De-icing salt frost scaling in concretes with fly ash or slag with low air void contents

Strand, Martin

2016

Document Version:
Publisher's PDF, also known as Version of record

Link to publication

Citation for published version (APA):
Strand, M. (2016). *De-icing salt frost scaling in concretes with fly ash or slag with low air void contents*.

Total number of authors:
1

LUND UNIVERSITY

PO Box 117
221 00 Lund
+46 46-222 00 00

De-icing salt frost scaling in concretes with fly ash or slag with low air void contents

Martin Strand

Licentiate Thesis

Report TVBM-3181

Division of Building Materials

Faculty of Engineering

Lund University

2016

Lund University
Division of Building Materials
www.byggnadsmaterial.lth.se

ISBN 978-91-7753-100-5 (print)
ISBN 978-91-7753-101-2 (pdf)
Report TVBM-3181

Printed in Sweden by Lund University
Lund 2016

Preface

I would like to thank the following persons for their contributions to the project:

Göran Fagerlund	…for initiating and formulating the project.
Skanska (especially Kyösti Tuutti)	…for contributing during the application process and making the project possible.
SBUF and Cementa AB	…for accepting and funding the project.
CBI	…for letting me work with the project at 60% rate, while continuing working at CBI, during an initial period of the project.
Katja Fridh	…for being my supervisor.
Anders Lindvall, Arvid Hejll, Erik Viggh, Kyösti Tuutti, Mikael Westerholm, Nils Rydén, Peter Utgenannt, and Ulf Jönsson	…(the reference group) for showing a great interest in my project and also supporting with input from their experience.
Sture Lindmark	…for contributing with some important input in the beginning of the project and by sharing some of his experience.
Lars Wadsö	…for comments on one of my papers and some helpful discussions.
The employees at the division of Building Materials	…for creating a nice working environment with interesting discussions during the lunch and coffee breaks and have generally being helpful and supportive.
My family	…for being very supportive.

Summary

Concrete is the most common building material because its versatility, however, the production of cement contributes to 5 to 8% of all manmade CO_2 emissions [1]. To reduce these emissions some of the cement can be replaced with a supplementary cementitious material such as fly ash or slag. The fly ash is a waste-product from coal power plants and the slag is a waste-product from the metal industry. These react with cement and water and will modify the properties of the concrete. This is important to be aware of to make sure that the concrete maintain its durability against certain damaging mechanisms and not reduce the expected service life of a structure. Concrete structures such as bridges are often expected to have a service life of 100 years, while being highly exposed to various damaging mechanisms. In countries where the temperature can vary between freezing and thawing several times per year, one important such damaging mechanism is de-icing salt frost scaling (DISFS). This occurs when a solution with a low concentration of salt freezes in contact with a concrete surface.

This licentiate thesis includes the following:

- Some background to why this project of DISFS of concrete containing fly ash or slag is important to study, and the specific questions this project have focused on.
- A literature review is presented which includes an introduction to the materials used in this project and basic information about the DISFS. After that, some information about the air void system inside the concrete and how it can be described (or quantified). Then some information about the DISFS test methods and finally a review of previous studies that have analysed DISFS in concrete containing fly ash (FA) or slag.
- The materials, which have been used in the project, are presented and then a summarized version of the methodology for the test that have been performed are presented.
- A summary of the results acquired from the DISFS tests.
- A discussion regarding the results.
- Conclusions drawn from the measurements that have been made so far.
- In the appendices, the articles can be found together with some complementary information regarding the development of the test methods. Last in the appendices are the results acquired from the tests performed on the binders and the measurements made on the air void systems of the hardened concrete.

The results from the DISFS measurements made on concrete test surfaces, which have never dried, show that the concrete with 20 mass% siliceous fly ash (SFA) and the concrete containing 100% ordinary Portland cement (OPC) acquire the most positive effect from additional air void content. The mass of DISFS is larger for concrete containing 100% OPC and cement blended with SFA than concrete containing ground granulated blast-furnace slag (GGBFS). However, the mass of DISFS is relatively large for the concrete with the smallest mass of DISFS. The reason for this is believed to be that the test surface is never dried and therefore (more or less) noncarbonated.

Sammanfattning

Betong är det vanligaste byggnadsmaterialet på grund av dess mångsidighet, dock är det så att cementproduktionen bidrar med 5 till 8% av alla CO_2 emissioner producerade av människor [1]. För att minska dessa emissioner från cementindustrin så kan en del av cementen ersättas med något annat som också kan bidra till cementreaktionen, exempelvis flygaska eller slagg. Flygaska är en biprodukt från kolkraftverken och slaggen är en biprodukt från metallindustrin. Dessa kan reagera med cementen och vattnet och bidra med vissa förändringar av egenskaperna hos betongen. På grund av att vissa egenskaper förändras är det viktigt att använda materialet på rätt sätt så att betongen inte får en lägre beständighet mot skademekanismer som skulle kunna sänka livslängden för en konstruktion. Broar är ett bra exempel på betongkonstruktioner då de har förväntad livslängd på cirka 100 år samtidigt som den utsätts för många skademekanismer. I länder där temperaturen kan variera mellan under och över 0 °C flera gånger om året, så är t.ex. en viktig skademekanism är saltfrostavskalningen. Denna sker då en salt lösning med låg koncentration fryser i kontakt med en betongyta.

Denna licentiat uppsatts innehåller följande:

- Bakgrunden till varför detta projekt som studerar saltfrost beständighet i betong med flygaska och slagg är viktigt, samt vilka specifika frågor detta projekt fokuserat på.
- En litteraturstudie som innehåller en introduktion till samtliga material som använts i projektet och grundläggande information om saltfrost skador. Därefter kommer information om luftporsstrukturer i betongen samt hur denna kan beskrivas (eller kvantifieras). Sedan kommer information kring metoder som testar saltfrostbeständighet och slutligen en genomgång av tidigare studier som studerat saltfrostbeständighet i betong som innehåller flygaska eller slagg.
- Materialen som använts i projektet och därefter en sammanfattning av metodologin för testerna som utförts.
- Summering av resultaten från saltfrostprovningen.
- En diskussion om resultaten.
- Slutsattser som dragits utifrån de hittills erhållna resultaten.
- I appendixen så finns artiklarna tillsammans med komplementerande information till testmetoderna. Sist i appendixen så finns resultaten från testen av bindemedlen som använts och mätningarna utförda på luftporsstrukturerna hos den hårdnade betongen.

Resultaten från saltfrost testerna utförda på betongytorna, som aldrig fått torka, visar att betong som innehåller 20 mass% kiselhaltig flygaska och betong som innehåller 100% vanlig Portlandcement erhåller störst positiv effekt från ett ökat luftinnehåll. Massan saltfrostavskalningar är större från betong med 100% vanlig Portland cement och betong som innehåller vanlig Portlandcement tillsammans med kiselhaltig flygaska, jämfört med betong som innehåller mald granulerad masugnsslagg. Dock, så är massan saltfrostavskalningar från betong med lägst mängd saltfrostavskalningar relativt stor. Anledningen till detta tros vara på grund av förkonditioneringen av testytan, som aldrig fått torka och därmed (mer eller mindre) inte karbonatiserad.

Symbols and abbreviations

A	Total volume of air voids per volume of concrete (usually called “total air content”)	[m³/m³]
α	Volumetric surface of air voids, boundary area per unit volume of air	[m²/m³]
c_i	Initial concentration	
c_T	Equilibrium concentration at temperature T	
l	Average distance across intersected voids along the line of traverse	[m]
L	Spacing factor	[m]
n	Number of voids intersected per unit length of traverse	[-]
p	Paste content, volume of paste per volume of concrete	[m³/m³]
Y_T	Fraction of ice at temperature T	
AEA	Air entraining agent	
Alite	Tricalcium silicate ($3CaO{\cdot}SiO_2$), abbreviated C_3S	
Aluminate	Tricalcium aluminate ($3CaO{\cdot}Al_2O_2$), abbreviated C_3A	
Belite	Dicalcium silicate ($2CaO{\cdot}SiO_2$), abbreviated C_2S	
bc	Binder content = mass of cementitious materials per cubic meter concrete	[kg/m³]
CH	Calcium hydroxide ($Ca(OH)_2$)	
CV	Coefficient of variation = standard deviation / mean value	[-]
DISFS	De-icing salt frost scaling	
FA	Fly ash (used e.g. when it is unclear if its siliceous or calcareous)	
Ferrite	Tetracalcium alumina ferrite ($4CaO{\cdot}Al_2O_3{\cdot}Fe_2O_3$), abbreviated C_4AF	
FTC	Freeze-thaw cycles	
GGBFS	Ground granulated blast furnace slag	
ITZ	Interfacial transition zone	
OPC	Ordinary Portland cement. This abbreviation is often used for “CEM I” cement according to the European standard and also to cement similar to CEM I.	
SCM	Supplementary cementitious material	
SFA	Siliceous fly ash	
SP	Superplasticizer	
Water	Dihydrogen monoxide (H_2O), abbreviated H	
wbr	Water binder ratio = mass of water / (mass of cement + mass of fly ash or slag)	[kg/kg]

Papers included and contributions

1. **Title:** "Methodology to analyse the Salt frost scaling mechanism(s) in concrete with different binders".
   Conference paper presented at the international RILEM conference "Materials, Systems and Structures in Civil Engineering 2016 - Segment on Frost action in Concrete", Lyngby, Denmark.
   Authors: Martin Strand, Katja Fridh.
   My contribution has been to perform the laboratory work, come up with a system to evaluate the results from the tests and I wrote the article. Katja have given input during the work and commented on the article.

2. **Preliminary title:** "Test Method for Salt Frost Scaling of Concrete using Climate Chambers with Air as Thermal Medium with an Upside Down Sample Setup".
   Manuscript (manuscript).
   Authors: Martin Strand, Katja Fridh.
   My contribution has been to develop the salt frost scaling method with various tests during the development to minimize the risk for errors. Also to teach, assist and co-supervise a master student, Henrik Sjöbeck, that performed some of the measurements presented in the article. I performed measurements not made by HS and I wrote the article. Katja has given input during the work, supervised the master student and commented on the article. Dr Sture Lindmark and Dr Peter Utgenannt provided with important input during the development of the method and sample setup.

3. **Preliminary title:** "Low Air Void Contents effect on the De-Icing Salt Frost Scaling in Uncarbonated Concrete containing Siliceous Fly Ash".
   Manuscript (manuscript).
   Authors: Martin Strand, Katja Fridh.
   My contribution has been to perform the de-icing salt frost scaling tests, evaluate the results and write the article. Katja has given input during the work and commented on the article.

4. **Preliminary title:** "Low Air Void Contents effect on the De-Icing Salt Frost Scaling in Uncarbonated Concrete containing Ground Granulated Blast-Furnace Slag".
   Manuscript (manuscript).
   Authors: Martin Strand, Katja Fridh.
   My contribution has been to perform the de-icing salt frost scaling tests, evaluate the results and write the article. Katja has given input during the work and commented on the article.

Table of content

Appendices

1. Development of the method to test combinations of AEA and SP
2. Methodology to analyse the Salt frost scaling mechanism(s) in concrete with different binders
3. Test Method for Salt Frost Scaling of Concrete using Climate Chambers with Air as Thermal Medium with an Upside Down Sample Setup
4. Complementary tests and measurements made for the DISFS method
5. Low Air Void Contents effect on the De-Icing Salt Frost Scaling in Uncarbonated Concrete containing Siliceous Fly Ash
6. Low Air Void Contents effect on the De-Icing Salt Frost Scaling in Uncarbonated Concrete containing Ground Granulated Blast-Furnace Slag
7. Results from Cementa CEM I, F20, F35, S20, S35, S70, K35
8. Results from Pelcon CEM I, F20, F35, S20, S35, S70, K35

1 Introduction

The purpose of this introduction is to give a general background to this project together with the aim and scope and a brief description of the thesis.

1.1 Background

Concrete is the most common building material because of the versatility with its high compressive strength and durability. However, the production of cement contributes to 5 to 8% of all manmade CO_2 emissions [1]. Considering the possible risks with climate change caused by manmade emissions, it is important to minimize them in order to minimize the possible impact of the climate change in the future. The CO_2 emissions from the cement production can be minimized by replacing a fraction of the cement with some other supplementary cementitious material (SCM). Two examples of SCMs are fly ash (FA) and slag which are waste-products from the coal power plants and metal industries respectively. However, when these are mixed in to the concrete will that change its microstructure and thus some of the properties. It is important that this change not will jeopardise the durability of the concrete.

This project studies concrete with wbr 0.40 that could be used in structures that are exposed harsh environment and several deterioration mechanisms, e.g. bridge decks. One important deterioration mechanism, is de-icing salt frost scaling (DISFS). The phenomenon occurs when a solution of water with a low concentration of de-icing salt freeze in contact with the concrete surface. Considering the fact that SCMs will change the properties and possibly the durability of the concrete there is a need for research. Some previous researchers have studied the DISFS mechanism(s) and also how various factors affect the mass of DISFS, however far from everything is known. In addition to this, the SCMs that are added to the concrete have been studied to a smaller extent. Therefore there is less knowledge regarding the DISFS of concrete containing SCM in comparison to the knowledge of DISFS of concrete that only contain ordinary Portland cement (OPC).

When studying DISFS of concrete the basic test method has a concrete surface in contact with a solution that consists of water with a specific concentration of salt. This setup is then frozen and thawed according to a continuous specified freeze-thaw cycle. After a certain number of cycles, the surface is brushed off, and the scaled concrete material is collected, dried and weighed. The mass of this DISFS will then act as a measurement for the DISFS durability of the concrete, i.e. how well a certain concrete recipe will resist the DISFS.

The DISFS mechanism(s) that inflict superficial damages has been studied for a long time. One of the oldest and among the most famous articles was written by Henry Arnfelt and published 1943 [2]. He studied how various de-icing agents affects the mass of DISFS and at which concentrations the largest mass of DISFS was produced. Verbeck and Klieger published a paper in 1957 [3] were they did a similar test matrix with both salts and non-salt de-icing agents. After these two large studies, it was concluded that there exist a so called "pessimum concentration" for each de-icing agent which contribute to the largest mass of damage.

A lot of research have also focused on how the test methodology affects the DISFS [4-8]. The studies clearly show that this is no simple task since there are several factors that have a large influence on the results. The methodology can be divided in to two groups where one group consist of the preconditioning of the test surfaces and the second consist of the DISFS test procedure. Some of the factors which can be included in to the preconditioning are e.g. hydration time of the concrete, the type of surface that is tested (e.g. sawed or trowelled), and if the surface have been dehydrated and/or carbonated prior to the test. Some of the factors that can be included in to the test procedure are e.g. the freeze-thaw cycle (e.g. minimum temperature and exposure time to the minimum temperature) and the type of de-icing agent (and the concentration) used in the solution. These factors only consider the methodology of the DISFS tests. When considering testing of concrete that contain various fractions of different SCMs, the complexity increase since the properties of the concrete will vary even more. If the concrete properties vary, this means that all the factors from the methodology affecting the DISFS results will most likely have different impact depending on the material. For example, a specific time for dehydration of the test surface will have different effect on DISFS results when comparing a concrete that only contain OPC with concrete that contain OPC blended with slag or FA with the same degree of hydration. The reason for this is that the permeability will be lower for concrete containing slag of FA, which means that the dehydration rate will differ and the samples will have different water contents that most likely will influence the DISFS results.

This thesis will introduce some basic knowledge and previous research in the literature review that will show the complexity of the DISFS tests. It will also present the methodology used to focus on the effect from the air void content for each concrete with a uncarbonated surface. Then the DISFS results are presented from tests performed during this study from the uncarbonated concrete containing siliceous fly ash (SFA), or ground granulated blast furnace slag (GGBFS). Finally, a discussion is given and the conclusions made during this project are listed.

1.2 Aim

The aim of this licentiate thesis is to investigate how various (low) air contents affect the DISFS for various fractions of added SFA or GGBFS for a never dried sawed concrete surface.

2 Literature study

The purpose of this literature study is to present relevant information regarding the materials that have been used and the measurements that have been performed in this study.

2.1 Concrete materials

The most important concrete property is generally considered to be the compressive strength which is obvious when designing a construction exposed to certain loads. Specifically the early compressive strength is important since this governs the time for demoulding on. However, when considering the durability, e.g. DISFS, inner frost damage, chloride penetration, and carbonation, other properties are also important. For inner frost damage, the air void content seems to have the largest influence on the frost resistance of the concrete. For chloride penetration in concrete, the permeability and the binding of chloride ions have the largest influence. For carbonation, the air permeability has a large influence. For DISFS the permeability, air content, porosity, capillary suction and others, all seem to affect the mass of DISFS for various concrete mixes and it is not agreed upon which property that is most important.

Concrete is made by mixing cement, water and aggregates in a mould. The reaction that occurs between the cement and the water result in a strong, porous and brittle glue between the aggregates. The materials properties, e.g. compressive strength, are strongly dependent on the extent of the reaction between the water and the cement, which is called the degree of hydration. High degree of hydration means that a large fraction of the cement has reacted with water. In addition to these three basic components, there are also supplementary cementitious materials that can be blended with the cement to alter the properties of the hardened paste. Finally, there are also some different admixtures that can be added to the concrete mix in order to change some property of the fresh or hardened concrete. In this study air entraining agents (AEA) and superplasticizers (SP) have been used to alter the air void structure and the workability of the concrete.

2.1.1 Cement

Cement is produced from burning limestone ($CaCO_3$) in approximately 1450 °C. During this process carbon dioxide (CO_2) is released from the limestone, which mean that calcium oxide (CaO) is obtained. After the CO_2 has been released, the limestone will eventually reach thermodynamic equilibrium in the kiln where the phases are created which cement consists of. The four main phases in a OPC are alite, belite, aluminate, and ferrite. After these phases have formed inside the kiln, the mass is cooled quickly to preserve these phases. Then it is grinded to a powder with gypsum and perhaps a small amount of additional limestone (< 5 mass%) to create a CEM I which is the name of ordinary Portland cement (OPC) according to the European standard. The size of the cement grains is governed by the grinding procedure. As the grains size decrease the surface area per kg of cement will increase, which means more cement is in contact with the water and can therefore react quicker and provide a higher early compressive strength. This also means that the heat created from the hydration process will be high, which can cause e.g. some early cracking. The surface area of the cement used in this project is relatively large since the CEM I is classified to generate a moderate amount of heat during the reaction. The sizes of these particles are approximately 4 to 50 µm across, (appendix 7).

Two of the basic reactions between the calcium silicates (C_3S and C_2S) and water (H_2O or H) can be approximated according to the following equations of equilibrium:

$$2C_3S + 6H \rightarrow C_3S_2H_3 + 3CH$$

$$2C_2S + 4H \rightarrow C_3S_2H_3 + CH$$

The products are called calcium silicate hydrate (CSH) and calcium hydroxide (CH). The notable difference between these two reactions is that the C_3S reaction produces more CH. The main difference between these is that C_3S react early, therefore contributes to early strength, while C_2S react later, and therefore contributes more to strength later on.

2.1.2 Supplementary cementitious materials (SCM)

The main reason for the use of SCMs in concrete is that the total CO_2 emissions from producing the concrete needed for the construction is therefore reduced. If the SCM is not used as filler in concrete, it will end up in a landfill since it is just a waste-product, which should be considered as a worse case since then it does not contribute to any reduction in CO_2 emissions and increase the total amount of wastes.

SCMs change the microstructure of the hardened cement paste and is thereby changing the basic conditions (concrete material properties, e.g. permeability) for the concrete to either become more or less resistant to various types of deterioration mechanisms. The different types of deterioration mechanisms can be related to what conditions the concrete is exposed to. The European standard [9] defines various exposure classes. In addition to this, it sets some minimum requirements on the concrete exposed to the various exposure classes. If these minimum requirements are met, the durability of the concrete should be high enough for a certain service life. These minimum requirements also specify limits of the fraction of SCMs which can be added. As an example, concrete exposed to sulphates (e.g. in sewer pipes) it is beneficial to have a large fraction of GGBFS since it increase the resistance to sulphate attacks. However, in the case of concrete exposed to freezing and thawing in combination with de-icing salts the standards have relatively low limits for the fraction of SCM replacement. This limit has been set due to studies that indicated that an increased fraction of SCMs result in an increased mass of DISFS (lower DISFS resistance).

There are also other factors, besides those regarding durability of the hardened concrete, which change when implementing SCMs in to the concrete. One example is the total heat produced from the reactions during the first day is reduced. This is because the reaction from e.g. SFA and GGBFS needs CH, which means that the cement reaction have to produce some CH before it can start. When these reactions start, they result in mostly CSH. This will contribute to a lower temperature inside the young concrete, which is beneficial in thick constructions, or when casting in environments with high temperatures. High temperatures inside the concrete during the hydration period can cause problems such as shrinkage during cooling, which leads to large tensions, which can cause cracks in the concrete. In addition to this, a low heat of hydration can also be a disadvantage when casting in a cold climate since the reaction rate will then be even slower. That will result in a lower degree of hydration rate and a slower increase in the early compressive strength that will increase the time before the moulds can be removed. These simple examples show that it is important to consider the changes when implementing SCMs to utilize them in an advantageous way.

2.1.2.1 Siliceous fly ash (SFA)

Fly ash (FA) consists of spheres of almost completely burnt ash (SiO_2), which is produced as a waste-product in a coal power plants. It is collected by filters, which are used to prevent the FA from escaping from the power plant into the environment. This waste-product can then be used as a supplementary cementitious material mixed with cement and contribute with some modifications to the properties in the concrete through its pozzolanic reactions of the FA.

The FA used in this project is siliceous fly ash (SFA), which consists mostly of silicon dioxide (SiO_2) and aluminium oxide (Al_2O_3). The size of these fly ash spheres are approximately 5 to 150 µm (appendix 7)

Bouzoubaâ and Fournier [10] analysed the use of fly ash, slag and silica fume in Canada 2001. They concluded that fly ash has the biggest potential for increased utilisation. However, the paper mentioned the DISFS to be an obstacle regarding the technical issues of expanding the production of concrete containing fly ash.

2.1.2.2 Ground granulated blast furnace slag (GGBFS)

Slag is created inside the blast furnace during the production of iron. It is a waste-product that mainly consists of calcium oxide (CaO), silicon dioxide (SiO_2), and aluminium oxide (Al_2O_3). After cooling, it is ground in to a powder where the fractions are usually around the same size (or slightly smaller) as the fractions of cement. The particle size of the GGBFS used in this project is approximately 3 to 56 µm (appendix 7).

According to Bouzoubaâ and Fournier [10], 90 % of the GGBFS produced during the year 2001 in Canada is used for the cement and concrete industry. It is also mentioned in the report that if the market demands it, more slag can be grounded into GGBFS for use. During the year 2001, the amount of GGBFS was approximately 25 % (380 000 out of the 1 438 000 tons slag produced) of the total blast furnace slag production with potential to be used in concrete. The rest is mainly used as lightweight aggregates or exported to USA. (No similar article has been found regarding the slag production and consumption in Sweden or Europe during the literature study.)

2.1.2.3 Lime stone filler (LSF)

Lime stone filler is limestone ($CaCO_3$) that has been ground down to a particle size distribution similar to that of cement. The lime filler contributes with increasing the fraction of calcium in the paste mix, which can contribute to a faster early hydration due to the so-called “seeding effect”. CEM I consist of 95% clinker and 5% of “something else”, the main constituents of the 5% is usually gypsum and lime filler.

2.1.3 Admixtures

In this section is the basic functions of the superplasticizer and the air-entraining agent briefly explained, chosen since there are the only admixtures used in the project.

2.1.3.1 Superplasticizer (SP)

Superplasticizers (SP) are used to increase the workability of the concrete, i.e. make it flow without increasing the w/b-ratio. These can generally be sorted in to four categories, sulfonated melamine-formaldehyde condensates, sulfonated naphthalene formaldehyde condensates, modified lignosulfonates, hydroxylated polymers, and other synthetic polymers (e.g. hydroxylated carboxylic acids and polyether-polycarboxylates) [11]. They adsorb to cement grains, which disperse the grains and prevents early agglomeration, and thereby increase the workability of the fresh concrete. The prevention of cement grain agglomerates is also positive for the cement hydration since more cement grains have direct access to water and thereby the paste can reach a higher degree of hydration (mass hydrated cement in relation to the total mass of cement added from the start) on shorter time. Since the strength increase with an increased degree of hydration, this is a positive effect.

2.1.3.2 Air entraining agent (AEA)

Air entraining agents are surfactants that end up on the border between air and water inside the cement paste. These can generally be sorted in to neutralized wood resin, They consist of one part that is hydrophilic (negatively charged), and the other part, which usually looks like a tail, is non-polar (or hydrophobic). One thing that can be designed for a synthetic surfactant is the length of the non-polar tail, which can have an impact on some of the AEA properties. Some examples of AEAs are neutralized wood resin and synthetic detergents from salts of organic acids and sulfonated hydrocarbons [12]. They should not bind chemically with cement or any other SCMs, they should only contribute with encapsulating air inside the cement paste. During the mixing, the AEA create many small air voids that are dispersed inside the cement paste, which will increase the frost resistance.

2.1.4 Aggregates

Aggregates usually make up approximately 75 mass% of a normal concrete mix, which implies that the aggregates have a significant impact on the concrete. One of the factors to consider regarding the choice of aggregates is that the fraction size distribution. This is important for the workability and it also have an impact on compaction of the concrete, which have an influence on the strength. The aggregate size distribution also determines the minimum required cement content since it is dependent on the total surface area of the aggregates. Generally, a smaller total surface area should require a lower minimum cement content, and by reducing the cement content, the total CO_2 emissions are also reduced.

One additional factor that can be considered regarding the strength is that aggregates contain different minerals, which have different Youngs modulus and different maximum compressive strengths. This will in turn affect the resulting strength of the concrete. However, considering that the compressive strength is a combination of the hardened cement pastes and the aggregates, the effect from the aggregates is dependent on the strength of the hardened cement paste. If the wbr is low, e.g. 0.40 and well hydrated, the hardened cement paste can have approximately the same compressive strength as the aggregates. This will result in a fracture going through the cement paste and aggregates, i.e. the strength of the aggregates matters for the total strength of the concrete. However, if the wbr is high, e.g. 0.60, fractures will most likely go through the cement paste, around the aggregates. This means that aggregates with a high Youngs modulus and high compressive strength will not contribute to a significant increase for the total compressive strength of a concrete recipe with a high wbr.

When considering durability there are also some things to consider before choosing the aggregates. Siliceous aggregates can contribute to alkali-silica reactions where the product from the reaction have a larger volume and therefore create a pressure which can make the concrete crack and thereby destroy it. This can be avoided more or less by using cement with low alkali content and/or aggregates with low silica content.

For construction that will be exposed to freezing temperatures, i.e. there is a risk for frost damage, frost resistant aggregates should be used in the concrete mix. In general, a frost resistant aggregate have a high strength and low absorption. To determine if aggregates are frost resistant or not, some tests can be made which are given in standards [13-16]. Petrographic examination can show if there are some minerals or particles present which are generally weak (low compressive and tensile strength). Water absorption tests can indicate if the aggregates are frost resistant or not. If an aggregate have a large volume of small voids that can be filled with water easily, the risk for frost damage is high. Aggregate that are frost resistant generally have either a small volume of larger voids that are not easily filled, or a small volume of small air voids where the mass of water that freeze is small. The absorption rate and the rate for which water then can escape are also important factors where a higher rate contributes to a higher frost resistance. Another test is to let the aggregates absorb water and then expose them to freeze-thaw cycles (FTC). After the exposure, the frost resistance is based on if any cracks have formed, there is a loss in mass or the strength has been reduced. In some special cases with high exposure to salt and de-icing agents, this test can be made with a salt solution or urea instead of pure water.

In Sweden, the bedrock consist of granite which is an igneous rock that contain the minerals quartz and feldspar among others. Granite among other rocks found in Sweden is usually frost resistant and overall the fraction of silica is low, if any, which mean that there is usually no risk for deleterious reactions between the aggregates and the paste.

2.2 Frost damage

This section will give a brief introduction to frost damages in concrete that can be separated in to two types, the inner frost damage and the superficial DISFS. Firstly, the so-called inner frost damage mechanism will be described briefly, and then some basic information regarding the DISFS phenomenon is given.

2.2.1 Inner frost damage and the critical degree of saturation

The inner frost damage mechanism has been studied by several researchers, a few examples of these studies are [17-21]. The basic mechanism can be explained with the following example. If you take a bottle made of glass, fill it with water and put it inside the freezer the bottle will break when the water freezes. The mechanism contributing to this is the volume increase that happens during the phase change when the H_2O transform from liquid phase (water) to solid phase (ice). This volume increase is approximately 9 vol%. The theory of critical degree of saturation is based on this volume increase due to the phase change [20]. The critical degree of saturation for a material is the point when it contains so much water that the inner pressure becomes so large that it damages the material. The critical degree of saturation for the bottle in the example mentioned above is therefore approximately 91.7 vol%. This can be calculated by multiplying the volume which is filled (91.7) with a nine percent volume increase (91.7·1.09=100.0%). This means that if the bottle is filled with more than 91.7 vol% water, the bottle will break if the water freeze and change phases from liquid (water) to solid (ice).

Considering ice forming inside a water filled air void in the concrete, this will create an inner pressure in the same way as for the bottle mentioned above. However, if there is an empty air void connected to the water filled air void where the freezing began, the pressure can be relieved since the water that have not yet frozen can be evacuated to the empty air void. This means that a homogenous air void system with many small air voids will decrease the pressures that otherwise build up during ice formation and therefore improve the frost resistance of the concrete. A high air void content with many small voids will also decrease the risk for the concrete to reach the critical degree of saturation. However, it is important to remember that the critical degree of saturation can always be reached given that there is unlimited time and unlimited access to water.

Fagerlund [20] presents a test method to determine the critical degree of saturation. In addition to this, results are presented where the critical degree of saturation have been determined for 41 different materials. This report clearly shows that the critical degree of saturation varies for different porous and brittle materials similar to concrete.

The inner frost damage and the DISFS is somewhat linked since the inner frost damage mechanism can occur in the concrete close to the surface during a DISFS test. This is why it is important to understand internal frost damage when doing DISFS tests. However, there are some important differences with the DISFS since the de-icing agent alters the freezing process.

2.2.2 De-icing salt frost scaling

This section will give some basic information about how a de-icing agent works in order to explain the differences between internal frost damages and DISFS. That is followed by a summary of some previous studies regarding the pessimum concentration, and then two general theories regarding the DISFS mechanism is briefly described,. The chapter ends with a list that show what researchers generally agree on regarding the DISFS mechanism.

2.2.2.1 Freezing of a De-Icing Agent Solutions

When studying the DISFS mechanism in concrete it is important to have a basic understanding about what happens when a solution with a low concentration of a de-icing agent freeze. In normal conditions without any de-icing agents, water freeze at 0 °C or slightly below 0 °C if the water is super cooled. However, when a de-icing agent is mixed with the water, the freezing temperature of the water in the solution is lowered. This enables de-icing agents to thaw ice on top of roads and bridges during the winter. Since NaCl solution is used in many DISFS tests, it will be used here as an example to visualise the effect of a de-icing agent. Figure 1 presents an overview of a phase diagram of a water and NaCl solution. “Area I” in the figure shows at what temperatures and concentrations the NaCl is completely dissolved when mixed with water. When the concentration increases from 0 to approximately 23 mass% the freezing depression for the water in the solution is lowered from 0 to -21.12 °C. The point where area 1, 2, 3 and 4 meet in the diagram is called the eutectic point. When a 23.3 mass% NaCl solution is cooled below -21.12 °C, it will change phases to ice and a crystal phase of $NaCl{\cdot}2H_2O$, which mean that the salt does not have any de-icing function below the eutectic point.

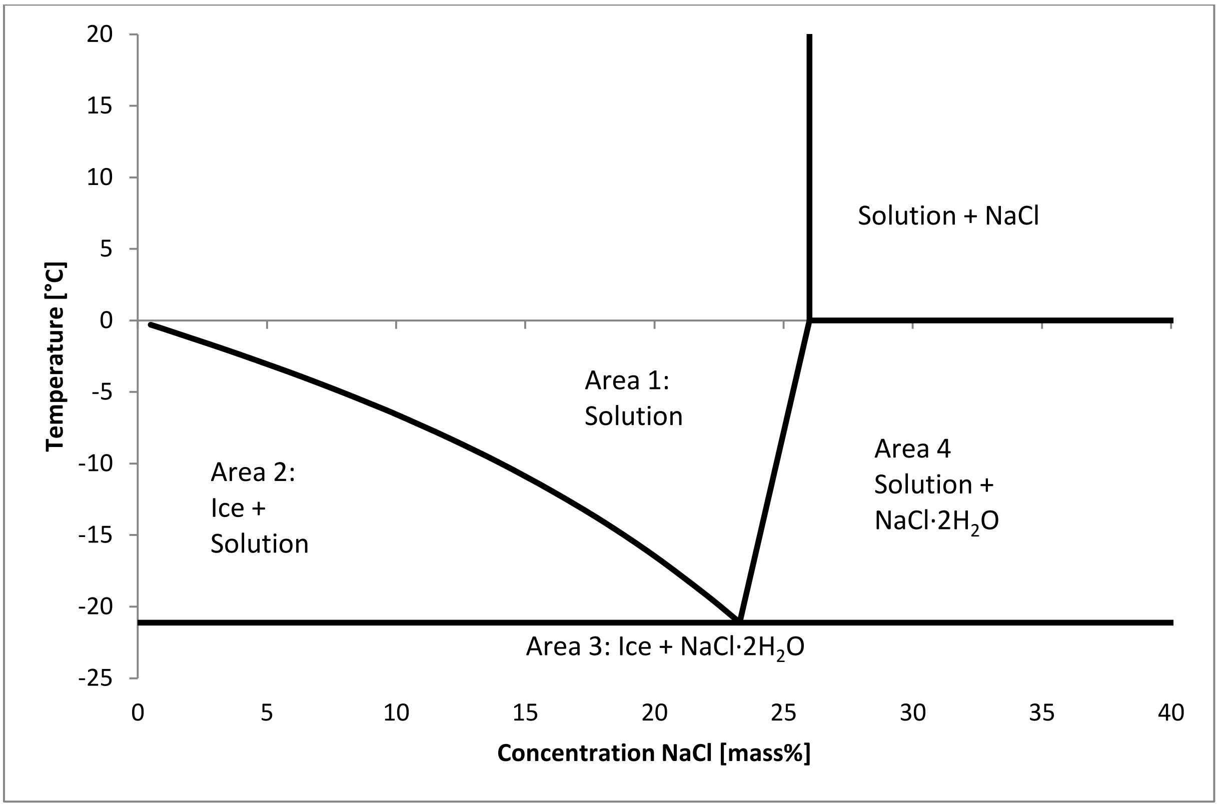

Figure 1. Phase diagram of NaCl mixed with H_2O, remade according to the phase diagram presented in [2].

Figure 2 presents a part of area 1 and area 2, where a 3 mass% NaCl solution will be in equilibrium during the regular DISFS tests. This area, is when the NaCl concentration is between 0 and 23.3 mass% and the temperature is between 0 and -21.12 °C.

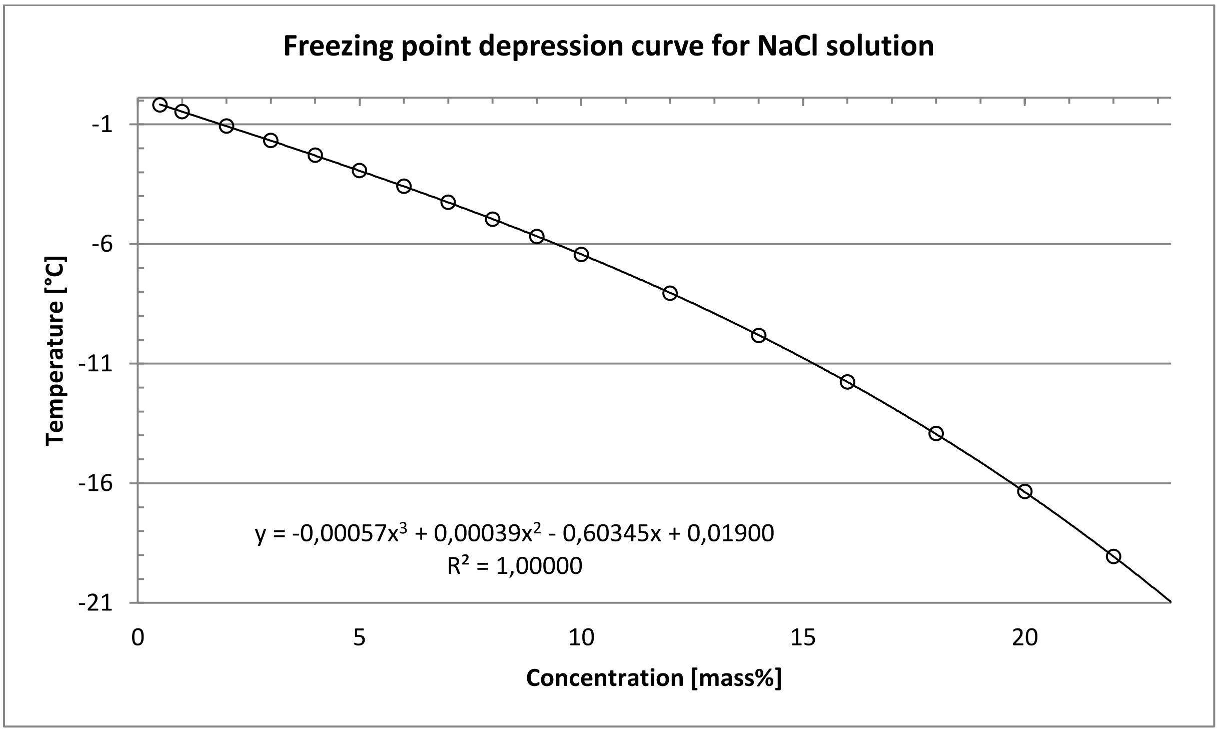

Figure 2. Freezing point depression curve for NaCl mixed with H_2O in thermodynamic equilibrium [22]. The data points of the freezing suppression is according to [22], and the equation presented is generated from the measurement points.

According to Figure 2, for a solution with 3 mass% NaCl concentration the freezing suppression is -1.79 °C. When a 3 mass% NaCl solution is exposed to temperatures below -1.79 °C, it is only some of the H2O that freeze, while the NaCl will still be dissolved in a solution. This means that there will be one part ice and one part solution. Because some of the water has frozen, the solution will have an increased NaCl concentration since the mass ratio between NaCl and unfrozen water has increased. The fraction of ice and solution can be calculated according to Equation (1).

$$Y_T = \frac{c_T - c_i}{c_T} \tag{1}$$

Where the concentration at temperature T is given by the equation presented in Figure 2.

In the following example the temperature is lowered to -6.56 °C for a solution with the initial concentration of 3 mass% NaCl. According to Figure 2, the concentration at temperature -6.56 °C is 10 mass%. The fraction of ice can then be determined according to the following calculation.

$$\frac{10 - 3}{10} = 0.70 = 70\%$$

This means that 70 % of the NaCl solution consists of ice and the rest (30 mass%) consist of a 10 mass% NaCl solution which can remain as a solution at -6.56 °C. In Figure 3 the fraction of ice formed at a given temperature is calculated with equation 1 and the data given in Figure 2. The different lines presents solutions with different initial concentrations, from 1 mass%

NaCl (curve with highest fraction of ice at -21 °C) to 10 mass% NaCl (curve with lowest fraction of ice at -21 °C).

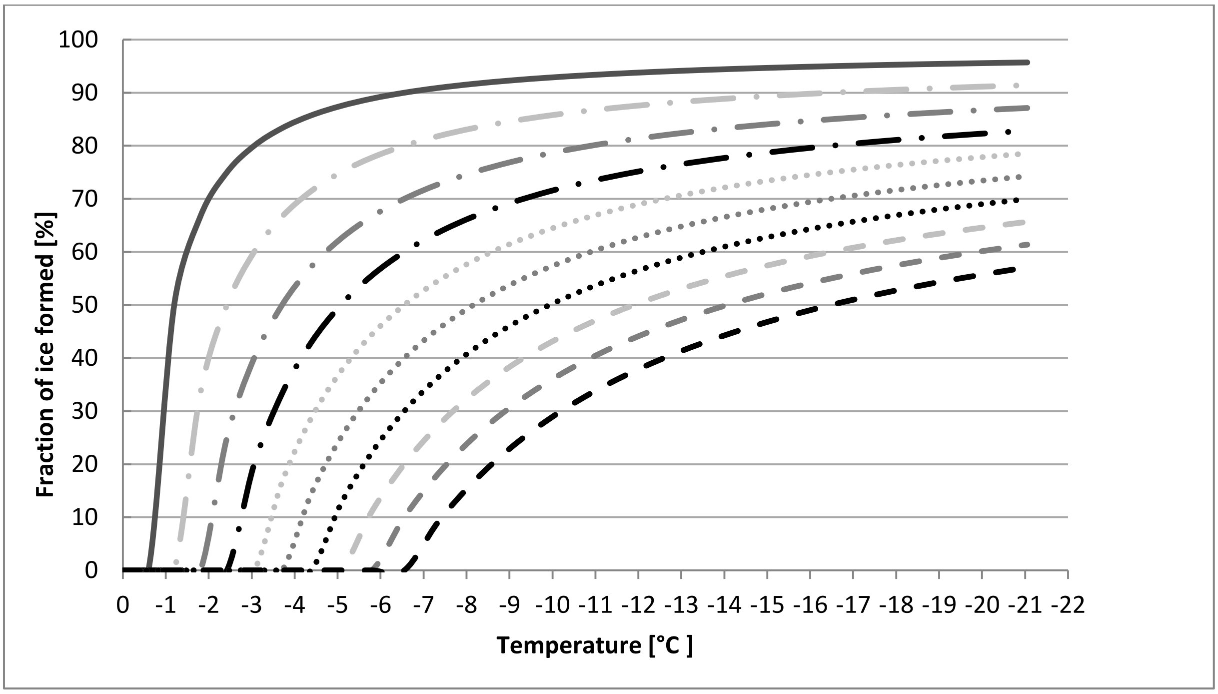

Figure 3. Fraction of ice formed at a certain temperature for NaCl solution with 1 to 10 mass% NaCl in steps of 1 mass%.

Here are some concluding notes regarding the function of de-icing agents.

- The addition of a de-icing agent to ice will lower the freezing point and thereby thaw ice when the addition is high enough.
- When the temperature is lowered only the water freeze and the NaCl will remain in a solution with an increased concentration.
- During the freezing process of a low concentration of de-icing agent solution (from when freezing start just below 0 °C to -21.1 °C) the fraction of ice will increase at the same time as the concentration of the surrounding solution will increase.

2.2.2.2 Pessimum Concentrations of De-Icing Agent Solutions

There exists a pessimum concentration for de-icing agents that will contribute to the largest mass of DISFS during freeze-thaw. This means that when freezing water with 0.1, 3 and 10 mass% NaCl, the 3 mass% solution will create a larger mass of DISFS in comparison to both the 0.1 and the 10 mass% solution.

The studies, which have done DISFS tests with various concentrations of de-icing agents, found during the literature study are Arnfelt [2], Verbeck and Klieger [3], Sellevold and Farstad [23], Fagerlund [24], Lindmark [25], Marchand [26], Setzer [27] and Liu and Hansen [28]. In Table 1 a rough summary of these studies are presented. In Table 2 some of the notable findings from the results are summarized.

Table 1. Summary of which factors have been varied in the DISFS studies where the pessimum have been analysed.

Researcher(s) [Article]	De-icing agents	Concentrations [mass%]	Material
Arnfelt [2]	$CaCl_2$	1 to 10, 20, 30, 40, 50, 60	OPC, concrete samples taken from roads
	NaCl	0, 2, 4, 6, 8, 10, 20, 30	wbr unknown
Verbeck and Klieger [3]	$CaCl_2$	2, 4, 8, 16	OPC,
	NaCl	2, 4, 8, 16	Non air entrained (ca 2 vol% ac) +
	Urea	2, 4, 8, 16	Air entrained (ca 7 vol% ac)
	Ethyl alcohol	2, 4, 8, 16	wbr 0.42, 0.63$^{1)}$
Sellevold and Farstad [23]	NaCl	0.5, 1, 1.5, 2, 3, 4, 4.5, 6, 8	OPC, OPC+silica fume, wbr 0.55, 0.45, 0.36, 0.27, initial salt solutions in pores
Fagerlund [24]	NaCl	0.0, 2.5, 5.0, 10.0	OPC, 3 various air contents, 3 wbr, 0.40, 0.60, 0.70
Lindmark [25]	NaCl	1.0, 1.5, 2.0, 2.5, 3.0, 3.5, 4.0, 4.5, 5.0	OPC, 0.35 initial salt solutions in pores Dried and remoistened, and never dried specimens
Marchand [26]	NaCl	1.5, 3, 6, 9, 12	OPC, initial, and no initial, salt solutions in pores wbr 0.25, 0.35, 0.45 hydrated 180 days in lime solution, dried and carbonated for 21 days
Setzer [29]	NaCl	0.1, 0.5, 1, 2, 3, 6, 8, 9, 10, 11, 12, 15, 18	OPC,
Liu and Hansen [28]	NaCl	0, 0.5, 1.5, 3, 6, 9, 12	OPC, wbr 0.45

[1)] 4.8 and 7.2 gal water per sack cement = 7.2*3.785/43 = 0.63. Mass for 1 sack of cement is uncertain (here it is assumed to be 43 kg).

Table 2. Summary of notable conclusions from the DISFS studies where the pessimum have been analysed [2, 3, 23-28].

Author	Notable comments
Arnfelt [2]	• Older and less permeable concrete (i.e. longer time for hydration and therefore most likely higher degree of hydration) will create smaller mass of DISFS. In addition, the chemical effect from the salt solution seems insignificant. • Results show that there exist a pessimum concentration both for NaCl and CaCl. • Results also indicate that seven other chemicals produced more damage than pure water when mixed to have a freezing point depression of 1.5 °C.
Verbeck and Klieger [3]	• Dissimilar de-icing agents can cause DISFS. • Low concentrations of de-icing agents contribute to a larger mass of DISFS when they freeze in contact with concrete with a pessimum of 2 to 4 mass%. • The results indicate that a larger mass of DISFS is produced when the same solution is kept in contact with the concrete during the FTC in comparison to when water have frozen then salt is applied (which thaws the ice) and finally the solution is rinsed from the surface and replaced with new water. • No DISFS occurs when the concrete test surface is only damp (i.e. there is no layer of solution on top that freeze and thaws).
Sellevold and Farstad [23]	• Concrete mixes with wbr 0.27 and a compressive strength of approximately 115 MPa seems to be unaffected by the DISFS. • Concrete mixes with wbr 0.36 and a compressive strength of approximately 91.5 MPa are clearly affected by the DISFS and the pessimum concentration of the NaCl seems to be 4.5 to 6 mass%. • Concrete mixes with wbr 0.55 and a compressive strength of approximately 50 MPa are clearly affected by the DISFS and the pessimum concentration of the NaCl seems to be 1 to 3 mass% NaCl. • No damage is produced on this concrete with wbr 0.5 when water is used while a 0.5 mass% NaCl concentration contributes to a significant mass of DISFS. • When the there is an initial NaCl concentration inside the pores before the test begin (with a 3 mass% NaCl outer solution) the mass of DISFS decrease in comparison to when the initial inner concentration is 0%.

Fagerlund [24]	• Results indicate that the pessimum NaCl concentration for DISFS is higher for a saturated sample (from approximately 2.5 mass% for a dried sample, to 5 (or 10) mass% for a saturated sample). • Results indicate that the uptake of NaCl solution is higher during freezing and thawing than during isothermal capillary suction with +20 °C, and the uptake of NaCl solution is generally higher than water uptake. • Mass of DISFS decrease when air content increase or when the wbr decrease. • Results from freezing samples saturated with either water or various NaCl solutions (with constant degrees of saturation) showed largest strain for the samples with 2.5 mass% NaCl which indicates a pessimum concentration.
Lindmark [25]	• No clear pessimum between 1.0 and 5.0 mass% NaCl solution (w/c 0.35). • The mass of DISFS is generally higher when the outer concentration is 3 mass% NaCl regardless of the inner concentration.
Marchand [26]	• Consistent pessimum around 1.5 to 3 % (for favourably hydrated concrete with w/c of 0.25, 0.35 and 0.45) which suggest that the pessimum chloride concentration is not related to the concrete quality. • It is stated that the mass of DISFS is related to the ice formation and therefore the pore structure. A low wbr will contribute to a denser pore structure and less ice formation, this is believed to be the reason for a lower mass of scaling in concrete with low wbr. • The results suggest that the outer solution has a larger influence on the DISFS.
Setzer [29]	• Results indicate that the minimum temperature of -20 °C result in larger mass of DISFS than when the minimum temperature is -10 °C. • A pessimum NaCl concentration can be seen around 3 mass% both when the minimum temperature is -10 °C and -20 °C. • The pessimum NaCl concentration seems to be the same for a CEM I and a CEM III/B with wbr 0.60 and bc 320 kg/m^3. • There is a clear difference in DISFS when comparing 0.0 mass% NaCl (water) with a 0.1 mass% NaCl solution.
Liu and Hansen [28]	• The results indicate that a NaCl concentration of around 0.5 to 6.0 mass% produce the largest mass of DISFS.

These are all observations that a DISFS mechanism should be able to answer. There are currently two different theories regarding the mechanisms that contribute to DISFS. These are the “glue-spall” mechanism and the “ice lens growth” mechanism, which are introduced in the following sections.

2.2.2.3 “Glue-spall”-mechanism

The glue-spall mechanism theory presented by Valenza II and Scherer [30] is based on that concrete and ice have different coefficients of thermal expansion. This principle is used to treat glass windows where the glass is sandblasted, then a film of epoxy is applied and the temperature is changed. The epoxy will shrink more than the glass that generate high stresses on the surface of the glass, this makes thin pieces of glass “spall” off and thereby a modified glass surface is created. In the glue-spall mechanism theory for DISFS on a concrete surface, the salt solution freeze and becomes strongly adhered to the concrete. When the temperature is lowered the ice shrinks and cracks (due to brine pockets inside the ice layer), which contribute to the same superficial stresses on the surface of the concrete.

This theory is based on warping tests made by Valenza II and Scherer [31]. The warping test setup is basically a beam of cement paste on which a solution is frozen. The ice will shrink more than the cement paste and make the beam bend. The deflection of the beam is measured and the stresses can then be calculated. Results from these tests are presented in [31].

2.2.2.4 Ice lens growth in porous systems

The ice lens growth mechanism is presented in [32] and is based on the fact that nature wants to even out differences in concentrations, e.g. air pressure, vapour in air or ion concentrations in a solution. The paper explains that the basic factor that contributes to the ice body growth is the free energy of the water, which is affected by the ion concentration and pressure among other things. Increased ion concentration increases the free energy of water inside small voids, which in turn contributes to a freezing point depression. The free energy also increase when the size of the voids decrease because when the curvature of the surrounding matrix is smaller the bond strength of the water increase. This means that there is a supply of water that will be transported to the ice body during freezing given the driving force that the differences in free energy provide. When the ice nucleation starts only the water freeze that creates differences in ion concentration and in the free energy of the unfrozen water surrounding the ice body. This driving force from the differences in the free energy is called osmotic pressures that results in a water transport from small voids connected to the larger voids where the ice nucleation started. In addition to this, there will also be unfrozen solution on the concrete surface (outside the concrete matrix) that also contributes with water that can be transported in to the ice bodies in the concrete matrix.

The process of the mechanism that Powers [32] present is that the ice nucleation will start in a large void and the ice body will start to grow given that it is supplied with water due to the osmotic pressures. When the ice body grows so-called hydraulic pressures will be created because of the 9 vol% increase when water change phase to ice if the surrounding voids are also filled with water. This pressure will decrease if water can transport to an empty adjacent air void, however, if the distance to the closest empty air void is large the pressure might exceed the strength of the concrete, which will damage the concrete.

Lindmark [25] also studied this mechanism and presented results which supports this theory. One of the tests presented showed that samples that had been stored in low concentrations of NaCl solutions (close to pessimum concentrations) then submerged in precooled salt solutions gained more weight than samples that had been stored in a higher concentration salt solutions. In addition to this, the mass increase was higher when the temperature of the precooled solution was lower. Cryogenic suction (absorption at low temperatures) has also been analysed in a study by Liu and Hansen [33] that found a connection between the cryogenic suction and the mass of DISFS. They conclude that the cryogenic suction mechanism is governed by “(I) freezable water (or the initial ice nucleation), (II) the presence of surface moisture transported through (III) the capillary pore system”.

2.2.2.5 Phenomena which researchers generally agree on

The following list have been made during the literature study summarize common findings.

1. DISFS demands that a solution which contribute with a freezing point depression is in contact with the concrete and freeze, i.e. if there is not a solution there will not be any damage and water (without any ions which could contribute to some freezing point depression) will not contribute to any damage [25].
2. The chemistry of the solution does not seem to matter, only the freezing point depression [2, 3].
3. There exist a pessimum concentration for the solution which is a low concentration (1-5 mass%) [2, 3, 23, 25-28, 34].
4. Without freezing temperatures no scaling occurs [25]. According to the glue spall theory the DISFS will start to occur when the temperature is approximately -10 °C, however this is dependent on the initial NaCl concentration of the solution [35].
5. The mass of DISFS increase with increasing mass of ice formed. This implies that the mass of DISFS increase when the minimum temperature decrease, and also with a longer time of exposure to the minimum temperature, i.e. the features of the FTC affect the mass of DISFS [25, 26, 35].
6. Tests performed with various initial internal salt solutions, inside the pores of the concrete, with various salt solutions on the outside, applied when the DISFS test begin, indicate that the initial internal salt solution also matters [23, 25, 26]. However, there does not seem to be a uniform answer of how much an initial de-icing agent solution inside the pores matter or exactly how it affects the DISFS mechanism(s).
7. An increased degree of hydration decrease the mass of DISFS [2].
8. A lower w/c ratio decrease the mass of DISFS [24, 26].
9. The mass of DISFS increase as the number of FTC increase.

2.3 The Air Void System

Increased air content by adding AEA can increase the frost resistance [32]. According to the glue spall theory, the reduction in mass of DISFS from the air void system is because the air void system contributes compressive tensions when the ice body create suction of water from adjacent capillary pores. This suction in combination with the ice, in the matrix, contribute with increasing the thermal expansion and therefore a smaller difference in shrinkage between the concrete surface and the ice [36]. The reduction in mass of DISFS due to the air void system, according to the theory of ice lens growth, is because of the shortened distance for water to be transported from a point in the capillary pores to an air void [37].

It is important to quantify the air void system to be able to decide if the system have the right features (small enough voids to have small distances between them but big enough not to be water-filled to easily). The measurements, from which these factors are calculated, are made on (two-dimensional) sections of a concrete sample. To identify the air voids, the concrete is painted black and the air voids are filled with zinc paste. Thereby, a contrast is created between the concrete and air voids. When this is done, a linear traverse measurement can be performed.

2.3.1 Linear traverse

Linear traverse measurements is done by shining a small light, ca 2 µm in diameter, on the painted concrete surface (black concrete surface and air voids filled with white zinc) and measure the reflection. When the light is on the black area the reflection will be low (i.e. solid concrete), when the light is on the white area the reflection will be high (i.e. an air void filled with zinc paste) and this enables measurements of the length of each white area crossed. These so-called cords are the length of each line over an air void that the light has passed. However, note that the light almost never go through the middle of each air void which introduce some difficulties. Because of this, many lines need to be measured on the same concrete surface to make the results statistically reliable for a sample [38].

2.3.2 Quantifying the Air Void System

The theory of micro ice lens growth lead Powers [39] to analyse the relationship between the average distance from any point in a cement paste to an air void and the mass of DISFS. With more entrained air, there will be a larger amount of small air voids that result in a shorter average distance called spacing factor. The paper conclude that concrete should have a spacing factor of approximately 0.01 inch (0.25 mm), but this number is only approximate and not a guarantee for frost resistance [39]. The paper present the following equations developed by Powers with contributions from T.F. Willis.

Equation (2) calculates the total air content by multiplying the number of voids intersected (cords) during the measurement with the average distance across all of the intersections (symbols are described on page VI).

$$A = n \cdot l \tag{2}$$

T.F. Willis has concluded that the boundary area of the air-voids per unit volume of air (m^2/m^3) can also be determined from the average cord length “l” [39].

$$\alpha = \frac{4}{l} \tag{3}$$

Hence, from Equation (2) and (3) gives Equation (4)

$$\alpha = \frac{4n}{A} \tag{4}$$

The third equation of interest in the paper is the void spacing factor that is calculated according to Equation 5.

$$L = \frac{3}{\alpha}\left(1.4\left(\frac{p}{A}+1\right)^{\frac{1}{3}} - 1\right) \tag{5}$$

After the spacing factor, there have been some other similar factors suggested to describe the DISFS resistance. These are the Philleo factor [40], the mean spacing factor [41] and the flow length [42]. These three are based on the same concept as the spacing factor, which says something about a probable distance to nearest air void.

Plante et al. [43] have suggested air-void stability index defined as the largest spacing factor minus the smallest spacing factor for two mixes (same recipe) where e.g. the mixing time have been changed to evaluate the air void system. The index could give some indication about the variation of air void systems created, but it should be noted that the spacing factors must be considered. If the air-void stability index is low (which is considered to be good), but the spacing factors are high the quality of the air void system is still very low. This index has been used in the evaluation process in the publication [44].

In a more recent article by Hasholt [45] scaling results are presented in relation to the total air content, specific surface, spacing factor and the total surface area of voids. The paper states that the total surface area of voids is as good as, or better, for indicating DISFS resistance than the spacing factor. The total surface area of voids is proportional to the total surface area multiplied with the specific surface area. The main difference between the spacing factor and the total surface area is explained as:

“The spacing factor expresses the likelihood that a capillary pore is located in the vicinity of an air void. The total surface area expresses the likelihood that the capillary pore is connected to an air void.”

This suggest that DISFS is more dependent on the connectivity between the the air void system and the capillary pore system than the shortest distances to air voids from different points inside the capillary pore system [45].

2.3.3 Alkalinity’s effect on the air voids

In the early publication [46] the following is stated:

“Because high concentrations of alkalis (Na^+ and K^+) in solutions such as are developed during the hydration of Portland cement strongly depresses the concentration of calcium in solution. It is expected that cements which provide an immediate high concentration of sodium or potassium ions in solution will cause production at air-water interfaces of precipitated films which are thinner and more soluble than those which would develop in the presence of low-alkali cements.”

In [46] results show that when $Na(OH)_2$ is added to the mixing water of a cement (to increase the Na_2O in the pore solution) the specific surface decreased, and the spacing factor increased for the air void system consistently for all (4) mixes. The paper conclude that the sodium hydroxide appears to decrease the probability for small air voids to form and be preserved in the fresh concrete.

It seems like the probability and possibility to create a large amount of small air voids (which contributes to frost resistance) increase when the pore solution in the fresh concrete contains a lower concentration of alkalis. Therefore, if the binder produces a high concentration of alkalis in the pore solution of the fresh concrete, the alkalis could contribute to an air void system with larger and fewer voids. However, different types of AEAs are affected by alkalis in various ways [47].

Another study [44] present a large study with two cements, three AEAs (sulfonated hydrocarbon, synthetic detergent, vinsol resin), two SPs (naphthalene, melamine) and two alkali boosters ($NaSO_4$, $Na(OH)_2$). Also, three different mixing procedures which are 10, 30 and 60 min long were tested. Some notable results are presented below.

For cement C1 (Na_2O-equivalent 0.4, LOI 2.8, limestone filler 4.5) the results indicate:

- When the C1 cement is mixed with the synthetic detergent (without an SP) the spacing factors increase as the mixing time increases, but when the $NaSO_4$ or $Na(OH)_2$ is added they are low (<200 µm) and seem stable as the mixing time increases.
- When the C1 cement is mixed with the vinsol resin the spacing factor is relatively low with each SP, and also when the $Na(OH)_2$ is added (174 to 286 µm). However, when $NaSO_4$ was added the spacing factor increase significantly (423 to 621 µm).
- The C1 cement mixed with the sulfonated hydrocarbon generally result in a very high spacing factor.

For cement C2 (Na_2O-equivalent 0.6, LOI 1.1, limestone filler 0.0) the results indicate:

- The C2 cement mixed with the synthetic detergent (SD) seems to result in low spacing factors with each SP, and there is relatively small changes in the spacing factor when the two different kinds of alkalis are added.
- When the sulfonated hydrocarbon or vinsol resin is used with C2 (without an SP) the concrete generally gets a higher spacing factor when the mixing time is prolonged.
- When SPs are added with the sulfonated hydrocarbon or the vinsol resin, the spacing factors remain low. However, prolonged mixing and agitation, as well as the addition of alkalis, generally increased the spacing factor.
    - There is one exception to this: vinsol resin combined with the melamine SP and the addition of $Na(OH)_2$ resulted in a low spacing factor even after prolonged agitation.

Dubovoy et al. published [47] which studied the interaction between the cement alkali level (0.21, 0.60, 1.20%) and different AEAs (salts of fatty acids, sulfonated hydrocarbons, alkylbenzyl-sulfonates, neutralized vinsol resin). Their results indicated that the AEA based on the fatty acids seemed to be unaffected by the prolonged agitation when the alkali content increased from 0.20 to 0.60. The air content only decreased slightly when the cement alkali level was 1.20. The results from the recipes containing vinsol resin seem to be more affected by the agitation when the cement alkali-level was 0.20 in comparison to when the alkali level was 0.60 or 1.20%. The AEA based on alkylbenzyl-sulfonates and sulfonated hydrocarbons seemed to be affected negatively by the agitation as well as the increased cement alkali level.

2.4 Interfacial transition zone

In the article by Scrivener et al. [48] they describe of the interfacial transitional zone (ITZ) and how it is created. The ITZ is a layer of paste around the aggregates that is known to be more porous than the bulk cement paste. The reason for it becoming more porous is due to “the wall effect” which contributes to that the closer you get to the aggregate surface the smaller the cement grains will be. This effect also infers that the creation of this zone depends on the sizes of the cement grains. The most significant change in the properties is the closest 15 to 20 µm from the aggregate when normal cement is used with cement grains from less than 1 up to 100 µm. The article makes it clear that this is a gradual transition and not a distinct zone. The wall effect also increase the effective water to cement ratio, which contributes to a more porous layer. One of the conclusions in the paper is that if smaller particles, such as silica fume, are added to the mix, the ITZ can be modified.

Silica fume is not used in this project. However, it can be good to note that the GGBFS used in this study has a larger fraction of small particles when compared to the SFA particles, which mean that the ITZ in the concrete containing SFA and GGBFS, which are tested, will most likely differ from each other. Considering that the ITZ zone is more porous this could suggest that the probability for ice nucleation to start there is most likely higher. At the same time, the tensile strength should naturally be lower in the ITZ that would make the probability higher for a crack to start from this zone and propagate from there. This zone may therefore have a significant impact on the mass of DISFS created.

The effect of three different types of aggregates effect on the ITZ, and how the mass of DISFS change depending on the different aggregates were studied in [49]. The three aggregates where carbonated steel slag aggregates, normal aggregates and crushed steel slag aggregates. They concluded that the properties of the ITZ change when changing between these three types of aggregates and the results regarding the properties of the ITZ have a strong correlation with the results from the D-ISTS tests. When changing from normal aggregates to carbonated steel aggregates the permeability seems to decrease, the hardness increase and the frost and DISFS resistance increase. The reason for these changes is believed to be that the high absorption of the carbonated steel aggregates contributes to a lower wbr in the ITZ around the aggregates. This means that the layer will become denser.

[50] present the variations in ITZ created when adding different fractions of LF and GGBFS. Both the LF and the GGBFS have slightly smaller particle size distributions in comparison to the cement they used. The results show that incorporation of LF and GGBFS contributes decreasing the porosity in the ITZ, decreasing the chloride migration coefficient and decreasing the sorptivity of the concrete.

2.5 DISFS methods

This section will give some basic information about standardized DISFS methods and some comparisons are made to show some difficulties of DISFS testing.

The standard freeze-thaw methods to test DISFS for a certain concrete is done by exposing the samples to a standardized preconditioning process and then use a standardized FTC while the concrete test surface is in contact with a certain salt solution. Since this is a very time consuming test, which is why researchers have been trying to find the properties strongest connected to the DISFS, which could enable a faster measurement of the DISFS resistance. However, the damage mechanism is complex and so far, no simple relationship has been found between the mass of DISFS and some material properties of concrete which would enable a prediction of the DISFS resistance.

MacInnis and Nathawad [51] came to the conclusion that it is doubtful if either absorptivity or permeability, by themselves, could ever be reliable indicators of the potential frost durability of concrete. In another paper [23], Sellevold and Farstad stated that the temperature and moisture history have a large impact on the DISFS and are also needed in addition to wbr, strength and air void structure before any prediction could be made regarding the DISFS of a concrete recipe.

2.5.1 Comparison between standard test methods

In Europe the CEN TS 12390-9:2006 is currently used which include the CDF method and the slab method. In USA and Canada (ASTM C672, MTO LS-412, BNQ NQ 2621-900) are used and ASTM C672 seems to be the most common. In a report by Hooton and Vassilev [52] they give a summarized comparison between the ASTM 672 and the BNQ NQ 2621-900. Here are some notable changes between these used in the North America and the ones used in Europe:

- ASTM C672 use a 4 mass% $CaCl_2$ solution.
    - BNQ-, CDF- and slab method use a 3 mass% NaCl solution.
- ASTM- and BNQ method tests a finished concrete surface.
    - A finished test surface will test the type of surfaces which are created from casting in the field and therefore much more dependent on the execution of the finishing procedure.
    - The slab method (and the one used in this study) use a sawed test surface. The sawed test surface result in a focus on the materials potential of DISFS by avoiding bleeding which can occur at the surface. However, this the results does not show the scaling for the first layer of a finished surface, which consist of a larger fraction of paste and small aggregates in comparison to the sawed test surface.
    - In the CDF method, the test surface is a mould surface, which has been created with a PTFE plate that has not been treated with any demoulding agent.
- Both the ASTM- and the BNQ methods measurements are made every fifth FTC (related to the workweek).
    - The slab-, and CDF method measures every 7th cycle. The CDF use an ultrasonic bath and the slab use a freezer.
- ASTM and BNQ precondition samples with 14 days in 100% RH and 14 days in 50% RH. After this the test begins for the ASTM test (28 days after casting) while the BNQ re-saturate the test surface for 7 days with a saline solution (35 days after casting).
    - The CDF- and slab method preconditioning begin with 1 day in mould, 6 days immersed in water.
        - The CDF conditioning continues (specimen age 7 days) with 21 days in a climate chamber with 20±2 °C and 65±5 % RH, and finally 7 days of

capillary suction with the 3 mass% NaCl solution at 20±2 °C before the test begins (35 days after casting).

- The slab method continues (specimen age 7 days) with 14 days in a climate chamber with 20±2 °C and 65±5 % RH, then (specimen age 21 days) the specimens are sawed and directly returned to the climate chamber for 7 more days. Finally, (specimen age 28 days) de-ionised water is poured onto the surface for re-saturation for 3 days ±2 hours at 20±2 °C before the test begins (31 days after casting).

Considering the mentioned standard methods the following points should be emphasized. The specimen's age, time for hydration, time for dehydration and carbonation varies between the methods when the test is started. Table 3 present a comparison between the amount of days each method expose the samples test surfaces to favourable hydration conditions and favourable dehydration and carbonation conditions.

Table 3. Comparison between standard DISFS methods.

	Slab	CDF	ASTM 672	BNQ
Hydration[1)]	7+14+3=24	7+7=14	14	14+7=21
Dehydration and carbonation[2)]	7	21	14	14

[1)] Test surface exposed to favourable hydration conditions, i.e. sealed, in contact with water or in room with 100% RH.

[2)] Test surface exposed to air with 20 °C and 50 to 70% RH (which is favourable for carbonation) and about , 0.04% CO_2, which are regular CO_2 levels in the atmosphere.

With all these variations and the fact that the moisture history affects the mass of DISFS, the masses of DISFS cannot directly be compared between the various methods. This is in accordance with the differences in acceptable masses of DISFS each standard have. However, they seem to be conservative, which means that some concrete fail according to the test methods even though the performance in field seems acceptable [53]. One reason for this could be that the concrete containing SFA or GGBFS have a slower hydration processes and a disadvantage when testing at a young age according to the standards. Also (assuming the same degree of hydration) other properties differ in comparison to concrete containing 100% CEM I such as permeability. This means that the dehydration and carbonation will affect the concrete in different ways during the set number of days for dehydration and carbonation according to the standard methods which also will lead to different amounts of scaling.

2.6 Scaling resistance in concrete containing OPC

Most research regarding the DISFS mechanism(s) have been made on concrete containing 100% OPC. In addition to this, almost all studies on concrete that contain OPC blended with a fraction of FA or GGBFS also include at least one control recipe with 100% OPC as the binder. This means that information about concrete containing 100% OPC can be found in almost all articles regarding the DISFS mentioned in this literature study.

Early studies showed that a concrete containing 100% OPC have a high DISFS resistance when an AEA have been used which produce an air void system with a large amount of small air voids. However, as mentioned in Chapter 2.3.4 some AEAs are sensitive to the fraction of soluble alkalis present in the pore solution. Therefore, some types of OPC perform poorly with high soluble alkali content in the pore solution of the fresh paste.

2.7 Scaling resistance in concrete containing fly ash (FA)

In this section, short summaries are presented of articles that present results tested the DISFS of concrete containing fly ash.

2.7.1 Summaries of studies on DISFS on concrete containing FA

In a study by Pigeon M. et al. [54], 2 types of cement and 1 type of SFA (52.7 % SiO_2 and 12.5% CaO) was studied. SEM measurement revealed a porous trowelled surface layer which seemed to increase when SFA was included. They concluded that the fly ash used tend to increase the bleeding which reduce the water/cement ratio at the surface. Sawed test surfaces were also tested with a slightly modified ASTM C672 method. The concrete containing 40 mass% fly ash had approximately 1 kg/m² (which is almost satisfactory) while 20 mass% fly ash and 100% OPC recipes had very low scaling.

In a study by Bilodeau A. and Malhotra V.M. [55], three different wbr (0.35, 0.45, 0.55) were tested according to ASTM C672 where 0, 20, or 30 mass% of the total binder content was replaced with SFA. The air contents in the fresh concrete was 6.5±0.5% and spacing factors was approximately 144 to 220 µm and a specific surface of 16 to 25 mm^{-1}. They also tested three wbr (0.27, 0.31, 0.39) with 0 or 58 mass% of SFAs where three different fly ashes were used (one type per cast). The air content in the fresh concrete of approximately 5.0±0.5% and a spacing factor of 167 to 286 µm. Moist curing conditions (for 3, 7 or 14 days) were followed by various periods of drying (3, 4, 5 or 6 weeks) before the salt frost test began. The results showed that the concrete containing up to 30 mass% SFA had an acceptable mass of DISFS and the scaling generally increased with increasing fraction of SFA. The mass of scaling was lower for concrete that had been cured with a membrane compared to moist cured and the scaling was generally reduced with a lower wbr. All concrete containing 58 mass% of one of the three types of fly ashes all performed poorly despite the low wbr.

In a study by Marchand J. et al. [56] they investigate if the fly ash only acts as inert grains after 14 or 28 days and if the fly ash affects the pore solution in a way which modifies the ice formation process. One type of cement with three types of more or less SFA (32.45, 46.25 and 52.68 % SiO_2) was used. Thermogravimetric analysis was made together with measurements on the evaporable water content, MIP, low temperature calorimetry and DISFS test according to ASTM C672. The thermogravimetric analysis showed that fly ash increased the non-evaporable water content which lead to the conclusion that fly ash does not act as an inert filler during the early hydration (after 1 and 14 days). The MIP results indicate that 40 mass% fly ash increased the fraction of pores in the range of 0.06 to 0.009 µm. The low temperature calorimetry showed approximately the same freezable water content for OPC and 20 mass% SFA. The recipe with 40 mass% SFA had slightly higher freezable water content at -20 °C.

In an article written by Thomas M.D.A. [57], he presents a summary of previous studies made on DISFS resistance of concrete containing siliceous and calcareous fly ashes and present results from field performances compared with laboratory testing with ASTM C671 on the same material. Results from the laboratory are presented elsewhere, however, the main point of the article is to emphasize that there is a difference between the laboratory results and the field performance.

In a study by Bilodeau et al. [58], one type of OPC was used with one type of SFA (56.96% SiO_2, 1.44% CaO) during this study. Concrete was made with 0, 25, 35 and 58 mass% FA and the wbr was 0.32, 0.35, 0.40 and 0.45. All of the recipes included an AEA and some also contained an SP. According to the air void analysis, the spacing factors were between 106 and 179 µm. These are generally is considered to be favourable air void systems which should contribute to increase the DISFS resistance of the concrete. This is a comprehensive study where many factors are tested, which enables interesting comparisons. Four major things are discussed in the article. The effect from various durations of moist curing, various duration of air, surfaces cast vertically vs horizontally, and the effect from curing compounds. The results show that an extended moist curing, from 14 to either 28 or 56 days, does not contribute to a decrease in the mass of DISFS concrete containing 25 or 35 mass% SFA with wbr of 0.40. Concrete containing 25 and 35 mass% SFA preconditioned with 14 days of moist curing and 14 days of drying resulted in an acceptable mass of scaling. When the moist curing was 14 days and air drying was 0 days the scaling was low for casts with 100% OPC and 25 mass% SFA, however, when the air drying increased to 4 and 14 days the DISFS increased for both casts. Curing compounds decreased the DISFS significantly for all recipes when compared to 14 days of moist curing. For concrete containing 0, 25 and 35 mass% SFA the scaling was close to 0, but for the casts with 58 mass% SFA there was still significant DISFS although reduced. The samples with curing compounds hydrated for 14 days with the compounds and then the compounds were removed by “vigorous brushing”, then the test surface were dried for 14 days. This could suggest that any bleeding effect on the surface of samples with the compounds would be brushed off while the samples with 14 days of moist curing might have had some bleeding on the surface.

In a study by Zhang M.H. et al. [59], two OPC, two SFAs (49.48 and 56.96 % SiO_2) and one calcareous FA (33.90 SiO_2 and 28.24 CaO) was used. The wbr used for the recipes was 0.32, 0.35, 0.40 and 0.45 and the replacement of fly ash was 0, 25, 35 and 58 mass%. All recipes included an AEA and some also an SP. Several things can be concluded from the (ASTM C672) results, some of which are that the type of SFA, the mass% replacement of fly ash used and also the wbr clearly had an impact on the mass of DISFS. Another general trend regarding the results was that when the mass% of SFA increase and/or the wbr increase, the mass of DISFS generally increase. However, there was one notable exception for one of the SFA where the cast with wbr 0.35 resulted in a scaling around 1 kg/m² while the cast with wbr 0.40 resulted in approximately 0.5 kg/m² after 50 FTC. Curing compounds, applied after bleeding had stopped and brushed off after 14 days, almost removed the mass of DISFS completely for recipes with wbr 0.40 and 0.45 where 25 mass% consisted of SFA. However, for the same SFA with wbr 0.32 and 58 mass% replacement the scaling was still significant, even though it had been reduced. The casts with a large mass of DISFS generally scaled the most between the fifth and tenth cycle, and the casts with least scaling had some scaling in the beginning then it seemed to stop, which is similar to results from the slab method [60]. The results indicate that mass of scaling for moist cured concrete seems to be related to mass of water absorption, increasing water absorption increase the mass of scaling. However, concrete hydrated with curing compound result in more water absorption than moist-cured concrete and at the same time a decrease in mass of DISFS. Backscattered electron images (BEI) after 28 days show a porous transitional zone around the fly ash particles and another BEI after 180 days show a significant densification of the transition zone. The microstructure after 180 days is described as more unified and the hydration and reaction products in general are more evenly distributed in the system when comparing to the 28 days images.

In a study by Baert G. et al. [61], wbr was kept constant at 0.30 and the FA replacement was 0, 10, 40, 60 mass% of binder. Results from the DISFS test, according to the NTN 018 (1998) standard made with 90 days old specimens, show that there is almost no scaling for 0 and 10 mass% replacement while 40 and 60 mass% have a significant mass of DISFS (ca 2.6 and 3.4 kg/m² respectively). At the same time the concrete containing 10 and 40 mass% FA had a chloride diffusion coefficient of 1.39 and $1.43 \cdot 10^{-12}$ m/s while 0 and 60% had a chloride diffusion coefficient of 2.76 and $2.61 \cdot 10^{-12}$ m/s. This means that the chloride diffusion coefficient does not correlate with the mass of DISFS according to their results. Results from an accelerated carbonation test in 10 % CO_2 the carbonation seemed to be relatively low up to 40 mass% while the depth increased significantly from 40 to 60 mass% FA.

Marchand J. et al. [62], reviewed nine papers are on laboratory studies which showed an unacceptable DISFS resistance in concrete containing fly ash and three papers on field studies which show satisfactory performance of concrete containing fly ash exposed to severe conditions. Samples cast and finished on site but moist cured in the laboratory, performed worse than cores extracted from the sidewalk at 60 days. “Lab specimens” had a scaling between 1.07 and 4.28 kg/m² and the “field cores” had a scaling between 0.03 to 0.52 kg/m². Three different fly ashes was tested ((49.60 + 14.91), (40.98 + 28.07), (50.06 + 2.75) of (SiO_2 + CaO)-content), with a set wbr of 0.40, and 20 mass% fly ash replacement. Air void analysis showed that the spacing factors was from 125 to 188 µm and measurements on the air content in fresh concrete between was 5.5 to 6.5 vol%. The results showed that specimens cured in the laboratory, where the test started at age 28 + 14 days (since 14 days of re-saturation with water was added to the ASTM C672 preconditioning procedure), had consistently more DISFS after 60 FTC in comparison to the field cores. The field cores were taken 60 days after casting and resaturated 14 days before the test began. The authors believe that the specimens cured in plastic forms in the laboratory had more bleeding in comparison to the field samples exposed to natural conditions. The results show an obvious difference between the samples with the two different processes for preconditioning the test surfaces.

In a study by Bouzoubaa et al. [63] they tested one CEM I and one SFA with either 25 or 35 mass% replacement of the binder, wbr 0.45 and approximately 400 kg/m² bc. The concrete was tested according to the ASTM- and BNQ test. All recipes included AEA and a water reducer (similar to SP). Fly ash concrete failed the ASTM test but generally performed satisfactorily according to the BNQ test. Results are also presented regarding the reproducibility between seven different laboratories when the BNQ method was used. These DISFS results varied between 0.17 and 0.94 kg/m² for 35 mass% SFA, and from 0.10 to 0.73

kg/m² for 25 mass% SFA. According the BNQ standard the limit for passing is 0.5 kg/m², which meant that two out of seven of 35 mass% SFA failed and one out of seven failed of the 25 mass% SFA. The ASTM test failed both concrete recipes containing SFA and according to the comments of the field test (a sidewalk exposed to four winters) the surface clearly had been affected by DISFS however in the concluding remarks it was deemed “acceptable”. One of the conclusions was that the BNQ test method, which results in lower mass of DISFS, gave a slightly better prediction of the DISFS resistance for field exposure.

In a study by Nili M. and Zaheri M. [64] two basic recipes were tested, first with wbr 0.36 and binder content 300 kg/m³ and second with wbr 0.43 and binder content 250 kg/m³. In both recipes 20 mass% of the binder was replaced with SFA and tested according to ASTM C672 with two different FTC. One cycle consist of 18 hours in -18 °C and 6 hours in 23 °C and the other consist of 6 hours in -18 °C and 18 hours in 23 °C. A water reducer was used without any air entraining agent. The results showed that the cycle with the longest freezing time (longer exposure to minimum temperature) consistently produced the largest mass of scaling for all recipes. The recipe with 20 mass% SFA had consistently larger mass of scaling in comparison to the reference with 100% OPC.

In a study by Sun C. et al. [65] one OPC was used with one fly ash and four factors were changed in the recipes, wbr, bc, FA replacement fraction and air content. Three casts was made with 30 mass% FA and ca 5 vol% air content with wbr 0.35 (514 kg/m³), 0.42 (429 kg/m³), 0.50 (360 kg/m³). Four casts was made with 429 kg/m³ bc and ca 5 vol% air content where the FA replacement fraction was 0, 10, 30 and 50 mass%. Three casts was made with 429 kg/m³ bc and 30 mass% FA placement fraction where the air content was 3.8, 4.8 and 5.8 vol%. The DISFS test seems to resemble the cube method where the specimen is submerged in a 3.5 mass% NaCl solution. The FTC used is 2-4 hours and the core temperature of specimen’s cycle between -17±2 °C and 8±2 °C. The results showed increased mass of DISFS when increasing the wbr at the same time as the binder content was reduced when 30 mass% of the binder was replaced with FA. The mass of DISFS increase when the fraction of FA replacement increased.

In a study by Ahani R.M. and Nokken M.R. [66] one OPC and one SFA was included where the wbr was 0.40 with 400 kg/m³ binder content and 25 mass% was replaced with SFA. All recipes included AEA to reach 6±1 vol% air content measured in the fresh paste. The ASTM C672 method was used with four versions of preconditioning the samples before the DISFS test begins. First was the standard procedure, 1 day in a mould, 13 days of moist curing, followed by 14 days of dehydration in +23±2 °C. Second procedure tested was 1 day in a mould, 2 days of moist curing followed by 25 days of dehydration in +23±2 °C. The third procedure tested was 14 days moist curing, 14 days in air, followed by 7 days where the test surface was covered with a 4 mass% $CaCl_2$ solution (which is used in ASTM C672 during the FTC). Forth version tested was 20 to 24 h hydration in a mould followed by 27 days of hydration with a curing compound before the DISFS test began according to ASTM C672. The fly ash recipe produced around 1 kg/m² for the standard procedure. The second and third procedures seemed to increase the mass of DISFS slightly and the forth seemed to contribute with the most scaling. However, previous articles mentioned in this chapter that tested curing compounds usually brush the curing compound off before the DISFS test began. In this article, the curing compound was not brushed off before the test began which is most likely the significant difference for the large mass of DISFS. However, the curing compound resulted in the least mass of DISFS for the concrete with 100 % OPC. This could suggest that the adhesion between the curing compound and the concrete is important, and that a more favourable adhesion was created for the concrete containing OPC in comparison to adhesion created for the concrete that contained SFA.

In a study by Nowak-Michta A. [67] two concrete recipes was tested according to the slab method where the wbr and bc was 0.38 and 450 kg/m³ for the first, and 0.45 and 400 kg/m³ for the second. All recipes contained a SP and an AEA (except one additional control recipe that excluded the AEA). The binder content was replaced with 0, 20, and 35 and 50 mass% of three similar SFAs. The main difference between these SFAs was the loss on ignition (LOI) which were 1.9, 5.1 and 9.0 mass%. The recipes with wbr 0.38 had a mass of scaling between 0.99 down to 0.05, which is rated “acceptable” to “very good” according to SS137244, while all recipes containing fly ash with wbr 0.45 had unacceptable masses of scaling. The recipes with wbr 0.45 with 35 and 50 mass% fly ash seemed to indicate that the increase in LOI contributed to an increase in DISFS. However, the recipes with wbr 0.38 did not seem to be affected to a large extent by the difference in LOI. The recipe with wbr 0.38 and 20 or 35 mass% of SFA with 9.0 mass% LOI resulted in 0.15 kg/m² scaling which is considered “good” according to the standard. It was concluded that the wbr have a significant impact on the DISFS, and when the wbr is 0.45 the LOI also have a significant impact. AEA had a large impact on concrete with OPC. When the wbr was 0.38 and the AEA was excluded the OPC was not DISFS resistant, while the same concrete with AEA was DISFS resistant. Also, the OPC concrete with AEA and wbr 0.45 was DISFS resistant. However, the AEA did not have the same effect for concrete containing fly ash when the wbr is 0.45.

In a study by Van den Heede P. et al. [68] they included one CEM I and two SFAs where six casts where made, three with AEA and three without. The two recipes with 100% CEM I with and without AEA had bc 340 kg/m³. The four recipes that contained SFA, with and without AEA, had bc 450 kg/m³ and 50 mass% SFA. All recipes included a polycarboxylic ether-based SP. For the OPC concrete without AEA the scaling increased slightly when comparing 28 with 91 days of hydration, but for the OPC with AEA the scaling was reduced when comparing 28 days and 1.5 years of hydration. For the concrete containing SFA the scaling consistently increased with increasing age which is believed to be because of the negative effect carbonation has on concrete with SFA (while it has a positive effect on concrete with OPC containing AEA).

2.7.2 Notable findings regarding DISFS in concrete containing FA

The list below is a summary of notable findings and trends that previous studies have found on the DISFS of concrete containing FA.

- The mass of DISFS increases as the mass of fly ash and replacement fraction of the total binder content increase [55, 56, 58, 59, 61, 63, 65, 67].

- The mass of DISFS increases as the wbr increase [55, 59, 64, 65, 67].
- Some studies present results indicating that curing compounds decreases the mass of DISFS [55, 58, 59, 62, 69] and all studies brushed off the curing compound before testing started. Ahani and Nokken [66] present results showing an increase in DISFS for concrete with fly ash when using curing compound, however, the curing compound was not brushed off in this study.
- The agreement between the results from the standard DISFS methods and field tests is somewhat lacking [62, 63, 69].
- The mass of DISFS increases as the degree of hydration decreases for concrete with CEM I [2, 70] and CEM I blended with fly ash [62, 63, 71] with wbr 0.45.
- The mass of DISFS increases when binder content decreases [64, 65].
- The bleeding (water separation in the paste) seems to increase when fly ash is used in the mix. This means that the effective wbr of the concrete surface increases which increase the autogenous shrinkage and this leads to an increases in the mass of DISFS [54].
- An increasing loss on ignition (fraction of unburnt carbon in fly ash) increases the DISFS for wbr 0.45 [67].

2.8 Scaling resistance in concrete containing GGBFS

In this section short summaries are presented of articles that present results tested the DISFS of concrete containing slag.

2.8.1 Summaries of studies on DISFS on concrete containing GGBFS

In a study by Fagerlund G. [72] one CEM I and one type of GGBFS was tested where the replacement fraction was 15, 40 and 65 mass% of the binder with wbr 0.431 to 0.451 and bc 380 to 425 kg/m³. Casts were made with and without air entrainment, which then were subjected to a DISFS test with an upside down sample setup where sawed surfaces were tested. The samples hydrated for 7 months, then dried at 50 °C (most likely low RH and therefore low carbonation) for one week to simulate some aging and put in to water for one week of re-saturation before the DISFS test began. Additionally a comparison was made between samples cut from the top of the concrete cylinders with samples cut from the bottom. The results indicate that an increased fraction of GGBFS decrease the mass of DISFS, and the air content seemed to generally reduce the mass of DISFS however the effect was small for concrete with 60 mass% GGBFS. The bottom sample generally seemed to have lower mass of DISFS than the top sample for concrete with a large mass of scaling. This could indicate e.g. a segregation of air voids or slightly more bleeding in the top of the cylinders created by the vibration procedure. The concrete with OPC resulted in a large mass of scaling even then the AEA had been used to produce low spacing factors between 90 and 150 µm. (However, this could be explained by the fact that the surface was probably not carbonated, which then agrees with results presented in the third article.)

In a study by Afrani I. and Rogers C. [73] two OPCs and one type of GGBFS was tested where the replacement fraction was 25 and 50 mass% of the binder with wbr 0.38 and 0.39 and bc 415 kg/m³. Three different preconditioning processes were used. The first was 14 days in a moist room and then 14 days in ambient laboratory air. The second was 14 days outdoors (temperatures between -4 and +26 °C) covered under wet burlap and plastic sheet and then 14 days in ambient laboratory air. The third was 28 days in laboratory air after curing compound had been applied (curing compound was left on the surface). The DISFS results showed that the concrete with 50 mass% GGBFS passed the acceptable scaling limit. The samples preconditioned 14 days in a moist room was slightly above 1 kg/m², the wet burlap samples had just below 2 kg/m² and the samples with curing compound had just above 3 kg/m² after 50 FTC. The concrete with 0 or 25 mass% had 0.54 kg/m² accumulated DISFS or lower, after 50 FTC for all preconditioning processes.

In a study by Bilodeau A. and Malhotra V.M. [55], two OPCs and three GGBFS are tested where the replacement fraction was 25 and 50 mass% of the binder with wbr 0.55 and bc 264 to 275 kg/m³. An AEA based on sulfonated hydrocarbon was used in all mixtures and produced 6.1 to 6.9 vol% air contents according to measurements in the fresh concrete and spacing factors from 98 to 141 µm. The preconditioning was 14 days moist curing and 14 days curing in 50% RH and 23±1.7 °C for the concrete with 50 mass% GGBFS and 14 days moist curing and 49 days curing in 50% RH and 23±1.7 °C for the concrete with 25 mass% GGBFS (due to break down of freezing equipment). The results show that increased fraction of GGBFS increase the mass of DISFS. The largest mass of scaling generally comes from the first five FTC of scaling for the concrete casts containing GGBFS. There also seems to be a small difference between the three types of GGBFS.

In a study by Hooton R.D. and Boyd A. [4] they included one OPC and one type of GGBFS where the replacement fraction was 25, 30, 35 and 40 mass% of the binder with wbr 0.45 and the bc 375 kg/m³. Three tests were made, first six different finishing procedures was tested, then six different preconditioning procedures were tested and thirdly the fineness of the GGBFS was varied together with the air content. For the preconditioning procedures, the mould was stripped after 1 or 4 days with form temperature at 25 or 50 °C (heated with infrared lamp) for the first 8 hours to simulate a hot summer day. One of the procedures was 14 days moist curing and 14 days in air (ASTM procedure). The ASTM procedure clearly produced the lowest mass of DISFS while the others scaled significantly more. When the temperature of the first 8 hours increased, the scaling generally increased. Regarding the fineness of the GGBFS the mass of DISFS decreased when the fineness increased from 432 to 499 m²/kg. For concrete with 25 mass% GGBFS the scaling increased slightly when the air content was increased from 6.3 to 7.6 and from 7.6 to 9.2 for both types of fineness. For concrete with 35 mass% GGBFS the scaling decreased slightly when the air content was increased from 6.2 to 7.6 and from 7.6 to 9.1 for both types of fineness. Additionally field trials was also made with concrete containing 25, 35 and 50 mass% GGBFS with wbr 0.42. Three laboratories tested these field samples where the results varied, however, 25 and 35 mass% GGBFS generally was fine while 50 mass% GGBFS failed. These results made Hooton and Boyd question the severity of the ASTM C672 method.

In a study by Stark J. and Ludwig H.-M. [74] an analysis is given regarding how the carbonation influence the mass of DISFS in concrete containing 60 mass% GGBFS. They conclude that the surface becomes more porous and the carbonates that are present after the carbonation contribute to the large mass of DISFS during the initial FTC (#0 to #4) compared to the ones that come later. The DISFS results clearly show a larger mass of scaling after the first few FTC, which is generally how DISFS results appear when tested with the slab method. This paper is an extended version of the paper [75].

In a study by Deja J. [76] tested a CEM III/A (57 mass% GGBFS) with and without a SP and AEA combination. The results show a decrease in DISFS from 10.5 kg/m² after 14 FTC to 1.1 kg/m² after 50 FTC when decreasing the wbr from 0.58 to 0.51 and at the same time increase the air from 1 to 6 vol%. In addition to this, the influence of polypropylene fibres was also tested, which also seemed to decrease the mass of DISFS (from 1.1 to 0.7 kg/m² after 50 FTC).

The PhD thesis written by Utgenannt P. [70] investigates what effect carbonation has on the DISFS on concrete containing GGBFS. There are several tests presented which is why only a few will be mentioned here. In chapter 3.5.3.4 of the thesis, results are presented from testing “micro concrete” with a maximum aggregate size of 8 mm, wbr 0.45 and replacement fractions of 20, 35, 65% GGBFS with bc 444.5, 452.0 and 444 kg/m³ (no AEA nor SP) together with a reference with 100% OPC and bc 448 kg/m³ with AEA (no SP). Air content of 13-14% in the paste was required to get approximately 0.2 mm spacing factor. In addition to the material variations, three preconditioning procedures were also tested. The first one was hydrated one day in the mould, and then cured in water until one day before the DISFS test began when it was taken out from the water, and finally is was sawed and prepared half an hour before the test began (no re-saturation before the test). The second procedure was one day in mould, and then cured in water until eleven days before the DISFS test began when it was removed from the water. Ten days before the test began the samples were sawn and put in a climate chamber with 20 °C, 65% RH and 0% CO_2, three days before the DISFS test began the surface was covered with de-ionized water for re-saturation. The third procedure is the same as the second procedure with the difference that the climate chamber has 1 vol% CO_2, which means there will be an accelerated carbonation. The results clearly show that carbonation significantly decrease the mass of DISFS in the recipes containing 0, 20 and 35 mass% GGBFS. Additionally it can be seen that for air entrained concrete containing 100% CEM I with wbr 0.35, 0.45 and 0.55, which have not been exposed to carbonation, the mass of DISFS increase when the wbr increase. However, all of these samples have a large mass of scaling, wbr 0.35 have around 2 kg/m², after 56 FTC. Then these noncarbonated samples can be compared to those exposed to carbonation (with 1% CO_2). The carbonated concrete with wbr 0.55 (with AEA) have approximately 0.5 kg/m² accumulated scaling after 56 FTC, which is significantly lower than the noncarbonated concrete with wbr 0.35. With consideration to some tests on the effect of hydration and drying before the DISFS test began one notable quote is:

“Although the effect of carbonation was different for materials with different binder types/combinations, it was found to be so strong that the other ageing effects were more or less insignificant in comparison, at least for older concrete (over 30 days of age).” (p. 322)

In a study, by Lang E. [77], binder combinations containing 25+10 mass% GGBFS+LF and concrete containing 35 mass% GGBFS has been tested according to the CDF method. According to the results the recipes containing both GGBFS and LF has a larger mass of DISFS in comparison to the concrete containing 35 mass% GGBFS after 28 FTC. However, all recipes have lower mass of DISFS than the acceptance limit of 1.5 kg/m² after 28 FTC. (The results from concrete containing 25+10 mass% GGBFS+LF is not presented.)

In a study by Marchand J. et al. [62] one type of OPC was used together with one type of GGBFS where the replacement fraction was 25 mass%, the wbr 0.40, bc 400 kg/m³. In addition to this, all recipes contained a water reducer, AEA and a retarder. The retarder was needed since all casts (6 m³/cast) where made in a concrete plant and transported by trucks to the site. The ASTM C672 freeze-thaw method was used, however, the preconditioning process varied. Samples that were cast and finished on site, and preconditioned in the laboratory (14 days moist curing and 14 days dehydration), was compared to samples extracted from the site after 60 days. The results show that the field cores from each cast had 0.31 and 0.09 kg/m² DISFS after 50 FTC (acceptable mass of scaling), while the samples cured in the lab from same casts had 1.68 and 2.19 kg/m² respectively. It is mentioned that the main reason for this could be due to more bleeding from the laboratory samples due to the plastic moulds contributing to more bleeding in comparison to the field samples. In any case, it shows a contrast between field and laboratory results on the same concrete.

In a study by Krishnan A. [78], results are presented from DISFS test according to ASTM C672 from a CEM I and a binder which contain 30 mass% GGBFS, with the wbr 0.44 and bc 305 kg/m³. These were tested with two different types of preconditioning procedures. One of these were 14 days moist curing and 14 days drying in 20 °C and 50% RH. The second procedure involved 3 days of moist curing and 3 days of drying in 20 °C and 50% RH. The results from this test was that the CEM I had a low mass of DISFS after both of these preconditioning processes while the concrete containing GGBFS had approximately 1.6 kg/m² after the 6 days procedure and approximately 0.3 kg/m² after the standard procedure. The scaling almost exclusively occurred during the first 5 FTC for the GGBFS concrete.

In a study by Boyd A.J. and Hooton R.D. [79] three blended binders are included with a CEM I and GGBFS where the replacement fraction was 25, 35 and 50 mass% with wbr 0.42 and bc 355 kg/m³. Both laboratory and field preconditioning processes was tested for the DISFS tests, the laboratory was according to the standard MTO LS-412 (14 days moist curing and 14 days dehydration), the field samples were subjected to 127 days in the outdoor climate (with either burlap and plastic or a curing compound during the early hydration) before the DISFS test. The results from lab showed consistently larger mass of DISFS from all samples in comparison to the field samples. The laboratory concrete specimens containing 25 mass% GGBFS had 0.60 and 0.52 kg/m² after 50 FTC while the field specimens had 0.14 kg/m² or lower. The laboratory concrete specimens containing 35 mass% GGBFS had 0.50 and 1.24

kg/m² after 50 FTC while the field specimens had 0.15 kg/m² or lower. The laboratory concrete specimens containing 50 mass% GGBFS had 1.60, 2.02 and 1.44 kg/m² after 50 FTC while the field specimens had 1.28 kg/m² or lower. These results show the importance of preconditioning of the concrete test surface before the DISFS test. Pull off tests were also made, however, there did not seem to be any correlation when considering the concrete specimens containing FA that had high strength and large mass of scaling.

In a study by Panesar D.K. and Chidiac S.E. [80] a statistical analysis was made on results from seven different publications some of which have been mentioned earlier. Some of the conclusions were that the wbr and OPC/binder ratios are controlling variables, as well as if the surface is formed or have been finished. In addition to this, mass of DISFS increase as the OPC/binder decrease for concrete containing GGBFS, and air entrainment does not seem to be a controlling variable to the DISFS on a finished surface. The analysis also indicates that NaCl- and $CaCl_2$ solutions will result in different masses of scaling for the same concrete during a DISFS test.

In a study by Chidiac S.E. and Panesar D.K. [81] tests of mechanical properties was made with DISFS tests. Measurements of the strength show that the 28 days compressive strength is equivalent or higher for concrete with wbr 0.31 and 0.38 containing 20, 25, 40, 50 or 60 mass% GGBFS than concrete with a 100% OPC binder with the same binder content. Additionally, the 28 days compressive strength is generally higher for the concrete with wbr 0.38, which could be explained by an increased degree of hydration in comparison to the concrete with wbr 0.31. Considering the DISFS results presented in the article it is considered slightly strange that the mass of DISFS from concrete with wbr 0.38, containing 100% CEM I or 20 mass% GGBFS, increase when the age of the concrete increase from 120 days to 2 years. Otherwise, the DISFS seems to be as one could expect where the mass of DISFS increase when the wbr increase from 0.31 to 0.38 for all recipes, and the scaling decrease when the time for hydration increase from 120 days to 2 years for concrete containing 40, 50 and 60 mass% GGBFS. Also, the mass of DISFS increase when the OPC/binder decrease for concrete, with wbr 0.31 and 0.38, hydrated for 28 and 120 days respectively.

In a study by Giergiczny Z. et al. [82] three types of binders was tested where the replacement fraction was 0, 30 and 57 mass% GGBFS (wbr 0.44, bc 350 kg/m³) and all recipes contained an SP and an AEA (each binder was given a separate AEA). The names of the binders according to the European standard is CEM I 42.5R, CEM II/B-S 42.5N and CEM III/A 42.5N-HSR/NA. The slab method was used for the DISFS test. The article compares scaling results in relation to measurements of the air void system on the fresh concrete (with the pressure method and with an Air void analyser) and also on hardened concrete (with linear traverse, standard method PN-EN 480-11). A conclusion is drawn that the slag corrupts the air void system. However, another explanation could be that the combination of SP and AEA contributed to bleeding for the binders containing GGBFS. The pressure method resulted in approximately the same air void content for the three recipes with the three different binders. However, when looking at the results from the linear traverse measurements the scaling results are expected. According to the linear traverse, the air content is lower, the spacing factor is higher and the specific surface is smaller for the slag mixes. Therefore, the increase in mass of DISFS, in comparison to the OPC reference cement without slag should follow (which it did). However, the binder containing 57 mass% GGBFS only got approximately 0.8 kg/m² DISFS after 56 FTC which is an acceptable mass according to the standard. This show additional evidence of the importance when choosing a combination of SP and AEA to make sure they work well together. When a combination is found for a certain binder, the mass of added AEA to acquire specific air contents in the concrete should be tested first. When the air void systems are comparable, then it could be possible to think about how the scaling results could be compared.

In a study by Panesar D.K. and Chidiac S.E. [83], one type of OPC and one type of GGBFS are used to cast concrete with wbr 0.31 or 0.38, and bc 360 or 450 kg/m³. The MSO LS-412 DISFS test was used on concrete containing 0, 25, 40, 50 and 60 mass% GGBFS. The casts with wbr 0.31 hydrated for 28 days before the DISFS test began and the casts with wbr 0.38 hydrated for 2 years before the DISFS test began. The mass of DISFS from recipes containing 0, 25 and 60 mass% GGBFS differs to a large extent between the 0.31 and 0.38 in comparison the recipes containing 40 and 50 mass% GGBFS. When comparing the mass of DISFS between the concrete with wbr 0.31 there is an increase when the fraction of GGBFS increase. The results from recipes with wbr 0.38 which have hydrated for 2 years show lowest mass of DISFS for 40 mass% GGBFS, then 25 and 50 mass% while 0 and 60 mass% have the largest mass of scaling. The mass of DISFS result for the concrete containing 0% GGBFS (100% OPC) with wbr 0.38 seems large, however, when considering the “Freeze-thaw salt scaling resistance factor” (which is introduced in the article) the scaling is more or less expected. The “Freeze-thaw salt scaling resistance factor” is dependent on the ionic sorptivity and tensile strength of the concrete.

In a study by Ahani R.M. and Nokken M.R. [66] one OPC and one GGBFS is included where the wbr was 0.40 with 400 kg/m³ binder content and 35 mass% was replaced with GGBFS. All recipes included an SP and an AEA. The ASTM C672 method was used with four versions of preconditioning the samples before the DISFS test begins. First procedure was 1 day in a mould, 13 days of moist curing, followed by 14 days of dehydration in +23±2 °C. The second procedure tested was 1 day in a mould, 2 days of moist curing followed by 25 days of dehydration in +23±2 °C. The third procedure tested was the 14 days moist curing and 14 days in air followed by 7 days where the test surface was covered with a 4 mass% $CaCl_2$ solution (which is used in ASTM C672 during the FTC). Forth version tested was 20 to 24 h hydration in a mould followed by 27 days of hydration with a curing compound before the DISFS test began according to ASTM C672. The GGBFS recipe accumulated around 0.30 kg/m² after 50 days for the standard procedure and approximately 0.45 kg/m² for the three day curing procedure and when the curing compound was used. The procedure with preconditioning the surface with a $CaCl_2$ solution accumulated around 0.15 kg/m² after 50 days. In this article the curing compound was not brushed off before the test began, which suggest that this curing compound works well with a concrete containing 35 mass% GGBFS. It is noticeable that the 14 days moist- and 14 days air curing procedure results in the largest mass of DISFS after the first 5 FTC, then the mass of DISFS is clearly less. The three days curing and curing compound seemed to start of in a linear curve and then accelerate while the procedure with the $CaCl_2$ preconditioning during one week resulted in a linear progression of the DISFS.

In a study by Schlorholtz S. and Hooton R.D. [84] bridge decks are analysed. Thereafter a follow up study was made by Hooton D.R. and Vassilev D. [52] where two types of OPC was used together with two types of GGBFS where concrete casts where made which contained 0, 20, 35 and 50 mass% GGBFS with wbr 0.42 and bc 338 kg/m^3. Three types of standard DISFS test methods where used together with each preconditioning procedure, which is included in the standards. These three was the ASTM C672, BNQ and VADOT. From this test matrix (along with complementary tests) they conclude that there was no direct relationship between the DISFS and the compressive strength or the charge passed through concrete. The results indicated a relationship between increasing fractions of slag with an increasing mass of DISFS. The bulk mass of the DISFS was accumulated during the first 15 FTC then the DISFS per cycle decreased. When samples are not allowed to dry (and almost no carbonation can occur since the relative humidity is so high) before test begins the scaling is more severe. According to the measurements, the carbonation depth increase with increasing slag content however chloride penetration depth decreased. Another conclusion drawn was that insulation, which contributes to a more one-dimensional heat flow, seemed to decrease the mass of DISFS. Additionally there is also a suggestion of linking the mass scaling rating system to the visual rating system.

In a study by Skripkiūnas G. et al. [85] concrete with wbr 0.48 and bc 360 kg/m^3 containing the following four binders was used, CEM I 42.5R, CEM II/A-S 42.5N, CEM II/A-LL 42.5R, and CEM III/B 32.5 N-LH. The “LST EN 1338:2003+AC:2006” standard DISFS test was used. All mixes contained a SP, and some also included a retarder. The CEM I, without retarder, had approximately accumulated 1 kg/m^2 DISFS after 28 days and the CEM III/B, without retarder, had less than 0.5 kg/m^2, otherwise the mass of DISFS was large. One conclusion was that the retarder seemed to generally increase the mass of DISFS.

In a follow up study, to [52], by Taylor P. and Wang X. [86] similar materials are included as those used in [52], i.e. wbr 0.42, bc 338 kg/m^3, 0, 20, 35 and 50 mass% GGBFS etc. A comparison is made between the results in the Figure 4, Figure 5 and Figure 6 below. The correlation between the two test series are varied according to the figures below which presents the scaling from ASTM test, and BNQ test where the results from 2012 and 2014 are presented.

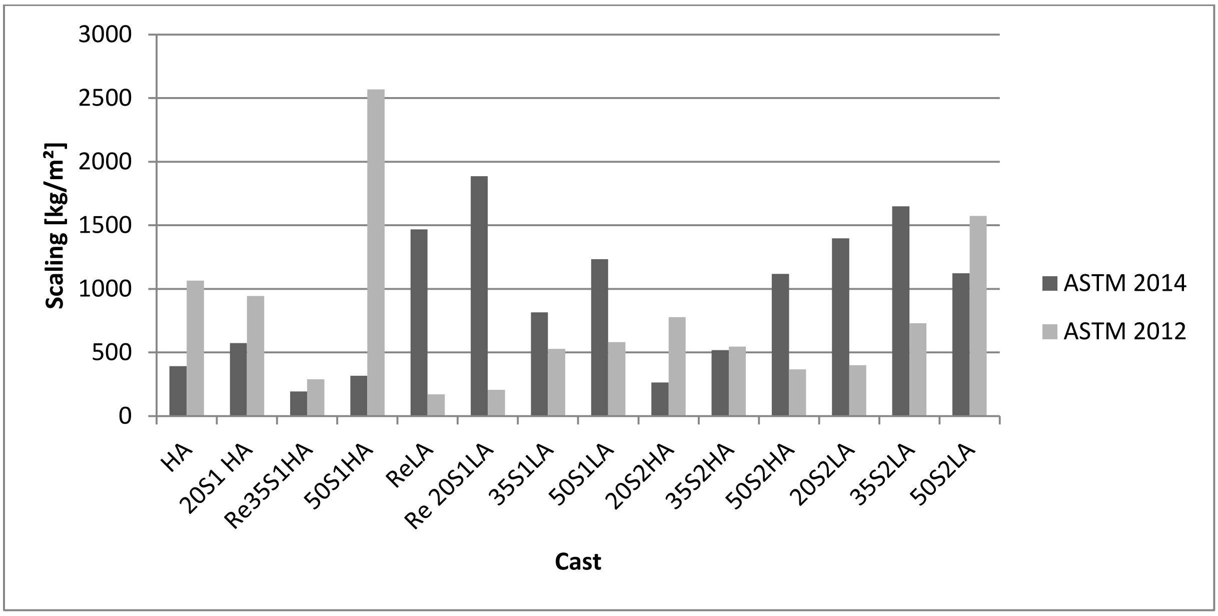

Figure 4. Results presented by Taylor P. and Wang X. [86] where the ASTM C672 method was used.

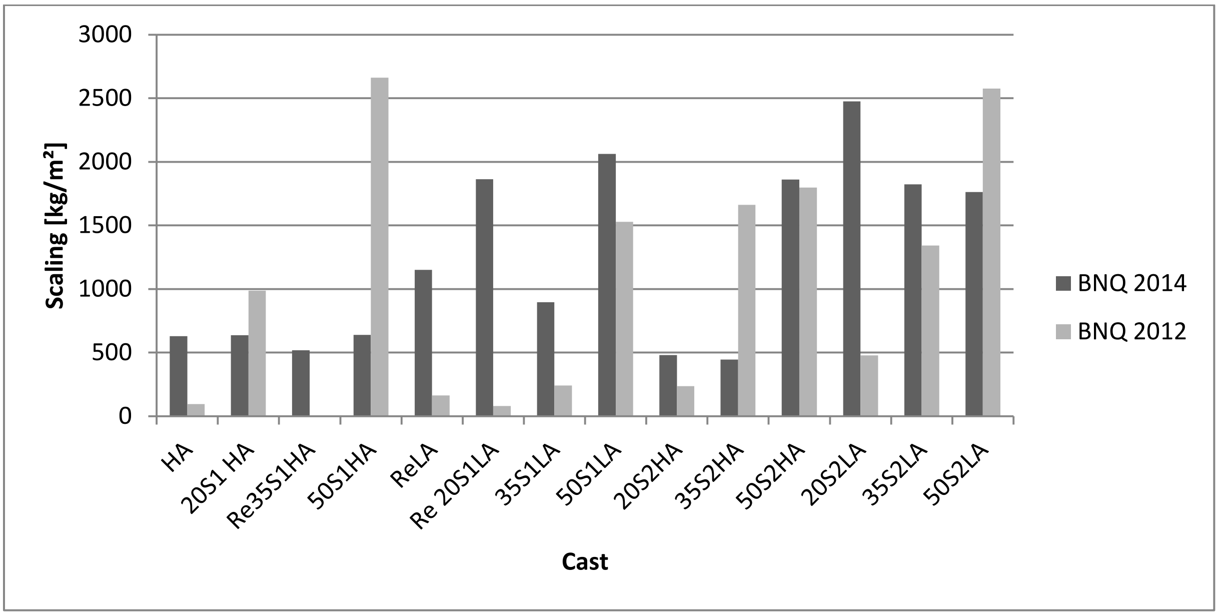

Figure 5. Results presented by Taylor P. and Wang X. [86] where the BNQ method was used.

In Figure 6 the results from 2014 is subtracted from the results from 2012, i.e. the positive values indicate more scaling for 2012 than 2014 and vice versa for negative values. According to these results the BNQ and ASTM seems to show the same trend in most cases, where both ASTM and BNQ show positive, negative or close to zero. If both test series resulted in almost the same scaling, the values would be close to zero. Since there are some high positive and low negative values, this suggests that the quality vary significantly between the concrete recipes cast in 2012 and 2014. For example, 50 mass% GGBFS #1 with 50 high alkali cement ("50S1HA"), the cast from 2012 clearly had significantly more scaling than the cast from 2014. This could suggest that the cast from 2012 was affected more from bleeding of the finished test surface. The reverse can be said regarding the low alkali cement content concrete ("ReLA") and the 20 mass% GGBFS #1 with low alkali cement ("Re20S1LA").

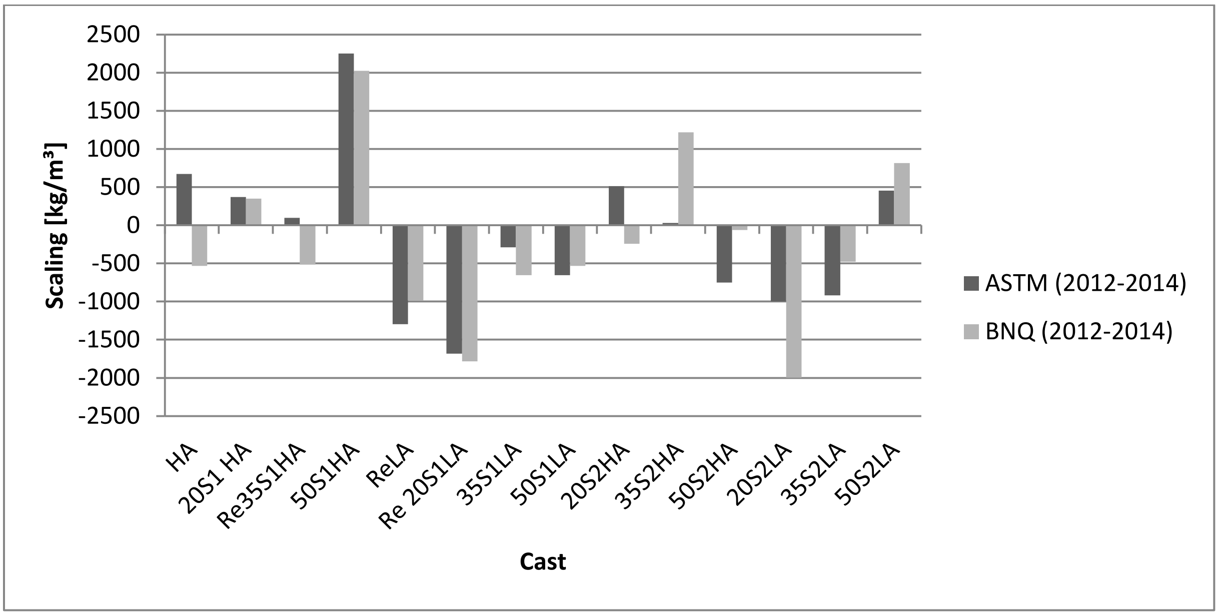

Figure 6. Analysis of results presented by Taylor P. and Wang X. [86] where the results from 2014 is subtracted from the results 2012.

In a study by Boubitsas D. et al. [53] the following four binders are included CEM I LA, CEM II/A-S with approximately 15 mass% GGBFS, 30 mass% GGBFS with the CEM I and a Dutch CEM III/B with approximately 70 mass% GGBFS. In the article they point out that for some of the mixes there could have been a problem with the compatibility between the binder, the SP (and the AEA for the ones containing AEA). The volume change results presented in figure 1 and 2, in the article, combined with the fact that there does not seem to be any internal damages in the slag mixes, indicate that the entrained air does not have any detrimental effect on the salt frost scaling resistance in these concrete mixes with wbr of 0.40. The difference between with and without air is much more noticeable for mixes with wbr larger than 0.40. Looking at the correlation between field and the slab test, all of the tested concrete containing GGBFS seems to be acceptable (or close to acceptable for CEM III/B) in the field considering the 2 to 3 % as an acceptable decrease in volume after the 19 years of field exposure which is marked in figure 3 (in the article). The slab test show acceptable results for 3 of these (CEM I with air, 70+30 CEM I+slag with air, and CEM III/B with air) while the other 5 (CEM I without air, CEM II/A-S with and without air, 70+30 CEM I+slag without air and CEM III/B without air) fail according to the slab test. It should be noted that the CEM III/B without air should be considered accurate since it have slightly over 3 vol% decrease and slightly over 1 kg/m² in the slab test. So according to these results, the slab method seems to be too hard for concrete recipes with wbr 0.40 containing 19 to 30 mass% GGBFS. However, only 19 years have passed, which mean that if the damage increases during the next e.g. 31 or 81 years they fail in the field and the slab method should then be considered accurate and well fit to predict DISFS. For 70% slag the DISFS resistance does not seem to be affected or improve by the air void system (which correlates with my results). They also conclude in the article that carbonation needs to be taken into consideration when testing and evaluating scaling resistance using laboratory test methods.

In a study by Helsing E. and Utgenannt P. [87] include two CEM I which are blended with 0, 20, 35 or 65 mass% GGBFS. In addition to this three different preconditioning procedures where tested. First procedure was according to the slab standard method where its 7 days moist curing, 14 days in 20 °C and 65% RH, then the sample is sawed and exposed to 20 °C and 65% RH for 7 days and finally saturation of the test surface during 3 days with water before the DISFS test begin. The second procedure is the same as the first 28 days in the first procedure, and then it proceeded with 7 days in a climate chamber with 1 vol% CO_2 and finally three days of re-saturation of the test surface before the DISFS test began. The third procedure was also the same as the first 28 days in the first procedure, and then it proceeded with 14 additional days in the 20 °C and 65% RH climate room, and finally three days saturation before the DISFS test began (21 days, in total, of dehydration and carbonation in climate room). Three mixes excluded AEA, among these were CEM I N and 20 mass% GGBFS. These results showed a smaller mass of DISFS when the GGBFS was included from all three preconditioning procedures. However, the samples with the smallest mass of DISFS, from the 20 mass% GGBFS cast, were larger than 1 kg/m² after 56 FTC. For both of these mixes the prolonged dehydration in the climate room (procedure 3) increased the mass of DISFS compared to the basic 7 days of in climate room (procedure 1). According to the results from the concrete with AEA, there seemed to be a difference between the CEM I N and the CEM I R when 35 mass% GGBFS were included. The CEM I N with 35 mass% GGBFS had 0.22 kg/m² after 56 FTC and the CEM I R with 35 mass% GGBFS had 0.12 kg/m² after 56 FTC. When comparing the binder containing 20 mass% GGBFS with and without AEA there is a significant reduction in scaling. The casts containing 100% CEM I N seemed to have slightly smaller mass of DISFS in comparison to the mix with 100% CEM I R for all three preconditioning procedures. However, the CEM I R samples with largest mass of scaling, out of these two concrete casts, had approximately 0.25 kg/m² after 112 FTC (they had been exposed to procedure 2 and 3). When testing concrete containing GGBFS with AEA all recipes had a larger mass of DISFS when the samples had been exposed to 1 vol% CO_2 in comparison to the two other preconditioning procedures. There also seemed to be a trend where the mass of DISFS increased as the fraction of GGBFS increased.

In a study by Löfgren I. et al. [88] two CEM I is included, where the CEM I LA is blended with two different GGBFS in fractions of 20, 30, 40 and 60 mass%. In addition to this one CEM II/B-S is also tested. The wbr and bc is either 0.40 and 425 kg/m³ or 0.45 and 400 kg/m³ (the matrix is not complete). The study also includes four preconditioning procedures. The first one (according to the slab method) is one day in mould, then 6 days in water, then 14 days in a climate room with 20±2 °C and 65±5% RH, then at age 21 days the samples are sawed, then put back in to the climate chamber where the test surface dehydrates and carbonates for 7 days. Then (age 28 days) de-ionized water is poured on the test surface and kept for 3 days of saturation before the test begin at age 31 days. The second procedure is according to the first procedure with one modification where the samples are exposed to 1% CO_2 (20±2 °C and 65±5% RH) from age 21 to 28 days. The third procedure is one day in the mould, then 20 days in water, then 14 days in a climate room (20±2 °C and 65±5% RH). Then (age 35 days) the samples are sawed, then placed 7 days in a climate chamber with 1 vol% CO_2 (20±2 °C and 65±5% RH), then de-ionized water is poured on the surface and kept for 3 days before the test begin (at age 45 days). The forth procedure is one day in the mould, then 62 days in water, then 14 days in a climate room (20±2 °C and 65±5% RH), then (at age 77 days) the samples are sawed, then placed 7 days in a climate chamber with 1 vol% CO_2 (20±2 °C and 65±5% RH). Then de-ionized water is poured on the surface and kept for 3 days before the test begin (age 87 days). When comparing carbonation depth from preconditioning procedure two, three and four, the depth was generally deepest for procedure two and most shallow for procedure four. For wbr 0.40, the mass of DISFS generally increase with increasing fraction GGBFS replacement, from 20 to 30 and 30 to 40 mass%. In addition to this, the scaling generally decrease when comparing preconditioning procedure two with three and three with four. The standard preconditioning procedure (number one) generally produced the lowest mass of scaling. According to the results, 40 mass% scaling with preconditioning #2 was the only one of the 0.40 GGBFS concrete mixes that had more than 0.50 kg/m² accumulated scaling after 112 FTC. Generally, concrete containing 20 mass% GGBFS was only slightly affected by the preconditioning procedures with accelerated carbonation when considering the DISFS. However, there seemed to be a significant effect from the accelerated carbonation on concrete containing more than 20 mass% where preconditioning procedure two, three and four greatly increased the DISFS in comparison to procedure one.

2.8.2 Notable findings regarding DISFS in concrete containing GGBFS

- The agreement between the results from the standard DISFS methods and field tests is somewhat lacking [4, 53, 62, 78, 79, 88].
- The mass of DISFS increases as the wbr increase [53, 70, 76, 88].
- The mass of DISFS decreases as the degree of hydration increases for concrete with CEM I [70] and CEM I blended with slag [71, 78].
- Increased air void content (from 6 to 9%) can improve concrete with 35 mass% slag, but it does not seem to have any effect on the scaling for concrete with 20 mass% slag scaling [4].
- Higher fineness value for the slag fractions (from 430 to 500 m²/kg) decreases the scaling [4].
- Carbonation reduces the DISFS for concrete containing up to 30 mass% slag [70].
- Carbonation have the most significant effect on the DISFS for all ages, however, the hydration and any exposure to drying will have an impact during the early ages (up to 30 days) [70].
- Finishing procedures and bleeding of the concrete surface affects the DISFS of concrete containing GGBFS [4, 62, 80]
- The mass of DISFS increase as the mass of GGBFS and replacement fraction of the total binder content increase when the test surface have been exposed to carbonation and dehydration [52, 55, 70, 80, 82, 88].

- Replacing up to approximately 35 mass% of the CEM I with GGBFS results in an acceptable mass of scaling in concrete (with wbr 0.40, a combination of SP and AEA which does not cause bleeding, and containing approximately 4.5 vol% air content) according to the slab method [53, 70, 87, 88]. In concrete with no AEA, replacing 15 to 20 mass% of CEM I with GGBFS can reduce the mass of scaling [53, 87].
- The mass of DISFS from the slab test decrease significantly when incorporating approximately 4.5 to 5.0 vol% air void content into concrete containing GGBFS with a combination of SP and AEA (which does no cause bleeding) [53, 87].
- The compatibility between the SP and AEA is important to avoid bleeding, and thereby scaling of the concrete [53]

3 Materials

3.1 Binders

Table 4 present the binders used in this study with the abbreviations used when presenting the results.

Table 4. Binder combinations and abbreviations for concrete recipes containing the binders.

Binder abbreviation	Blended content
CEM I	100 % CEM I 42.5 N - SR 3 MH LA[1)]
F20	80 mass% CEM I 42.5 N - SR 3 MH LA[1)] 20 mass% SFA[2)]
F35	65 mass% CEM I 42.5 N - SR 3 MH LA[1)] 35 mass% SFA[2)]
S20	80 mass% CEM I 42.5 N - SR 3 MH LA[1)] 20 mass% GGBFS[3)]
S35	65 mass% CEM I 42.5 N - SR 3 MH LA[1)] 35 mass% GGBFS[3)]
S70	80 mass% CEM I 42.5 N - SR 3 MH LA[1)] 20 mass% GGBFS[3)]
K35	65 mass% CEM I 42.5 N - SR 3 MH LA[1)] 25 mass% GGBFS[3)] 10 mass% LF[4)]

1) Degerhamn Anläggningscement.
2) Siliceous fly ash from Emineral A/S.
3) Merit 5000 from Merox.
4) Limus 25 from Nordkalk.

Below are some brief descriptions of the characterization methods used, on the binders. Results these measurements are presented in the appendix 7.

3.1.1 Characterization of the binders

To characterize the tested materials the following measurements have been made.

- LOI with a Leco apparatus according to “ER 9213:2005”-method
- XRF oxide analysis (Bogue calculation)
- Density
- Blaine value and laser diffraction for particle size distribution
- Vicat
- Compressive strengths
- ICP-analysis for K_2O and Na_2O with water
- SO_3, CO_2, and limestone content

Loss on ignition (LOI) with a Leco apparatus is a measurement of the loss in mass when the binder is heated up to 950 °C. This loss in mass can be due to bound water evaporating, carbon dioxide being released from carbonated cement or unburnt coal when fly ash is tested. In a study by Nowak-Michta [67] the results clearly indicate that the loss on ignition have an impact on the DISFS, which is why this is important to measure. When slag is tested, the oxidisation of sulphur can contribute to a negative loss on ignition, i.e. the mass increase.

XRF (X-ray fluorescence) measures secondary X-rays that have been reflected from the material, which usually consist of a powder. This is an elemental analysis that shows which oxides and how large fraction of each oxide exists in cement, which enables a comparison between cement from various studies. From these results, a Bogue calculation can be made which results in the potential amount of Alite, Belite, tri-calcium aluminate, and tetra-calcium alumina ferrite.

The Blaine fineness measurement is a relative measurement of the air permeability by drawing a defined quantity of air through a bed of cement with a defined porosity. The measurement results in a Blaine value which is the total surface area of the particles per mass of material, usually [m^2/kg]. A higher value means smaller particles in the cement and vice versa. This is also important to consider when comparing with other SFA or GGBFS since the sizes of the particles will have an impact on the hydration process, considering that a larger specific surface of the grains will contribute to more reactions [4].

Laser diffraction measurements are made to complement the Blaine measurement. Considering that the particle size distribution of the binder can affect the ITZ (which could be a crucial area for the DISFS) this additional information could be an interesting factor to evaluate. The results are presented as a particle size distribution from 1 µm to 315 µm.

The Vicat test consist of a needle pressed down into the fresh paste with a certain force at different specified times after the water was added to the cement. As the cement reacts with the water the paste will become more stiff and the depth of which the needle can be pressed will decrease. The results is presented as a time which says something about how long before the fresh paste hardens, or ”sets”. Measurements on the fresh pastes refer to initial and final setting times to give some information about the early hydration.

The ICP analysis is made to investigate how much K_2O and Na_2O from the cement is dissolved in water. This is interesting to know since the solved alkali content is believed to affect the creation of air voids in the fresh paste.

Measurements are also made on the SO_3, CO_2 and limestone content. Since the measurements are done on a CEM I this will give some information about the 5 % fraction of the cement, which is not clinker, consist of limestone.

3.2 Aggregates

The three types of aggregates have been used during the study. These are called “0-8 sand”, “8-12 stones” and “12-16 stones” in this chapter. The 0-8 sand is from “Kvidinge stenkross AB” and consists to most part of quartz and feldspars. The 8-12 and 12-16 stone are from “Hardeberga stenkross” and consist mostly of quartzite.

When modifying the fractions of sand and stones, an attempt was made to make them contribute to a better contrast between the mixes that performed better or worse. This was done by controlling the fraction of sand and larger stones, where a large fraction of the 0-8 sand was added. The sand contained approximately 17 mass% the fractions 2 to 8 mm. In addition to the sand, the 8-12 and 12-16 stones were added to enable the concrete to mix in the “free fall mixer” and disabling the mix from creating agglomerations during the mixing procedure. The mass of concrete per cast was approximately 22 dm³, the main reason for the small mixing size was that many casts where thrown away due to an unwanted air content in the fresh concrete. In Figure 7 the sieving curves for the aggregates respectively and the combined curve “50-20-30” which was used in the concrete recipes is presented.

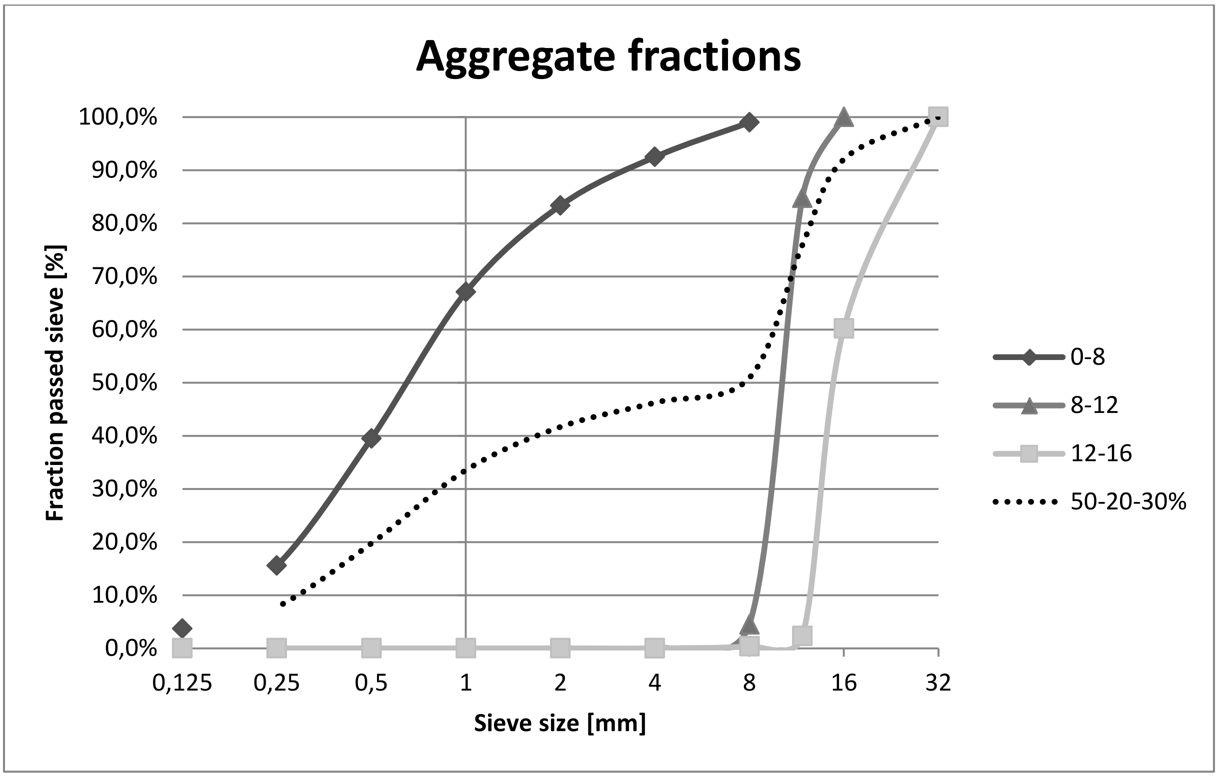

Figure 7. Sieving curves of the aggregates respectively together with the combined sieving curve used in the recipes.

3.3 Admixtures

3.3.1 Superplasticizers

During the test of combinations of SP and AEA six different types of SP was tested with each AEA. Five of these were modified polycarboxylates and one was a sulphonate melamine-fomaldehyde condensate. The brand names of the SPs that were tested are Glenium 51, Glenium SKY 558, Glenium SKY 612, Pozzolith 475-S, Sika ViscoCrete RMC-520 and Sikament EVO 26. One of these was selected for the concrete recipes with the FA and one of these was selected for the concrete recipes (used for the DISFS test) containing GGBFS and 100% CEM I.

3.3.2 Air entraining agents

During the test of combinations of SP and AEA three different types of AEA were tested with each SP. Two of these were synthetic detergents and one was a vinsol resin. The brand names of the AEAs that were tested are Micro Air 100, Sika 88L and Sika AirPRO. One of these was selected for the concrete recipes.

4 Methodology

This chapter gives a summary of the methodology and DISFS test, additional information is given in appendix 2 and 3. The methodology used in this thesis was designed to focus on the question of how the air void content affect the DISFS of concrete containing various fractions of SFA and GGBFS. To make this possible each concrete recipe should contain both SP and AEA, in addition to this the wbr and bc of the concrete recipes were set to meet the requirements of the present Swedish standards for concrete exposed to DISFS [89]. The methodology contain two main parts, first a test to find a combination of SP and AEA for each binder combinations used and second part is the DISFS test.

4.1 Test of admixture combinations

The purpose of finding a combination of an SP and an AEA that work well together with each binder, is to enable casting of concrete with small variations in air void contents by varying the mass of AEA added. The procedure included three parts, measurement of the air void content, workability, and estimation of the air voids stability. The casts were 4 dm³, containing 0-8 sand, with wbr 0.4 and the sand/binder ratio was 3. The mixing procedure consisted of 2.5 min of blending sand with the binder, then water mixed with AEA was added and blended for 2.5 min, and finally SP was gradually added to attempt to acquire approximately the same workability for each cast.

Directly after the mixing was finished, the air content was measured in 1 dm³ of the mix with an air content device using a pressure meter. Then the workability was measured using a Hägermann cone. The third test of the air void stability was made by taking 5 large spoons with mortar and disperses it in a bucket of water. The air voids created in the fresh mix would then emerge at the surface and generally either create a thick layer of foam with small and stable bubbles, or burst. The results showed a clear relation between a relatively high air void content, no bleeding visible during the workability measurement and a layer of foam with bubbles that did not burst directly after they emerged to the water surface. This enabled a selection of a combination of SP and AEA for each binder combination that has been used in the DISFS test.

4.2 DISFS test

The DISFS test was designed to acquire results that show what effect the air void content has on the DISFS for each binder combination. This was done by minimizing factors affecting the DISFS associated to two main groups, the preconditioning and the DISFS method.

The following considerations were made for the current preconditioning process. To investigate the effect from carbonation combined with dehydration for each concrete, two series of samples was made.. The test surface hydrated for 7 days submerged in water and 299 days sealed in 20 °C before the samples were sawn, and then one day submerged in water before the DISFS test, or the dehydration/carbonation, began. The purpose of the hydration process was to enable pozzolanic reactions to occur prior to the DISFS test, minimize any continued hydration to occur during the DISFS test. This should help to minimize the variation in degree of hydration and therefore the variation of the microstructure for the samples containing the same binder. 336 samples were made for the DISFS test where 168 were tested at age 307 days when the surface had never dried and never been exposed any to favourable conditions for carbonation. The other 168 were put in to a climate room with 20±0.2 °C, 60±2 % RH and approximately 0.04 vol% CO_2, which means that there is favourable conditions for natural carbonation of the concrete test surfaces. In this thesis the samples with a test surface that had never dried prior to the DISFS test will be presented, the carbonated samples will be presented in the PhD-thesis.

The following factors were considered for the DISFS method. When using a DISFS method with the de-icing agent solution on top of the concrete there is a risk for the edges of the test surface to crack and enable the solution to leak from the test surface. To avoid this risk an upside down sample setup was used. The sample setup is presented in Figure 8 (left) and the freezers (containing 9 samples on each shelf) used during the DISFS test is presented Figure 8 (right).

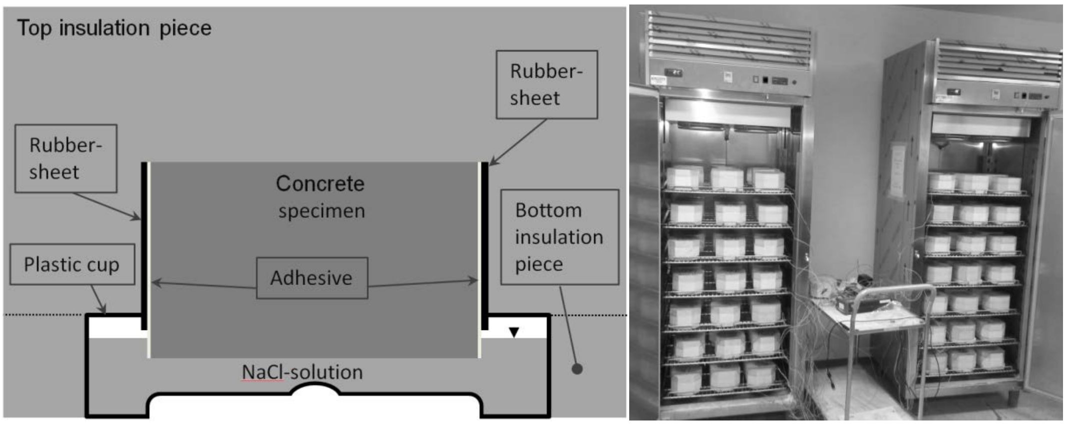

Figure 8. Sample setup for the DISFS test (left). Freezers and sample positioning (nine samples per shelf) inside the freezers (right).

Using this sample setup together with these freezers, which cycle between +20 and -23 °C, the FTC measured inside the seven different solutions on seven different shelfs can be seen in Figure 9.

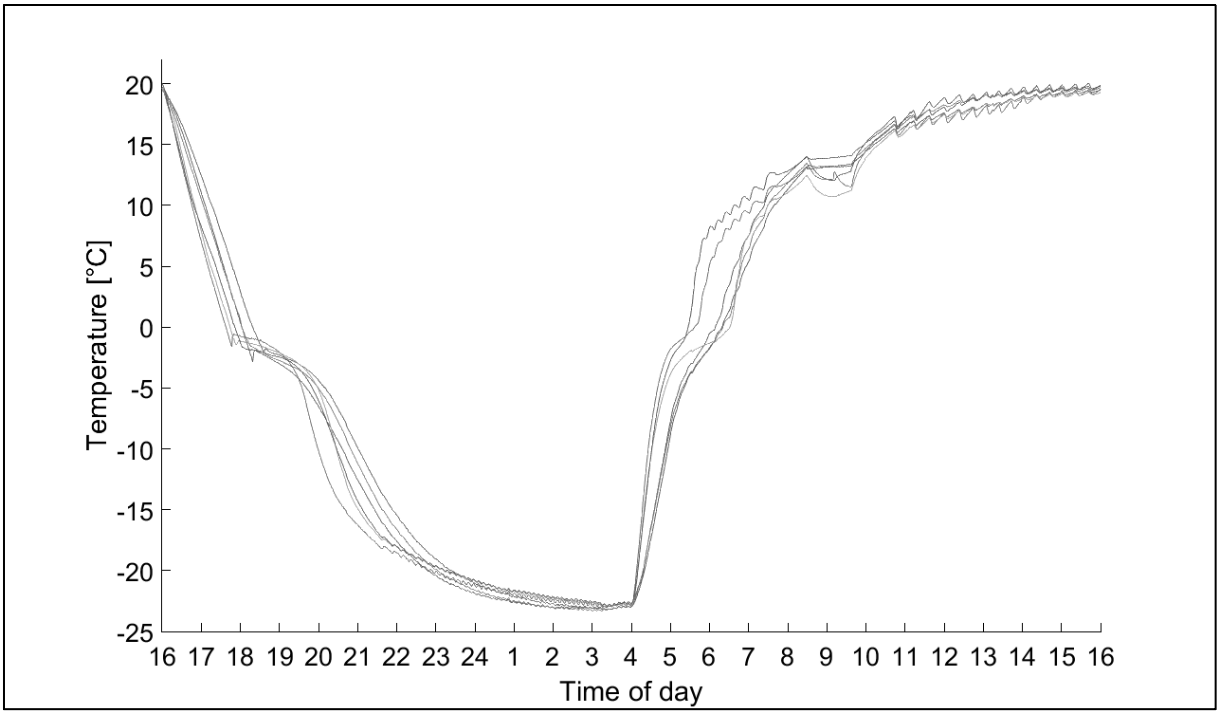

Figure 9. Freeze-thaw cycle measurements inside seven different NaCl solutions standing on seperate shelfs inside the freezer.

DISFS measurements were made once every week on each sample where the scaling was brushed off and collected in separate filters. The filters was dried in 105±5 °C for 22±2 hours and weighed. Figure 10 present a sample with the test surface 100Ø mm² that has been exposed to 112 cycles.

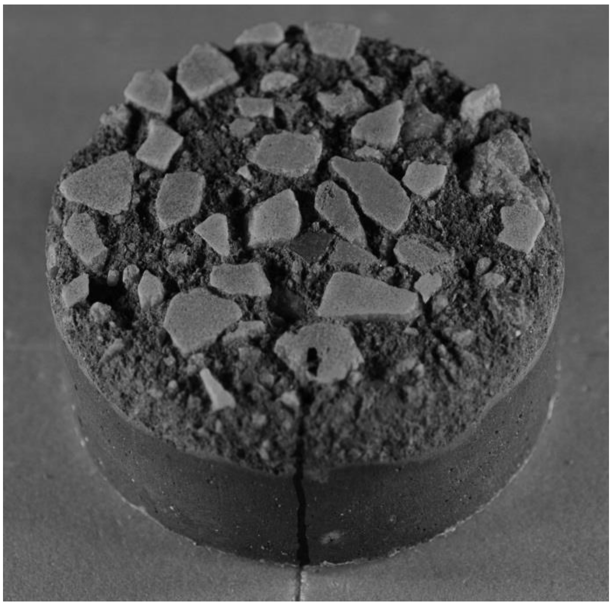

Figure 10. Sample O-41 after 112 freeze-thaw cycles.

5 Results

This chapter will present some figures that summarize the results presented in the articles regarding the DISFS in concrete containing SFA and GGBFS.

5.1 DISFS

Figure 11 to Figure 16 present comparisons between the mean accumulated mass of DISFS with the standard deviation from all concrete recipes tested. The names for each cast are presented along the x-axis with four bars each that present the four casts with the respective binder. The four bars for each binder combination represents the four casts with 6 samples per cast where the #1 was cast without any AEA, #2 had the target air content 2.5 vol%, #3 present the cast with target air content 3.5 vol% and #4 the cast with the target air content 4.5 vol%. The results from the air void analysis are presented in appendix 8. Figure 11 and Figure 12 presents comparisons between the DISFS for the concrete containing GGBFS in relation to the CEM I after 56 and 112 FTC. Figure 13 and Figure 14 presents the accumulated mass of DISFS from the concrete with 20 mass% replacement of the binder in relation to the CEM I after 56 and 112 FTC. Figure 15 and Figure 16 presents the accumulated mass of DISFS from the concrete with 35 mass% replacement of the binder in relation to the CEM I after 56 and 112 FTC.

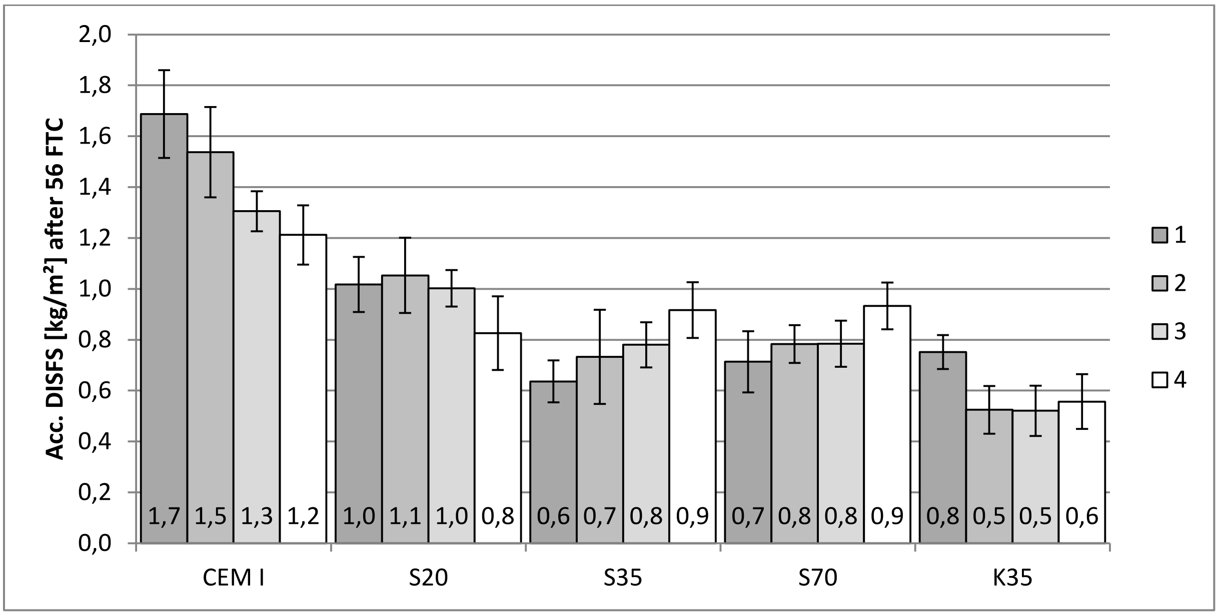

Figure 11. Comparison between accumulated DISFS after 56 FTC from the concrete casts containing 100% CEM I and the concrete casts containing GGBFS. Each mean value and error bar represent six samples. Bar #1 to #4 present casts with the target air content (in the fresh concrete) of 1.5 to 4.5 vol%.

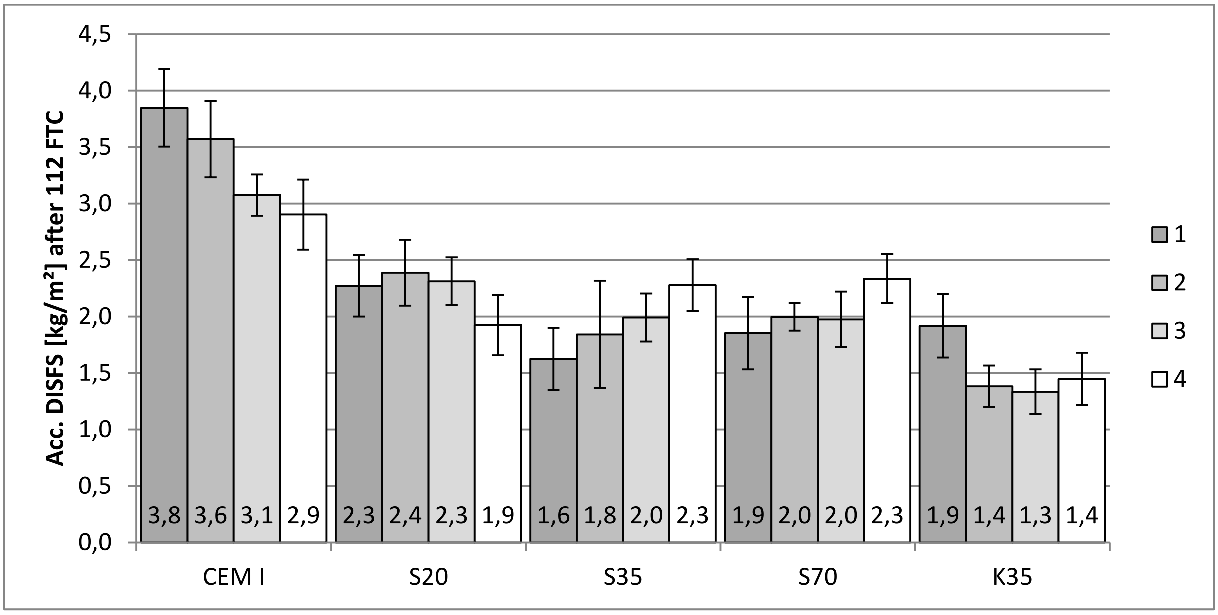

Figure 12. Comparison between accumulated DISFS after 112 FTC from the concrete casts containing 100% CEM I and the concrete casts containing GGBFS. Each mean value and error bar represent six samples. Bar #1 to #4 present casts with the target air content (in the fresh concrete) of 1.5 to 4.5 vol%.

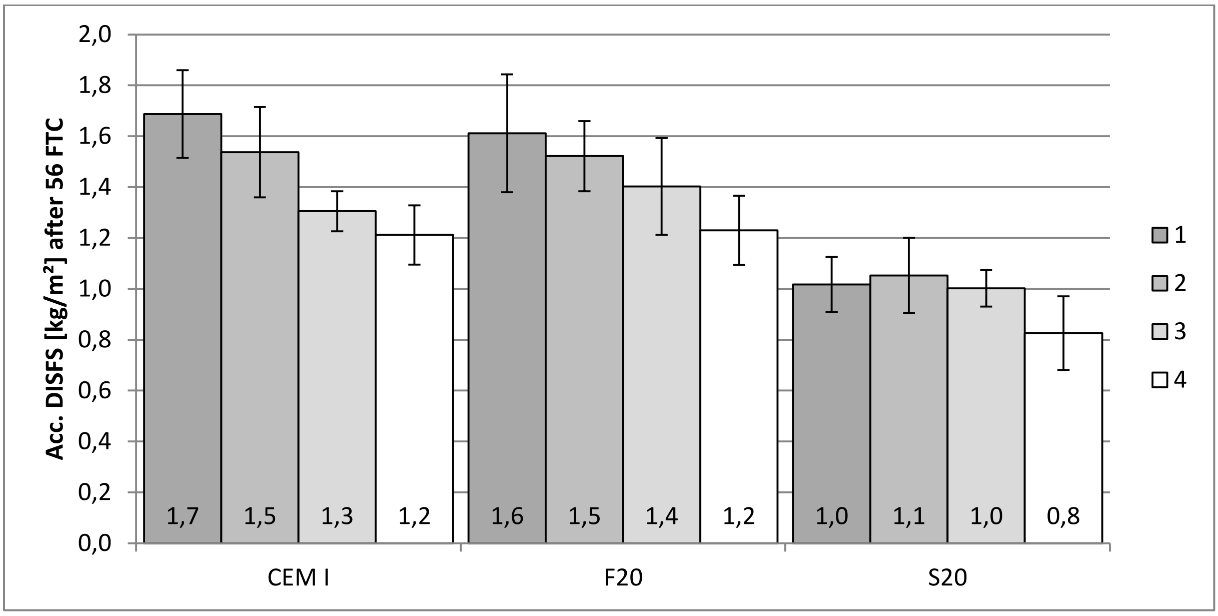

Figure 13. Comparison between accumulated DISFS after 56 FTC from the concrete casts containing 100% CEM I, and the concrete casts containing 20 mass% SFA or GGBFS. Each mean value and error bar represent six samples. Bar #1 to #4 present casts with the target air content (in the fresh concrete) of 1.5 to 4.5 vol%.

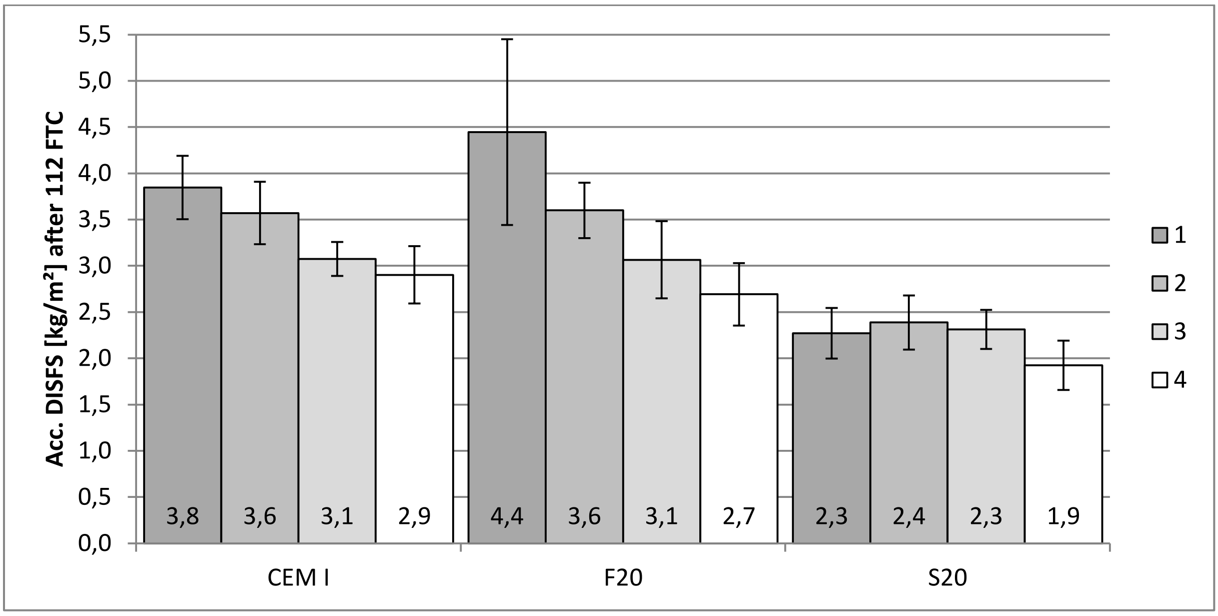

Figure 14. Comparison between accumulated DISFS after 112 FTC from the concrete casts containing 100% CEM I, and the concrete casts containing 20 mass% SFA or GGBFS. Each mean value and error bar represent six samples. Bar #1 to #4 present casts with the target air content (in the fresh concrete) of 1.5 to 4.5 vol%.

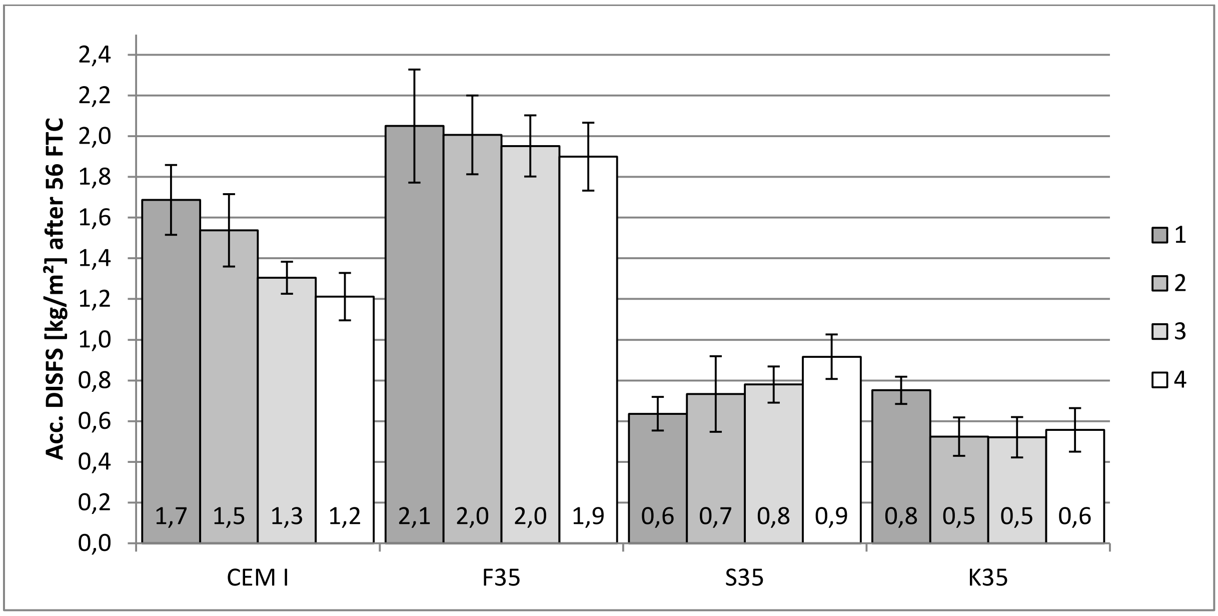

Figure 15. Comparison between accumulated DISFS after 56 FTC from the concrete casts containing 100% CEM I, 35 mass% GGBFS or SFA and the concrete containing 25+10 mass% GGBFS+LF. Bar #1 to #4 present casts with the target air content (in the fresh concrete) of 1.5 to 4.5 vol%.

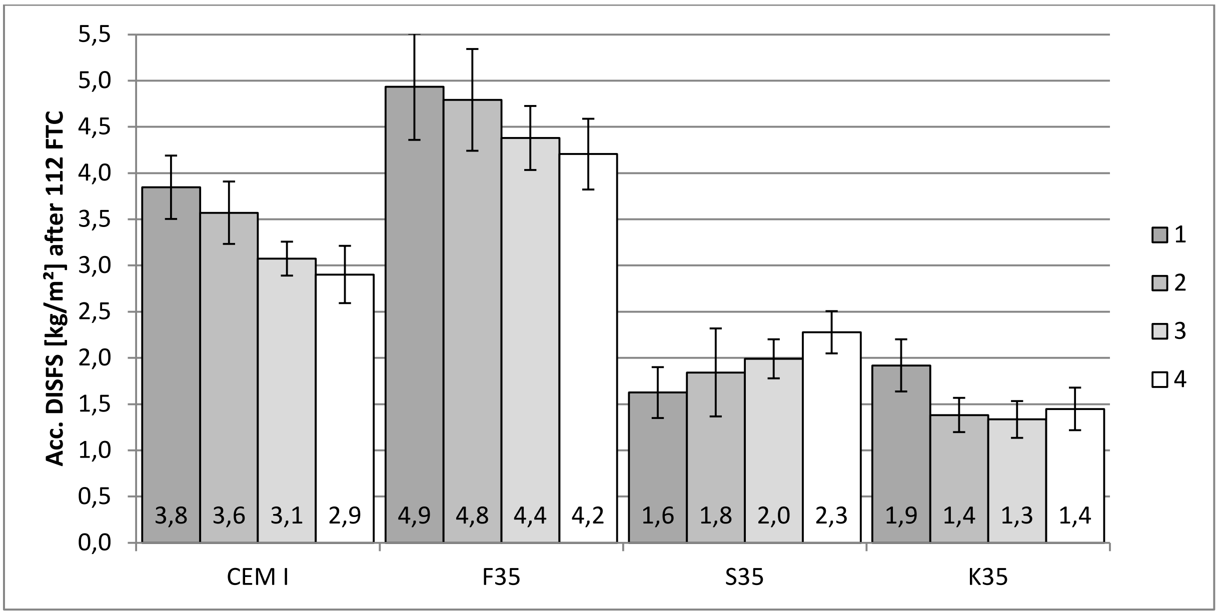

Figure 16. Comparison between accumulated DISFS after 112 FTC from the concrete casts containing 100% CEM I, 35 mass% GGBFS or SFA and the concrete containing 25+10 mass% GGBFS+LF. The error bar of F35-1 ends at 5.5 kg/m². Bar #1 to #4 present casts with the target air content (in the fresh concrete) of 1.5 to 4.5 vol%.

5.2 Calculated "absorption"

The diagrams in this section present mean values with standard deviation for the calculated "absorption". The "absorption" is calculated according to Equation 6:

$$\text{Calculated "absorption" after 56 cycles} = m_1 - m_2 + m_3 \tag{6}$$

m_1 = The mass of sample + insulation + rubber + glue (according to the sample setup) after 56 cycles. Visible NaCl-solution were dryed off, from the outer surfaces of the sample setup, with a paper towel before wheighing.
m_2 = The mass of sample + insulation + rubber + glue (according to the sample setup) right before the first cycle. Free water were dryed off, from the outer surfaces of the sample setup, with a paper towel before wheighing.
m_3 = The dry mass of the accumulated scaling for the sample after 56 cycles for the sample (note: dry mass for scaling is used, i.e. this does not result in the actual absorption during the test for each sample therefore it is called "Absorption").

The y axis is set to show 0 to 19 g for all diagrams to make the comparison easier for the reader.

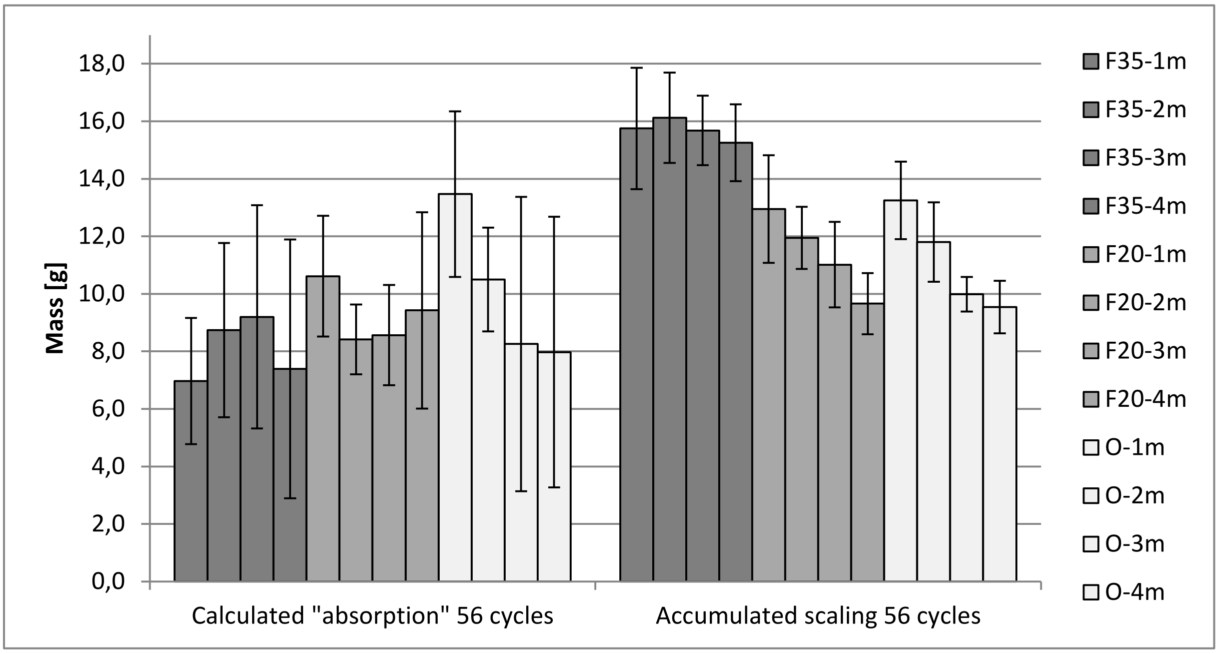

Figure 17. Calculated "absorption" in relation to the accumulated scaling after 56 cycles for concrete containing 65+35 mass% CEM I+SFA, 80+20 mass% CEM I+SFA and 100% CEM I. The legend present each cast (6 samples/cast) from left to right.

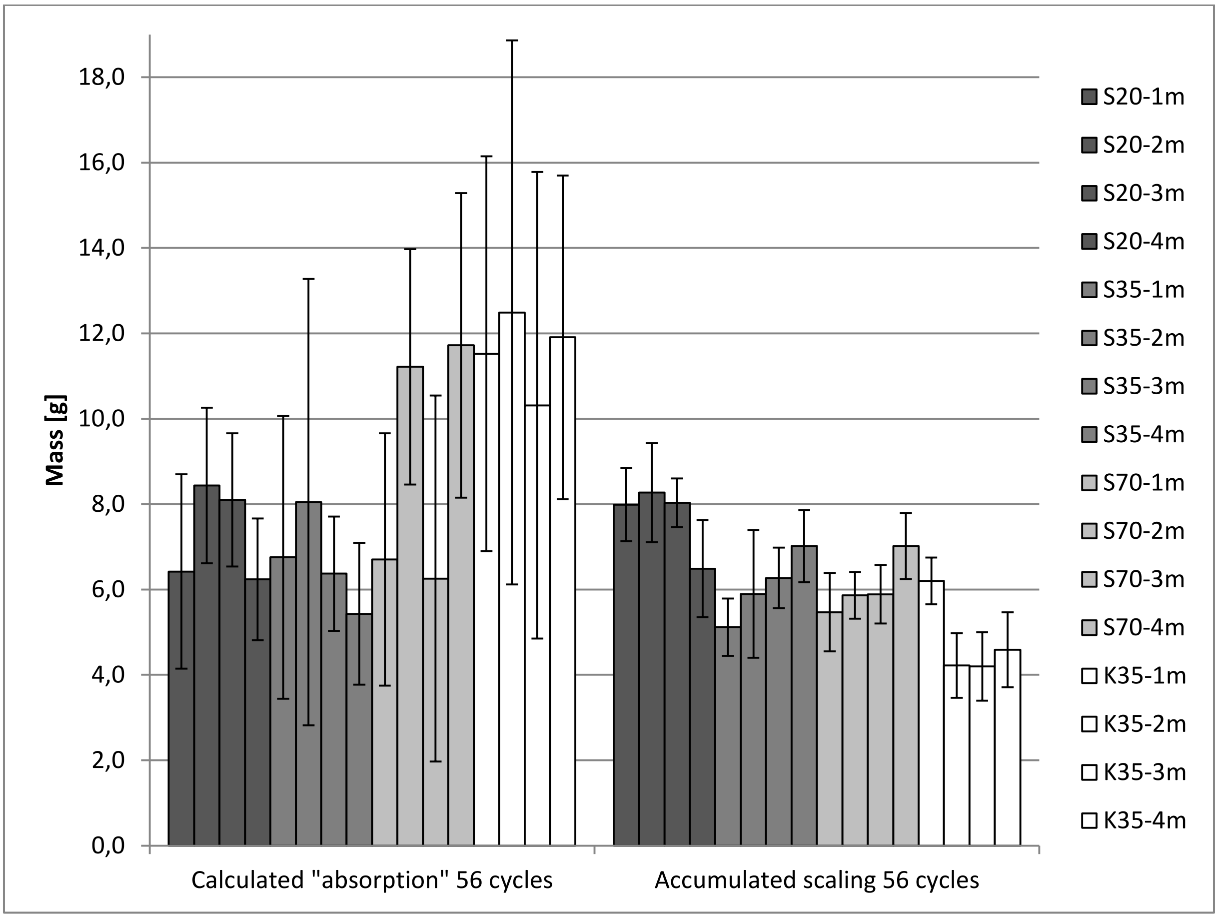

Figure 18. Calculated “absorption” in relation to the accumulated scaling after 56 cycles for concrete containing 80+20 mass% CEM I+GGFS, 65+35 mass% CEM I+GGBFS and 30+70 mass% CEM I+GGBFS. The legend present each cast (6 samples/cast) from left to right.

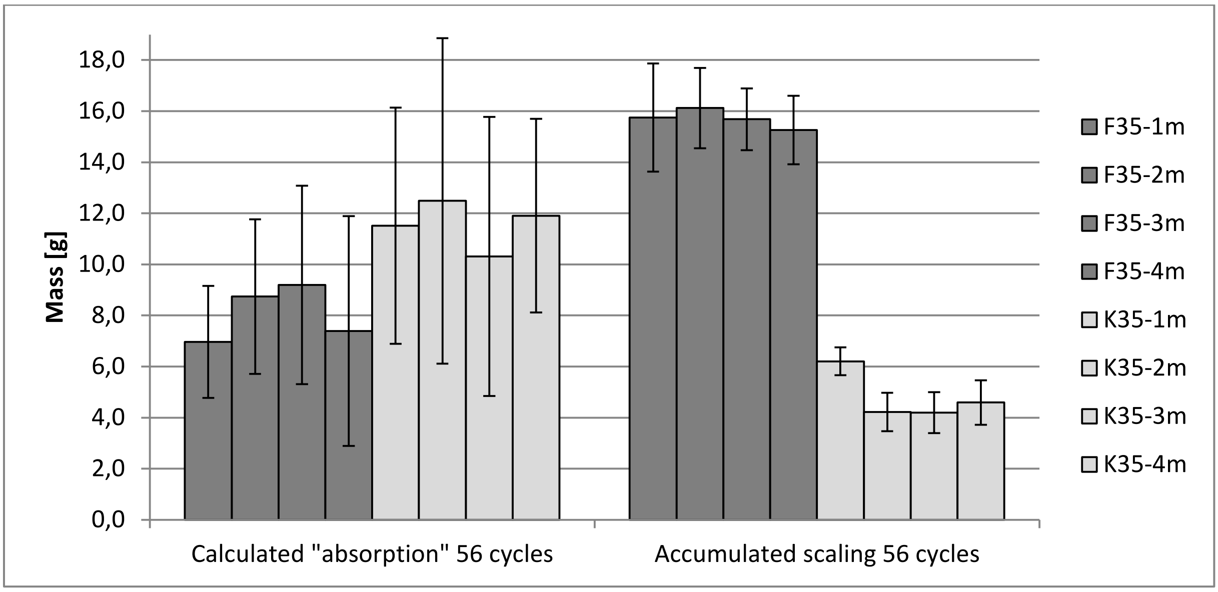

Figure 19. Calculated "absorption" in relation to the accumulated scaling after 56 cycles for concrete containing 65+35 mass% CEM I+GGBFS and 65+25+10 mass% CEM I+GGBFS+LF. The legend present each cast (6 samples/cast) from left to right.

5.3 Coefficient of variation

Figure 20 and Figure 21 presents a compilation of the CV each cast has based on the accumulated mean scaling and the standard deviation for the six samples after 56 and 112 FTC.

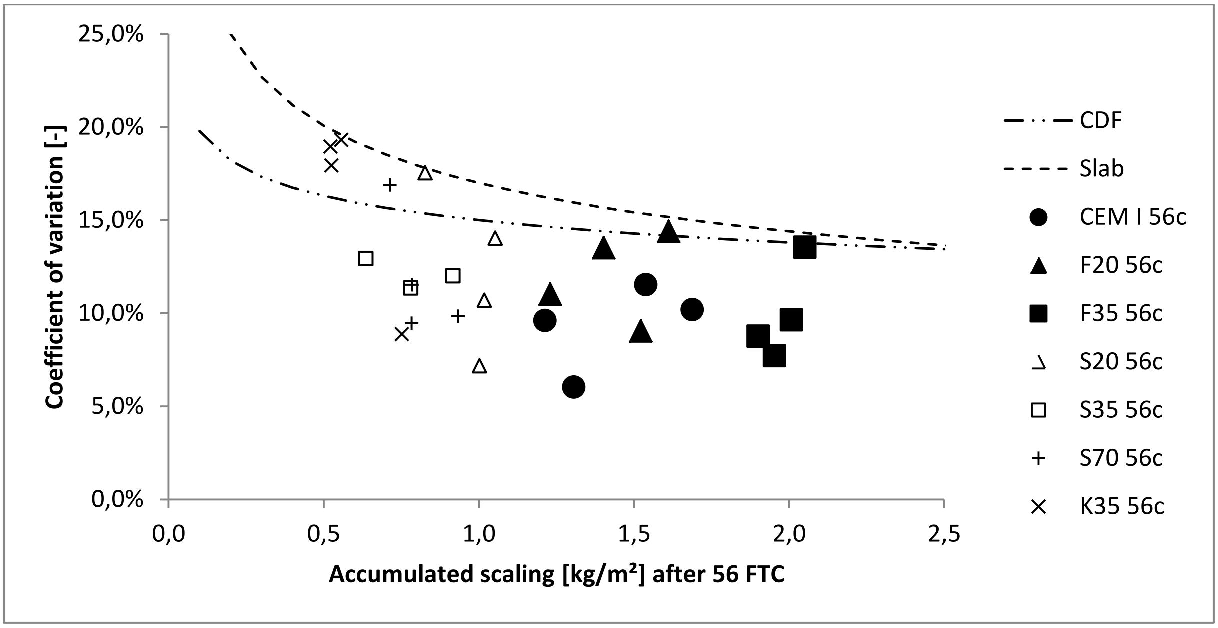

Figure 20. Compilation of CV-values based on the accumulated DISFS and standard variation after 56 FTC.

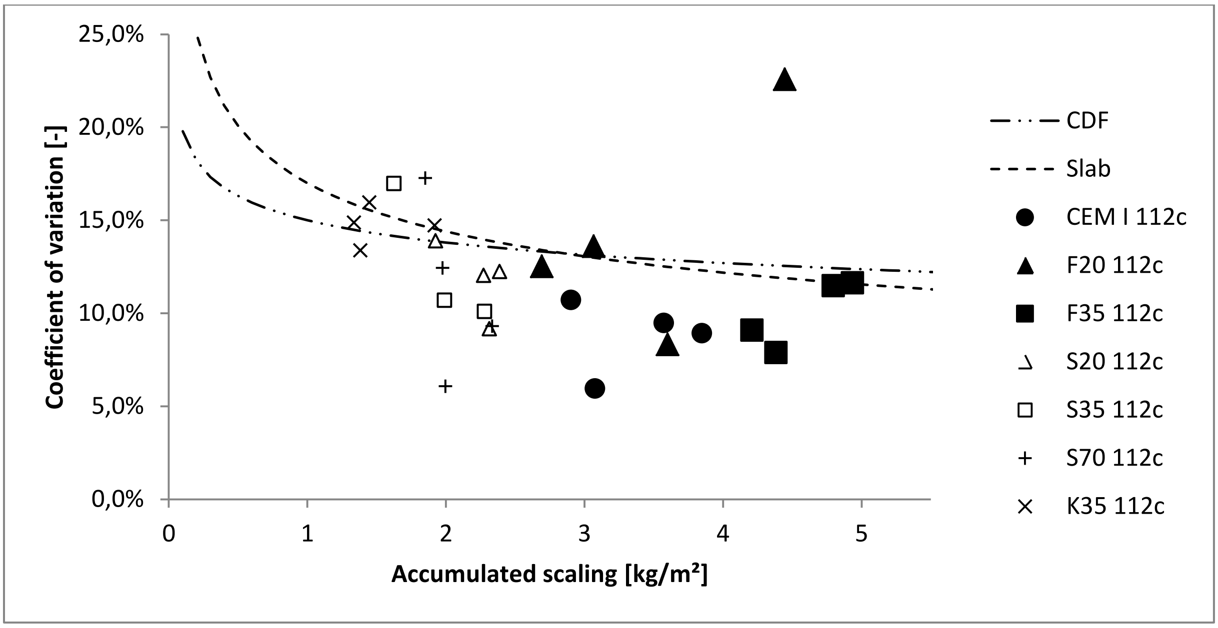

Figure 21. Compilation of CV-values based on the accumulated DISFS and standard variation after 112 FTC.

6 Discussion

This chapter presents some complementary discussion to paper three and four, since the discussions in the articles only focus on the results for each binder.

6.1 DISFS rate

When testing concrete with relatively good DISFS resistance the ASTM C672-, the CDF- and the slab method is used there seems to be a large mass of DISFS created during the first few FTC, and then the rate is significantly reduced for concrete with relatively high DISFS resistance. When only considering the ASTM C672- and CDF method and the test surfaces used, the explanation could be that the test surface is trowelled or resembles a form-surface. This would infer that there is more paste and small fraction aggregates which could scale of in the beginning, and as more aggregates covers the test surface the scaling is reduced. Alternatively, some bleeding has occurred on the test surface, which contributes to a large mass of DISFS in the beginning. However, neither of these two theories explains why a sawed test surface (i.e. no "surface bleeding" or an initial larger fraction of paste and small fraction of aggregates) exposed to the slab method also have the highest DISFS rate during the first few FTC and followed by a significant decrease.

Another factor that clearly affects the DISFS is the preconditioning. In the current study, the results show a slightly accelerating mass of DISFS, the samples have been hydrated for a long time and never dried (except for the self-desiccation, which can occur for concrete with wbr 0.40). In the study by Utgenannt [70], which use a similar DISFS method, never dried and water saturated samples are tested together with dried and uncarbonated samples. The difference between the "never dried"-procedure used by Utgenannt and the procedure used in the current study is that Utgenannt did not re-saturate the samples before the DISFS test began while there was a one day re-saturation before the test in the current test method. The results from Utgenannt show that there is a more or less constant DISFS of the "never dried test surface-samples", similar to the DISFS rate of the current study.

Another factor, which could contribute to the acceleration in the current method, is the fact that the probability for larger aggregates to come off increase as the mass of DISFS increase. This could explain why the concrete in the current study accelerate while the micro concrete (max aggregate size is 8 mm) used by Utgenannt [70] seems to have a more constant DISFS rate. However, it is unlikely that this is the only factor contributing to this. According to the positive values for the calculated "absorption", the moisture content inside the concrete will increase during the DISFS test, which is believed to contribute to altering the DISFS rate.

When comparing the masses of scaling per week, there seems to be almost the same increase in the DISFS rate. Most casts for CEM I, F20, S20, S35, S70 and K35 all increase approximately 0.1 kg/m² when comparing the scaling during the first few cycles (up to 14) with the last cycles (98 to 112). However, F35 increase up to 0.3 kg/m² then it seems to stop, and one should consider that the results for F35 are influenced by larger stones during the later cycles. Another thing to note is that the differences of the initial scaling between the first

14 cycles for F35 and K35 differ. F35 has approximately 0.2 kg/m² and K35 has approximately 0.05 kg/m². This could indicate that the scaling is deeper for F35.

6.2 Effect from the air content on the DISFS

The results from concrete containing 100% CEM I show that there is a clear decrease in the mass of DISFS when the air content, and the amount of small voids, increase. This effect has been shown previously for concrete which have been exposed to carbonation and dehydration according to the standard slab method, e.g. [53, 70, 87]. However, the effect from different air contents on uncarbonated and never dried concrete have not been analysed in this way before. It is however unknown if the mass of D-ISFS decrease to 0 kg/m² with increasing air content or if the scaling will decrease until a certain point when added air voids does not have any more affect. Increased air content far above 5 vol% is not practically relevant, however it could give some additional information regarding the DISFS mechanism(s).

The effect on the DISFS from the air void content differs significantly when comparing concrete containing SFA and GGBFS. One important factor affecting this is believed to be the connectivity of the capillary pores. Since SFA reacts much later in comparison to GGBFS, the OPC cement have reacted much more and created a more complete hardened matrix. This could mean that the late reaction from the SFA will fill some of the capillary pores and decrease the connectivity of the hardened paste. This could lead, according to the glue spall mechanism, to a reduction of the strain created from the ice inside the matrix close to the surface. That will lead to larger difference in resulting strain, therefore larger tension, between the concrete surface and the outer ice, which will increase the mass of DISFS. When considering the theory of ice growth, a decrease in connectivity will increase the distances the water must travel inside capillary and gel pores before it reach a void. If this distances increases, the hydraulic pressures will also increase and an increase in mass of DISFS is expected. Considering that the concrete containing 20 mass% SFA and 100 mass% CEM I appears to produce the same mass of DISFS, there seems to some limit somewhere between 20 and 35 mass% SFA where the decrease in connectivity begins to change the amount of scaling significantly. This hypothesis needs to be verified with a characterization of the materials microstructure.

According to the DISFS results presented in Figure 11 and Figure 12, the mass of DISFS is reduced when GGBFS is added in comparison to the concrete containing 100% CEM I. The results clearly show a difference in how each concrete recipe is affected by the addition of AEA. The mass of DISFS seems to be reduced for the concrete containing CEM I, 20 mass% GGBFS and 25+10 mass% GGBFS+LF while it seems to increase for concrete containing 35 and 70 mass% GGBFS. This suggests that the addition of air voids has different effect on the DISFS depending on the properties of each uncarbonated never dried hardened paste, with each given microstructure.

6.3 Calculated “absorption”

The calculated “absorption” is presented to give some idea about the absorption during the test since the absorption have been found to correlate to some degree with the mass of DISFS

[90]. However, it is important to consider the difficulties with estimating the mass of absorption for a specific sample.

In the current case the sample is weighed just before the first cycle start and then at every measurement of the DISFS. However, between every measurement some paste and aggregates will have scaled off. This means that some estimate must be made regarding the mass of absorption that the scaled material contributed with just before it scaled off. In this study, the dry weight of the scaled material is added to the calculated “absorption”, meaning the current “absorption” does not consider the absorption that the scaled material contributed with. In addition to this, the scaled material consists of hardened paste and aggregates. To enable an accurate estimate of the absorption in the scaled material, the porosity is needed. However, the porosity of scaled material varies greatly depending on if a stone is included in the scaled material because the frost resistant stones have much lower porosity than the hardened air entrained cement paste. In addition to this, because the scaled material has been dried in 105 °C, the microstructure will have changed. This means that it is not possible to measure the absorption of the dried scaled off material since this most likely will result in a mass of absorption that is too large when compared to the accurate absorption in the material just before it scaled off.

This difficulty is visualised by Figure 19 that show the concrete casts containing 35 mass% SFA together with the concrete casts containing 65+25+10 mass% CEM I+GGBFS+LF. According to the diagram the concrete with 35 mass% SFA have a lower “absorption”. However, considering that the accumulated scaling is much higher for the F35 than K35, the author believes that the mass of absorption of the F35 was most likely larger than the K35.

Considering the factors stated above, the calculated “absorption” will be revisited in this project when measurements have been made on the porosity in each material. These measurements of the porosity would enable a calculation of an estimated mass of “absorption” which is more accurate than the calculated “absorption” currently presented.

6.4 Coefficient of variation

Figure 20 and Figure 21 presents the coefficients of variation that are calculated from the mean value and standard deviation for each cast which consist of six samples. According to the results the coefficients are either around or below the limits given in the European standard [60]. This indicate that the DISFS test method, which have been used in this study, have an adequate accuracy to investigate how various factors affect the DISFS mechanism(s).

7 Conclusions

7.1 Methods

- The test method for finding combinations of AEA and SP clearly indicate if a certain combination will have a high or low risk for bleeding when used in a concrete. When using a combination with a low risk for bleeding, according to the test method, small differences can be generated in the air void system by changing the mass in AEA added to the mix.
- The DISFS method is considered to be suited to analyse the salt frost scaling mechanism(s). The DISFS method exposes the samples to a temperature cycle with a small variation, which mean that there is a negligible variation added to the DISFS results due to the F-TC used in the method. This contributes to a more constant DISFS load. According to the coefficient of variation presented for each batch (6 samples/batch), no significant variations are believed to be added to the results because of to the DISFS method.

7.2 DISFS measurements

- The results from the concrete containing 65+35 mass% CEM I+SFA show that when increasing the air void content, the DISFS decrease less in comparison to 100% CEM I and the binder combination 80+20 mass% CEM I+ SFA. In addition to this, the mass of scaling is significantly higher for concrete containing 65+35 mass% CEM I+SFA in comparison to 100% CEM I and the binder combination 80+20 mass% CEM I+ SFA.
- The mass of DISFS slightly decrease for concrete containing 80+20 mass% CEM I+GGBFS and 4.5% air content. When adding a larger mass of AEA, the mass of DISFS seems to increase from the uncarbonated concrete containing 35 or 70 mass% GGBFS. The mass of DISFS in concrete containing CEM I blended with 25 mass% GGBFS and 10 mass% lime filler seems be reduced slightly when adding AEA, however increasing the mass of added AEA slightly, does not seem to decrease the mass of DISFS.
- When testing well hydrated, sawed, uncarbonated and never dried test surfaces the DISFS rate seems to be slightly accelerating for binders containing SFA, GGBFS or GGBFS with LF when using the developed DISFS method.

8 Future studies

During the second half of this PhD project, dried carbonated concrete from the same batches will be tested with the developed DISFS method to enable a comparison with the results presented in paper three and four. This will hopefully increase our knowledge of the impact the carbonation and drying have on each binder and also be able to study if the effect of the air void systems change or not.

In addition to this, complementary tests will be made to study the microstructure of the test surface to try to connect the different mechanisms with the results from the DISFS tests. The goal of these tests are to analyse differences in the microstructure, e.g. the porosity and connectivity, between the various binder combinations to see how the DISFS relates to the properties of the, approximately, 2 mm thick test surface. Another factor, which could be interesting to study, is the self-desiccation and degree of hydration of the different binder combinations to give more information about starting conditions of the concrete before the DISFS test.

9 References

1. Scrivener, K.L., *Options for the future of cement.* The Indian Concrete Journal, 2014. **88**(7): p. 11.
2. Arnfelt, H., *Damage on Concrete Pavements by Wintertime Salt Treatment*. 1943, Statens Väginstitut. p. 28.
3. Verbeck, G.J. and P. Klieger, *Studies of "Salt" Scaling of Concrete*, H.R.B. 150, Editor. 1957: Washington D.C. p. 13.
4. Hooton, R.D. and A. Boyd, *Effect of finishing, forming and curing on de-icer salt scaling resistance of concretes*, in *Frost Resistance of Concrete*, M.J. Setzer and R. Auberg, Editors. 1997, E&FN Spon: University of Essen. p. 174-183.
5. Jacobsen, S., D.H. Saether, and E.J. Sellevold, *Frost testing of high strength concrete: Frost/salt scaling at different cooling rates.* Materials and Structures/Materiaux et Constructions, 1997. **30**(195): p. 33-42.
6. Powers, T.C., *Basic Considerations Pertaining to Freezing-and-Thawing Tests.* ASTM Proceedings, 1955. **55**: p. 24.
7. Jacobsen, S., et al., *Frost deicer salt scaling testing of concrete: Effect of drying and natural weathering.* Cement Concrete and Aggregates, 1997. **19**(1): p. 8-16.
8. Setzer, M.J. and R. Auberg. *Testing of Freeze Thaw and Deicing Salt Resistance*. in *CBP Second International Workshop*. 1994. Oslo, Norway.
9. Anonymous, *SS-EN 1097-6:2013*, in *Tests for mechanical and physical properties of aggregates - Part 6: Determination of particle density and water absorption*. 2013.
10. Bouzoubaâ, N. and B. Fournier, *Current situation with the production and use of supplementary cementitious materials (SCMs) in concrete construction in Canada.* Canadian Journal of Civil Engineering, 2005. **32**: p. 129-143.
11. Edmeades, R.M. and P.C. Hewlett, *15 - Cement Admixtures*, in *Lea's Chemistry of Cement and Concrete (Fourth Edition)*. 1998, Butterworth-Heinemann: Oxford. p. 841-905.
12. E-701, A.C., *Chemical admixtures for concrete*, in *ACI Education Bulletin E4-12*. 2013.
13. SS-EN1367-1, *SS-EN 1367-1:2007*, in *Tests for thermal and weathering properties of aggregates - Part 1: Determination of resistance to freezing and thawing*. 2007.
14. SS-EN12620, *SS-EN 12620+A1:2008*, in *Aggregates for concrete*. 2008.
15. Standard, S., *SS-EN 1097-6:2013 Tests for mechanical and physical properties of aggregates - Part 6: Determination of particle density and water absorption*. 2013.
16. SS-EN1367-2, *SS-EN 1367-2:2009*, in *Tests for thermal and weathering properties of aggregates - Part 2: Magnesium sulfate test*. 2009.
17. Powers, T.C., *The mechanism of frost action in concrete (Part I).* Cement, Lime and Gravel, 1966. **41**(5): p. 6.
18. Warris, B., *The Influence of Air-Entrainment on the Frost-Resistance of Concrete*. 1963, The Royal Institute of Technology. p. 45.
19. Collins, A.R., *The Destruction of Concrete by Frost.* Journal of the Institution of Civil Engineers, 1944. **23**: p. 29-41.
20. Fagerlund, G., *Critical degrees of saturation at freezing of porous and brittle materials*. 1972, The Lund Institute of Technology: Lund, Sweden.
21. Fridh, K., *Internal frost damage in concrete Experimental studies of destruction mechanisms*, in *Department of Building and Environmental Technology*. 2005, Faculty of Engineering, LTH, Lund University: Lund. p. 276.
22. *CRC Handbook of Chemistry and Physics 93rd edition*, ed. W.M. Haynes. 2012.
23. Sellevold, E.J. and T. Farstad, *Frost/Salt-testing of Concrete: Effect of Test Parameters and Concrete Moisture History.* 1991.
24. Fagerlund, G., *Studies of the Scaling, the Water Uptake and the Dilation of Mortar Specimens Exposed to Freezing and Thawing in NaCl Solutions*, in *Freeze-Thaw and De-Icing Resistance*

of Concrete, G. Fagerlund and M.J. Setzer, Editors. 1992, Lund Institute of Technology: Lund, Sweden. p. 36-66.

25. Lindmark, S., *Mechanisms of Salt Frost Scaling of Portland Cement-bound Materials: Studies and Hypothesis*, in *Department of Building and Environmental Technology*. 1998, Faculty of Engineering, LTH, Lund University: Lund. p. 266.
26. Marchand, J., et al., *Influence of Chloride Solution Concentration on Deicer Salt Scaling Deterioration of Concrete.* ACI Materials Journal, 1999. **96**(4): p. 429-435.
27. Setzer, M.J., *Frost-attack on concrete - modeling by the micro-ice-lens model - evaluating by RILEM CIF test.* Creep, Shrinkage and Durability Mechanics of Concrete and Concrete Structures, 2009: p. 971-977.
28. Liu, Z. and W. Hansen, *Freezing characteristics of air-entrained concrete in the presence of deicing salt.* Cement and Concrete Research, 2015. **74**: p. 10-18.
29. Setzer, M.J., S. Palecki, and F. Tauscher, *Einfluss der NaCl konzentration auf das abwitterungsverhalten von beton unter frost-tausalzbelastung.* Forschungsbericht BAST, 2007.
30. Valenza II, J.J. and G.W. Scherer, *A review of salt scaling: II. Mechanisms.* Cement and Concrete Research, 2007. **37**(7): p. 1022-1034.
31. Valenza II, J.J., *Mechanism for Salt Scaling*, in *Civil and Environmental Engineering*. 2005, Princeton University. p. 362.
32. Powers, T.C., *The mechanism of frost action in concrete (Part II).* Cement, Lime and Gravel, 1966. **41**(6): p. 5.
33. Liu, Z. and W. Hansen, *A hypothesis for salt frost scaling in cementitious materials.* Journal of Advanced Concrete Technology, 2015. **13**: p. 403-414.
34. Setzer, M.J., H.-J. Keck, and S. Palecki, *Entwicklung eines prufverfahrens fur beton in der expositionsklasse XF2*, in *Berichte der bundesanstalt fur srassenwesen*. 2007, Brucken- und Ingenierurbau: BAST. p. 141.
35. Valenza II, J.J. and G.W. Scherer, *Mechanism for salt scaling.* Journal of the American Ceramic Society, 2006. **89**(4): p. 1161-1179.
36. Sun, Z. and G.W. Scherer, *Effect of air voids on salt scaling and internal freezing.* Cement and Concrete Research, 2009. **40**: p. 260-270.
37. Powers, T.C. and R.A. Helmuth, *Theory of volume changes in hardened portland-cement paste during freezing.* Proceedings, Highway Research Board 32, PCA Bull 46, 1953.
38. ASTM, *ASTM C457 / C457M - 12, Standard Test Method for Microscopical Determination of Parameters of the Air-Void System in Hardened Concrete*. 2012.
39. Powers, T.C. *The Air Requirement of Frost-Resistant Concrete*. 1949. Highway Research Board 29, PCA Bull 33.
40. Philleo, R., *A method for analysing void distribution in air-entrained concrete.* Cement, Concrete and Aggregates, 1983. **5**(2): p. 128-130.
41. Attiogbe, E.K., *Mean Spacing of Air Voids in Hardened Concrete.* Aci Materials Journal, 1993. **90**(2): p. 174-181.
42. Pleau, R. and M. Pigeon, *The use of the flow length concept to assess the efficiency of air entrainment with regards to frost durability: Part I - Description of the test method.* Cement, Concrete and Aggregates, 1996. **18**(1): p. 19-29.
43. Plante, P., M. Pigeon, and F. Saucier, *Air-Void Stability .2. Influence of Superplasticizers and Cement.* Aci Materials Journal, 1989. **86**(6): p. 581-589.
44. Pigeon, M., et al., *Influence of soluble alkalies on the production and stability of the air-void system in superplasticized and nonsuperplasticized concrete.* ACI Materials Journal, 1992. **89**(1): p. 24-31.
45. Hasholt, M.T., *Air void structure and frost resistance: a challenge to Powers' spacing factor.* Materials and Structures, 2012. **47**(5): p. 911-923.
46. Mielenz, R.C., et al., *Origin, evolution, and effects of the air void system in concrete. Part 1 - Entrained air in unhardened concrete.* ACI, 1958. **30**(1): p. 95-121.

47. Dubovoy, V.S., S.H. Gebler, and P. Klieger, *Cement-alkali level as it affects air-void stability, freeze-thaw resistance and deicer scaling resistance of concrete*, in *RD128, Portland cement association*. 2002: Skokie, Illinois, USA. p. 24.
48. Scrivener, K.L., A.K. Crumbie, and P. Laugesen, *The interfacial transition zone (ITZ) between cement paste and aggregate in concrete.* Interface science, 2004. **12**(4): p. 411-421.
49. Pang, B., et al., *ITZ properties of concrete with carbonated steel slag aggregate in salty freeze-thaw environment.* Construction and Building Materials, 2016. **114**: p. 162-171.
50. Wu, K., et al., *Microstructural characterization of ITZ in blended cement concretes and its relation to transport properties.* Cement and Concrete Research, 2016. **79**: p. 243-256.
51. MacInnis, C. and Y.R. Nathawad, *The effects of a deicing agent on the absorption and permeability of various concretes*, in *Durability of Building Materials and Components ASTM STP 691*, P.J. Sereda and G.G. Litvan, Editors. 1980, American Society for Testing and Materials: Ottawa, Canada. p. 474-484.
52. Hooton, R.D. and D. Vassilev, *Deicer Scaling Resistance of Concrete Pavements, Bridge Decks, and Other Structures Containing Slag Cement: Phase 2: Evaluation of Different Laboratory Scaling Test Methods*. 2012.
53. Boubitsas, D., et al., *Frost resistance of concrete - Experience from long term exposure*, in *Materials, Systems and Structures in Civil Engineering 2016*, M.T. Hasholt, K. Fridh, and R.D. Hooton, Editors. 2016, RILEM publications S.A.R.L: Technical University of Denmark, Lyngby, Denmark. p. 21-30.
54. Pigeon, M., et al., *Surface microstructure and scaling resistance of concrete.* Cement and Concrete Research, 1996. **26**(10): p. 1555-1566.
55. Bilodeau, A. and V.M. Malhotra. *Deicing salt scaling resistance of concrete incorporating supplementary cementing materials CANMET research*. in *Freeze-Thaw Durability of Concrete - rilem proceedings 30*. 1997. E & FN SPON.
56. Marchand, J., et al., *Effects of fly ash on microstructure and deicer salt scaling resistance of concrete*, in *Frost Resistance of Concrete*, M.J. Setzer and R. Auberg, Editors. 1997, E&FN Spon: University of Essen. p. 11-20.
57. Thomas, M.D.A., *Laboratory and field studies of salt scaling in fly ash concrete*, in *Frost Resistance of Concrete*, M.J. Setzer and R. Auberg, Editors. 1997, E&FN Spon: University of Essen. p. 21-30.
58. Bilodeau, A., et al., *Effect of Curing Methods and Conditions on the Performance of Fly Ash Concrete in De-Icing Salt Scaling*, in *Sixth CANMET/ACI International Conference on Fly Ash, Silica Fume, Slag, and Natural Pozzolans in Concrete*, V.M. Malhotra, Editor. 1998, ACI: Bangkok, Thailand. p. 361-384.
59. Zhang, M.H., et al., *De-Icing Salt Scaling of Concrete Incorporating Different Types and Percentages of Fly Ashes*, in *Sixth CANMET/ACI International Conference on Fly Ash, Silica Fume, Slag, and Natural Pozzolans in Concrete*, V.M. Malhotra, Editor. 1998, ACI: Bangkok, Thailand. p. 493-525.
60. CEN/TS, *CEN/TS 12390-9* in *Testing hardened concrete - Part 9: Freeze-thaw resistance - Scaling*. 2006. p. 24.
61. Baert, G., A.-M. Poppe, and N. De Belie, *Evaluation and comparison of mechanical characteristics and durability of concrete with different cement replacement levels by fly ash*, in *Cement Combinations for Durable Concrete*, R.K. Dhir, T.A. Harrison, and M.D. Newlands, Editors. 2005, MPG Books: University of Dundee, Scotland, UK. p. 787-797.
62. Marchand, J., M. Jolin, and Y. Machabée, *Deicer salt scaling resistance of supplementary cementing material concrete: laboratory results against field performance*, in *Cement Combinations for Durable Concrete*, R.K. Dhir, T.A. Harrison, and M.D. Newlands, Editors. 2005, MPG Books: University of Dundee, Scotland, UK. p. 579-590.
63. Bouzoubaâ, N., et al., *Deicing salt scaling resistance of concrete incorporating supplementary cementing materials: laboratory and field test data.* Canadian Journal of Civil Engineering, 2008. **35**: p. 1261-1275.

64. Nili, M. and M. Zaheri, *Deicer salt-scaling resistance of non-air-entrained roller-compacted concrete pavements.* Construction and Building Materials, 2011. **25**(4): p. 1671-1676.
65. Sun, C.T., W.H. Li, and B.R. Hou, *Study on Frost-Salt Resistance of Fly Ash Concrete.* Architecture and Urban Development, 2012. **598**: p. 432-437.
66. Ahani, R.M. and M.R. Nokken, *Salt scaling resistance – The effect of curing and pre-saturation.* Construction and Building Materials, 2012. **26**(1): p. 558-564.
67. Nowak-Michta, A., *Water-binder Ratio Influence on De-icing Salt Scaling of Fly Ash Concretes.* Procedia Engineering, 2013. **57**: p. 823-829.
68. Van den Heede, P., J. Furniere, and N. De Belie, *Influence of air entraining agents on deicing salt scaling resistance and transport properties of high-volume fly ash concrete.* Cement and Concrete Composites, 2013. **37**: p. 293-303.
69. Bouzoubaâ, N., et al., *Deicing salt scaling resistance of concrete incorporating fly ash and (or) silica fume - laboratory and field sidewalk test data.* Canadian Journal of Civil Engineering, 2011. **38**: p. 373-382.
70. Utgenannt, P., *The influence of ageing on the salt-frost resistance of concrete*, in *Department och Building and Environmental Technology*. 2004, Faculty of Engineering, LTH, Lund University: Lund. p. 346.
71. Strand, M.J. and K. Fridh, *Test Method for Salt Frost Scaling of Concrete using Climate Chambers with Air as Thermal Medium with an Upside Down Sample Setup*. Manuscript, Lund University.
72. Fagerlund, G., *The influence of slag cement on the frost resistance of the hardened concrete*. 1982, Swedish Cement and Concrete Research Institute: Stockholm.
73. C., A.I.R., *The effects of different cementing materials and curing on concrete scaling.* Cement, Concrete and Aggregates, 1994. **16**(2): p. 132-139.
74. Stark, J. and H.M. Ludwig, *Freeze-thaw and freeze-deicing salt resistance of concretes containing cement rich in granulated blast furnace slag.* Aci Materials Journal, 1997. **94**(1): p. 47-55.
75. Stark, J. and U. Knaack. *Freeze-deicing salt resistance of concretes containing blast-furnace slag-cement*. in *Freeze-thaw durability of concrete*. 1997. United Kingdom, London: E & FN Spon.
76. Deja, J., *Freezing and de-icing salt resistance of blast furnace slag concretes.* Cement and Concrete Composites, 2003. **25**(3): p. 357-361.
77. Lang, E., *Durability aspects of CEM II/B-M with blastfurnace slag and limestone*, in *Cement Combinations for Durable Concrete*, R.K. Dhir, T.A. Harrison, and M.D. Newlands, Editors. 2005, MPG Books: University of Dundee, Scotland, UK. p. 55-64.
78. Krishnan, A., et al., *Technical issues related to the use of fly ash and slag during late-fall (low temperature) construction season*. 2006, Indiana department of transportation, Purdue University. p. 358.
79. Boyd, A.J. and R.D. Hooton, *Long-Term Scaling Performance of Concretes Containing Supplementary Cementing Materials.* Journal of Materials in Civil Engineering, 2007. **19**(10): p. 820-825.
80. Panesar, D.K. and S.E. Chidiac, *Multi-variable statistical analysis for scaling resistance of concrete containing GGBFS.* Cement and Concrete Composites, 2007. **29**(1): p. 39-48.
81. Chidiac, S.E. and D.K. Panesar, *Evolution of mechanical properties of concrete containing ground granulated blast furnace slag and effects on the scaling resistance test at 28 days.* Cement and Concrete Composites, 2008. **30**(2): p. 63-71.
82. Giergiczny, Z., et al., *Air void system and frost-salt scaling of concrete containing slag-blended cement.* Construction and Building Materials, 2009. **23**(6): p. 2451-2456.
83. Panesar, D.K. and S.E. Chidiac, *Capillary suction model for characterizing salt scaling resistance of concrete containing GGBFS.* Cement and Concrete Composites, 2009. **31**(8): p. 570-576.

84. S., S. and R.D. Hooton, *Deicer Scaling Resistance of Concrete Pavements, Bridge Decks, and Other Structures Containing Slag Cement: Phase 1: Site Selection and Analysis of Field Cores*. 2008.
85. Skripkiūnas, G., et al., *The Cement Type Effect on Freeze – Thaw and Deicing Salt Resistance of Concrete.* Procedia Engineering, 2013. **57**: p. 1045-1051.
86. Taylor, P. and X. Wang, *Deicer Scaling resistance of Concrete Mixtures Containing Slag Cement*. 2014.
87. Helsing, E. and P. Utgenannt, *The salt-frost resistance of concrete with supplementary cementitoius materials (SCM)*, in *Materials, Systems and Structures in Civil Engineering 2016*, M.T. Hasholt, K. Fridh, and R.D. Hooton, Editors. 2016, RILEM publications S.A.R.L: Technical University of Denmark, Lyngby, Denmark. p. 51-60.
88. Löfgren, I., O. Esping, and A. Lindvall, *The influence of carbonation and age on salt frost scaling of concrete with mineral additions*, in *Materials, Systems and Structures in Civil Engineering 2016*, M.T. Hasholt, K. Fridh, and R.D. Hooton, Editors. 2016, RILEM publications S.A.R.L: Technical University of Denmark, Lyngby, Denmark. p. 91-100.
89. Standard, S., *SS 137003:2015 Concrete - Application of SS-EN 206 in Sweden*. 2015, Swedish Standards Institute. p. 52.
90. Jacobsen, S. and E.J. Sellevold, *Frost/Salt scaling testing of concrete - Importance of absorption during test.* Nordic Concrete Research, 1994. **14**: p. 26-44.

Appendix 1

Development of the method to test combinations of AEA and SP

To study the effect from various combinations of SP and AEA with various binder combinations, an effort was first made to recreate the foam-test made by Fagerlund [62] (presented on pages 40 to 42). Fagerlund developed and used this method to enable a fast and simple way of studying the foam stability of various AEA by extracting an electrolyte 15 after mixing started from a paste mix (AEA not added yet). Then the electrolyte was poured in to a 250 ml glass and based on the mass electrolyte, AEA was added in the correct mass to simulate the concentration that should have been in the concrete. These were then gently mixed w/o causing foaming, then a water reducer or SP was added, and lastly the glass was shaken in a standardized way. The height and degradation of the foam was then measured to see which combinations seemed to cause a collapse or to reduce the foam stability. The mixes that caused a collapse, or was considered to reduce the foam stability, could then be considered less suited to create an air void system that would increase the frost resistance.

This concept was taken and the test setup presented in Figure 1 below show the technique to extract the so called electrolyte. However, some things were changed from the method used by Fagerlund. The AEA and SP was added to the paste to force them to interact during the mixing process which would occur when the concrete was cast.

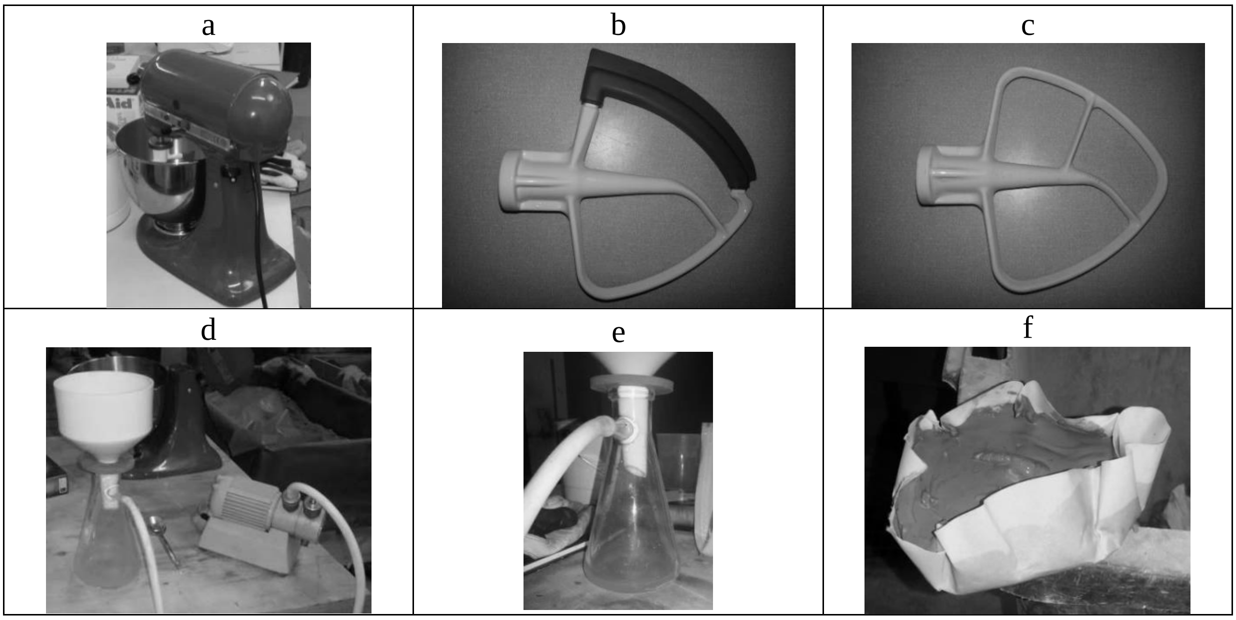

Figure 1. 1a shows the Kitchen aid used for the mixes. 1b show the mixer used for paste-mixes. 1c show the mixer used for mortar (0-8 fraction with paste) mixes. 1d show the setup which enables an extraction (by suction) of a liquid from the paste or mortar. 1e show approximately how much liquid is extracted during one test. 1f show paste inside a filter where the liquid have been extracted.

In Figure 2 below some results are shown from tests were water and an AEA was mixed to see how the mass of electrolyte could influence the results.

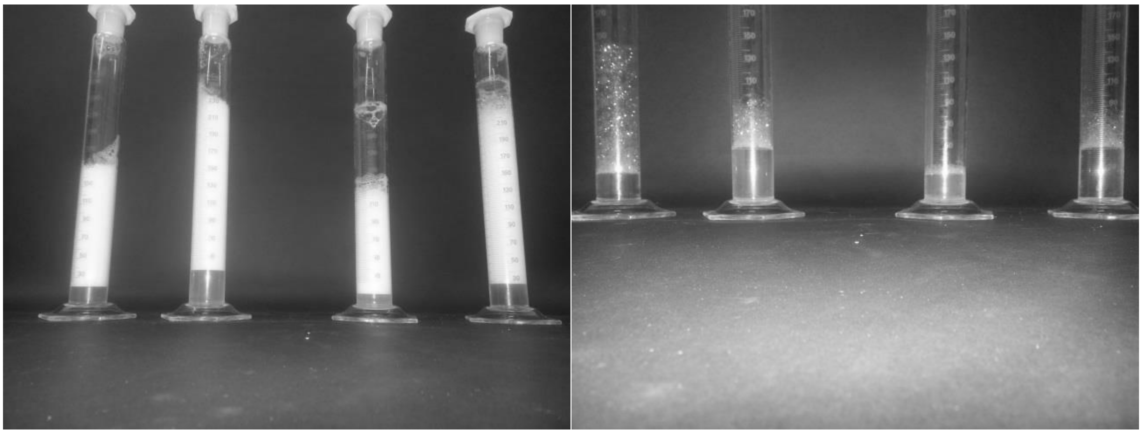

Figure 2. Left picture was taken 2014-02-12 kl 08:51. Right picture was taken 2014-02-12 kl 16:12
Mixes from the left to right: Total volume 25 ml, ”micro air 100”, diluted 1:19, Total volume 50 ml ”micro air 100”, diluted 1:19, Total volume 25 ml, ”micro air 100”, diluted 1:9, Total volume 50 ml ”micro air 100”, diluted 1:9

The time it took to weigh the material, mix, extract the electrolyte, wash and dry the equipment until the next recipe could be started was approximately 45 min. Then photographs needs to be taken at specific times during the mixing of the next batch which increase the time for the procedure. Another factor which was considered before was the evaluation of the results (pictures) where the height of the foam pillar inside the glass could be misleading. According to the pictures a better way would be to do image analysis where the fraction of pixels that where white would be plotted over time. However, before any development of image analysis code was done a decision was made to change the method to test AEA and SP combination to the method described in the methodology article.

Appendix 2 - Paper 1

International RILEM Conference on Materials, Systems and Structures in Civil Engineering
Conference segment on Frost Action in Concrete
22-23 August 2016, Lunds University, Lund, Sweden

METHODOLOGY TO ANALYSE THE SALT FROST SCALING MECHANISM(S) IN CONCRETE WITH DIFFERENT BINDERS

Martin Strand (1), Katja Fridh (1)
(1) Building Materials, Lunds University, Lund, Sweden

Abstract

The purpose of this article is to present a methodology which can be used to evaluate how the salt frost scaling mechanism(s) affects concrete with different air void systems. First, a test is made where the binder is mixed with various combinations of superplasticizer and air entraining agent to find one combination which performs well. The combination is then used when casting concrete to produce four air void systems, from approximately 1.5% to 4.5% in total air content, which are quantified with an air void analysis made on the hardened concrete. The concrete is sealed and hydrated until for over 300 days which results in a high degree of hydration for any binder. Then a salt frost scaling method is used with a temperature cycle which increases the salt frost scaling mechanism(s) load. The results present scaling from concrete with a high degree of hydration, regardless of hydration rate, and the effect the air void system has on the salt frost scaling damage in various binders given an even microstructure since each sample is fully hydrated. This enables a study of how various microstructures are affected by a constant load from the salt frost scaling mechanism(s) and of the salt frost scaling process.

1. Introduction

The purpose of this article is to present a methodology for a salt frost scaling analysis of close to fully hydrated binders with an analysis of the effect various air void systems has on each binder. The degree of hydration has a significant influence when analysing salt frost scaling resistance for different binders [1]. The binders with a slow rate of hydration will produce more scaling when testing after the same amount of time given equal conditions during the hydration. However, by allowing any binder to hydrate in sealed conditions for over 300 days salt frost scaling test results will give information about how the salt frost scaling mechanism affect various binders with fully developed microstructures. The air void system also has a significant effect on the salt frost scaling in concrete containing various binders, therefore it is interesting to study the effect from slight changes in the air void system for various binders.

This paper presents a description of the methodology used, starting with a method to find a combination of superplasticizer (SP) and air entraining agent (AEA) for each binder to enable the creation of various air void systems with small differences. These differences were then quantified by an air void system analysis (linear traverse). Then the article presents the hydration process and briefly mention the salt frost scaling test method which is presented in [2] together with some results from four casts of CEM I concrete. Lastly the methodology is discussed and conclusions are drawn.

2. Test of superplasticizer and air entraining agent combinations

The purpose of this test was to get indications of the difference in performance and learn about the risk of water separation for various combinations of admixtures (one AEA and one SP) given the same recipe (binder and aggregate fractions). The results then enable a choice of a AEA and SP combination (for each binder) which perform well and have a low risk for bleeding, which in turn enables a creation of various air void systems with only small differences. The test measured workability, the air content inside the fresh mortar, and a foam test which gives an idea of the risk for air voids to merge. The mortar recipe contained 2.000 kg binder, 6.000 kg of “0-8” aggregate fraction, and 0.800 kg water.

2.1 Method for the mortar tests

To enable an attempt to produce an acceptable workability for all binders, the AEA was mixed with the water, and then the superplasticizer was added. The following mixing procedure was used:

- The binder and aggregates were blended for 2.5 min ±5 sec
- Water was added and mixed for 2.5 min ±5 sec,
- Mixing continues for 2.5 min ±5 sec and a pipette was used to drip the superplasticizer in to the mix and stop when one of the following occurred
    - the workability looked acceptable.
    - bleeding started (before an acceptable workability was acquired).

The average recommended mass for each AEA was used. When mixing the concrete for the salt frost scaling test a smaller mass of AEA were used to get close to 5% air content. However, at this stage it was assumed that if a larger (average recommended) mass of AEA work well with a specific superplasticizer, then a smaller mass also will perform well.

2.2 Results from the mortar tests

After the mixing procedure was done the workability was measured with a Hägermann cone which is presented in Figure 1a. When the workability was measured the edge of the mortar was studied to look for indications of bleeding (Figure 1b and 1c). The indication of risk for separation was graded “clear”, “slight”, and “no” from visual observation.


1a 1b 1c

Figure 1. 1a) The Hägermann cone filled with mortar. 1b) When the edge of a mortar is considered to indicate no risk for water separation according to the grading system. 1c) A combination with clear risk for water separation, which happened before the mortar acquired an acceptable workability.

Then the air content was measured on 1 dm³ mortar 5 min after the mixer had stopped. Then circa 0.5 dm³ of mortar were put in to a bucket of water, slowly mixed and dispersed with a large spoon which enabled a comparison between the foam created at the surface when the air inside the mortar ascend. Two different results are shown in Figure 2. In Figure 2b less foam is created since the bubbles come up to the surface and bursts quicker than the bubbles in Figure 2a. The foam created for each mix was graded from zero to two from visual observation in combination with photographs.

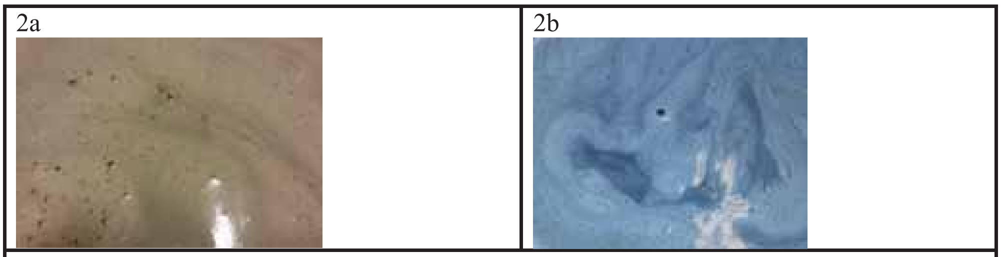
2a 2b

Figure 2. Both figures show an area of approximately 15x15 cm². 2a shows thick foam created at the surface with the foam rating 2. 2b shows less foam created with the foam rating 1.

The results from the admixture combination tests should be compiled according to Table 2. The results presented are from the variation where each of three AEAs has been combined with each of five different superplasticizers for the same binder. Since the recommended average mass of each AEA was used for all mixes, the total air content in the mixes with different SPs should only vary by a few percent if the SPs do not affect the air content.

According to the examples of results in table 2 there is clearly a wide spread of how well different combinations seems to work together with the binder. When evaluating the results a system was made to find the combination which seems to perform best out of the combinations which have been tested. First considerations were taken to the estimated risk for bleeding; the combinations that showed a clear risk were disregarded and focus was put on combinations considered to have no risk for water separation. Then the air content was studied by comparing the air contents for each AEA. As an example, when looking at AEA1 (in table 2) the combination with SP5 resulted in no risk for water separation, therefore approximately 12.5% was considered to be a minimum (or target) air content that the specified mass of AEA1 should result in when mixed with a SP with an acceptable interaction (i.e. the approximate minimum air content was decided depending on the results from a combination without bleeding). This means that SP4 was also considered since it only had a slight indication of water separation and air content above 12.5%. The third factor which was considered was the workability. Since the SP is added until it looked like the mortar had a workability which was approximately 150 mm (an approved flow-measurement was set to be 130 mm or more). The addition of SP was also stopped when the water started to separate from the paste, hence the mass of SP could become more than the maximum recommended amount. When focusing on the combinations which performed well, the results presented a strong correlation between no indication of separation, high air content and a larger volume of stable foam.

Table 2. Compiled results from the mortar test of one binder.

Combination	Indication of water separation	Air content [%]	Workability [mm]	Superplasticizer[1)] [%]	Foam
SP1[2)]+AEA1[3)]	Slight	9,6	170	112,0	1
SP2[2)]+AEA1	Clear	5,2	170	126,8	1
SP3[2)]+AEA1	Clear	7,2	175	126,5	1
SP4[2)]+AEA1	Slight	15,1	155	257,8	2
SP5[2)]+AEA1	No	12,5	170	196,7	2
SP1+AEA2[3)]	Clear	4,3	175	417,3	0
SP2+AEA2	Clear	6,0	165	244,8	1
SP3+AEA2	Clear	18,5	120	103,8	1
SP4+AEA2	Slight	5,2	150	318,0	1
SP5+AEA2	No	11,5	180	125,7	2
SP1+AEA3[3)]	Slight	13,5	225	65,0	2
SP2+AEA3	Slight	18,5	140	37,0	2
SP3+AEA3	Slight	15,0	185	33,0	2
SP4+AEA3	No	20,0	120	69,5	2
SP5+AEA3	No	21,5	130	68,3	2

[1)] Mass of superplasticizer used divided by mass of maximum recommended amount.

[2)] SP4 is based on a sulphonate melamine-formaldehyde condensate. The rest of the SPs is based on different modified polycarboxylates.

[3)] AEA1 and AEA3 are based on a synthetic detergent. AEA2 is based on Vinsol resin.

When a combination which performed well had been found from evaluating the results another complementing test was made to get an indication if this combination would release air over time from the fresh concrete. This was done by measuring the air content after 5 min (same as before), 30 min and 60 min on the same recipe as before. Results from these tests were also considered before a combination of AEA and SP for each binder was determined for the concrete recipe which was used for the salt frost scaling test. The measurements made on the combination SP5+AEA3 showed the air content between 17.0 and 19.0% for the three measurements and not indicating a decrease over time. This was considered a good result, therefore the combination was chosen without doing the same test with other combinations.

3. Concrete for salt frost scaling test

3.1 Recipe and casting the concrete

To keep the binder content close to 430 kg/m³ the mass of aggregates was adjusted with consideration to the anticipated air content. The anticipated air content was 1.5, 2.5, 3.5 and 4.5 % and the mass of AEA was adjusted with the goal for the measured air content in the fresh concrete to be close to the anticipated air content for each cast. The air content was measured in a 8 dm³ of the fresh concrete, which was approximately 35% of the total mass of concrete mixed. Considering that the air content measurement was made on a large fraction of the cast, the measurement should be a good indication for the entire cast. When casting the concrete the mass of superplasticizer was constant for the four recipes which resulted in a slump of more than 150 mm (when no AEA was added) to facilitate the casting.

3.2 Curing

To enable the tested binder to come as close as possible to fully hydrated conditions, the concrete was cured for 1 day inside a covered steel mould, 7 days submerged in water (approximately 20°C), and 300 days sealed inside a climate room with 20.0±0.1°C. The purpose of the relatively short hydration in water counteracted any early drying shrinkage at the same time as should have added a negligible additional mass of water to the concrete surfaces. Therefore the long hydration in the climate room was constantly 100% RH with a limited mass of water at the set temperature.

3.3 Air void analysis

The air void analysis was done with the linear traverse methodology, according to the ASTM C 457 standard method [3], with one sample per cast. Linear traverse measurements are done by scanning a sample with a small light beam and at the same time measure the reflection. It requires thorough sample preparations to get accurate results from the reflections. First the sample surface is polished, then it is coloured with a black paint and the air voids are filled with zinc paste. When the light beam hits the zinc there is a strong reflection and the machine starts to draw a cord (line), when the light beam has past the air void filled with zinc and is back on the surface painted black there is much less reflecting light and the cord is finished. When approximately 3.5 meters has been measured on a sample (100x150 mm²), calculations are made to estimate the air content, spacing factor and specific surface from all of the cords. In table 4 results from linear traverse measurements are presented for four casts of concrete with 100 mass% CEM I as binder. Cast #4 contained ca 0.015 mass% of the air entraining agent.

Table 4. Results from four casts made with 100% CEM I. The variables presented are calculated from the linear traverse analysis.

Cast	**Fresh Concrete [%]1)**	**Air void content**			**Air void content in paste**		**Specific surface**	**Spacing factor**
		Total [%]2)	**<2 mm [%]2)3)**	**<0.35 mm [%]2)4)**	**<2.00 mm [%]2)5)**	**<0.35 mm [%]2)6)**	**[mm^{-1}]2)7)**	**[mm]2)8)**
#1	1,10	3,6	0,8	0,3	2,3	0,9	15	0,76
#2	2,40	5,8	2,5	1,2	7,0	3,4	19	0,37
#3	3,50	5,2	3,9	1,7	11,1	4,9	19	0,30
#4	4,80	2,2	2,2	1,5	6,7	4,6	33	0,22

The results show that the specific surface increase and the spacing factor decrease when an increased mass of AEA is added to the mix. This trend is consistent when comparing the results from all voids and when looking at voids less than 2 mm. When all results was considered a general conclusion was drawn that the air void system was improved when the mass of AEA was increased.

4. Salt frost scaling test

4.1 Method

The salt frost scaling method is developed for the methodology described in this paper where concrete with a high degree of hydration and with various air void systems are tested. During development some factors were chosen to enhance the effect from the salt frost scaling damage e.g. the temperature cycle which is used has been shown to increase the salt frost scaling damage in comparison to the CDF-cycle [1, 4]. This enabled the present methodology to test how the salt frost scaling mechanism(s) is affected by different factors and the effect the mechanism(s) has on concrete with favourable conditions (high degree of hydration and various air void systems) with a high resolution while using climate chambers with air as a thermal conductor. This enables a study as to which properties have the biggest impact on concrete salt frost scaling resistance. These must be considered when varying the binders used for the concrete in structures which is exposed to de-icing salts and freezing temperatures. A detailed description is given in [2].

4.2 Scaling results

The figures below show scaling results from four CEM I concrete casts presented in table 4.

Figure 3 presents non-cumulative results from each separate cast including the mean scaling from all (six) samples together with the standard deviation. In [2] an argument is made that the salt frost scaling method contributes to a relatively constant salt frost scaling load. Considering this with the fact that Figure 3 shows non-cumulative results with measurements of the total scaling per seven cycles, the general gradient of the curve highlights information about an acceleration or deceleration of the scaling damage.

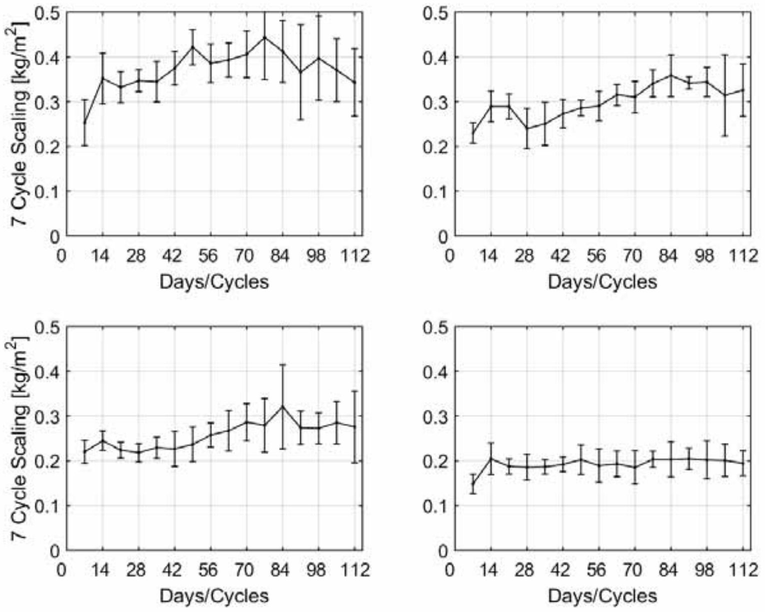

Figure 3. Scaling results measured at each measurement occasion (not cumulative). The line presents the mean scaling from the six samples from each cast after 112 cycles. The error bars present the standard deviation for the six samples at each occasion measurements were done. Upper left show the results from cast #1. Upper right show the results from cast #2. Lower left show the results from cast #3. Lower right show the results from cast #4.

Figure 4 presents a compilation of all mean values of the results, 4a non-cumulative and 4b cumulative. Both highlight the decrease in salt frost scaling damage when improving the air void system, however, they should be presented together to complement each other. 4a shows indications of acceleration and the rate of the salt frost scaling process, while 4b highlights distinctions between each cast at the same time as it presents the total average scaling.

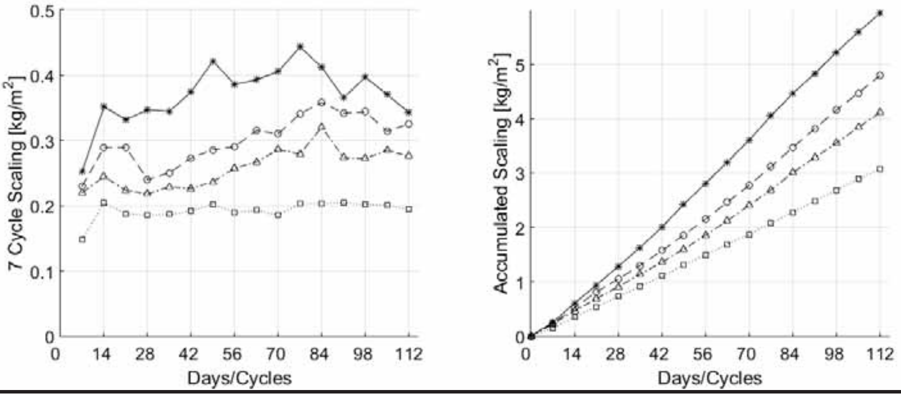

Figure 4. The average mass of scaling for one sample for each cast. 4a shows scaling measured at each measurement occasion. 4b shows the cumulative mass of scaling.

Figure 5 shows a general summary of the results by presenting the total average mass of scaling for all samples, and the error bars show the total mass of scaling from the sample with the most and least mass of scaling after 112 cycles from each cast. This highlights the decrease in salt frost scaling damage, but a slight con is that there is no information provided about the salt frost scaling process for each material.

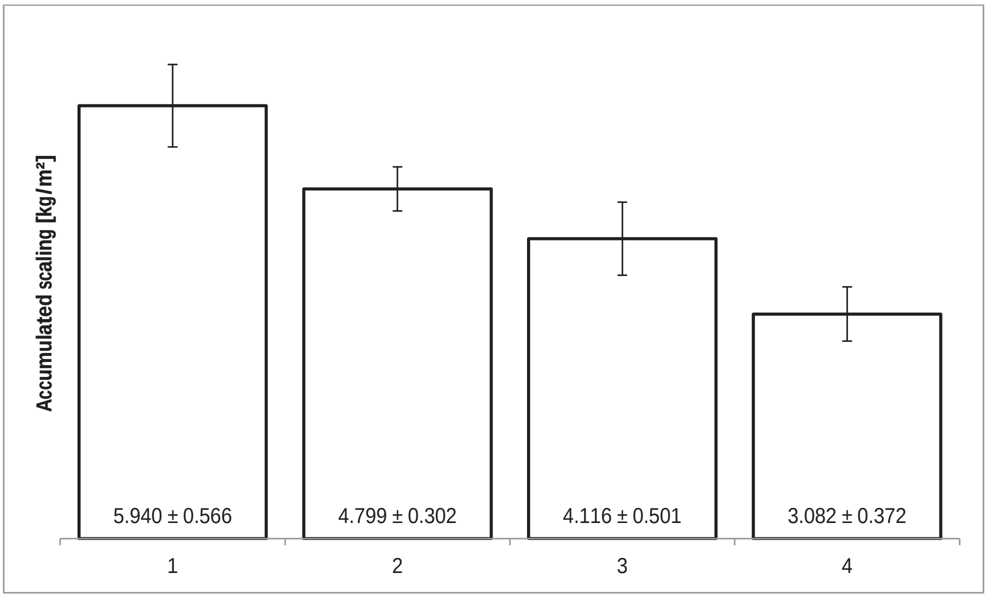

Figure 5. The numbers present the average mass of scaling per sample (6 samples per cast) after 112 cycles. The error bars present the total mass of scaling for the sample with the most and least mass of scaling after 112 cycles.

5. Discussion

When analysing the results from the mortar test, air void analysis and salt frost scaling test it is clear that they seem to agree with three main ideas. First, the mortar test showed that the combination of AEA and SP is vital for minimizing the risk of bleeding and to enable the creation of a relatively stable air void system. Secondly, the results from the air void analysis show that it is also possible to create slightly different air void systems by changing the amount of AEA when using the combination from the mortar test. Finally, by testing concrete which have been sealed for a long time all samples from the same batch will have a high degree of hydration with little variation. This means that the microstructure will not change due to hydration during the testing which contributes to more constant conditions for the material during the test. By using the salt frost scaling method with a high precision and presenting the results according to the diagrams used in chapter 4, the air void systems effect on the salt frost scaling damage on the concrete can be observed for the binder (or binder combination) of interest.

Considering results presented in the current article, the methodology is considered to contribute information of the salt frost scaling mechanism(s) and how it affects various binders given favourable conditions. When a binder is hydrated according to this methodology it will be as close to fully hydrated as can be, given the water binder ratio used. When testing cast #1 (which is the fully hydrated concrete, only containing a SP which provides an excellent workability) with a salt frost scaling method which contributes a relatively constant salt frost scaling load, a non-accumulative and cumulative baseline is acquired for the binder's (or concrete's) salt frost scaling resistance. When this baseline for the binder is known, the impact in salt frost scaling resistance from adding AEA and thereby improving the air void system can then be measured for the specific binder. The salt frost scaling method used also contributes information about the salt frost scaling process over time for the binder.

5.2 Future studies

To obtain more information about the salt frost scaling mechanism(s) and how it varies for concrete with various properties (e.g. concrete containing different SCMs) a grading analysis should be made on the scaled material. The grading will contribute more information about how the average size of the scaled material varies from the beginning of the test until the end of the test, which will give information about the salt frost scaling process. This would also enable an analysis of how the average scaling size varies when the air void system changes. When considering different additives it would be interesting to compare the difference in average scale size between different additives.

Additional salt frost scaling tests should be made with AEA and SP combinations which do not seem to perform well according to the first mortar test results. This would acquire more information about the effectiveness and reliability of the mortar test used. It would also give a better comprehension about the difference in scaling for the salt frost scaling method which increases the mass of scaling damage and enhance knowledge about the salt frost scaling mechanism(s). The results from these complementary tests could also give information about the robustness of a certain binder to various admixtures combinations.

Since the salt frost scaling test method which has been used differs from the standard methods the following should be noted. This method is designed to contribute to a large amount of scaling damage from the salt frost scaling mechanism(s) and provide a higher resolution in the results when testing concrete with a water binder ratio of 0.40 (which could concrete considered when building e.g. a bridge). This means that any claim of a limit for the mass of scaling for a concrete to be considered salt frost scaling resistant cannot be made without much more testing preferably with a lot of field tests to verify the lab results. Another option could be a large round robin test where concrete with various salt frost scaling resistances is tested according to the method presented in [2] together with some of the standard methods [5, 6]. This would provide information about how the salt frost scaling method used in this methodology compares to the other methods, considering relative mass of scaling when testing concrete with the same binder/binder combination. The results would also show if all methods give the same indications about how the salt frost scaling damage increase or decrease when testing various factors, e.g. when varying binder combination, binder content, or air content in the same binder.

6. Conclusions

- The methodology enables a study of the salt frost scaling mechanism(s) in concrete with a high degree of hydration which contributes to an optimal microstructure for any binder regardless of hydration rate. Therefore more constant material conditions during the salt frost scaling test in comparison to tests of young concrete.
- This methodology enables an analysis of how differences in the air void system affects the mass of salt frost scaling damage from a relatively constant salt frost scaling mechanism(s) load for a concrete with a given microstructure.

References

[1] Sjöbeck H (2015) The time dependency of salt-frost damage at low temperature on concrete with SCMs. Lund University, (in Swedish), Master of Science thesis, https://lup.lub.lu.se/student-papers/search/publication/7454864

[2] Strand MJ (2016), Salt frost scaling in uncarbonated concrete containing fly ash and slag with various air void contents, Licenciate thesis, Lunds University, TVBM 3181

[3] ASTM (2012) ASTM C457 / C457M - 12, Standard Test Method for Microscopical Determination of Parameters of the Air-Void System in Hardened Concrete.

[4] Jacobsen S, Saether DH, Sellevold EJ (1997) Frost testing of high strength concrete: Frost/salt scaling at different cooling rates Materials and Structures/Materiaux et Constructions 30:33-42

[5] Setzer MJ, Fagerlund G, Janssen DJ (1996) CDF Test - Test method for the freeze-thaw resistance of concrete - tests with sodium chloride solution (CDF) Materials and Structures 29:523-528 doi:10.1007/bf02485951

[6] SS137244 (2005) Concrete Testing – Hardened Concrete – Scaling at freezing, Swedish Standards Institute, (in Swedish) 10 p.

Appendix 3 – Paper 2

Test Method for Salt Frost Scaling of Concrete using Climate Chambers with Air as Thermal Medium with an Upside Down Sample Setup

Martin Strand, Katja Fridh

Division of Building Materials, Lund University, Lund, Sweden

Corresponding author's info.

E-mail: martin.strand@byggtek.lth.se

Telephone: (+46)7 02 95 68 75

Abstract

This article presents a salt frost scaling test method which can be used to study the salt frost scaling mechanism(s). An effort has been made to remove or minimize factors increasing the variations in the results due to the method. This includes minimizing the variation in temperature cycles for different samples when a climate chamber with air as thermal medium is used. The method has been tested on concrete with three different binder combinations which was hydrated in sealed conditions for two different time periods. All concrete was tested with three temperature cycles, the one used in the presented method and with two modified cycles. The results show that the mass of scaling is larger for samples with a shorter period of sealed hydration for each binder. The amount of scaling damage also increases when prolonging the time of which the concrete is exposed to the minimum temperature during the freezing period. In conclusion, the method is considered credible and time- and cost efficient which enables a quantitative and qualitative analysis of concrete which can be considered when building structures exposed to de-icing salt and freezing temperatures, i.e. with water binder ratio ≤0.40. The precision of the method makes it possible to analyse the salt frost scaling mechanism(s) with concrete containing various binder combinations and how the salt frost scaling mechanism(s) is affected by factors such as concrete with different degrees of hydration and various freeze-thaw cycles.

Keywords: Concrete, Salt frost scaling, Test method, Temperature cycle, Supplementary cementitious materials (SCMs)

Acknowledgement

This research was carried out with the financial support of SBUF (The Development Fund of the Swedish Construction Industry) and Cementa AB (a part of Heidelberg Cement Group). We gratefully acknowledge the support from Henrik Sjöbeck who tested the method in his Master thesis. Additional thanks to Sture Lindmark and Peter Utgenannt who contributed with some important input during the development of the method and sample setup.

1. Introduction

Concrete is the most common building material in the world but every kilogram of standard concrete produced results in approximately 0.130 kg of carbon dioxide emissions (Scrivener 2014). This means that approximately 5 to 8% of all manmade CO_2 emissions are produced by the cement industry (Scrivener 2014). To reduce the emissions the industry increases the extent of blending supplementary cementitious materials (SCMs) in to the ordinary Portland cement (OPC). Fly ash and blast furnace slag (waste products from coal power plants and the iron and steel industry) are two commonly used SCMs. However, when SCMs are added, the concrete properties change and this will influence the durability of the concrete. One important form of deterioration that can occur in countries where the climate cycles between freezing and thawing temperatures is salt frost scaling. This superficial damage occurs when a de-icing salt water solution freezes in contact with concrete and results in scaling of the concrete surface. If the concrete cover protecting the reinforcement is damaged by scaling it decreases in thickness. This leads to a decrease in the time needed for the concrete cover to carbonate, and for the chloride ions to reach the reinforcement, which results in a high risk for corrosion to initiate. This deterioration results in a need for more frequent repairs, and thereby higher repair costs, and a shorter service life. Consequently it is important to study how each SCM in different concentrations affects the salt frost scaling mechanism(s) and the durability of the concrete. To be able to do this the salt frost scaling method presented in this paper has been developed.

To estimate the salt frost scaling resistance there are standardized methods available where concrete samples are put in contact with a salt solution which is frozen and thawed. When the concrete has been exposed to a certain number of freeze-thaw cycles, the surface is brushed and then the dry mass of the scaled material is weighed. If the mass of scaled material after a specified number of cycles is less than a certain amount (this amount varies since the standard methods differs), the concrete will be considered salt frost resistant. There are a significant number of studies which form the foundation of the standardized methods (Powers 1955; Setzer et al. 1996) and the current knowledge about the salt frost scaling mechanism(s) (Lindmark 1998; Liu 2014; Powers 1966a; Powers 1966b; Utgenannt 2004; Valenza II and Scherer 2007a; Valenza II and Scherer 2007b; Verbeck and Klieger 1957).

Research concerning the salt frost scaling mechanism(s) has shown that the features of the temperature cycle during the freeze-thaw test affect the amount of scaling damage. These features are divided in to three parts in the current article, the minimum temperature, the temperature gradient and the time samples are exposed to the minimum temperature. According to Sellevold and Farstad (1991), Petersson (1994), Studer (1997) and Lindmark (1998), the scaling increase when the minimum temperature decrease. Results from Jacobsen et al. (1997b) indicate that a lower temperature gradient increase the salt frost scaling damage in concrete without any air entraining agent, he also found that a prolonged exposure time to the minimum temperature increase the damage. However, regarding the affect from the temperature gradient some results from Lindmark (1998) and Jacobsen et al. (1997b) seems contradictory. Results presented by Lindmark (1998) indicate that a low freezing gradient with a short time at the lowest temperature cause a smaller mass of scaling damage than a high temperature gradient with a long exposure time to the minimum temperature while Jacobsen et al. (1997b) found the opposite. This information about how the temperature cycle affects the salt frost scaling mechanism(s) implies that the amount of scaling from different methods (using different cycles and sample setups) should not be compared. However, the results from different salt frost scaling methods should provide the same indication of relative salt frost scaling damage when testing different factors.

Jacobsen et al. (1997a) and Utgenannt (2004) have studied the affect preconditioning have on the scaling results. Jacobsen et al. (1997a) concluded that different degrees of dehydration affects the scaling in different ways while Utgenannt (2004) concluded that the carbonation of concrete is another important factor which must be considered when presenting salt frost scaling results. Therefore all samples must be preconditioned in the same way to enable a relative comparison between scaling results from different samples.

The focus for the present work has been to minimize the risk for errors and variation in results due to the method, e.g. leakage of solution and large variation in the temperature cycles between samples. A combination of low variation in results (high precision) together with an aggressive temperature cycle could contribute to a high resolution, i.e. an increased contrast in the results for different materials. This could enable studies of how different factors are affected by the salt frost scaling mechanism(s) which will contribute to more information and a better understanding of the deterioration mechanisms. The paper contains information about the tests conducted during the development phase, the final version of the method, results from testing the method, a discussion about the method and conclusions drawn.

2. Description of Method

In this section a description of the sample setup, freeze-thaw cycle and measurements procedure is presented together with some of the tests conducted during the development. When testing and adjusting the setup, the goal was to minimize the risk that the method would increase the variation in results at the same time as making the measurement procedure as consistent and time efficient as possible. Comparisons will be made to the Swedish SS137244:2005-method (SS137244:2005) and the German CDF-method (CEN/TS 12390-9:2006), but other previous research also contributed with inspiration when designing the present salt frost scaling setup (Fagerlund 1982; Lindmark 2010; Utgenannt 2004).

2.1 Sample Setup and Equipment

First it was decided to have an upside down sample setup since this removes the risk for the solution to leak from the test surface. An upside down setup also contributes to a higher thermal conductivity in comparison to the SS137244:2005-standard method, which has the solution on top of the concrete surface together with an air layer and a plastic film on top which stops the water from evaporating. The CDF standard method is also upside down, where the samples stand on distances and the test surface is submerged in to a 3 mass% NaCl solution.

The sample size, shown in Figure 1a, was set to be 100 mm in diameter and 50 mm thick resulting in a mass less than 1 kg per sample which made the sample easy to handle. To draw any conclusions from a salt frost scaling test results the total test surface area should be as big as possible, this mean that the number of Ø100 mm samples should be enough to give a strong indication regarding the precision of the method. The SS137244:2005-standard method use at least four samples with the test surface area 150x150 mm² per sample, and the CDF method use a minimum of five samples with the test surface area approximately 140x150 mm² (CEN/TS 12390-9). However, when testing concrete from an existing structure the recommend test surface area according to SS137244:2005 is six cylinders with a diameter of 100 mm. When deciding the minimum amount of samples per concrete recipe considerations must be taken to that fact that a larger test surface (more samples) will enable fewer recipes to be tested during the same period. The minimum criterion allowed by the standard (6 samples with Ø100 mm) was therefore set as the minimum required amount of samples per concrete recipe in the presented method.

Given the premise that climate chambers with air as thermal medium would be used, some sealant was needed to stop the solution from evaporating. This led to the use of insulation which works as a sealant at the same time as it creates a one dimensional heat flow at the surface of the concrete, according to Figure 1a. The XPS insulation used has a dry thermal conductivity of 0.035 W/(mK), a dry density of 28-42 kg/m³, and a vapour permeability of $0.25 \cdot 10^{-6}$ to $0.30 \cdot 10^{-6}$ m²/s according to information given by the producer.

When using an upside down sample setup for a salt frost scaling test, consideration must be taken with regard to the extra scaling which occurs along the edges of the sample (in contact with the adhesive according to Figure 1a) to minimize the variation in results. Fagerlund (1982) solved this problem by having a smaller cup inside a larger cup which separated the edge scaling. Another way of dealing with the additional scaling from the edges is to reduce it by fastening e.g. rubber with adhesive along the sides of the sample. This technique is commonly used with upside down setups, e.g. the CDF-method, and was also chosen to be used in the presented method according to Figure 1a. This does not remove the edge scaling completely but it is greatly reduced, as was concluded from tests made during the development of the present method where a comparison was made between nothing on the sides and a combination of six various adhesives and one type of rubber.

The choice of adhesive used to fasten the rubber sheet to the concrete sample was selected after the effectiveness of six different types had been tested. Two samples were prepared with each type of adhesive from the same cast of concrete. A SMP-polymer based adhesive was chosen which had good adhesion and the least mass of edge scaling after 14 cycles. The adhesion could be improved when the sides of the concrete samples had been brushed with a steel brush before fastening.

With the use of 3 mm ethylene propylene diene monomer (EPDM) rubber (120±20 kg/cm³) on the side, the samples could be squeezed into the insulation which is shown in Figure 1a. According to the technical data sheet for the rubber, the SHORE hardness 00 according to “ASTM D 2240” was 50±5. This removes air movements caused by convection around the samples and removes the need for supports for the samples stand on which interferes with the surface.

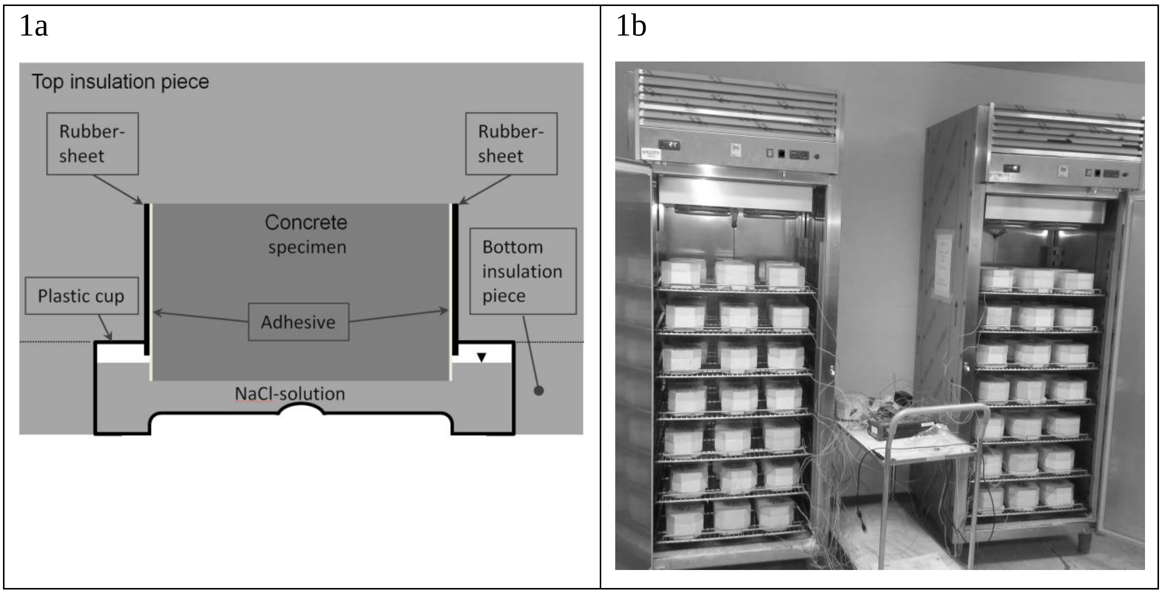

Figure 1. 1a presents the cross section of the sample setup. The insulation shape around the sample resembles an octagon. The insulation thickness above the sample is about 30 mm and the thickness around the sample is 25±5 mm. The insulation thickness around the plastic cup is about 12±2 mm. The top insulation together with the sample is resting on the plastic cup and the insulation surrounding it. 1b show the setup inside the freezers.

The removal of convection around the samples also contributes to a more defined one-dimensional heat flow according to measurements made with three samples where three thermocouples were cast inside the centre of each sample. The first was placed about 10 mm from the bottom surface, the second in the middle and the third about 10 mm from the top surface of the sample. The measurements confirmed that the temperature cycle for the top of the sample, closest to the insulation, was delayed during freezing and thawing in comparison to the temperature in to bottom of the sample closest to the NaCl solution. Results from the thermocouples inside the samples showed consistent temperature cycles at each depth.

After testing different plastic- and glass cups of different sizes, a polypropylene plastic cup with a diameter of 118 mm was chosen to be used as a container for the NaCl solution.

During the measurements all samples were weighed to monitor the absorption for each sample to look for any indication of a relation between absorption and scaling for different concrete recipes. To enable a fast measurement with this setup the sample was weighed with the insulation above the plastic cup, the adhesive and the rubber. Therefore a test was made to see how much moisture the rubber and insulation absorbed when going from a dry state to direct contact with water for seven days. The total absorption from the rubber and insulation was measured to be approximately 0.1 g/week, which was considered negligible when measuring absorption of the sample. According to the technical data sheet for the rubber the water absorption is 0.13% when tested with “ASTM D 1056–3min”.

After testing four different paint brushes, one with synthetic straws which had the highest straw density (estimated to 2800 straws/cm²) out of the four was chosen. The straws were cut to 2.0 to 3.0 cm in length which made them stiff enough to remove loose scaling in a fast way and flexible enough to bend and go in between stones that stuck out from samples with a large amount of scaling damage.

Research has shown that there exists a pessimum salt concentration which maximizes the salt frost scaling damage in concrete (Arnfelt 1943; Verbeck and Klieger 1957). This pessimum concentration, which is approximately 3 mass%, is used in all standard tests, and was also used with the current method, with de-ionized water.

2.2 Temperature Cycle

The temperature cycles created in the salt solutions are a result of cycling the thermal medium (air) between two temperatures inside the climate chamber, which is also done in the SS137244:2005-method. The settings used with the climate chambers in this method are +20 °C for 12 h and -25 °C for 12 h, which result in an air temperature inside the freezer of +20 °C to +24 °C and -25 °C to -21 °C. The average temperature in the air during the thawing period was +22 °C, and -23 °C during the freezing period. These settings differ from the settings used in SS137244:2005 where the freezing time is longer and thawing time shorter. The minimum temperature was set to freeze the solutions below the eutectic point of a NaCl solution which is -21.12 °C. By setting the temperature slightly lower than the eutectic point (-25 °C) in the climate chamber, the temperature gradient is kept relatively high (see Figure 2) from the freezing begins until the eutectic point which means that the variation in the time samples are exposed to temperatures below -21 °C was kept short. This setup for the freezers results in more than 8 h for the scaling measurements to be made without interrupting the freezing period.

Some tests were made to optimize positioning of the samples inside the climate chamber where the number of shelfs and samples per shelf were varied. The goal was to acquire the maximum number of samples, at the same time as the circulation of air was high enough to get a minimized variation in temperature cycle between all samples, for each climate chamber. Thermocouples were used to measure the temperature inside the NaCl solutions. One practical factor considered was that a larger space (≥6 cm) between the top of samples and shelf above simplifies the handling of the shelfs and the samples during the measurement procedure which reduce risk for spillage of solution. The best positioning (out of the tested shelf setups inside a freezer) was found to be nine samples (3 rows with 3 columns) per shelf with seven shelfs per climate chamber which results in 0.495 m² test surface (63 samples of Ø100 mm) according Figure 1 (1b). When compared to the SS137244:2005-method, the same climate chamber is used and the (normal) total test surface area is 0.630 m² (28 samples of 150x150 mm²). If more samples are put in the same climate chamber there is a risk for bigger temperature variations since the air circulating inside becomes more obstructed. When compared to the CDF method the bath which is used can contain 0.225 m² (10 samples of 150x150 mm²) test surface area. However, the CDF uses a 12 h cycle (the presented method and the SS137244:2005-method has 24 h cycles) which means that 0.450 m² can be tested during 56 days for a comparable standard SS137244:2005-method test.

The accuracy and precision of the thermocouples was measured at -10 °C and -20 °C in an insulated container with water. The accurate value is assumed to be the mean value of all thermocouples measurements at each time measurements were made. This enables a calculation for each thermocouple of how much the average deviation is from the accurate value. The mean deviation is calculated for all measurement at -10 °C and -20 °C, which then enables a calculation of the overall average deviation. This average deviation is added as a constant correction factor for each thermocouple to the raw data. These factors varied between -0.5 °C to +0.2 °C.

Temperature measurements were done for all positions on the seven shelfs during one week and the sample in the middle on each shelf has been measured continuously. Some of the results are presented in Figure 2 which shows measurements (for two separate weeks) made on the fourth and seventh shelf during the freezing period of temperature cycles. These two shelfs where chosen to show an indication of the variation in temperature cycles for different samples. Shelf number four was in the middle of the climate chamber and shelf number seven was in the bottom of the climate chamber. The fans distributing the air inside the climate chamber are positioned in the top which means shelf number seven is furthest away from the fans.

All diagrams in Figure 2 show the freezing period. A4 and A7 present the highest, lowest and mean temperatures measured during seven cycles for all samples on the fourth (middle) and seventh (bottom) shelf. B4 and B7 present the temperature cycles for the nine salt solutions on each respective shelf during one freeze cycle of the week. C4 and C7 present all measurements during seven cycles for the samples in the middle on both shelfs. It should be noted that the thawing period last for as long as the freezing period, i.e. 12.0±0.5 h, and during this time the test surfaces are in constant contact with the NaCl solution.

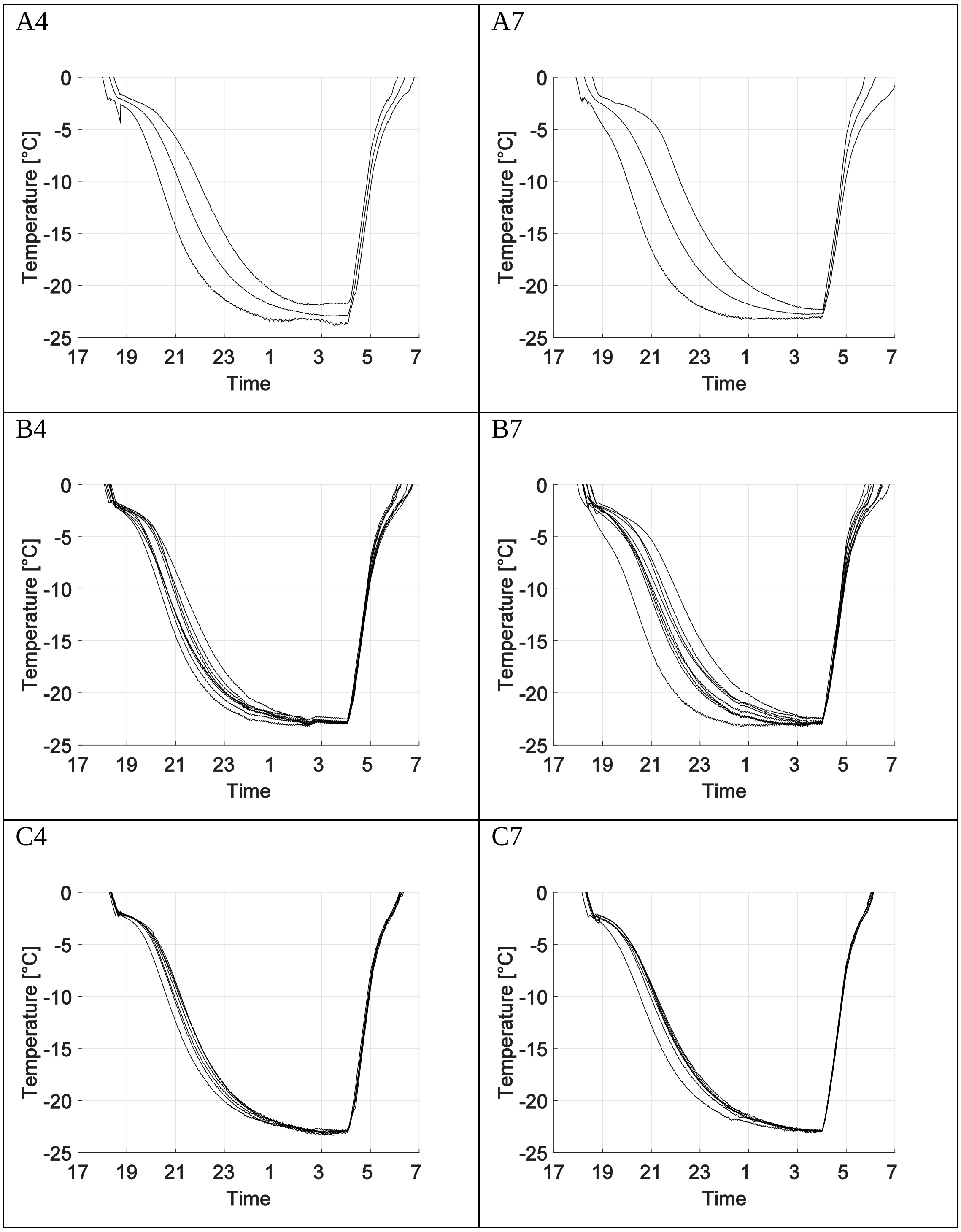

Figure 2. All figures only show the freezing periods measured inside the salt solutions.

“A-“ present the highest, lowest and mean temperatures during seven cycles for all samples on the specified shelf.

“B-“ present temperature cycles for all samples on the same shelf during one freeze cycle.

“C-“ present all measurements during seven cycles for the sample in the middle on the shelf.

“-4” is shelf 4 (middle in Figure 1b) and “-7” is shelf 7 (bottom in Figure 1b).

In Table 1 the freezing periods presented in Figure 2 are described with four parameters. These are the mean freezing rates, maximum freezing rate, the variation in minimum temperatures, and the different time spans when samples are exposed to temperatures below -21.1 °C. The mean freezing rate is defined as the average rate between -1.8 °C, when the solution begins to freeze, and the eutectic point at -21.1 °C. The maximum freezing rate is defined as the average rate between -10.0 and -11.0°C.

Table 1. Freezing rate and time samples are exposed to the minimum temperature in Figure 2.

Fig. 2	**Mean freezing rate [°C/h]**		**Variation in minimum temperature [°C]**	**Hours samples are exposed to T≤-21 °C**
	-1.8<T<-21 °C	**-10<T<-11 °C**		
A4	-3.0 to -4.4	-5.0 to -7.5	-21.9 to -23.8	3.0 to 5.5
A7	-2.8 to -4.6	-5.7 to -7.2	-22.3 to -23.2	2.5 to 5.5
B4	-3.0 to -4.4	-5.7 to -7.5	-22.6 to -23.2	3.5 to 5.5
B7	-2.8 to -4.6	-5.2 to -6.5	-22.4 to -23.1	2.5 to 5.5
C4	-3.4 to -3.8	-5.8 to -7.1	-22.9 to -23.3	4.2 to 4.8
C7	-3.5 to -3.9	-5.3 to -6.3	-22.9 to -23.1	3.5 to 4.5

When observing the measurements it is important to note that each measurement is in one point inside the salt solution. The difference in mean temperature cycles (middle curves) according to A4 and A7 is negligible and the majority of temperature cycles barely differ from these mean cycles. The change in gradient at approximately -1.8 °C is due to the exothermic phase change of the water in the NaCl solution freezing.

According to the SS137244:2005-method, the minimum temperature can vary from -18 to -22 °C and the exposure time to the minimum temperature during the cycles can vary from 0 hours to approximately 7 hours depending on the temperature. The CDF method has a bath which contributes to a small variation in temperature cycle. The allowed temperature during the minimum temperature (-20 °C) is ±0.5 °C, and the temperature gradient during freezing and thawing is -10 °C/h with an acceptable temperature deviation of ±1.0 °C.

2.3 Measurement procedure

By mixing a total of 5000.0±0.10 g of salt solution, consisting of 4850.0±0.05 g deionized water and 150.0±0.05 g of NaCl(s), measurements could be made on 48 samples and each salt solution could be replaced. This means that the 48 samples acquire the same concentration contributing to equal conditions for the salt frost scaling mechanism(s).

Filters used to collect the scaling damage were marked with sample name and the total number of cycles each sample had been exposed to. This enabled an easy way of storing all of the scaled material from each measurement occasion.

Each samples test surface were brushed about 15 to 25 times in four perpendicular directions, fewer times when there were less scaling and vice versa. After the surface had been brushed it was rinsed with tap water. The NaCl solution and scaled material in the plastic cup was poured into a filter together with the scaling that came off from the brushing the sample. The dry masses were then acquired by placing the filters inside an oven at 105±5 °C. For a filter containing scaled material with a total weight of 3.5 g (which is higher than the average mass after 7 cycles for all measurements), the minimum time for drying was determined to be 5 h inside the oven to dry all free water. During the test the filters was weighed after drying for about 18 to 22 h in 105±5 °C. The dry weight of the scaled off concrete was recorded with a balance which had a precision of ±0.0005 g. The mass of the sample, including the insulation, rubber sheet and adhesive, was recorded after the excess water from rinsing the sample had been dried with paper. The balance used for the sample weights had a precision of ±0.05 g. Before the sample was placed back in to the new solution in the cup, a mould was used to make sure the concrete test surface was 1 cm from the insulation to ensure about 2 mm of all samples were submerged in to the solution. To enable a quick way of filling the cups with 100±2 ml of 3 mass% NaCl solutions a 100 ml plastic syringe is used.

To minimize the risk of mixing up samples during the measurements, and at the same time minimizing the variation in temperature cycle for each sample, all samples were kept in the same position inside the climate chamber during all cycles.

The measurements was made once every week to get information regarding an acceleration or deceleration in the salt frost scaling process and enable a fast intervention if e.g. a power outage occurred.

2.4 Factors from the Method Affecting the Results

In the following section the factors which are considered to have the biggest influence on the results are noted. However, all of these are considered negligible which means that the variations which can be noticed from the results are due to the natural variation in the material. One important factor affecting the natural variation is how much of the test surface was covered with large salt frost resistant aggregates and how much was covered with paste which contributes to most of the scaling.

There were some random occurrences of the sample not touching the surface of the solution after 7 cycles. This occurred at approximately 2.5% of the measurement instances when using the method. This did not occur every week and when it did, the amount of scaling was similar to, or more than, the amount from the previous week suggesting that only a few or none of the seven cycles were effected.

There is an edge effect which makes the samples scale off more along the edges. Concrete with lower salt frost resistance, with a higher amount of scaling damage, are affected more by this edge phenomenon which could increase the contrast between high and low frost resistance. However, the edge effect seems to be proportional to the total amount of scaling for all samples which means that all samples are affected consistently.

When NaCl solutions with the scaling from the cup were poured in to the filter some of the salt seemed to have stayed in the filter and contributed to a larger variation in mass of the filters. The increase in variation due to the salt in the filters was up to ±0.01 g which is generally less than 2% of variation since the average scaling per week was more than 1 g, therefore considered insignificant.

Since there are so many local differences in properties affected by the micro structure and the variation in the air void distribution, salt frost scaling test methods can only give an indication of potential salt frost resistance from testing many samples, or a large surface area. When considering the variation contributed by the local differences in the different samples the variation contributed due to this method was considered to be negligible.

The preconditioning also have a big impact on the results, hence it is crucial that all samples which are being tested are preconditioned in the same way to enable a comparison. Jacobsen et al. (1997a) tested OPC and OPC mixed with silica and exposed the samples test surface to various amount of drying, from none at all to “severe drying”. The results showed that a sample with a low degree of dehydration decreased the scaling while no dehydration and a moderate to high degree of dehydration increased the scaling. Utgenannt (2004) studied OPC and OPC blended with slag where the samples had never dried, dried without carbondioxide (non-carbonated) and dried with carbondioxide (carbonated). The results showed that the effect from carbonation can increase scaling in concrete containing slag and decrease the scaling in concrete with a CEM I. This infer that when presenting salt frost scaling results it is important to state if the test surface is carbonated or not since the carbonation can change the concrete properties to increase or decrease the salt frost scaling for different binder combinations.

3. Test of method

The test of the method was done to see if the method can differentiate between three binders with different degrees of hydration exposed to three cycles (Sjöbeck 2015). Information about the recipes is presented in Table 2. The concrete cylinders were hydrated for one day in a mould, seven days in lime saturated water and 28 or 56 days hydrated in sealed conditions in +20 °C. With this information it can be concluded that all results presented in the current article are from concrete which has been hydrated in sealed conditions and could only was affected by self-desiccation. The samples were sawed about 20 to 24 h before the freeze-thaw test began and directly put into a box with fresh water where the test surface was averted from carbonating, hence only uncarbonated surfaces were tested.

Table 2. Specifications of the materials used in the test of the method.

Batch	w/(c+s)[1]	Binder[2] kg/m³	Aggregate[2] kg/m³	SP[3] kg/m³	AEA[4] kg/m³	Slump mm	Air[5] vol-%	Density[6] kg/m³
O[7]	0.40	428	1765	5.41	0.08	100	5.0	2364
F35[8]	0.40	432	1764	8.11	1.22	190	3.8	2369
S35[9]	0.40	433	1779	5.41	0.08	200	4.1	2385

1) Water binder ratio = water/(cement+SCM)
2) Binder- and aggregate content is calculated with consideration to the air content measured in the fresh concrete.
3) A super plasticizer based on a polycarboxylate was used in batch #1 and #3, and another super plasticizer based on sulphonate melamine-formaldehyde condensate was used in batch #2.
4) The air entraining agent for all batches was one based on a synthetic surfactant.
5) Air content is measured in 8 dm³ of the fresh concrete.
6) Density was determined on the same concrete as the air content.
7) The binder consists of 100 mass% CEM I 42,5 N - SR 3 LA.
8) The binder consists of 65 mass% CEM I 42,5 N - SR 3 LA and 35 mass% siliceous fly ash.
9) The binder consists of 65 mass% CEM I 42,5 N - SR 3 LA and 35 mass% fresh water ground granulated blastfurnace slag.

The temperature cycle in Figure 3 marked “4h” was produced with the settings mentioned in chapter 2.2. The temperature cycles in Figure 3 marked “2h” and “12h” cycles were produced with two other climate chambers creating similar temperature gradients and minimum temperatures. The only changes were made to the time when the samples are exposed to temperatures below -21.1 °C and the time when samples are exposed to temperatures above ±0.0 °C. The scaling from samples subjected to the cycle marked “4h” is compared with the scaling subjected to the cycles marked “2h” and “12h”. These are similar to the temperature cycles tested by Jacobsen et al. (1997b), with exception to the thawing period.

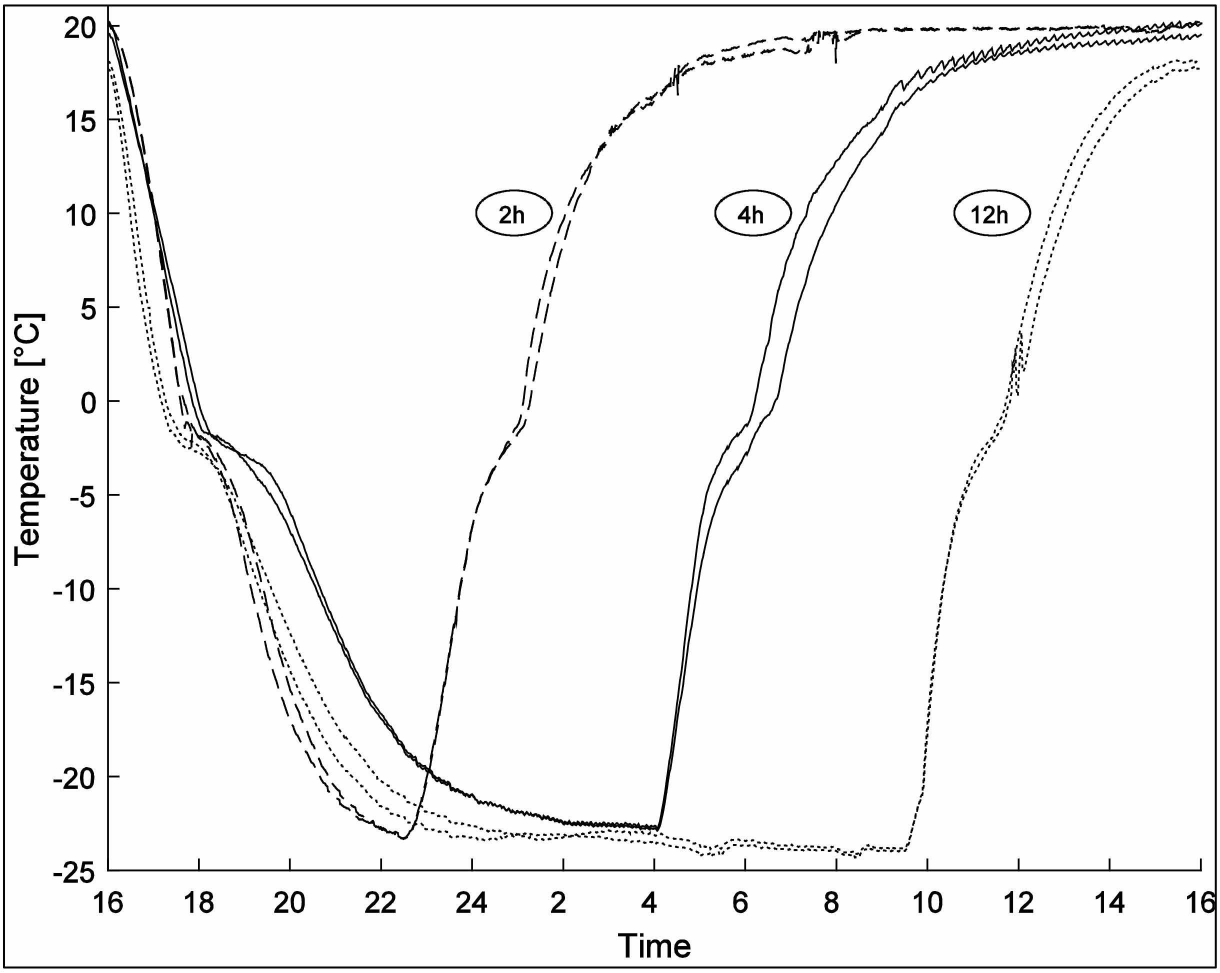

Figure 3. Freeze thaw cycles studied by Sjöbeck (Sjöbeck 2015). The graph shows 2 measurements on each cycle. All measurements where made inside the salt solution. The dents in the curves at approximately -1.8 °C are due to the exothermic phase change of water to ice in the 3 mass% NaCl solutions which reveal the freezing temperature.

Detailed information about the freezing for each cycle is presented in Table 3. The “2h”-cycle and the CDF-cycle have the same length on the freezing period with approximately the same gradients. The only difference is that the CDF-cycle has a minimum temperature of 20.0±0.5 °C, while the “2h” cycle is below -21 °C and the thawing period is approximately 18 h in the presented “2h” cycle compared to the 5 h thawing period in the CDF-cycle.

Table 3. Information about the freezing period for each cycle presented in Figure 3. During the test of the method temperature measurements in the solutions were made continuously on two samples per cycle.

Temperature cycle in Figure 3	**Mean freezing rate [°C/h] -1.8<T<-21 °C**	**Hours samples are exposed to T≤-21 °C**
2h	-5.0 to -6.0	1.5 to 2.5
4h	-3.0 to -4.0	4.0 to 5.0
12h	-4.0 to -5.0	11.5 to 12.5

Two test series has been done for all three binders. In the first series the “2h” cycle and the “4h” cycle was tested with concrete which had been hydrated for a total of 36 days. In the second test series the “4h” cycle and the “12h” cycle was tested with concrete which had hydrated for a total of 64 days. This enables an analysis of concrete exposed to the “4h” cycle with different time periods of sealed hydration. The results will also provide some indication if the materials tested in this study is affected in the same way as the materials tested by Jacobsen at al. (1997b) when changing the temperature cycle. Table 4 presents a summary of all D-ISFS results from each recipe.

Table 4. Results from the D-ISFS test.

Binder	Hydration [days]	Cycle[1)]	Mean scaling[2)] [kg/m²]	Standard deviation[3)] [kg/m²]	CV[4)] [%]
O	36	2h	0.575 (0.564)	0.146 (0.087)	25.5 (15.5)[5)]
O	36	4h	1.017	0.167	16.4
O	64	4h	0.645	0.102	15.8
O	64	12h	0.789 (0.845)	0.182 (0.134)	23.1 (15.8)[6)]
F35	36	2h	2.106	0.208	9.9
F35	36	4h	2.681	0.200	7.5
F35	64	4h	1.738	0.105	6.0
F35	64	12h	1.840	0.229	12.4
S35	36	2h	0.505	0.068	13.5
S35	36	4h	0.630	0.080	12.8
S35	64	4h	0.390	0.065	16.6
S35	64	12h	0.379	0.050	13.2

[1)] Freeze-thaw cycle according to Figure 3.

[2)] Total mean scaling after 28 cycles from six samples for each cast.

[3)] Standard deviation for six samples with Ø100 mm² test surface.

[4)] Coefficient of variation = Standard deviation / Mean scaling.

[5)] O-36d (2h), CV=20.2% when ignoring the sample deviating most from the mean mass of scaling. CV=15.5% when ignoring the two samples deviating most from the mean mass of scaling after 28 cycles.

[6)] O-64d (12h), CV=15.8% when ignoring the sample deviating most from the mean mass of scaling after 28 cycles.

The results from casts hydrated for 36 days show a trend of the “4h” cycle increasing the mass of scaling damage when compared to the “2h” cycle for all binders. Casts hydrated for 64 days indicate a slight increase in scaling damage when exposing O and F35 samples to the “12h” cycle compared to the “4h” cycle. The results also show a clear trend that the mass of scaling damage decrease when the degree of hydration increases for all binders. When using the CDF method the coefficient of variation should be 14 % when the mean total scaling is

1.50 kg/m², and when using the SS137244:2005 method the coefficient of variation should be 17 % when the mean total scaling is 1.00 kg/m² (CEN/TS 12390-9). Figure 4 shows a presentation of scaling in relation to the repeatability of the CDF- and SS137244:2005 method.

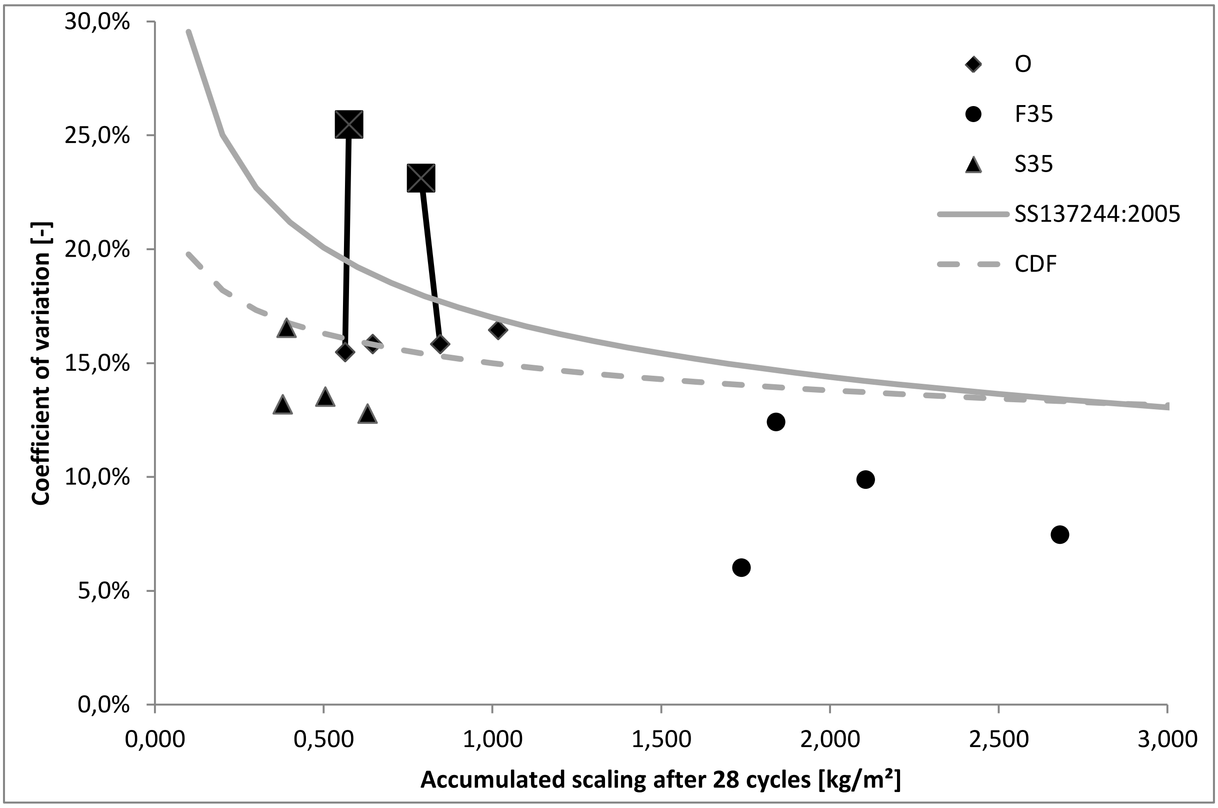

Figure 4. The relation between the mean accumulated scaling after 28 cycles with the coefficient of variation for the six samples of each cast. The solid line presents repeatability for SS137244:2005, $v_r=0.17 \cdot m^{-0.24}$ and CDF $v_r=0.15 \cdot m^{-0.12}$. The squares present values including the samples which are considered outliers (left 2 samples, right 1 sample), the lines connect these values to the adjusted values where the outliers are ignored. Order for O from left to right: "O36-2h", "O64-4h", "O64-12h", "O36-4h". Order for F from left to right: "F64-4h", "F64-12h", "F36-2h", "F36-4h". Order for S from left to right: "S64-12h", "S64-4h", "S36-2h", "S36-4h".

4. Discussion

This article has presented a method to test the relative salt frost scaling resistance for concrete using climate chambers with air as the thermal medium and where efforts was made to minimize the variation in the results due to the method. In the following text the temperature cycle and the results from the test of the method will be discussed, and then a few general comparisons are made between the presented method and the CDF- and SS137244:2005 method.

4.1 The Temperature Cycle

To enable an analyse of the relative differences in salt frost scaling damage in various materials a method with a consistent “load” from the salt frost scaling mechanism(s) per cycle is desired. If the load from the salt frost scaling mechanism(s) is kept constant by the method (which includes the cycle) and measurements are done regularly, this will show if the scaling created by a concrete recipe is constant, accelerates or decelerates over time. This could contribute to a deeper knowledge about how the salt frost scaling mechanism affect each material given a certain salt frost scaling load, which mean a better indication about the materials durability over time. This could in turn give a life expectancy when more data has been collected from tests with this method and field studies.

The air circulation is high inside the freezer and the differences between the mean temperature cycles on the different shelfs are negligible. Considering this, the average temperature measurement presented in Figure 2 A4 and A7 are a fair representation of the cycle which contributes to the salt frost scaling load in the presented method. Therefore the variations from the measurements do not imply that there is a large variation in temperature cycles, it only show how much the temperature can differ at different points inside the solutions. This variation is believed to have been created due to the placement of each thermocouple in relation to where the exothermic phase change of water to ice began. Since the ice formation is a stochastic process there will be differences in measured temperature cycles from the same thermocouple. This highlights a difficulty of measuring temperature cycles in a salt solution where water freeze and salt is concentrated to the remaining solution. This in turn increases the concentration in the unfrozen solution at the same time as it lowers the freezing temperature which makes the ice formation a complex process. However, the small amount of solution and the low variation in concentration should contribute to less variation in the salt frost scaling load due to the ice formation of the solution.

According to Sellevold and Farstad (1991), Petersson (1994), Studer (1997), Jacobsen et al. (1997b) and Lindmark (1998), the salt frost scaling damage (or load) increases or decreases due to the appearance of the temperature cycle. This is why efforts were made to minimize the variations of the cycle in the present method. The minimum temperature can vary from -21.9 °C to -23.8 °C inside the same climate chamber according the measurements, which is due to the freezer cycling between -21 °C to -25 °C. This variation in minimum temperature is assumed to contribute to a negligible variation in salt frost scaling load from the salt frost scaling mechanism(s).

According to the measurements, the entire solutions have a temperature below the eutectic point for a few hours. This means that the solution will strive towards a thermodynamic equilibrium, according to the phase diagram for H_2O-NaCl solutions, which consists of ice together with the dihydrate of NaCl (Hydrohalite, $NaCl{\cdot}2H_2O$). This consistent creation of these solid materials just below the eutectic point may also contribute to a more even salt frost scaling load.

4.2 Results from the Test of the Method

The purpose of the tests of the method was to see if the method has a precision high enough to detect differences between binders with various degrees of hydration tested with three different the temperature cycles. To estimate the precision of the method, the results from Figure 4, Figure 5 and Figure 6 is discussed in the following paragraphs.

In Figure 4 there is a trend where equal samples have a higher salt frost scaling damage when exposed to the “4h” cycle compared to the “2h” cycle. These results agree with the results from previous research (Jacobsen et al. 1997b). The previous study by Jacobsen et al. (1997b) tested two recipes containing OPC and three recipes containing OPC mixed with silica fume. Considering that concrete containing fly ash and slag showing the same indications as OPC and OPC blended with silica fume adds to the general perception shared among researchers who have studied this, such as Valenza II and Scherer (2007a), that the salt frost scaling mechanism(s) is a physical phenomenon and not a chemical.

In Figure 6 a clear trend can be observed for the three concrete materials where longer sealed hydration decreases the amount of salt frost scaling damage. This highlights the importance of considering the different hydration rates of different binders when doing salt frost scaling tests. These results agrees with previous research from Jacobsen et al. (1997a) among others which also found that a higher degree of hydration increases the salt frost scaling resistance, given the same moisture condition for the tested samples.

In Figure 5, equal samples hydrated for 64 days are compared. The results for O and F35 seem to show a slight indication of more damage when exposed to the “12h” cycle compared to the “4h” cycle. However, the longer hydration clearly reduces the damage, according to Figure 6, which probably has reduced the effect from a prolonged exposure time to temperatures below the eutectic temperature. When looking at the results from the slag recipe there seem to be no significant effect at all. However, the test only lasted for 28 cycles which infer that a prolonged test, e.g. 112 cycles, would result in a more information and probably a higher resolution when trying to see if the studied effect from changing the cycle from “12h” to “4h”.

When looking at the results considerations should be taken to the fact that all test surfaces were non-carbonated and never dried, except for the self-desiccation due to the low water binder ratio (0.40). According to Jacobsen et al. (1997a) and Utgenannt (2004) the amounts of scaling for OPC and CEM I increase when the test surface has never been exposed to drying or carbonation. This probably contributes to increase the contrast between the results in the current test of various concrete recipes which was exposed to the different temperature cycles. The amount of scaling from each concrete recipe should not be compared with any other method without considering how the preconditioning and the temperature cycle differ.

4.3 Comparisons to the Swedish and German Standard Methods

The method can be viewed as a combination of the CDF and the SS137244:2005-method with some pros and cons in comparison to each standard. The total surface area tested per 56 days is larger in the presented method than the one in the CDF-method and smaller than the one in the SS137244:2005-method. The variation in temperature cycle is lower in the presented method than the allowed variation in SS137244:2005-method but higher than the allowed variation in the CDF-method. When doing a comparison, the presented method can therefore complement the CDF method by enabling a quantitatively analysis (larger test surface area) with a tougher temperature cycle. Another comparison suggests that the presented method would complement the SS137244:2005-method (in a cost efficient way since the same type of climate chamber is used) with a more qualitative analysis of relative salt frost resistance since the temperature cycle variation is lower.

It can be suggested that different methods have different resolutions when testing concrete with high or low salt frost scaling resistances. The presented method use the pessimum salt concentration at the same time as it has a temperature cycle which also increases the amount of scaling damage compared to the CDF method (“2h” cycle compared to “4h” cycle). This might enable the method to have a higher resolution and perhaps increase the contrast between scaling results when analysing concrete recipes which could be considered in environments with exposure to de-icing salts and freezing temperatures (≤0.40 water binder ratio).

This method is developed to analyse the salt frost scaling mechanism(s) which means that no mass of scaling limit can be set to the method for a “salt frost scaling resistant” concrete.

Before this is possible additional field studies and round robin tests with the other standard methods are required.

Given the results, the method is considered to enable an analysis of the salt frost scaling mechanism(s) and how different factors affect the salt frost scaling mechanism(s).

5. Conclusion

- Considering that at least 48 samples can be measured per person and day, and it allows 0.495 m² test surface (63 samples of Ø100 mm) per freezer, this method is considered time- and cost efficient.
- The method exposes the samples to a temperature cycle with a small variation at the same time as a negligible variation is added to the scaling results due to the method which contribute to a high precision.
- The low variation in temperature cycle is believed to contribute to an even salt frost scaling load per cycle and when this is combined with regular measurements the results contributes to information about acceleration or deceleration in the long term salt frost scaling process.
- The method can detect differences in salt frost scaling resistance (for three different binder combinations with two different degrees of hydration, exposed to three different temperature cycles) and all of the results agree with previous researchers which confirm a high credibility for the method and that the results has a high precision.
- The method is considered to give a high amount of scaling damage which enables a high resolution and contrast when testing concrete which is considered for structures exposed to de-icing salts and freezing temperatures.
- The method is considered to be suited to analyse the salt frost scaling mechanism(s) and how various factors affect the salt frost scaling mechanism(s).

References

Arnfelt H (1943) Damage on Concrete Pavements by Wintertime Salt Treatment. Statens Väginstitut,

CEN/TS 12390-9 (2006) Testing hardened concrete - Part 9: Freeze-thaw resistance - Scaling. 24 p.

Fagerlund G (1982) The influence of slag cement on the frost resistance of the hardened concrete vol 1. Swedish Cement and Concrete Research Institute, Stockholm

Jacobsen S, Marchand J, Boisvert L, Pigeon M, Sellevold EJ (1997a) Frost deicer salt scaling testing of concrete: Effect of drying and natural weathering Cement Concrete and Aggregates 19:8-16

Jacobsen S, Saether DH, Sellevold EJ (1997b) Frost testing of high strength concrete: Frost/salt scaling at different cooling rates Materials and Structures/Materiaux et Constructions 30:33-42

Lindmark S (1998) Mechanisms of Salt Frost Scaling of Portland Cement-bound Materials: Studies and Hypothesis. Doctoral, Faculty of Engineering, LTH, Lund University

Lindmark S On the Relation between Air void system parameters and Salt frost scaling. In: Bager D (ed) Nordic Miniseminar: Freeze-thaw testing of concrete, Vedbaek, Denmark, 2010. Nordic Concrete Federation, pp 41-58

Liu Z (2014) Frost Deterioration in Concrete due to Deicing Salt Exposure: Mechanism, Mitigation and Conceptual Surface Scaling Model. University of Michigan

Petersson P-E (1994) Influence of Minimum Temperatures on the Scaling Resistance of Concrete. Part 1: Portland Cement Concrete. SP Swedish National Testing and Research Institute,

Powers TC (1955) Basic Considerations Pertaining to Freezing-and-Thawing Tests ASTM Proceedings 55:24

Powers TC (1966a) The mechanism of frost action in concrete (Part I) Cement, Lime and Gravel 41:6

Powers TC (1966b) The mechanism of frost action in concrete (Part II) Cement, Lime and Gravel 41:5

Scrivener KL (2014) Options for the future of cement The Indian Concrete Journal 88:11

Sellevold EJ, Farstad T (1991) Frost/Salt-testing of Concrete: Effect of Test Parameters and Concrete Moisture History

Setzer MJ, Fagerlund G, Janssen DJ (1996) CDF Test - Test method for the freeze-thaw resistance of concrete - tests with sodium chloride solution (CDF) Materials and Structures 29:523-528 doi:10.1007/bf02485951

Sjöbeck H (2015) The time dependency of salt-frost damage at low temperature on concrete with SCMs. Lund University

SS137244 (2005) Betongprovning – Hårdnad betong – Avflagning vid frysning. Concrete Testing – Hardened Concrete – Scaling at freezing, in Swedish, 10 p.

Studer W (1997) Internal comparative tests on frost-deicing-salt resistance. In: Marchand J, Pigeon M, Setzer M J (ed) Paper presented at the International Workshop in the Resistance of Concrete to Scaling Due to Freezing in the Presence of De-icing Salts, Sainte-Foy, Québec, Canada, pp. 259-270.

Utgenannt P (2004) The influence of ageing on the salt-frost resistance of concrete. Doctoral Thesis, Faculty of Engineering, LTH, Lund University

Valenza II JJ, Scherer GW (2007a) A review of salt scaling: I. Phenomenology Cement and Concrete Research 37:1007-1021 doi:10.1016/j.cemconres.2007.03.005

Valenza II JJ, Scherer GW (2007b) A review of salt scaling: II. Mechanisms Cement and Concrete Research 37:1022-1034 doi:10.1016/j.cemconres.2007.03.003

Verbeck GJ, Klieger P (1957) Studies of "Salt" Scaling of Concrete. Washington D.C.

Appendix 4

Complementary tests and analysis made for the D-ISFS method

During the development of the D-ISFS method some tests were made regarding the sample setup. In the final version of the sample setup a plastic cup is used as container for the NaCl solution. This is made from cutting the bottom of a plastic bucket, which is why it does not have a flat bottom. Before this plastic bottom was found petri dishes made from “Pyrex” glass was also tested, however, these cracked after only a few F-TC.

Another factor that was tested before the official test series began regarding the sample setup, was the adhesive used to fasten the rubber to the sample. In the beginning of the selection process, any adhesive that required a fume cupboard during use was disregarded. Three adhesives were used during an initial test before one was selected to be used during the official test series. The brand names on these are SuperFix, XtremFix and Glue Seal. The test involved fastening rubber to concrete samples and then subject them to 14 F-TC. The XtremFix was selected to be used, since it was considered to have the best adhesion after the 14 F-TC.

Before and during the test an error seemed to occur randomly for different samples where the test surface would not be in contact with the NaCl solution after 7 F-TC. To test why this occurred, various things were changed in the sample setup. One example of such test is that, the adhesion for some samples between the sample surface and the adhesive was poor. This could perhaps enable water to be absorbed in a fast rate from this small space by capillary suction. However, this were proved to not be the case since some had a bad adhesion while there was no problem with the test surface not being in contact with the NaCl solution. Another analysis performed was to look for any pattern for the samples that did not have contact with the NaCl solution, this could perhaps show if certain positions inside the freezers were more frequently affected than others. However, the results did not show any pattern, nor did it show that some positions seemed to result in more or less mass of scaling. Table 3 below presents an overview of how many samples that were affected by this and how many times these samples were affected by this phenomenon. It is important to remember that the measurements were made 16 times on each sample. This means that (looking at the table) two samples was affected by this five times out of the total 16 times they were measured, and these five times was not following each other. Hence, the mechanism contributing to this problem is still considered to be random and not yet found.

Table 1. Number of samples not in contact with the NaCl solution for a certain number of times.

n[1)]	0	1	2	3	4	5
Amount of samples	136	15	7	3	5	2

[1)] The number of times the sample was not in contact with the solution out of the 16 times when measurements of the mass of D-ISFS were performed.

According to Table 3, the fraction of samples exposed to this phenomenon at all is approximately (32/168) 19% and the fraction when this occurred out of all the measurements occaisions was ((15+14+9+20+10)/(168·16)) 2.5%.

Appendix 5 – Paper 3

Low Air Void Contents effect on the De-Icing Salt Frost Scaling in Uncarbonated Concrete containing Siliceous Fly Ash

Martin Strand, Katja Fridh

Division of Building Materials, Lund University, Lund, Sweden

Corresponding author's info.
E-mail: martin.strand@byggtek.lth.se
Telephone: (+46)7 02 95 68 75

Abstract

The purpose of this article is to present results which give more information about how various air void contents affect the de-icing salt frost scaling (D-ISFS) in uncarbonated concrete containing 20 or 35 mass% siliceous fly ash (SFA). A combination of superplasticizer and air entraining agent have been found, which provides a low risk for bleeding, to create four slightly different air void contents, from approximately 1.5 to 4.5 vol%, in concrete containing SFA blended with a CEM I. The concrete was sealed and hydrated for a long time before the D-ISFS test started in an attempt to decrease the risk for any significant changes in the microstructure during the test, e.g. due to continued hydration. The results show approximately the same reduction in mass of D-ISFS from the air void system for the uncarbonated concrete with 100 mass% CEM I binder as the uncarbonated concrete with 80 mass% CEM I with 20 mass% SFA. The air void system in the uncarbonated concrete with 65 mass% CEM I with 35 mass% SFA did not seem to decrease the mass of D-ISFS to the same extent as the other two.

Keywords: Concrete, De-Icing Salt Frost Scaling, Siliceous Fly Ash, Uncarbonated, Never Dried, Air Void System

Acknowledgement

This research was carried out with financial support from SBUF (The Development Fund of the Swedish Construction Industry) supported by Skanska and Cementa AB (a part of Heidelberg Cement Group).

1 Introduction

Due to climate change, everyone is pressured to reduce the CO2 emission including the cement production factories. One way for the cement factories to reduce the CO2 emissions is to increase the use of blended binders with supplementary cementitious materials (SCM) to reduce the mass of clinker used in concrete. One SCM being used in concrete is siliceous fly ash (SFA) which is a waste product from coal power plants. However, before increasing the use of the binder combinations in constructions exposed to tougher climate, such as bridges, these materials needs to be tested to a great extent to ensure that there is no reduction in durability.

One important factor to consider is the risk and consequences of de-icing salt frost scaling (D-ISFS) when building bridges in Nordic countries where the temperatures often are -20 °C or below during the winters when de-icing salts are used. This problem have been managed by implementing restrictions on which binder can be used in these tough environments together with requirements on the air void content [1, 2]. This have been proven to increase the D-ISFS resistance for concrete with ordinary Portland cement (OPC) as binder [3, 4]. The air content can be managed by using an air entraining agent (AEA) in the correct dosage for the specific recipe. When using a superplasticizer (SP) it is important to make sure that the combination of SP and AEA admixtures is robust to minimize the risk for water to separate from the paste (bleeding). As long as bleeding does not occur to any large extent it is possible to control the air void content with a precision of a few percent. This makes it practically enough to control the air content within a few percent around the minimum required air content which is required to provide a frost resistance. The minimum air content required for concrete set by the Swedish standard [1] is between 4.0 and 5.0 % depending on the size of the aggregates used for the second and third toughest “frost-exposure-class”, “XF2” and “XF3”. The toughest exposure class, “XF4”, requires approved results from the SS137244 (aka slab) test method (no minimum requirement on the air content according to [1]). Considering the exposure class XF2 and XF3 it is important to minimize the air content and get close to 5% to keep a high strength of the concrete since it decrease with an increased amount of air content.

When studying the D-ISFS resistance of concrete containing fly ash (FA) in combination with SP and AEA it is important to consider that the FA adsorbs some of the surfactants (SP or AEA) [5-7]. This will reduce the effectiveness of the AEA (or SP), which is added in to the mix first, and thereby increase the required mass of that surfactant to acquire the same air content (or workability) when compared to concrete only containing OPC (without any FA). Results from Gebler and Klieger [6] indicate that SFA (low fraction of CaO, Class F [8]) seems to require more AEA compared to calcareous FA (moderate fraction of CaO, Class C [8]). Another important difference between siliceous and calcareous FA is that calcareous FA contain alkalis that are soluble in water, which seems to have a negative impact on the creation of the air void system [9-11], while SFA does not contain alkalis that are soluble in water.

Most of the previous research on concrete containing SFA has been done according to standard methods, such as the slab method [12]. However, this study uses a modified test method where the preconditioning and the freeze-thaw cycle differ from the standard test methods. The standard methods condition the samples in climate rooms, which usually have 20 °C in 50% relative humidity (RH). This imply that evaporation and carbonation of the test surface will occur affect the scaling results on OPC [13, 14]. In addition to this the standard test methods test samples when the concrete is relatively young (31 days according to the slab method [12]).

Previous studies on D-ISFS on concrete containing SFA seem to agree on the following things. The mass of D-ISFS damage increase as the wbr increase [15-19].

The bleeding (water segregating in the paste) of concrete seems to increase when FA is used in the mix. This means that the effective wbr of the concrete surface will increases which increase the autogenous shrinkage and this seems to lead to an increase in the mass of surface scaling [20]. The mass of D-ISFS damage increase as the mass of FA and replacement fraction of the total binder content increase [15-17, 19, 21-23]. The agreement between the results from the standard D-ISFS methods and field tests is somewhat lacking [24-26].

In this article, results are presented from two binder combinations containing SFA which have been tested with a D-ISFS method. The reference binder is 100 mass% of a CEM I (referred to as “O” in this article) and the two other binder combinations consist of 20 and 35 mass% SFA blended with the CEM I (referred to as “F20” and “F35” in this article) with the same binder content and wbr. Each binder combination was made with four different air void contents by varying the mass of AEA added and hydrated for 307 days to decrease the probability for the microstructure to change during the D-ISFS test. These four air void contents ranges from the content created when a superplasticizer (SP) is used without any air-entraining agent (AEA), then in three steps up to where the air content in the fresh concrete has been measured to be approximately 4.5 to 5.0%. Recipes are presented and binder properties have been measured by XRF and ICP analysis. Results are presented from the air void analysis measured in the concrete according to ASTM C 457 [27] which gives an indication about the air void structure. Then the D-ISFS results are presented which give quantitative information about the impact various air void systems have on the D-ISFS created by the mechanism(s). This implies that the D-ISFS mechanism(s) should be able to explain and the differences between the results, and therefore this contribute to more information about the D-ISFS mechanism(s).

2 Method and Materials

The methodology for the tests is the same as the one presented in [28]. The main purpose of the methodology is to minimize the possibility for any change in the microstructure due to e.g. hydration in an attempt to facilitate what effect different air void systems has on the D-ISFS damage for the binder combinations that has been tested. First tests were made to find a combination of SP and AEA that perform well with each binder with the goal of enabling the creation of various air void systems without any risk for bleeding. This enables the creation of slightly varying air void systems by changing the mass of air entraining agent added to the mix. The selection of casts that were used was based on the measurement of the air content in the fresh concrete. The mixing procedure process consisted of 2.5 min dry blending the binder and aggregates, then water and AEA was added and mixed for 2.5 min, and finally SP was added and mixed for 2.5 min. After casting the samples hydrated 7 days in water and then sealed and left to hydrate for approximately 300 days in 20 °C. One sample from each cast was sent for an air void analysis according to ASTM C 457 [27] to enable a quantification of each air void system for each cast. The specimens were sawn and put in to water 1 day before the freeze-thaw test began to avoid carbonation of the test surface. Hence, each recipe has hydrated and self-desiccated as much as the specific binder combination is able to in this climate, note that the degree of hydration and self-desiccation will most likely vary when comparing different binder combinations.

2.1 Materials

Table 1 present the recipes used for each batch which have been tested in this study with consideration to the measured air content in the fresh concrete. The binder content was set to be close to 430 kg/m³ for each recipe given the target air contents of 1.5, 2.5, 3.5 and 4.5 vol%. The grain fraction curve of the aggregates used had a fineness modulus of 4.79, and it was designed to have a small amount of fractions between 4 and 8 mm. The purpose of this was to increase the contrast in the scaling results between samples with a small and large mass of D-ISFS. Samples with a small mass of D-ISFS was expected to scale of cement paste and aggregates smaller than 4 mm, while samples with a large mass of D-ISFS was expected to scale of aggregates larger than 8 mm which would contribute to significant spikes in the D-ISFS results.

Tabell 1. Concrete recipes.

Batch	Binder1) 2)	Aggregate [kg/m³]2)			SP2)3)	AEA2)4)	Air5)	Slump	Density6)
	[kg/m³]	0-8	8-12	12-32	[kg/m³]	[kg/m³]	[%]	[mm]	[kg/m³]
O-17)	423	951	280	528	1.068	0.000	3.20	165	2399
O-27)	428	948	280	526	1.081	0.023	3.00	160	2405
O-37)	426	930	274	516	1.076	0.045	4.50	200	2375
O-47)	428	920	271	511	1.081	0.068	5.10	220	2331
F20-18)	429	965	285	536	2.926	0.000	1.60	190	2413
F20-28)	429	952	281	528	2.927	0.497	2.60	220	2367
F20-38)	430	939	277	521	2.932	0.543	3.45	200	2371
F20-48)	430	926	273	514	2.933	0.680	4.45	210	2339
F35-18)	427	961	284	533	2.835	0.000	2.05	220	2382
F35-28)	429	951	280	528	2.845	0.813	2.70	230	2327
F35-38)	428	934	276	518	2.836	0.990	4.05	230	2309
F35-4 9)	428	921	272	511	2.838	1.216	5.05	240	2277

1) CEM I + SFA content.
2) Calculated with consideration to the air content measured in the fresh concrete according to the “Air”-column.
3) The super plasticizer based on a polycarboxylate was used for batches with 100% CEM I, and another super plasticizer based on sulphonate melamine-formaldehyde condensate was used for the batches containing SFA.
4) Calculated total dry mass per m³ concrete of the admixture added to the recipe.
5) Air content is measured in 8 dm³ of the fresh concrete.
6) Density was determined on the same concrete as the air content.
7) The binder consists of 100 mass% CEM I 42,5 N - SR 3 LA.
8) The binder consists of 80 mass% CEM I 42,5 N - SR 3 LA and 20 mass% SFA.
9) The binder consists of 65 mass% CEM I 42,5 N - SR 3 LA and 35 mass% SFA.

When using admixtures with SFA some part of the admixtures will be adsorbed by the SFA which then is ineffective [5-7]. According to the methodology by Strand and Fridh [28] the AEA is added to the mix before the SP. Therefore, a fraction of the AEA is adsorbed to the SFA, and that is believed to be the reason for the large mass of AEA required for the SFA recipes. If the SP would have been added before the AEA, a fraction of the SP would be adsorbed and a larger mass of SP would be needed (with a smaller mass of AEA).

Table 2 presents XRF analysis of the SFA and each binder combination which has been tested. The CEM I contained 2.36 % lime filler.

Table 2. X-ray fluorescence analysis (XRF) of the binders. Cement-wroxi standard.

Binder	CaO1) [%]	$SiO_2$1) [%]	$Al_2O_3$1) [%]	$Fe_2O_3$1) [%]	MgO1) [%]	K_2O1) [%]	Na_2O [%]	Na_2Oe2) [%]	$SO_3$1) [%]	LOI1) [%]
CEM I	63.60	21.30	3.80	4.56	0.86	0.65	0.07	0.50	2.45	1.84
SFA2)	3.53	57.00	21.60	7.33	1.95	2.16	0.00	1.42	0.65	2.71
F204)	52.40	28.60	7.38	5.17	1.09	1.00	0.25	0.91	2.05	2.00
F354)	44.00	33.50	9.88	5.52	1.26	1.24	0.38	1.20	1.78	2.09

1) The precision in the measurements are CaO±0.233%, SiO_2±0.100 %, Al_2O_3±0.052 %, Fe_2O_3±0.019 %, MgO±0.025 %, K_2O±0.032 %, SO_3±3%, (loss on ignition=) LOI ±0.18 %.

2) Na_2O-equivalent from K_2O and Na_2O.

3) Calculated oxide composition from the SFA and CEM I measurements.

4) Measured oxide composition from the blended SFA and CEM I.

In Table 3 results from ICP-, Blaine-, laser diffraction and compressive strength measurements are presented. The ICP-analysis shows how large fraction of the alkalis contained in each binder combination are soluble in water. According to the results the mass of soluble alkalis decrease when increasing the mass of SFA, which was expected. The Blaine and laser diffraction measurement shows that the SFA has a smaller specific surface in comparison and therefore has on average larger particle sizes than the CEM I.

Tabell 3. H_2O soluble alkalis, Blaine value, laser diffraction and compressive strength measurement.

Binder	ICP analysis1) [%]			Blaine2)	LD3)	Strength after presented days of hydration4) [MPa]			
	K_2O	Na_2O	Na_2Oe	[m²/kg]	[µm]	2 days	28 days	56 days	91 days
CEM I	0.44	0.03	0.32	343	17.305	21.8±0.3	55.1±0.3	62.3±1.2	66.1±2.0
F20	0.35	0.03	0.26	340	18.097	17.0±0.3	45.5±1.0	56.4±0.6	62.7±1.5
F35	0.29	0.04	0.23	328	18.556	13.3±0.2	37.4±0.4	49.6±1.1	56.9±0.6

1) ICP analysis of soluble K_2O, Na_2O and Na_2O-equivalent in H_2O according to the “CR 0401”-method.

2) Blaine value of specific surface area per mass binder measured according to [29].

3) Laser diffraction measurement on the size of the 50th percentile particles size.

4) Compressive strength measured according to the [30] with the standard deviation.

2.2 De-Icing Salt Frost Scaling Method

The D-ISFS method used is presented in Strand and Fridh [31], where results are presented from a test of the together with a discussion about the precision and possibilities with the method. The method use an upside down sample setup and a sawn test surface is used to remove any influence from surface bleeding. The freeze thaw cycle has been shown to be tough and produce more damage in non-dried samples than a cycle which is similar to the one used in the CDF method [31]. The large mass of D-ISFS produced is thought to increase the resolution in the results when comparing different concrete recipes with low wbr (around 0.40) which can be considered to be used in constructions with exposure to freezing, chlorides and cyclic wetting and drying, e.g. bridge decks. [31] also present all the measures taken to reduce any variation in the results caused by the method, to increase the precision of the measurements.

3 Results

3.1 Air Void Analysis

Table 4 presents results from the air void measurements made on the fresh and hardened concrete to describe and quantify the systems. Measurements on the hardened concrete were made on one sample per batch using linear traverse according to the ASTM C 457 standard method. The specific surface and spacing factor presented are calculated with regards to the chords smaller than 2 mm since air pores bigger than 2 mm contribute very little to the D-ISFS resistance in relation to smaller air voids. The results indicate that the increased mass of AEA increase the fraction of smaller air voids and the specific surface and shorten the spacing factor for each bindercombination.

Table 4. Air content measured in fresh concrete and results from linear traverse measurements according to ASTM C 457.

Cast	**Fresh Concrete $[\%]^{1)}$**	**Air void content**			**Air void content in paste**		**Specific surface $[mm^{-1}]^{2)7)}$**	**Spacing factor $[mm]^{2)8)}$**
		Total $[\%]^{2)}$	**<2 mm $[\%]^{2)3)}$**	**<0.35 mm $[\%]^{2)4)}$**	**<2.00 mm $[\%]^{2)5)}$**	**<0.35 mm $[\%]^{2)6)}$**		
O-1[9)]	3.20	2.6	2.4	0.9	7.1	2.8	17	0.41
O-2[9)]	3.00	2.7	2.4	0.9	6.8	2.8	19	0.38
O-3[9)]	4.50	2.8	2.7	1.3	8.0	3.9	21	0.32
O-4[9)]	5.10	4.1	3.4	1.9	9.4	5.7	24	0.25
F20-1[10)]	1.60	3.5	1.9	0.3	5.5	0.9	10	0.78
F20-2[10)]	2.60	2.0	1.9	0.9	5.8	2.6	25	0.32
F20-3[10)]	3.45	3.1	2.5	1.1	7.3	3.3	18	0.37
F20-4[10)]	4.45	3.5	3.4	2.0	9.6	5.9	22	0.27
F35-1[11)]	2.05	1.8	1.1	0.3	3.4	1.0	24	0.41
F35-2[11)]	2.70	3.8	2.4	0.8	6.9	2.2	20	0.35
F35-3[11)]	4.05	3.2	2.9	1.6	8.5	4.7	34	0.19
F35-4[11)]	5.05	4.8	3.4	2.0	9.5	5.8	27	0.22

[1)] Total air content measured in 8 dm³ fresh concrete. Read and rounded to closest 0.05 %.

[2)] Calculated from results from linear traverse measurements according to ASTM C 457.

[3)] Total air content from air voids <2.0 mm.

[4)] Total air content from air voids <0.350 mm.

[5)] Voids <2.0 mm / (vol% cement paste + vol% of total voids). Vol% cement paste is calculated to 31%.

[6)] Voids <0.350 mm / (vol% cement paste + vol% of total voids). Vol% cement paste is calculated to 31%.

[7)] Specific surface ($mm^2/mm^3=mm^{-1}$) calculated from results of voids <2.0 mm.

[8)] Spacing factor calculated from results of voids <2.0 mm.

[9)] O-1, 2, 3 and 4 were sealed 93, 92, 92, 93 days when delivered for the linear traverse analysis.

[10)] F20-1, 2, 3 and 4 were sealed 42, 36, 40, 40 days when delivered for the linear traverse analysis.

[11)] F35-1, 2, 3 and 4 were sealed 120, 114, 114, 115 days when delivered for the linear traverse analysis.

3.2 De-Icing Salt Frost Scaling

Figure 1 presents two different diagrams that show the accumulated scaling (left) and the 7 cycle scaling measured every week (right). All lines in the 7 cycle scaling diagram gives information about a slight to moderate acceleration of scaling which means that the accumulated scaling curves bends slightly upwards. The last few measurements from F20-1 that contain SP without AEA can be ignored since there were large aggregate falling off from two of samples. The top two diagrams show concrete containing 100% CEM I. The middle two diagrams show concrete containing 80+20 mass% CEM I+SFA. The bottom two diagrams show concrete containing 65+35 mass% CEM I+SFA.

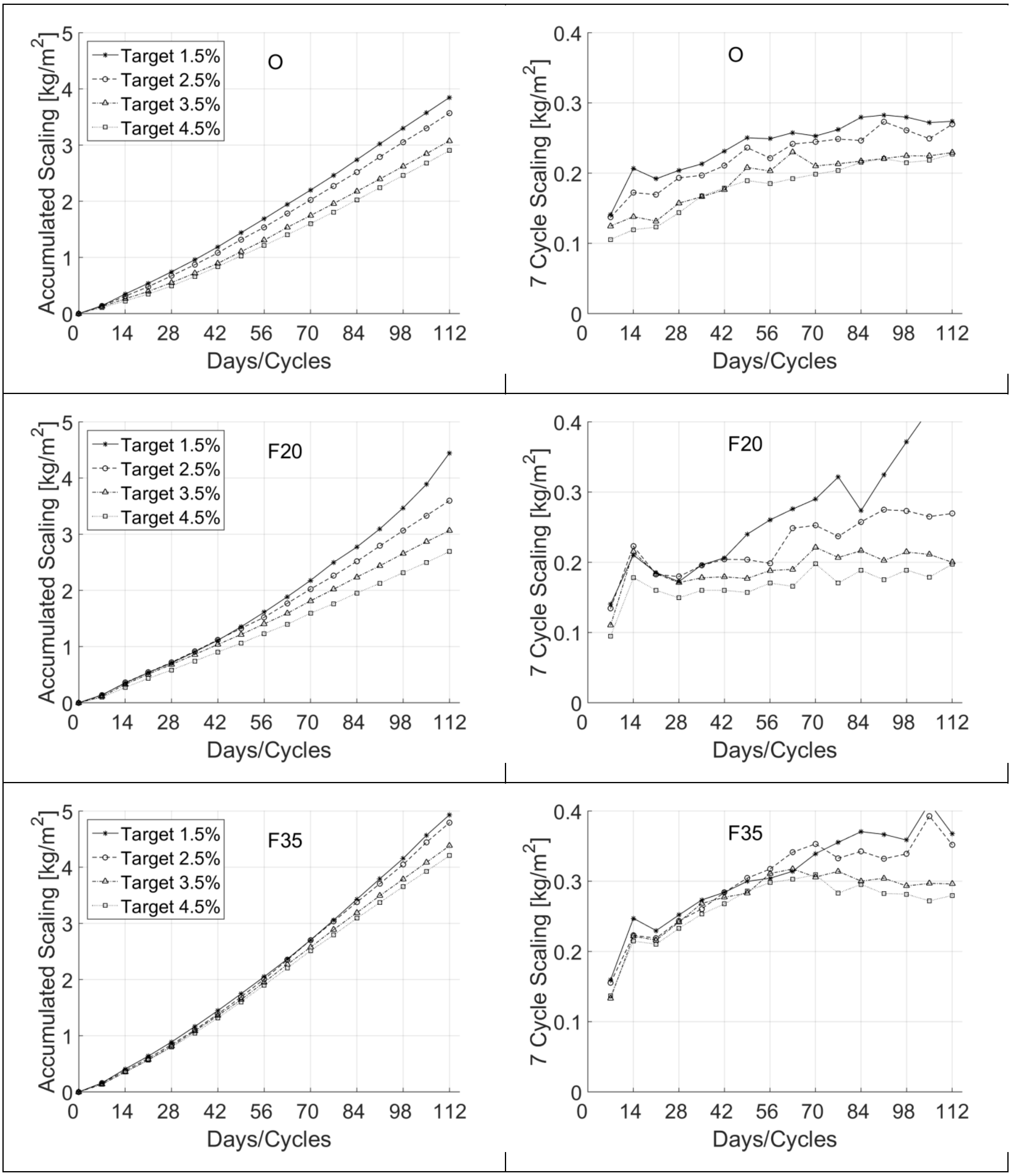

Figure 1. In the left column the total accumulated- and in the right column the mean D-ISFS per week for each cast during the D-ISFS test. Line 1 presents cast 1 with target air content 1.5 vol%. Line 2 presents cast 2 with target air content 2.5 vol%. Line 3 present cast 3 with target air content 3.5 vol%. Line 4 present cast 4 with target air content 4.5 vol%. Each point presents the mean value of six Ø100 mm² samples.

Figure 2 and Figure 3 presents the mean accumulated D-ISFS damage from the six samples after 56 and 112 cycles with the standard deviation highlighting the middle and end sections of the accumulated scaling diagrams with an indication of the variation for each cast.

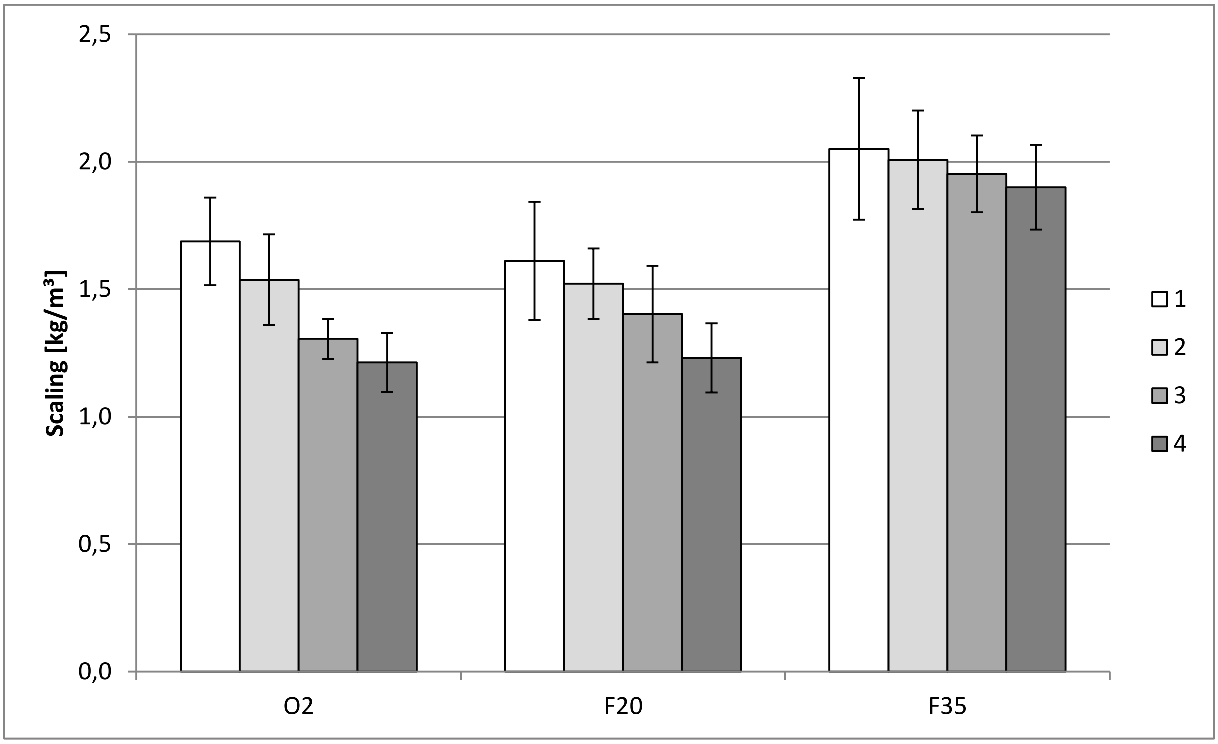

Figure 2. Accumulated average D-ISFS damage after 56 cycles with the standard deviation for each cast.

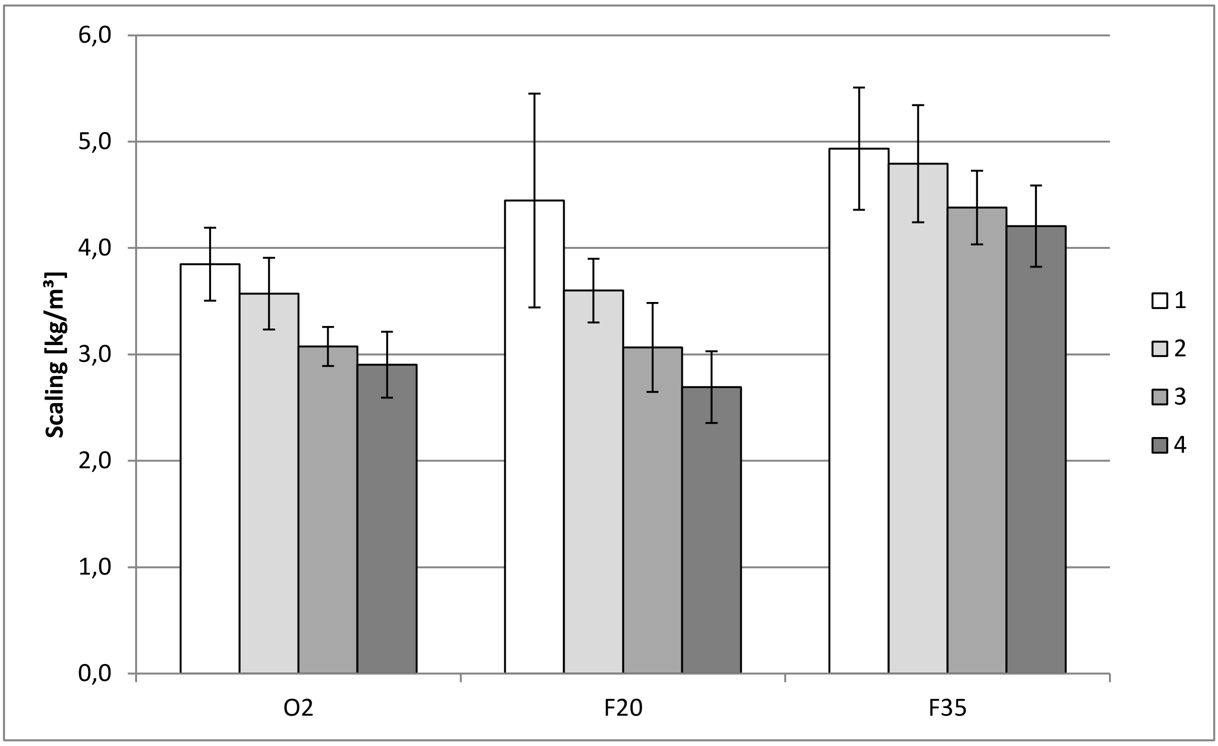

Figure 3. Accumulated average D-ISFS damage after 112 cycles with the standard deviation for each cast.

Figure 6 presents the accumulated scaling in relation to the coefficient of variation for each cast tested together with the repeatability of the CDF- and the SS137244:2005 method (CEN/TS 12390-9). The casts with the same binders after 28, 56 and 112 cycles are presented to present the coefficient of variation and an indication about how it change over time. In general, those points close to or above the repeatability levels according to the standard methods all have one or a few samples where stones scaled off which increase the standard variation and thereby the coefficient of variation. Only F20-1 after 112 cycles is unacceptable due to 2 samples where large stones came off close to the end of the test, otherwise the coefficients of variation from these D-ISFS measurements are considered acceptable or lower than acceptable.

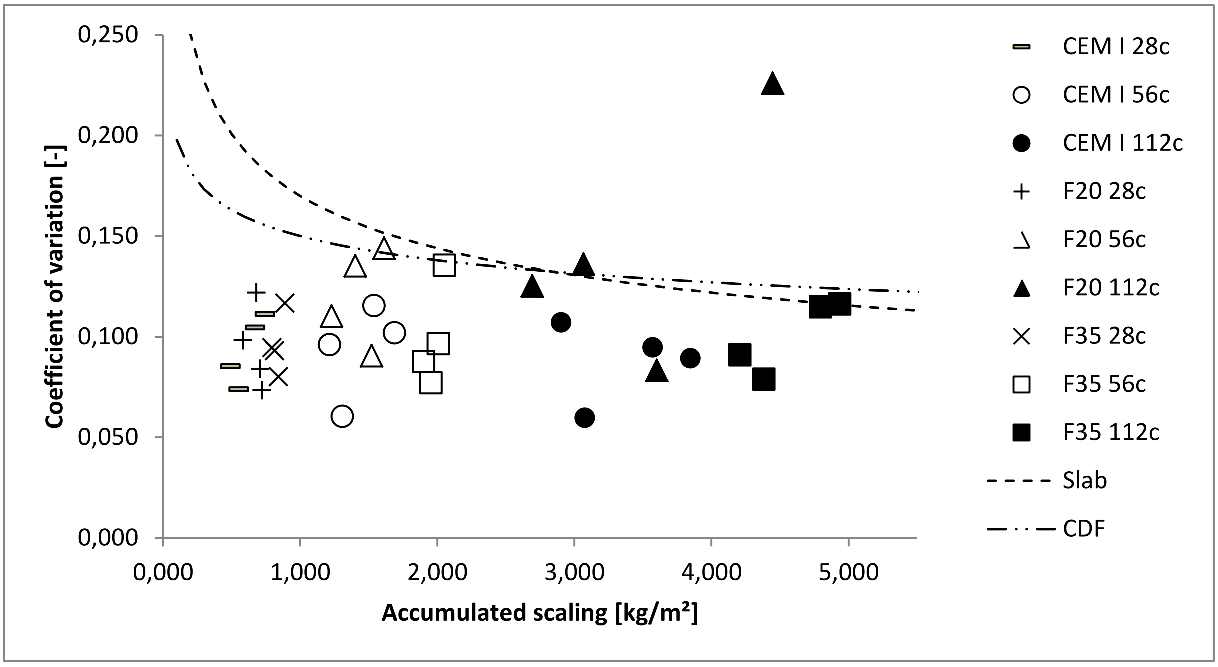

Figure 6. The relation between the mean accumulated scaling with the coefficient of variation for the six Ø100 mm² samples tested from each cast. The “dash-dot-dot” and dashed lines presents repeatability for Slab, $v_r=0.17 \cdot m^{-0.24}$ and CDF $v_r=0.15 \cdot m^{-0.12}$ [12].

4 Discussion

This paper has presented results from D-ISFS tests and air void analysis for concrete allowed to hydrate for a long time in favourable conditions to reach a relatively high degree of hydration and an even quality in the microstructure given the binder combination used along with data to help specify the material. The following discussion contains three main focuses. Firstly, some relevant previous research is mentioned to enable some general comparisons of concrete containing SFA tested according to one of the standard D-ISFS methods and the method used in the present article. Secondly, a discussion is given regarding what effect the different air void systems had on the D-ISFS damage for each of the tested materials considering the results presented in the article. Thirdly, some suggestion for future research needed to get some more information regarding the D-ISFS mechanism(s) from testing concrete containing various binders.

4.1 De-icing Salt Frost Scaling Results

Pigeon M. et al. [20] concluded that the SFA, used in the study, tend to increase the bleeding which reduce the water/cement ratio at the concrete surface which increase the scaling. This can explain high mass of scaling in concrete containing FA when testing a trowelled surface. However, the present article analyse sawed surfaces that enable a study of the material unaffected by any surface bleeding.

Most previous studies on the D-ISFS of concrete containing SFA have used one of the standard methods. Therefore, it is important to know the differences between the standard methods and the method used in the current article when comparing any trends shown in the scaling results. The ASTM C672-, CDF- and SS137244:2005 (aka slab) method all precondition the samples in a climate room with (approximately) 20 °C and 50 % RH. This preconditioning both dehydrates, and enables carbonation, of the samples test surfaces. Jacobsen et al. [14] studied the effect from drying the samples before the D-ISFS test began using concrete with two different OPCs (and also concrete that contain silica fume). The results from that study show that a short exposure-period to carbonation and dehydration before D-ISFS test begin will decrease the mass of scaling in comparison to results from never dried and noncarbonated concrete. Utgenannt [13] showed in one study that carbonation of concrete containing CEM I have a large impact on the D-ISFS. In the study, samples exposed to drying in the absence of CO_2 with samples exposed to drying and 1 vol% CO_2 for one week, and also samples which had never dried. The results showed a reduction of D-ISFS from approximately 7 kg/m² (uncarbonated) to 0.2 kg/m² (carbonated), and the samples that had never dried had approximately 9 kg/m². The effect from the preconditioning in the standard of two weeks of exposure to approximately 0.04 vol% carbon dioxide in 20 °C and a favourable relative humidity (50 to 60 %) for carbonation is however unclear. The results from Bilodeau and Malhotra [16] indicate that drying and carbonation, of concrete samples containing 100% OPC, for three weeks have approximately the same effect as six weeks in "air" (temperature and relative humidity is not presented). For concrete containing 20 and 30 mass% FA with wbr 0.35 there seems to be a reduction when increasing the drying from three to six weeks. For concrete containing FA with wbr 0.45 and 0.55 the results are not so clear regarding how the prolonged drying affect the D-ISFS.

Results of low temperature calorimetry measurements in combination with the D-ISFS test according to ASTM C672 (on sawed test surfaces) from Marchand et al. [21] indicated that the microstructure does not have a large impact on the D-ISFS damage. The low temperature calorimetry showed that there was approximately the same mass of freezable water in a paste containing OPC and another containing 80 mass% OPC and 20 mass% SFA down to -35 °C. However, the D-ISFS test showed that the OPC accumulated 0.09 kg/m² after 50 cycles while the 20 mass% SFA recipe accumulated 0.45 kg/m². One explanation to these D-ISFS results could be that the test surface of the OPC was carbonated from the preconditioning, and thereby produce a low mass of D-ISFS, while the samples used for the low temperature calorimetry test not completely carbonated. If this was the case, the low temperature will test the porosity in the entire sample and not exclusively the porosity of the test surface exposed to the D-ISFS. Then the D-ISFS test show the D-ISFS of a carbonated surface and the low temperature calorimetry would show the freezable water content inside a sample with an uncarbonated porosity. The results presented in this article for O-4 and F20-4 after approximately 50 cycles are 1.03 and 1.06 kg/m², which when compared to 0.09 and 0.45 kg/m² suggest that both recipes will benefit from carbonation. However, the recipe containing 20 mass% SFA does not benefit as much as the one only containing CEM I. The F35-4 cast have approximately 1.60 kg/m² after 50 cycles while the recipe containing 40 mass% SFA by Marchand et al. [21] only have 0.74 kg/m². This suggest that the recipe with 40 mass% SFA also can benefit from carbonation of the OPC, however not as much as the recipes with a smaller fraction of SFA. The low temperature calorimetry measurements presented by Marchand et al. [21] showed that the recipe containing 40 mass% SFA had more freezable water in comparison to the recipe with 20 mass% SFA down to -35 °C which could also be a factor contributing to a larger mass of scaling damage for the recipe containing 40 mass% SFA.

According to Figure 6, the coefficient of variation for the six samples from each batch is generally the same or lower than the coefficient of variations which are given according to [12] for the slab and CDF standard methods. The coefficient of variation for F20 after 120 cycles is very high because of two samples where large stone scaled off close to the end of the test which is also visible in Figure 1 where the accumulated scaling every seventh cycle for F20 is shown.

4.2 Air Void System Parameters

According to the air void analysis the amount of air voids smaller than 350 µm increase when increasing the mass of added AEA for all three binders (100% CEM I, 20 and 35 mass% SFA). The air void analysis and D-ISFS results from these uncarbonated and well hydrated specimens indicate that a binder consisting of 80+20 mass% of CEM I+SFA will be affected by a larger amount of small air voids in the same way as 100% CEM I. Both of these binders will produce a smaller mass of D-ISFS when the hardened cement paste contain a larger amount of air voids smaller. The concrete containing a binder combination consisting of 65+35 mass% CEM I+SFA seems to gain a small reduction in the mass of D-ISFS with the addition of a larger mass of AEA, however, not as significant as the other two binders. In addition to this, the mass of D-ISFS is notably higher than the other two binders tested. This suggest that the added 15 mass% (from 20 to 35 mass%) contribute to a significant change in the hardened paste which makes the material more susceptible to the D-ISFS mechanism(s). The results from the strength test indicate that the strength of the concrete with 35 mass% SFA is lower when hydrated for 91 days in 20±1 °C water. This could indicate a more porous microstructure. According to the measurements presented in [21] the same amount of ice is formed in concrete with 100 mass% Type 10 cement as when the cement is blended with 20 mass% FA at -10, -20 and -35 °C. However, when the measurements are made on a binder containing 40 mass% FA there is a larger mass of freezable water at these temperatures.

For the concrete tested with the largest mass of AEA tested in the present article the air to paste ratio was close to 10 vol%. Van den Heede et al. [32] tested two recipes with 50 mass% with two different SFAs where the D-ISFS resistance improved when increasing the air content from approximately 5% to 7%. The recipes with an air content of 7%, which corresponded to approximately 20% air in the paste, had an acceptable mass of scaling according to NBN EN 1339 [33]. The results presented in the current study together with the results from [32] indicate that the mass of D-ISFS will decrease further when increasing the air content.

Feldman [34] presents results from mercury intrusion porosimetry indicate that there are more “ink bottle pores” in hardened paste with FA. The reason for this could be that the pozzolanic FA reactions occur late than the cement reaction, which means there is already a solid matrix. This could increase the risk for the products created by the pozzolanic reaction to seal some of the capillary pores, which makes the air void system less continuous. This could in turn contribute to larger hydraulic pressures when ice is formed during the freezing process [35].

4.3 Future Research

The importance of carbonation of the concrete surface exposed to D-ISFS needs to be studied further. Samples taken from the same batches as the samples tested in this article will be tested after exposure to carbonation. These samples have been exposed to the same sealed hydration, however, they have also been carbonated in approximately 2 years in a climate of 60±5 % RH, 20.0±0.1 °C and 0.04 vol% carbon dioxide. The results from the uncarbonated concrete presented in the current article will then be compared to the results from the carbonated concrete. This means that the effect which the air void contents has on the D-ISFS damage for each binder can be evaluated for carbonated concrete and compared to noncarbonated concrete. Another factor that would be interesting to study to gain more knowledge regarding the D-ISFS mechanism is if the added amount of small air voids will continue to decrease the mass of D-ISFS for uncarbonated concrete until it is 0 kg/m². If not, this would answer when added effect from the air voids stop decreasing the mass of D-ISFS. Further analysis of the variation in microstructure of the concrete surface and its impact on the D-ISFS damage is also needed to give a better understanding about the D-ISFS mechanism(s). With a better understanding of relation between the surface microstructure and the D-ISFS mechanism(s) it could perhaps lead to new developments and possibilities to predict the D-ISFS damage of binders.

5 Conclusions

- The results from the D-ISFS method used in the present article indicate that the air void system have approximately the same efficiency in reducing the D-ISFS damage in the uncarbonated and well hydrated concrete containing 100% CEM I and 80+20 mass% CEM I+ siliceous fly ash.
- The results from the uncarbonated and never dried concrete containing 65+35 mass% CEM I+siliceous fly ash show that the air void system seems to have a lower efficiency in comparison to the other two binders tested.
- The total D-ISFS damage indicate that the uncarbonated and well hydrated concrete, containing a SP in combination with an AEA, with binder containing 100% CEM I is affected by the D-ISFS mechanism(s) to the same extent as the binder containing 80+20 mass% CEM I+ siliceous fly ash. The results from the uncarbonated and well hydrated concrete containing the “F35” binder show that the additional 15 mass% of fly ash in comparison to the “F20” binder increase the D-ISFS damage.

References

1. Standard, S., *SS 137003:2015 Concrete - Application of SS-EN 206 in Sweden*. 2015, Swedish Standards Institute. p. 52.
2. Standard, S., *SS-EN 206:2013 Concrete - Specification, performance, production and conformity*. 2013.
3. Powers, T.C., *The mechanism of frost action in concrete (Part II).* Cement, Lime and Gravel, 1966. **41**(6): p. 5.
4. Verbeck, G.J. and P. Klieger, *Studies of "Salt" Scaling of Concrete*, H.R.B. 150, Editor. 1957: Washington D.C. p. 13.
5. Bach, T., *Performance of air-entraining agents in concretes containing fly-ash*. 1980. p. 118.
6. Gebler, S.H. and P. Klieger, *Effect of fly ash on the air-void stability of concrete.* ACI, 1983. **79**: p. 103-142.
7. Du, L. and K.J. Folliard, *Mechanisms of air entrainment in concrete.* Cement and Concrete Research, 2005. **35**(8): p. 1463-1471.
8. ASTM, *ASTM C618-12a Coal fly ash and raw or calcined natural pozzolan for use in concrete*, in *ASTM C618 Standard Spec. Coal Fly Ash and Raw or Calcined Natural Pozzolan*. 2013.
9. Dubovoy, V.S., S.H. Gebler, and P. Klieger, *Cement-Alkali Level as it Affects Air-Void Stability, Freeze-Thaw Resistance, and Deicer Scaling Resistance of Concrete*. 2002, RD128: Portland Cement Association. 24.
10. Pistilli, M.F., *Air-Void Parameters Developed by Air-Entraining Admixtures, as Influenced by Soluble Alkalies from Fly Ash and Portland Cement.* Journal of the American Concrete Institute, 1983. **80**(3): p. 217-222.
11. Pigeon, M., et al., *Influence of soluble alkalies on the production and stability of the air-void system in superplasticized and nonsuperplasticized concrete.* ACI Materials Journal, 1992. **89**(1): p. 24-31.
12. CEN/TS, *CEN/TS 12390-9* in *Testing hardened concrete - Part 9: Freeze-thaw resistance - Scaling*. 2006. p. 24.
13. Utgenannt, P., *The influence of ageing on the salt-frost resistance of concrete*, in *Department och Building and Environmental Technology*. 2004, Faculty of Engineering, LTH, Lund University: Lund. p. 346.
14. Jacobsen, S., et al., *Frost deicer salt scaling testing of concrete: Effect of drying and natural weathering.* Cement Concrete and Aggregates, 1997. **19**(1): p. 8-16.
15. Nowak-Michta, A., *Water-binder Ratio Influence on De-icing Salt Scaling of Fly Ash Concretes*. Procedia Engineering, 2013. **57**: p. 823-829.
16. Bilodeau, A. and V.M. Malhotra. *Deicing salt scaling resistance of concrete incorporating supplementary cementing materials CANMET research*. in *Freeze-Thaw Durability of Concrete - rilem proceedings 30*. 1997. E & FN SPON.
17. Zhang, M.H., et al., *De-Icing Salt Scaling of Concrete Incorporating Different Types and Percentages of Fly Ashes*, in *Sixth CANMET/ACI International Conference on Fly Ash, Silica Fume, Slag, and Natural Pozzolans in Concrete*, V.M. Malhotra, Editor. 1998, ACI: Bangkok, Thailand. p. 493-525.
18. Nili, M. and M. Zaheri, *Deicer salt-scaling resistance of non-air-entrained roller-compacted concrete pavements.* Construction and Building Materials, 2011. **25**(4): p. 1671-1676.
19. Sun, C.T., W.H. Li, and B.R. Hou, *Study on Frost-Salt Resistance of Fly Ash Concrete.* Architecture and Urban Development, 2012. **598**: p. 432-437.

20. Pigeon, M., et al., *Surface microstructure and scaling resistance of concrete.* Cement and Concrete Research, 1996. **26**(10): p. 1555-1566.
21. Marchand, J., et al., *Effects of fly ash on microstructure and deicer salt scaling resistance of concrete,* in *Frost Resistance of Concrete,* M.J. Setzer and R. Auberg, Editors. 1997, E&FN Spon: University of Essen. p. 11-20.
22. Baert, G., A.-M. Poppe, and N. De Belie, *Evaluation and comparison of mechanical characteristics and durability of concrete with different cement replacement levels by fly ash*, in *Cement Combinations for Durable Concrete*, R.K. Dhir, T.A. Harrison, and M.D. Newlands, Editors. 2005, MPG Books: University of Dundee, Scotland, UK. p. 787-797.
23. Bilodeau, A., et al., *Effect of Curing Methods and Conditions on the Performance of Fly Ash Concrete in De-Icing Salt Scaling*, in *Sixth CANMET/ACI International Conference on Fly Ash, Silica Fume, Slag, and Natural Pozzolans in Concrete*, V.M. Malhotra, Editor. 1998, ACI: Bangkok, Thailand. p. 361-384.
24. Marchand, J., M. Jolin, and Y. Machabée, *Deicer salt scaling resistance of supplementary cementing material concrete: laboratory results against field performance*, in *Cement Combinations for Durable Concrete*, R.K. Dhir, T.A. Harrison, and M.D. Newlands, Editors. 2005, MPG Books: University of Dundee, Scotland, UK. p. 579-590.
25. Bouzoubaâ, N., et al., *Deicing salt scaling resistance of concrete incorporating supplementary cementing materials: laboratory and field test data.* Canadian Journal of Civil Engineering, 2008. **35**: p. 1261-1275.
26. Bouzoubaâ, N., et al., *Deicing salt scaling resistance of concrete incorporating fly ash and (or) silica fume - laboratory and field sidewalk test data.* Canadian Journal of Civil Engineering, 2011. **38**: p. 373-382.
27. ASTM, *ASTM C457 / C457M - 12, Standard Test Method for Microscopical Determination of Parameters of the Air-Void System in Hardened Concrete*. 2012.
28. Strand, M.J. and K. Fridh, *Methodology to analyse the salt frost scaling mechanism(s) in concrete with different binders*, in *Materials, Systems and Structures in Civil Engineering 2016*. 2016: Technical University of Denmark, Copenhagen, Denmark.
29. EN196-6, *Methods of testing cement- Part 6: Determination of fineness*. 2010.
30. EN196-1, *Methods of testing cement - Part 1: Determination of strength*. 2005.
31. Strand, M.J. and K. Fridh, *Test Method for Salt Frost Scaling of Concrete using Climate Chambers with Air as Thermal Medium with an Upside Down Sample Setup*. Manuscript, Lund University.
32. Van den Heede, P., J. Furniere, and N. De Belie, *Influence of air entraining agents on deicing salt scaling resistance and transport properties of high-volume fly ash concrete.* Cement and Concrete Composites, 2013. **37**: p. 293-303.
33. CEN, *NBN EN 1339*, in *Concrete paving flags - requirements and test methods*. 2003: Brussels.
34. Feldman, R.F., *Pore structure damage in blended cements caused by mercury intrusion.* Journal of the American Ceramic Society, 1984. **67**(1): p. 30-33.
35. Powers, T.C. and R.A. Helmuth, *Theory of volume changes in hardened portland-cement paste during freezing.* Proceedings, Highway Research Board 32, PCA Bull 46, 1953.

Appendix 6 – Paper 4

Low Air Void Contents effect on the De-Icing Salt Frost Scaling in Uncarbonated Concrete containing Ground Granulated Blast-Furnace Slag

Martin Strand, Katja Fridh

Division of Building Materials, Lund University, Lund, Sweden

Corresponding author's info.
E-mail: martin.strand@byggtek.lth.se
Telephone: (+46)7 02 95 68 75

Abstract

This article present the results showing how various air void contents (0 to 5 vol%) affect the de-icing salt frost scaling (D-ISFS), for uncarbonated never dried concrete containing 20, 35 and 70 mass% slag and a ternary blend with 25+10 mass% slag+lime filler blended with the CEM I. A combination of superplasticizer (SP) and air entraining agent (AEA) have been used to produce four slightly different air void systems. This enables a study of what effect different air void systems has on the D-ISFS for the binder combinations containing various fractions of slag in concrete. The concrete was sealed and hydrated for a 307 days before the D-ISFS test started to decrease the risk for changes in the microstructure, e.g. due to hydration, during the D-ISFS test. The results show low effect from the different air void systems for the binder with 20 mass% slag, and there seems to be an increase in mass of D-ISFS with an increased air content for 35 and 70 mass% slag. The uncarbonated concrete with the ternary binder containing 65 mass% CEM I with 25 mass% slag and 10 mass% lime filler seems to be least affected by the D-ISFS mechanism(s), however there seem to be a negligible effect from an increased air content when SP and AEA is used.

Keywords: Concrete, De-Icing Salt frost scaling, Ground granulated blast furnace slag, Uncarbonated, Never dried

Acknowledgement

This research was carried out with the financial support of SBUF (The Development Fund of the Swedish Construction Industry), Cementa AB (a part of Heidelberg Cement Group) and Skanska.

1 Introduction

To decrease the cement productions impact on the climate, due to its carbon dioxide (CO_2) emissions from the production of clinker, supplementary cementitious materials (SCMs) are used. These SCMs does not act as inert filler since they can react with the hydration products and create additional calcium-silica-hydrates which will give the hardened cement paste, and at the same time the concrete, different properties. One example of a SCM is ground granulated blast furnace slag (GGBFS) from the iron industry. When GGBFS is included in the binder some properties of the concrete change, e.g. the permeability of the concrete decreases [1] and the diffusion speed of chloride ion migration also decrease [2]. When considering using these materials in constructions with a tough climate exposure, e.g. chlorides from de-icing salts in combination with freezing and thawing, the effect these changes in material properties have on the durability must be considered. Therefore the materials must be tested to get some knowledge about how it is affected by various deleterious mechanisms and to ensure concrete with high durability is used in constructions with tough climate exposure. Material failure could mean that the construction must be rebuilt or it needs to be repaired which would lead to more CO_2 emissions.

Exposure to de-icing salt in combination with freezing and thawing can lead to de-icing salt frost scaling (D-ISFS) deterioration on the surface of the concrete. This deterioration problem can be prevented for concrete containing ordinary Portland cement (OPC) by adding an air entraining agent (AEA) to the mix which creates an air void system with small air voids distributed relatively homogeneously in the hardened cement paste [3, 4]. To create a concrete with workability which reduces risk for errors during casting and at the same time have an air void system, which reduce D-ISFS, both an AEA and a superplasticizer (SP) is needed. However, when using a combination of AEA and SP the risk for water separating from the paste (bleeding) can increase and the SP can decrease the efficiency of the AEA. To enable the creation of an air void system, which consists of small air voids distributed in the concrete to reduce D-ISFS, it is important the SP and AEA work well together. According to the Swedish standard [5] the minimum requirements set on the air void system in concrete is around 4.5 % depending on the maximum aggregate size for the second toughest “frost-exposure-class, XF3” (the toughest exposure class XF4 requires acceptable results from the slab test method [6]).

The previous research regarding D-ISFS has mostly tested concrete with OPC as a binder when trying to study the D-ISFS mechanism(s) [3, 7-9]. However, since the use of SCMs has increased more studies have been done with concrete containing GGBFS, which also can give some information about the D-ISFS mechanism(s).

Previous studies agree seems to agree on the following things. The mass of D-ISFS increase as the mass of GGBFS and replacement fraction of the total binder content increase when the test surface has been exposed to carbonation and dehydration [10-15]. When up to approximately 35 mass% GGBFS is blended with a CEM I there seems to result in an acceptable mass of scaling in concrete (wbr 0.40 and approximately 4.5 vol% air content) according to the slab method [14-17]. In concrete with no AEA, replacing 15 to 20 mass% of CEM I with GGBFS can reduce the mass of scaling [16, 17]. The mass of D-ISFS from the slab test decrease significantly when incorporating approximately 4.5 to 5.0 vol% air void content into concrete containing GGBFS with a combination of SP and AEA (which does no cause bleeding) [16, 17]. However, these previous D-ISFS studies on concrete containing slag are made according to standard test methods. The standard methods condition the samples in climate rooms which usually have 20 °C in 50% relative humidity (RH). This implies that the test surface is exposed to evaporation and carbonation which affect the scaling results significantly when compared to uncarbonated and never dried [15, 18].

In this article concrete with four types of binder combinations are tested with a D-ISFS method presented in [19] and where the methodology presented in [20] have been used. The aim for the methodology is to reduce the factors involved in D-ISFS tests which could increase the variation in the D-ISFS results. Therefore the samples have been hydrated for a 307 days to decrease the variation in the degree of hydration, and thereby the variation in microstructure in different samples from the same batch. In addition to this, any affect from dehydration and carbonation have also been removed by the preconditioning procedure where the test surface has never been in direct contact with air before the D-ISFS test begins. This is done to focus on what effect various air contents have on the D-ISFS for various binder combinations. Three binder combinations are made with CEM I blended with 20, 35, and 70 mass% GGBFS (referred to as “S20”, “S35” and “S70”) and one combination where the CEM I is blended with 25 mass% and 10 mass% lime filler (referred to as K35). Each binder combination is made with four different air void structures, from approximately 1.5 to approximately 4.5 vol%. Recipes are presented and some material properties have been measured by XRF and ICP analysis. Results are presented from the air void analysis (which has been made according to ASTM C 457 [21]) together with the D-ISFS results which will give information about how big impact the various air void systems have on the D-ISFS created by the D-ISFS mechanism(s) for each of the binder combinations.

2 Method and Materials

The methodology for this experiment is the same as the one presented in the conference article [20]. It can be summarized as according to the following. First a test has been made to find a SP and AEA which perform well with each binder. Then a concrete recipe was cast, according to the recipes below. When casting, the mass AEA was adjusted slightly and then the air content measured in the fresh concrete was used to ensure small differences between the various batches that contain the same binder combination. The samples were then sealed and left to hydrate for approximately 307 days in 20 °C. One sample from each cast was sent for an air void analysis according to ASTM C 457 [21] to get some information about the air void system created in each cast. The specimens for the D-ISFS test were sawn and put in to de-ionized water 22±2 hours before the freeze-thaw test began. Any carbonation of the test surface was only possible during the 24 hours while it was submerged in water, therefore, the surface is considered to be uncarbonated. The hydration rate decrease over time as the degree of hydrated binder increase, therefore the long and sealed hydration contributes to a lower variation in the microstructure of the paste between various samples from the same batch. This is done to facilitate what effect the air void content has on the D-ISFS for each binder combination, when the paste is uncarbonated.

2.1 Materials

Table 1 present the recipes used for each batch which have been tested in this article with consideration to the measured air content in the fresh concrete. The binder content was set to be close to 430 kg/m³ for each recipe given an increased amount of air content. The grain fraction curve of the aggregates used had a fineness modulus of 4.79, and it was designed to have a small amount of fractions between 4 and 8 mm. The purpose of this was to increase the contrast in the scaling results from only sand in combination with cement paste scaling off to the larger aggregates started to fall off.

Tabell 1. Concrete recipes for each cast used in this study.

Batch	Binder[1][2]	Aggregate [kg/m³][2]			SP[2][3]	AEA[2][4]	Air[5]	Slump	Density[6]
	[kg/m³]	0-8	8-12	12-32	[kg/m³]	[kg/m³]	[%]	[mm]	[kg/m³]
S20-1[7]	428	962	284	534	1,080	0,000	2,00	210	2417
S20-2[7]	428	949	280	527	1,082	0,009	2,85	210	2391
S20-3[7]	429	937	276	520	1,084	0,045	3,70	220	2375
S20-4[7]	429	924	272	513	1,085	0,081	4,70	220	2345
S35-1[8]	426	959	283	532	1,077	0,000	2,30	210	2398
S35-2[8]	424	941	277	522	1,072	0,022	3,80	220	2354
S35-3[8]	426	930	274	516	1,076	0,045	4,50	220	2336
S35-4[8]	427	919	271	510	1,080	0,067	5,20	240	2314
S70-1[9]	423	951	280	528	1,068	0,000	3,20	220	2364
S70-2[9]	423	938	277	521	1,069	0,022	4,10	230	2332
S70-3[9]	426	930	274	516	1,076	0,045	4,50	240	2328
S70-4[9]	429	924	272	513	1,085	0,068	4,70	240	2324
K35-1[10]	421	948	280	526	1,065	0,000	3,50	210	2389
K35-2[10]	425	942	278	523	1,073	0,013	3,70	210	2379
K35-3[10]	424	926	273	514	1,071	0,027	5,00	220	2327
K35-4 [10]	428	920	271	511	1,081	0,041	5,10	220	2338

[1] CEM I + GGBFS content.
[2] Calculated with consideration to the air content measured in the fresh concrete according to the “Air”-column.
[3] The super plasticizer was based on a polycarboxylate.
[4] The air entraining agent for all batches was one based on a synthetic surfactant.
[5] Air content is measured in 8 dm³ of the fresh concrete.
[6] Density was determined on the same concrete as the air content.
[7] The binder consists of 80 mass% CEM I 42,5 N - SR 3 LA and 20 mass% GGBFS.
[8] The binder consists of 65 mass% CEM I 42,5 N - SR 3 LA and 35 mass% GGBFS.
[9] The binder consists of 30 mass% CEM I 42,5 N - SR 3 LA and 70 mass% GGBFS.
[10] The binder consists of 65 mass% CEM I 42,5 N - SR 3 LA, 25 mass% GGBFS and 10 mass% LF.

Table 2 presents XRF analysis of the siliceous fly ash and each binder combination which has been tested. The CEM I contained 2.36 % lime filler.

Table 2. XRF – Cement – wroxi

Binder	**$CaO^{1)}$** [%]	**$SiO_2^{1)}$** [%]	**$Al_2O_3^{1)}$** [%]	**$Fe_2O_3^{1)}$** [%]	**$MgO^{1)}$** [%]	**$K_2O^{1)}$** [%]	**Na_2O** [%]	**$Na_2Oe^{2)}$** [%]	**$SO_3^{1)}$** [%]	**$LOI^{1)}$** [%]
CEM I	63.60	21.30	3.80	4.56	0.856	0.650	0.07	0.50	2.45	1.84
S20[3)]	57.80	23.90	5.61	3.78	3.68	0.699	0.17	0.63	2.60	1.17
S35[3)]	52.70	25.90	7.10	3.11	5.92	0.748	0.26	0.75	2.76	0.56
S70[3)]	41.60	29.90	10.20	1.67	10.7	0.842	0.44	1.00	3.02	-0.59
K35[3)]	54.10	22.90	5.94	3.11	4.77	0.685	0.21	0.66	2.40	5.04

[1)] The precision in the measurements are CaO±0.233%, SiO_2±0.100 %, Al_2O_3±0.052 %, Fe_2O_3±0.019 %, MgO±0.025 %, K_2O±0.032 %, SO_3±3%, (loss on ignition=) LOI ±0.18 %. Na

[2)] Na_2O-equivalent.

[3)] Measured oxide composition from the blended GGBFS and CEM I.

Table 3 present results from Blaine-, laser diffraction- and compressive strength measurements are presented. The Blaine- and laser diffraction measurement results indicate that the slag particles have a bigger specific surface and a smaller average size than the CEM I particles and the lime filler particles have smaller specific surface and a larger average particle size than the slag. When replacing 20 and 35 mass% of the CEM I content there is no significant difference in strength other than the early 2 day strength, however when replacing 70 mass% there is a significant difference up to 91 days. The lime filler seems to have a negative impact on the strength, in comparison to the GGBFS, according to these measurements.

Table 3. Blaine-, laser diffraction- and compressive strength measurements for each binder combination.

Binder	**Blaine[1)]**	**LD[2)]**	**Strength after given days of hydration[3)] [MPa]**			
	[m²/kg]	**[µm]**	**2 days**	**28 days**	**56 days**	**91 days**
CEM I	343	17.305	21.8±0.3	55.1±0.3	62.3±1.2	66.1±2.0
S20	371	16.142	16.5±0.2	52.1±0.8	63.3±1.3	65.3±1.3
S35	395	15.339	12.9±0.1	53.9±0.6	63.5±0.7	67.4±0.5
S70	448	13.957	4.4±0.1	42.4±0.4	49.3±0.9	51.8±1.1
K35	397	16.439	12.8±0.3	47.9±1.2	55.2±0.6	58.3±0.6

[1)] Blaine value of specific surface area per mass binder measured according to EN 196-6:2010.

[2)] Laser diffraction measurement on the size of the 50th percentile particles size.

[3)] Compressive strength measured according to EN 196-1:2005 with the standard deviation.

2.2 De-Icing Salt Frost Scaling Method

The D-ISFS method that has been used in this study is presented in Strand and Fridh [22]. It is an upside down sample setup with freezers, which have air as thermal conductor, that cycle between +20 and -22 °C (just below the eutectic temperature). The exposure time to each temperature is 12 hours, which means that the total time per cycle is 24 hours. The samples are 100 mm in diameter, six samples are tested per batch of concrete and measurements are done on each sample once every seventh day.

3 Results

3.1 Air Void Analysis

Table 4 presents results from the air void measurements which have been made on the fresh and hardened concrete to describe and quantify the air void systems. The air void content is calculated for different air void sizes from the cords which a linear traverse measurement results in. The paste content is 31 vol% of the concrete and the air content when only considering the paste is presented in the columns “Air void content in paste” (two different air void ranges). The specific surface and spacing factor is also included for each cast, calculated with regards to the voids <2 mm since air pores bigger than 2 mm contribute very little to the D-ISFS resistance in relation to smaller air voids.

Table 4. Air content measured in fresh concrete and results from linear traverse measurements according to ASTM C 457.

Cast	**Fresh Concrete [%]** 1)	**Air void content**			**Air void content in paste**		**Specific surface**	**Spacing factor**
		Total [%] 2)	**<2 mm [%]** 2)3)	**<0.35 mm [%]** 2)4)	**<2.00 mm [%]** 2)5)	**<0.35 mm [%]** 2)6)	**[mm^{-1}]** 2)7)	**[mm]** 2)8)
S20-1 9)	2,00	3,6	2,3	0,7	6,6	2,2	13	0,55
S20-2 9)	2,85	5,1	2,9	1,1	8,0	3,0	17	0,38
S20-3 9)	3,70	2,3	1,9	1,2	5,4	3,7	27	0,29
S20-4 9)	4,70	3,7	3,4	2,1	9,8	6,1	30	0,20
S35-1 10)	2,30	3,1	1,5	0,5	4,4	1,5	16	0,54
S35-2 10)	3,80	3,6	2,9	1,3	8,4	3,9	19	0,33
S35-3 10)	4,50	3,1	2,7	1,5	7,9	4,3	25	0,27
S35-4 10)	5,20	5,6	4,5	2,4	12,6	6,7	23	0,23
S70-1 11)	3,20	2,9	2,5	0,9	7,4	2,6	14	0,48
S70-2 11)	4,10	2,7	2,2	1,1	6,8	3,2	21	0,35
S70-3 11)	4,50	4,3	3,3	1,4	9,3	4,1	18	0,35
S70-4 11)	4,70	3,3	2,7	1,2	8,2	3,5	17	0,38
K35-1 12)	3,50	3,3	2,7	1,0	7,9	3,0	17	0,40
K35-2 12)	3,70	3,7	2,9	1,2	8,4	3,5	18	0,35
K35-3 12)	5,00	3,5	3,1	1,5	8,7	4,5	23	0,27
K35-4 12)	5,10	3,2	3,1	1,6	8,8	4,9	23	0,27

1) Total air content measured in 8 dm^3 fresh concrete.

2) Calculated from results from linear traverse measurements according to ASTM C 457.

3) Total air content from air voids <2.000 mm.

4) Total air content from air voids <0.350 mm.

5) Voids <2.000 mm / (vol% cement paste + vol% of total voids). Vol% cement paste is calculated to 31%.

6) Voids <0.350 mm / (vol% cement paste + vol% of total voids). Vol% cement paste is calculated to 31%.

7) Specific surface ($\text{mm}^2/\text{mm}^3=\text{mm}^{-1}$) calculated from results of voids <2.00 mm.

8) Spacing factor calculated from results of voids <2.00 mm.

9) S20-1, 2, 3 and 4 were sealed 35, 29, 34, and 22 days when delivered for the linear traverse analysis.

10) S35-1, 2, 3 and 4 were sealed 128, 121, 121, 126 days when delivered for the linear traverse analysis.

11) S70-1, 2, 3 and 4 were sealed 101, 100, 100, 101 days when delivered for the linear traverse analysis.

12) K35-1, 2, 3 and 4 were sealed 108, 106, 106, 107 days when delivered for the linear traverse analysis.

The results from the linear traverse analysis are made on one sample per batch to give an indication of how the air void systems vary when changing the mass of AEA. The purpose of this is to enable an estimate of how big impact the air void system has on the amount of D-ISFS produced by the D-ISFS method for each of the concretes containing CEM I with 20, 35, 70 mass% GGBFS and 25+10 mass% GGBFS+LF.

3.2 De-Icing Salt Frost Scaling

Figure 1 presents two different diagrams which show the accumulated scaling and the 7 cycle scaling measured every week. All lines in the 7 cycle scaling diagram gives information about a slight to moderate acceleration of scaling which means that the accumulated scaling curves bends slightly upwards.

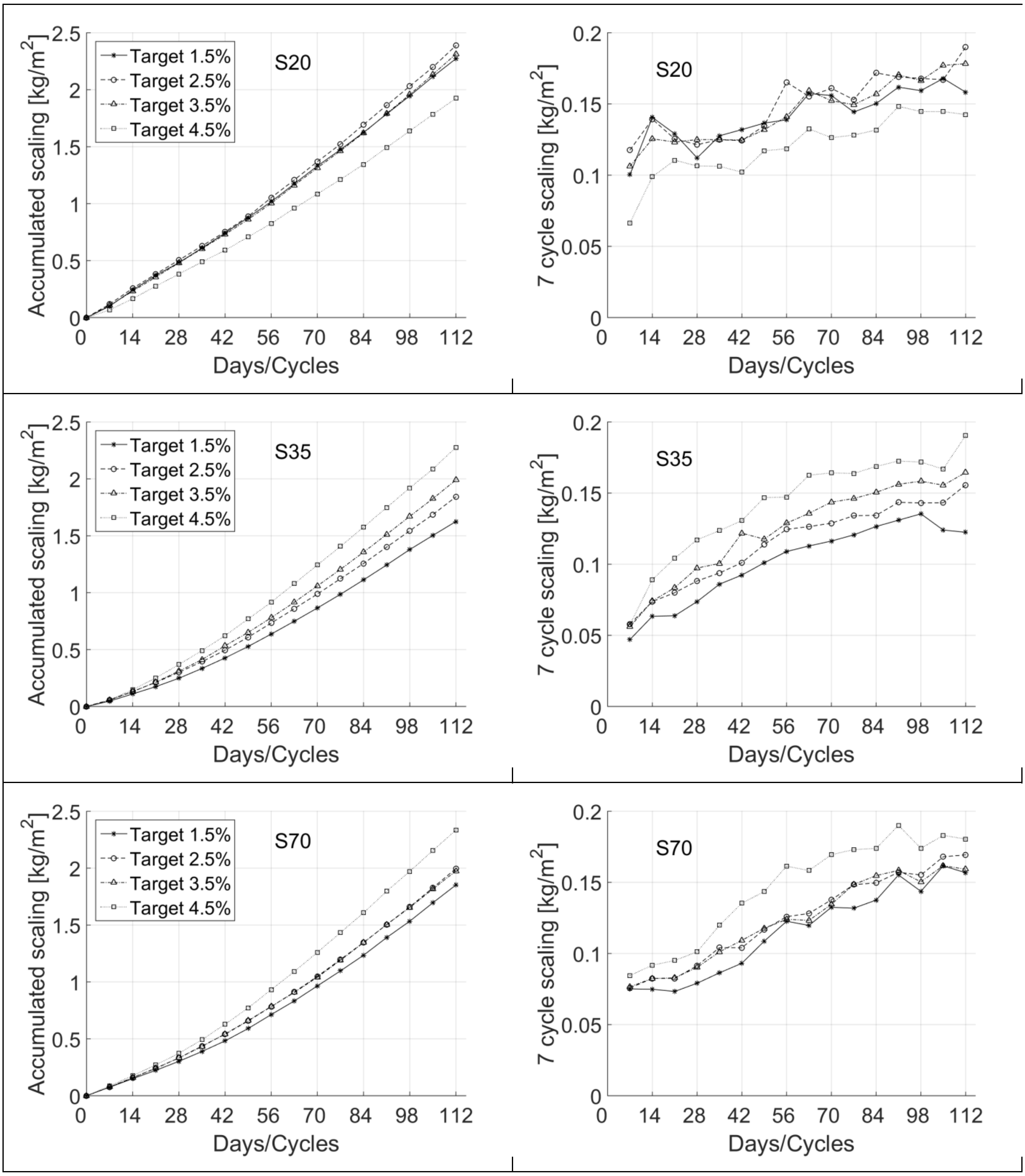

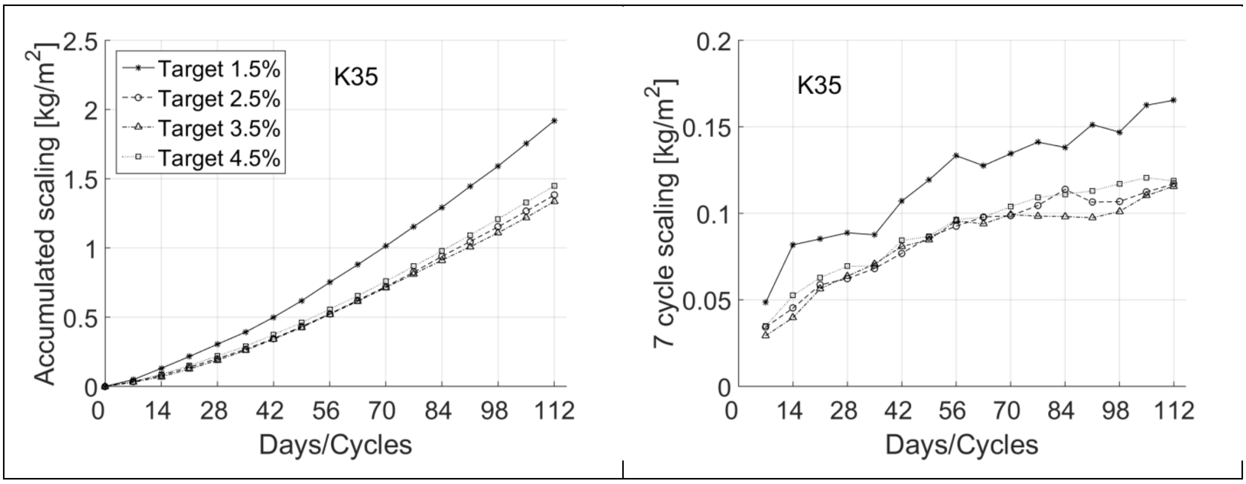

Figure 1. In the left column the total accumulated- and in the right column the mean D-ISFS per week for each cast during the D-ISFS test. Line 1 presents cast 1 with target air content 1.5 vol%. Line 2 presents cast 2 with target air content 2.5 vol%. Line 3 present cast 3 with target air content 3.5 vol%. Line 4 present cast 4 with target air content 4.5 vol%. Each point presents the mean value of six Ø100 mm² samples.

Figure 2 and 3 present the mean accumulated D-ISFS damage from the six samples after 56 and 112 cycles with the standard deviation highlighting the middle and end sections of the accumulated scaling diagrams (left column of Figure 1) with an indication of the variation for each cast.

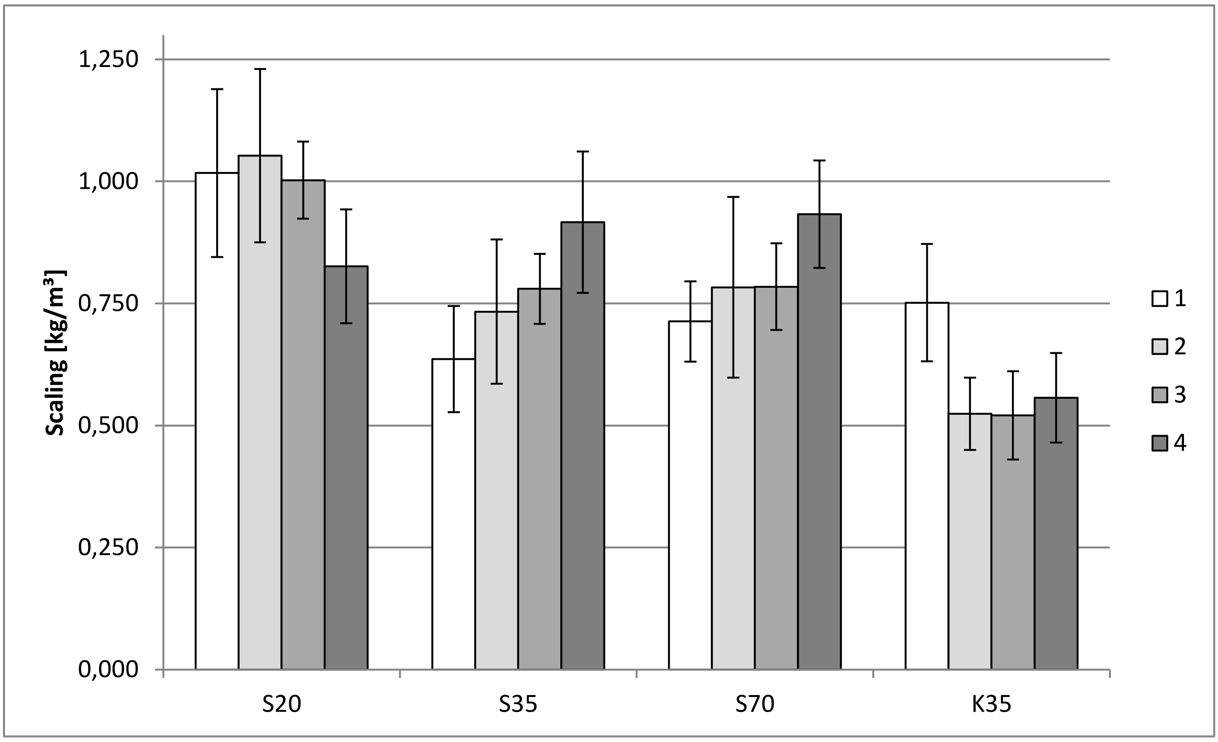

Figure 2. Each accumulated scaling with standard variation from six Ø100 mm² samples after 56 cycles.

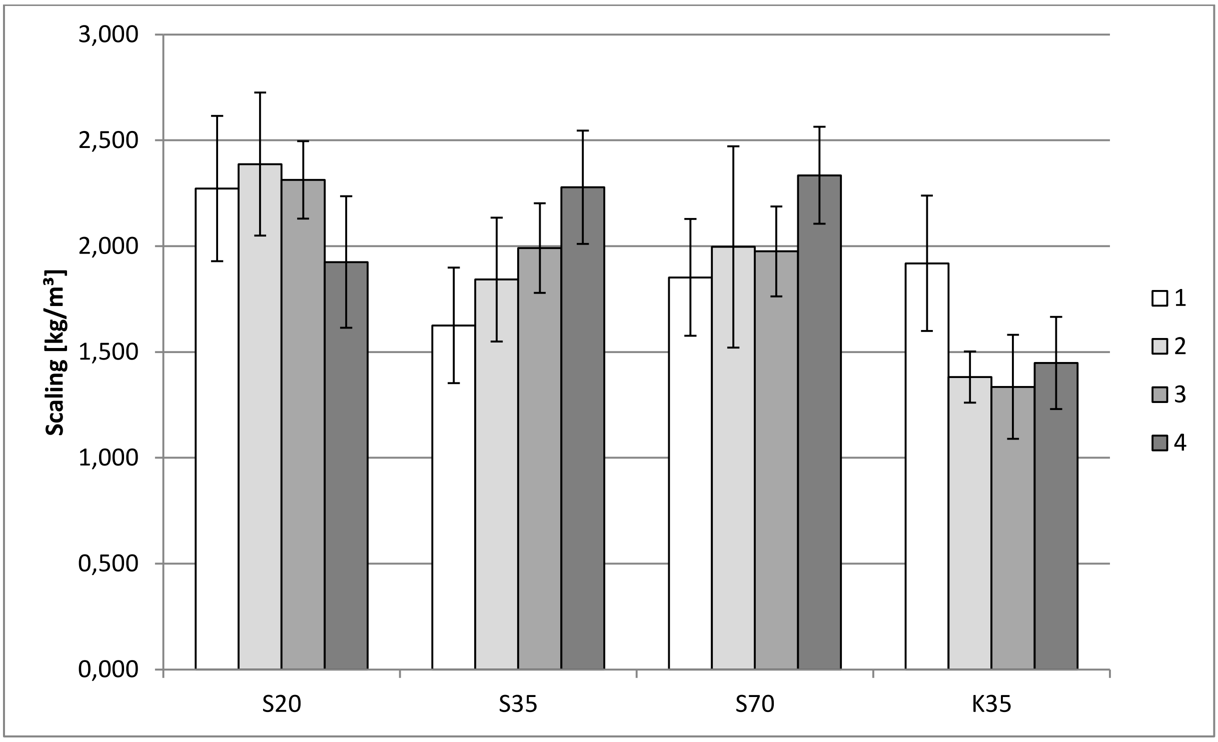

Figure 3. Each accumulated scaling with standard variation from six Ø100 mm² samples after 112 cycles.

Figure 5 presents the accumulated scaling in relation to the coefficient of variation for each cast tested together with the repeatability of the CDF- and the Slab method (CEN/TS 12390-9). The casts with the same binders after 56 and 112 cycles are presented to present the coefficient of variation and a rough idea about how it seems to vary over time. In general, those points close to or above the repeatability levels according to the standard methods all have one or a few samples where stones (which constitute part of the test surface) have not been frost resistant and therefore scaled off which increase the standard variation and thereby the coefficient of variation. S35 had one sample with two non-frost resistant stones which was destroyed during the first weeks which explain the high coefficient of variation after 56 cycles.

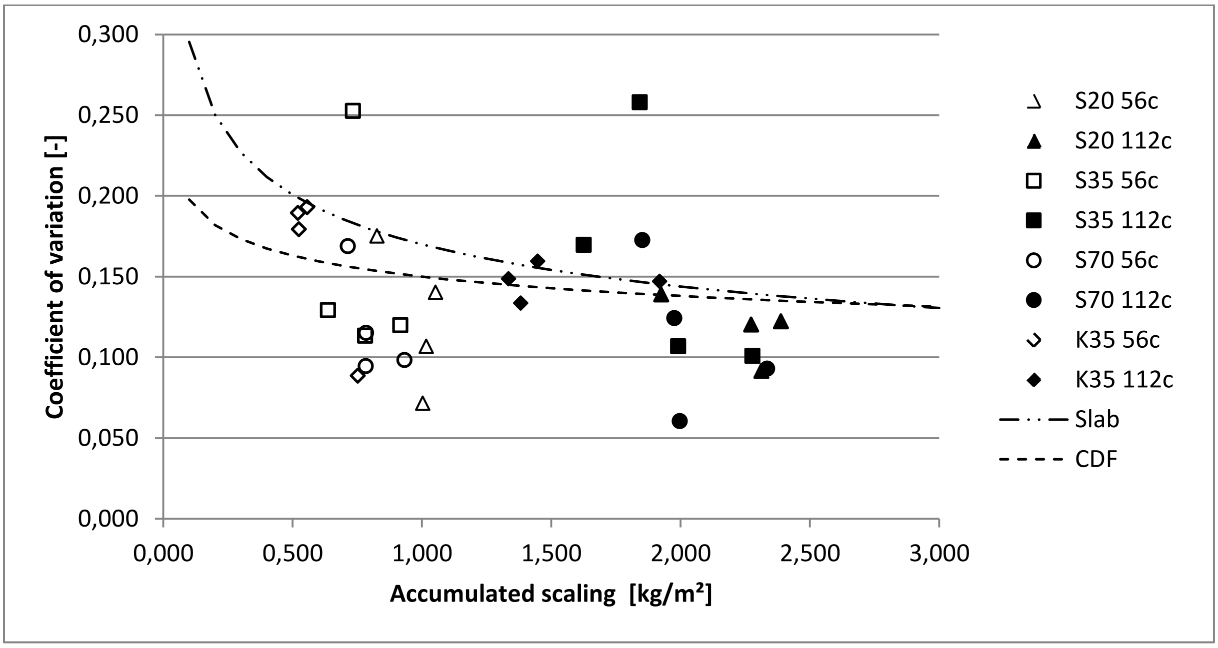

Figure 5. The relation between the mean accumulated scaling with the coefficient of variation for the six Ø100 mm² samples tested from each cast. The "dash-dot-dot" and dashed lines presents repeatability for Slab, $v_r=0.17 \cdot m^{-0.24}$ and CDF $v_r=0.15 \cdot m^{-0.12}$.

4 Discussion

4.1 De-Icing Salt Frost Scaling

The mass of D-ISFS differ very little between S35 and S70, while S20 seems to have a slightly larger mass of D-ISFS and K35 have the lowest mass of scaling when mixed with both SP and AEA.

According to Figure 3, the mass of D-ISFS varies between approximately 1.5 and 2.5 kg/m² after 112 cycles which is a larger mass of scaling than the acceptable limit for the slab method which is 1.0 kg/m². However, these results agree with [15] that tested concrete containing GGBFS with test surfaces that were "never dried+uncarbonated", "dried+uncarbonated" and "dried+carbonated". The results from that study showed that all of the uncarbonated and never dried surfaces also produced a mass of D-ISFS clearly larger than 1 kg/m². Based on these D-ISFS results along with some complementary low temperature calorimetry measurements the conclusion was drawn that the carbonation of the hardened paste is crucial for the D-ISFS damage. In addition to this, in [15] the accumulated D-ISFS curve of the uncarbonated concrete seems to be linear, i.e. the D-ISFS rate is high during the entire test. This also agrees with the results presented in Figure 3. The slight acceleration in the current study is believed to be because the probability for larger stones to scale off increase when the number of cycles increase. The D-ISFS rate [15] seems to be more constant, however, this is most likely because a “micro concrete” was used where there were no aggregates larger than 8 mm (no SP or AEA was included either). This probably also contributed to a lower standard deviation in the results in comparison to the standard deviation in the current study.

Results from [18] also indicate that never dried test surfaces scale more than test surfaces dried in climate chamber with ca 50 to 70 % RH and 20 °C for 14 days. This, along with [15], highlight the importance of preconditioning. In addition to this they also contribute with an explanation for the low masses of D-ISFS from the standardized methods when concrete with similar CEM I blended with low fractions of GGBFS is tested [17].

Some results presented in [15] indicate that when uncarbonated and never dried, the mass of D-ISFS is larger for micro concrete containing 20 mass% compared to 35 mass% slag. Also the mass of D-ISFS is larger for micro concrete containing 35 mass% compared to 70 mass% slag when the test surface is uncarbonated and never dried. According to the results presented in the current article the mass of D-ISFS is slightly smaller for S35 and S70 than S20 when comparing the casts only containing SP, which also seems to agree with the results from [15]. Results presented in the current article varies approximately from 0.6 kg/m² to 1.1 kg/m² after 56 cycles, while the variation of mass of D-ISFS from 20, 35 and 65 mass% according to Utgenannt [15] is approximately from 3.3 to 4.5 kg/m². The reason for the larger mass of D-ISFS in the results presented by Utgenannt believed to be that the wbr is higher (0.45), the micro concrete have hydrated for a shorter period (31 days), max fraction used in the micro concrete is 8 mm, and no SP or AEA was used in comparison to the current article.

The results from the recipe containing 25+10 mass% GGBFS+LF seems to have a slightly larger mass of D-ISFS in comparison to 35 and 70 mass% GGBFS the recipes only contain SP. This suggests that when including a 10 mass% of LF in to the binder, instead of only using 35 mass% GGBFS, will increase the mass of D-ISFS. However, there is a clear decrease in the mass of D-ISFS when the AEA is added. According to the air void analysis there seems to be an increase in the amount of small air voids when the mass of AEA increase. However, there is only a difference in scaling when comparing the recipes with AEA and the one without.

When considering the D-ISFS results in relation to the compressive strength, the results agree with a previous study by [13] which also show that there is no direct correlation between the mass of D-ISFS and the compressive strength for each binder. This is clearly shown just by looking at the compressive strength for S35 and S70 where S35 have approximately 15.6 MPa higher compressive strength than S70, yet they still produce approximately the same mass of D-ISFS. Another study by [23] tested pull-off strength, which can be considered related to the tensile strength of the material, in relation to the scaling test, however there was no correlation between these results. Considering that the carbonation change the micro structure and that is has an effect on the mass of D-ISFS, when doing pull off tests the rupture surface should be in the same condition as the test surface for the D-ISFS test. This means that if a carbonated surface is tested in a D-ISFS test, the surface where the rupture appeared in the pull-off test should also be carbonated to confirm that the same type of microstructure is tested in both of the tests.

According to Figure 5, the coefficient of variation was approximately as high as the coefficients given by the standard methods or lower as long as there were not non-frost resistant stones on the test surface. This can be considered to indicate that the efforts made to minimize the variation in results have been effective and this thereby enables a relatively accurate analysis of what effect the air contents have on the D-ISFS for each binder combination.

4.2 Air Void System Parameters

In concrete, containing 20 mass% GGBFS, the mass of D-ISFS seem to decrease slightly when a the mass of AEA added resulted in almost 5 vol% air content, and 6.1 vol% of the hardened paste consisted of air voids smaller than 350 µm. This indicate that the effect from the air voids is negligible in the hardened paste containing 20 mass% GGBFS until this amount of small air voids is obtained. In addition to this, the results could also suggest that the mass of D-ISFS could decrease even more if additional AEA was added to increase the amount of small air voids.

Considering the results from the linear traverse measurements both S35-1 and S70-1 clearly have longer spacing factor, smaller specific surface and less small air voids than the other casts with the same binder combinations. However they both have the lowest mass of D-ISFS out of the four concrete casts with the same binder combination. There seems to be a trend where the D-ISFS seem to increase with an increasing mass of AEA added for the concrete containing 35 and 70 mass% GGGBFS. According to the air void analysis, there seems to be clear differences for S35 casts where the amount of small air voids increase when the mass of AEA increase. The air void analysis for the S70 does not show the same clear trend, which mean that additional testing would be required to discover differences between the samples which could give some information about why the mass of D-ISFS increase with increasing mass of AEA added. The reason for the increase in mass of D-ISFS, when the amount of small air voids increase, is uncertain.

In the article [24] results are presented for concrete containing 100% of the same CEM I. Those results clearly show an increase in the amount of small air voids with an increase in mass of AEA added, and at the same time there is a clear decrease in the mass of D-ISFS. These results clearly indicate that the effect an increase amount of small air voids have on the mass of D-ISFS differs when various binder combinations are used. In the current study the results show that for uncarbonated concrete, the addition of GGBFS will decrease the mass of D-ISFS significantly in comparison to concrete with 100% CEM I. However, an increased amount of small air voids in concrete containing 35 or 70 mass% GGBFS seems to increase the mass of D-ISFS. This means that the effect from an increase amount of small air voids varies when it is combined with different unique microstructures with certain properties.

4.3 Future Studies

In a future study, samples from the same batches of concrete will be tested with the same D-ISFS test with the only difference that they have been carbonating inside a climate chamber with 60 % RH and 20 °C for approximately 2 years before the D-ISFS test begin. The combination of these “extreme” cases with uncarbonated and never dried with carbonated and dried for a very long time will give valuable information about how the D-ISFS mechanism(s) affect concrete with fly ash or slag.

Further studies will also be made on the microstructure, and the differences in the microstructures, between the uncarbonated and carbonated of the hardened pastes.

The question also remain why there does not seem to be any change in the mass of D-ISFS in the first three casts for concrete with 20 mass% GGBFS. Also, to look for some answer to why there seems to be a negative effect from additional air voids when 35 and 70 mass% GGBFS is included in the binder. To answer this more tests are needed to quantify differences between the microstructure and material properties of the concrete surfaces.

The reason why the mass of D-ISFS does not decrease with the increasing amount of small air voids for concrete containing 25+10 mass% GGBFS+LF is unknown. The differences between the uncarbonated and never dried concrete surfaces with and without AEA should be analysed further to look for any differences which could possibly explain the large difference in the mass of D-ISFS.

5 Conclusions

- The results from the D-ISFS method used in the present article indicate that the air void system created by the AEA have various effect depending on the unique never dried and uncarbonated hardened concrete created by the various binder combinations.
- When the air content is close to 5 vol%, concrete containing 20 mass% GGBFS seems to acquire a reduction in mass of D-ISFS from the air void system. However, when the air void content is lower than approximately 5 vol% the air void system does not seem to have any significant effect on the mass of D-ISFS.
- The results indicate that when including 20 mass% GGBFS in the binder there is a significant decrease in the mass of D-ISFS compared to when 100% CEM I is used for never dried and uncarbonated concrete. In addition to this, the mass of D-ISFS decrease even further when including 35 or 70 mass% GGBFS in comparison to concrete containing 20 mass% GGBFS.
- When adding a larger mass of AEA to concrete containing 35 and 70 mass% GGBFS, the mass of D-ISFS seem to increase when an uncarbonated and never dried surface is tested.
- The mass of D-ISFS in concrete containing CEM I blended with 25 mass% GGBFS and 10 mass% lime filler seems be reduced when both AEA and SP is included. However, increasing the mass of added AEA does not seem to decrease the mass of D-ISFS.

References

1. Özbay, E., M. Erdemir, and H.İ. Durmuş, *Utilization and efficiency of ground granulated blast furnace slag on concrete properties – A review.* Construction and Building Materials, 2016. **105**: p. 423-434.
2. Lang, E., *Durability aspects of CEM II/B-M with blastfurnace slag and limestone*, in *Cement Combinations for Durable Concrete,* R.K. Dhir, T.A. Harrison, and M.D. Newlands, Editors. 2005, MPG Books: University of Dundee, Scotland, UK. p. 55-64.
3. Powers, T.C., *The mechanism of frost action in concrete (Part II).* Cement, Lime and Gravel, 1966. **41**(6): p. 5.
4. Verbeck, G.J. and P. Klieger, *Studies of "Salt" Scaling of Concrete*, H.R.B. 150, Editor. 1957: Washington D.C. p. 13.
5. Standard, S., *SS 137003:2015 Concrete - Application of SS-EN 206 in Sweden*. 2015, Swedish Standards Institute. p. 52.
6. CEN/TS, *CEN/TS 12390-9* in *Testing hardened concrete - Part 9: Freeze-thaw resistance - Scaling*. 2006. p. 24.
7. Lindmark, S., *Mechanisms of Salt Frost Scaling of Portland Cement-bound Materials: Studies and Hypothesis*, in *Department of Building and Environmental Technology*. 1998, Faculty of Engineering, LTH, Lund University: Lund. p. 266.
8. Valenza II, J.J. and G.W. Scherer, *A review of salt scaling: II. Mechanisms.* Cement and Concrete Research, 2007. **37**(7): p. 1022-1034.

9. Liu, Z., *Frost Deterioration in Concrete due to Deicing Salt Exposure: Mechanism, Mitigation and Conceptual Surface Scaling Model*. 2014, University of Michigan. p. 211.
10. Bilodeau, A. and V.M. Malhotra. *Deicing salt scaling resistance of concrete incorporating supplementary cementing materials CANMET research*. in *Freeze-Thaw Durability of Concrete - rilem proceedings 30*. 1997. E & FN SPON.
11. Panesar, D.K. and S.E. Chidiac, *Multi-variable statistical analysis for scaling resistance of concrete containing GGBFS.* Cement and Concrete Composites, 2007. **29**(1): p. 39-48.
12. Giergiczny, Z., et al., *Air void system and frost-salt scaling of concrete containing slag-blended cement.* Construction and Building Materials, 2009. **23**(6): p. 2451-2456.
13. Hooton, R.D. and D. Vassilev, *Deicer Scaling Resistance of Concrete Pavements, Bridge Decks, and Other Structures Containing Slag Cement: Phase 2: Evaluation of Different Laboratory Scaling Test Methods*. 2012.
14. Löfgren, I., O. Esping, and A. Lindvall, *The influence of carbonation and age on salt frost scaling of concrete with mineral additions*, in *Materials, Systems and Structures in Civil Engineering 2016*, M.T. Hasholt, K. Fridh, and R.D. Hooton, Editors. 2016, RILEM publications S.A.R.L: Technical University of Denmark, Lyngby, Denmark. p. 91-100.
15. Utgenannt, P., *The influence of ageing on the salt-frost resistance of concrete*, in *Department och Building and Environmental Technology*. 2004, Faculty of Engineering, LTH, Lund University: Lund. p. 346.
16. Boubitsas, D., et al., *Frost resistance of concrete - Experience from long term exposure*, in *Materials, Systems and Structures in Civil Engineering 2016*, M.T. Hasholt, K. Fridh, and R.D. Hooton, Editors. 2016, RILEM publications S.A.R.L: Technical University of Denmark, Lyngby, Denmark. p. 21-30.
17. Helsing, E. and P. Utgenannt, *The salt-frost resistance of concrete with supplementary cementitoius materials (SCM)*, in *Materials, Systems and Structures in Civil Engineering 2016*, M.T. Hasholt, K. Fridh, and R.D. Hooton, Editors. 2016, RILEM publications S.A.R.L: Technical University of Denmark, Lyngby, Denmark. p. 51-60.
18. Jacobsen, S., et al., *Frost deicer salt scaling testing of concrete: Effect of drying and natural weathering.* Cement Concrete and Aggregates, 1997. **19**(1): p. 8-16.
19. Strand, M.J., *Low Air Void Contents effect on the De-Icing Salt Frost Scaling Damage in Uncarbonated Concrete containing Siliceous Fly Ash and Slag*, in *Building Materials*. 2016, Lunds University.
20. Strand, M.J. and K. Fridh, *Methodology to analyse the salt frost scaling mechanism(s) in concrete with different binders*, in *Materials, Systems and Structures in Civil Engineering 2016*. 2016: Technical University of Denmark, Copenhagen, Denmark.
21. ASTM, *ASTM C457 / C457M - 12, Standard Test Method for Microscopical Determination of Parameters of the Air-Void System in Hardened Concrete*. 2012.
22. Strand, M.J. and K. Fridh, *Test Method for Salt Frost Scaling of Concrete using Climate Chambers with Air as Thermal Medium with an Upside Down Sample Setup*. Manuscript, Lund University.
23. Boyd, A.J. and R.D. Hooton, *Long-Term Scaling Performance of Concretes Containing Supplementary Cementing Materials.* Journal of Materials in Civil Engineering, 2007. **19**(10): p. 820-825.
24. Strand, M.J. and K. Fridh, *Salt Frost Scaling of Uncarbonated Concrete containing Siliceous Fly Ash with various Air Void Systems* Manuscript, Lund University.

Appendix 7

SWEDAC ACKREDITERING
2026
ISO/IEC 17025

PROVRESULTAT

utfärdat av ackrediterat provningslaboratorium

CEMENTA
HEIDELBERGCEMENTGroup
Cementa Research

Provnr: 168949

Cementa AB
Stefan Sandelin, ref 205875
Box 47210
10074 STOCKHOLM

2015-10-05

Provnr	168949		
Märkning	LTH Referensprov 0; Degerhamn anläggningscement		
Uppdrag / grupp	Analyser för LTH-doktorand		
Variant		Ankomstdatum	2015-06-18
Handläggare	Karin Lindhe	Klardatum	2015-10-05
Provtagningsdatum	2015-06-17		
Provtagning	Insänt av kund		
Provtagare			

Namn (Karin Fagerström)

* ej ackrediterad analys

	Analys	Metod	Resultat	Mätosäkerhet	Kommentar
	Leco Apparatur				
	Gl.f 950°C	ER 9213 :2005	1,84 **%**	**0,18 %**	
	Bogue Beräkningar				
*	C2S	Saknas	15,7 **%**		
*	C3S	Saknas	60,4 **%**		
	C3A	ER 9226	2,4 **%**		
*	C4AF	Saknas	13,9 **%**		
	Fysikaliska Bestämningar				
	Densitet	ER 9228	3226 **kg/m3**	**40 kg/m3**	
	Blaine, manuell	EN 196-6 :2010	343 **m2/kg**	**3 %**	
	Bindetid				
	Vatten	EN 196-3 :2005	26,0 **%**	**3,7 %**	
	Vicat vatten	EN 196-3 :2005	195 **min**	**4 %**	
	Normprov Tryckhållfasthet				
	2 d	EN 196-1 :2005	21,8 **MPa**	**5 %**	
	28 d	EN 196-1 :2005	55,1 **MPa**	**5 %**	
	56 d	EN 196-1 :2005	62,3 **MPa**	**5 %**	
	91 d	EN 196-1 :2005	66,1 **MPa**	**5 %**	
	Std.av. 2 dygn	EN 196-1 :2005	0,3 **MPa**	**5 %**	
	Std.av. 28 dygn	EN 196-1 :2005	0,3 **MPa**	**5 %**	
	Std.av. 56 dygn	EN 196-1 :2005	1,2 **MPa**	**5 %**	
	Std.av. 91 dygn	EN 196-1 :2005	2,0 **MPa**	**5 %**	
	ICP-Analys				
*	K2O H2O-lösl	CR 0401	0,21 **%**		
*	Na2O H2O-lösl	CR 0401	0,02 **%**		
	XRF - Cement - wroxi				
	Na2O-ekvivalent	ER 9214	0,50 **%**		
	CaO	ER 9214	63,6 **%**	**0,233 %abs**	
	SiO2	ER 9214	21,3 **%**	**0,100 %abs**	
	Al2O3	ER 9214	3,80 **%**	**0,052 %abs**	
	Fe2O3	ER 9214	4,56 **%**	**0,019 %abs**	

	MgO	ER 9214	0,856 **%**	**0,025 %abs**
	K2O	ER 9214	0,650 **%**	**0,032 %abs**
	Na2O	ER 9214	0,07 **%**	

Partikelstorleksdistribution (Laserdiffraktionsteknik)

	D(0.5)	ER 9322	17,305 **µm**	

LECO instrument CS 230

	SO3	ER 9212	2,45 **%**	**3 %**
	CO2	ER 9212	0,93 **%**	**3 %**
*	Kalksten beräknad Degerhamn	Saknas	2,36 **%**	

Partikelstorleksdistribution (Laserdiffraktionsteknik)

Analys	**Siktstorlek**	**Passerande på sikt**
Enhet	µm	%
Metod	ER 9322	ER 9322
Mätosäkerhet		
RAD		
1	1,00	0,49
2	1,20	0,86
3	1,40	1,30
4	1,60	1,78
5	1,80	2,32
6	2,00	2,90
7	2,20	3,51
8	2,60	4,81
9	3,00	6,20
10	3,50	7,99
11	4,00	9,83
12	4,50	11,68
13	5,00	13,52
14	5,50	15,34
15	6,30	18,19
16	7,00	20,62
17	8,00	23,98
18	9,00	27,22
19	10,00	30,33
20	12,00	36,23
21	15,00	44,33
22	16,00	46,85
23	18,00	51,62
24	20,00	56,04
25	22,00	60,13
26	25,00	65,67
27	28,00	70,54
28	32,00	76,07
29	36,00	80,65
30	40,00	84,41
31	45,00	88,16
32	50,00	91,06
33	56,00	93,68
34	63,00	95,84
35	75,00	98,06
36	90,00	99,35
37	106,0	99,93
38	125,0	100,0

39	150,0	100,0
40	175,0	100,0
41	200,0	100,0
42	225,0	100,0
43	250,0	100,0
44	280,0	100,0
45	315,0	100,0

Delges **Cementa AB , Stefan Sandelin, ref 205875**
Cementa AB , Erik Viggh, ref 183100
Cementa AB , Mikael Westerholm

Mätosäkerhet enligt "SWEDAC:s policy för mätosäkerhet vid kalibrering och provning", SWEDAC DOC 04:05. Den angivna mätosäkerheten är beräknad med täckningsfaktor 2, vilket ger konfidensnivå på ca 95%. Mätosäkerheten anges som (%) relativ eller absolut(abs%) eller i övrigt gällande enhet t.ex. Mpa, mg/kg.

* SLUT PÅ RAPPORTEN *

PROVRESULTAT

CEMENTA
HEIDELBERGCEMENT Group
Cementa Research

Sid: 1 (1)
Provnr: 171102

Cementa AB
Erik Viggh, ref 183100
Dockplatsen 1
211 19 MALMÖ

2016-04-29

Provnr	171102		
Märkning	Anl.cem.		
Uppdrag / grupp	Analyser för LTH-doktorand - Refnr: 121034856142		
Variant		Ankomstdatum	2016-04-11
Handläggare	Stina Hammar	Klardatum	2016-04-29
Provtagningsdatum	2016-04-25		
Provtagning	Insänt av kund		
Provtagare		Namn (Stina Hammar)	

* ackrediterad analys

Analys	Metod	Resultat	Mätosäkerhet	Kommentar
ICP-Analys				
Na2O-ekvivalent H2O-löslig	Saknas	0,32 %		
K2O H2O-lösl	CR 0401	0,44 %		
Na2O H2O-lösl	CR 0401	0,03 %		

Delges **Cementa AB , Erik Viggh, ref 183100**
Cementa AB , Mikael Westerholm

Mätosäkerhet enligt "SWEDAC:s policy för mätosäkerhet vid kalibrering och provning", SWEDAC DOC 04:05. Den angivna mätosäkerheten är beräknad med täckningsfaktor 2, vilket ger konfidensnivå på ca 95%. Mätosäkerheten anges som (%) relativ eller absolut(abs%) eller i övrigt gällande enhet t.ex. Mpa, mg/kg.

* SLUT PÅ RAPPORTEN *

SWEDAC ACKREDITERING
2026
ISO/IEC 17025

PROVRESULTAT

utfärdat av ackrediterat provningslaboratorium

Cementa Research

Cementa AB
Stefan Sandelin, ref 205875
Box 47210
10074 STOCKHOLM

2015-10-14

Provnr	168951		
Märkning	LTH F20; Degerhamn anläggningscement + FA		
Uppdrag / grupp	Analyser för LTH-doktorand		
Variant		Ankomstdatum	2015-06-18
Handläggare	Karin Lindhe	Klardatum	2015-10-14
Provtagningsdatum	2015-06-17		
Provtagning	Insänt av kund		
Provtagare			
		Namn (Karin Lindhe)	

* ej ackrediterad analys

Analys	Metod	Resultat	Mätosäkerhet	Kommentar
Leco Apparatur				
Gl.f 950°C	ER 9213 :2005	2,00 **%**	**0,18 %**	
Gravimetrisk Analys				
* Flygaska-halt inkl. gips	Saknas	17,4 **%**		
Fysikaliska Bestämningar				
Densitet	ER 9228	2988 **kg/m3**	**40 kg/m3**	
Blaine, manuell	EN 196-6 :2010	340 **m2/kg**	**3 %**	
Bindetid				
Vatten	EN 196-3 :2005	26,0 **%**	**3,7 %**	
Vicat vatten	EN 196-3 :2005	215 **min**	**4 %**	
Normprov Tryckhållfasthet				
2 d	EN 196-1 :2005	17,0 **MPa**	**5 %**	
28 d	EN 196-1 :2005	45,5 **MPa**	**5 %**	
56 d	EN 196-1 :2005	56,4 **MPa**	**5 %**	
91 d	EN 196-1 :2005	62,7 **MPa**	**5 %**	
Std.av. 2 dygn	EN 196-1 :2005	0,3 **MPa**	**5 %**	
Std.av. 28 dygn	EN 196-1 :2005	1,0 **MPa**	**5 %**	
Std.av. 56 dygn	EN 196-1 :2005	0,6 **MPa**	**5 %**	
Std.av. 91 dygn	EN 196-1 :2005	1,5 **MPa**	**5 %**	
ICP-Analys				
* K2O H2O-lösl	CR 0401	0,35 **%**		
* Na2O H2O-lösl	CR 0401	0,03 **%**		
TGA				
* CaCO3	Saknas	2,12 **%**		
XRF - Cement - wroxi				
Na2O-ekvivalent	ER 9214	0,91 **%**		
CaO	ER 9214	52,4 **%**	**0,233 %abs**	
SiO2	ER 9214	28,6 **%**	**0,100 %abs**	
Al2O3	ER 9214	7,38 **%**	**0,052 %abs**	
Fe2O3	ER 9214	5,17 **%**	**0,019 %abs**	
MgO	ER 9214	1,09 **%**	**0,025 %abs**	

K2O	ER 9214	0,996 **%**	**0,032 %abs**
Na2O	ER 9214	0,25 **%**	

Partikelstorleksdistribution (Laserdiffraktionsteknik)

D(0.5)	ER 9322	18,097 **µm**	

LECO instrument CS 230

SO3	ER 9212	2,05 **%**	**3 %**

Partikelstorleksdistribution (Laserdiffraktionsteknik)

Analys	**Siktstorlek**	**Passerande på sikt**
Enhet	µm	%
Metod	ER 9322	ER 9322
Mätosäkerhet		
RAD		
1	1,00	0,46
2	1,20	0,86
3	1,40	1,33
4	1,60	1,85
5	1,80	2,43
6	2,00	3,04
7	2,20	3,69
8	2,60	5,07
9	3,00	6,50
10	3,50	8,36
11	4,00	10,23
12	4,50	12,10
13	5,00	13,95
14	5,50	15,77
15	6,30	18,61
16	7,00	21,00
17	8,00	24,27
18	9,00	27,38
19	10,00	30,34
20	12,00	35,85
21	15,00	43,26
22	16,00	45,53
23	18,00	49,80
24	20,00	53,73
25	22,00	57,34
26	25,00	62,22
27	28,00	66,52
28	32,00	71,43
29	36,00	75,54
30	40,00	78,98
31	45,00	82,50
32	50,00	85,33
33	56,00	88,00
34	63,00	90,37
35	75,00	93,13
36	90,00	95,17
37	106,0	96,43
38	125,0	97,29
39	150,0	97,92
40	175,0	98,29
41	200,0	98,56
42	225,0	98,77

43	250,0	98,95
44	280,0	99,13
45	315,0	99,32
46	355,0	99,48
47	400,0	99,63
48	450,0	99,77
49	500,0	99,88
50	560,0	99,97
51	600,0	100,0
52	677,0	100,0

Delges **Cementa AB , Mikael Westerholm**
Cementa AB , Erik Viggh, ref 183100
Cementa AB , Stefan Sandelin, ref 205875

Ingen hänsyn tagen till renheten på kalkstenen.

Mätosäkerhet enligt "SWEDAC:s policy för mätosäkerhet vid kalibrering och provning", SWEDAC DOC 04:05. Den angivna mätosäkerheten är beräknad med täckningsfaktor 2, vilket ger konfidensnivå på ca 95%. Mätosäkerheten anges som (%) relativ eller absolut(abs%) eller i övrigt gällande enhet t.ex. Mpa, mg/kg.

* SLUT PÅ RAPPORTEN *

PROVRESULTAT

Cementa Research

Sid: 1 (1)

Provnr: 171103

Cementa AB
Erik Viggh, ref 183100
Dockplatsen 1
211 19 MALMÖ

2016-04-29

Provnr	171103		
Märkning	F20		
Uppdrag / grupp	Analyser för LTH-doktorand - Refnr: 121034856142		
Variant		Ankomstdatum	2016-04-11
Handläggare	Stina Hammar	Klardatum	2016-04-29
Provtagningsdatum	2016-04-25		
Provtagning	Insänt av kund		
Provtagare		Namn (Stina Hammar)	

* ackrediterad analys

Analys	Metod	Resultat	Mätosäkerhet	Kommentar
ICP-Analys				
Na2O-ekvivalent H2O-löslig	Saknas	0,26 %		
K2O H2O-lösl	CR 0401	0,35 %		
Na2O H2O-lösl	CR 0401	0,03 %		

Delges **Cementa AB , Mikael Westerholm**
Cementa AB , Erik Viggh, ref 183100

Mätosäkerhet enligt "SWEDAC:s policy för mätosäkerhet vid kalibrering och provning", SWEDAC DOC 04:05. Den angivna mätosäkerheten är beräknad med täckningsfaktor 2, vilket ger konfidensnivå på ca 95%. Mätosäkerheten anges som (%) relativ eller absolut(abs%) eller i övrigt gällande enhet t.ex. Mpa, mg/kg.

* SLUT PÅ RAPPORTEN *

SWEDAC ACKREDITERING
2026
ISO/IEC 17025

PROVRESULTAT

utfärdat av ackrediterat provningslaboratorium

Cementa Research

Cementa AB
Stefan Sandelin, ref 205875
Box 47210
10074 STOCKHOLM

2015-10-14

Provnr	168952		
Märkning	LTH F35; Degerhamn anläggningscement + FA		
Uppdrag / grupp	Analyser för LTH-doktorand		
Variant		Ankomstdatum	2015-06-18
Handläggare	Karin Lindhe	Klardatum	2015-10-14
Provtagningsdatum	2015-06-17		
Provtagning	Insänt av kund		
Provtagare			

Namn (Karin Lindhe)

* ej ackrediterad analys

Analys	Metod	Resultat	Mätosäkerhet	Kommentar
Leco Apparatur				
Gl.f 950°C	ER 9213 :2005	2,09 **%**	**0,18 %**	
Gravimetrisk Analys				
* Flygaska-halt inkl. gips	Saknas	33,4 **%**		
Fysikaliska Bestämningar				
Densitet	ER 9228	2822 **kg/m3**	**40 kg/m3**	
Blaine, manuell	EN 196-6 :2010	328 **m2/kg**	**3 %**	
Bindetid				
Vatten	EN 196-3 :2005	26,0 **%**	**3,7 %**	
Vicat vatten	EN 196-3 :2005	210 **min**	**4 %**	
Normprov Tryckhållfasthet				
2 d	EN 196-1 :2005	13,3 **MPa**	**5 %**	
28 d	EN 196-1 :2005	37,4 **MPa**	**5 %**	
56 d	EN 196-1 :2005	49,6 **MPa**	**5 %**	
91 d	EN 196-1 :2005	56,9 **MPa**	**5 %**	
Std.av. 2 dygn	EN 196-1 :2005	0,2 **MPa**	**5 %**	
Std.av. 28 dygn	EN 196-1 :2005	0,4 **MPa**	**5 %**	
Std.av. 56 dygn	EN 196-1 :2005	1,1 **MPa**	**5 %**	
Std.av. 91 dygn	EN 196-1 :2005	0,6 **MPa**	**5 %**	
ICP-Analys				
* K2O H2O-lösl	CR 0401	0,28 **%**		
* Na2O H2O-lösl	CR 0401	0,04 **%**		
TGA				
* CaCO3	Saknas	1,75 **%**		
XRF - Cement - wroxi				
Na2O-ekvivalent	ER 9214	1,19 **%**		
CaO	ER 9214	44,0 **%**	**0,233 %abs**	
SiO2	ER 9214	33,5 **%**	**0,100 %abs**	
Al2O3	ER 9214	9,88 **%**	**0,052 %abs**	
Fe2O3	ER 9214	5,52 **%**	**0,019 %abs**	
MgO	ER 9214	1,26 **%**	**0,025 %abs**	

K2O	ER 9214	1,24 **%**	**0,032 %abs**
Na2O	ER 9214	0,38 **%**	

Partikelstorleksdistribution (Laserdiffraktionsteknik)

D(0.5)	ER 9322	18,556 **µm**	

LECO instrument CS 230

SO3	ER 9212	1,78 **%**	**3 %**

Partikelstorleksdistribution (Laserdiffraktionsteknik)

Analys	**Siktstorlek**	**Passerande på sikt**
Enhet	µm	%
Metod	ER 9322	ER 9322
Mätosäkerhet		
RAD		
1	1,00	0,56
2	1,20	0,88
3	1,40	1,22
4	1,60	1,58
5	1,80	1,96
6	2,00	2,38
7	2,20	2,84
8	2,60	3,85
9	3,00	4,98
10	3,50	6,55
11	4,00	8,25
12	4,50	10,04
13	5,00	11,88
14	5,50	13,74
15	6,30	16,71
16	7,00	19,26
17	8,00	22,78
18	9,00	26,13
19	10,00	29,30
20	12,00	35,08
21	15,00	42,58
22	16,00	44,81
23	18,00	48,93
24	20,00	52,65
25	22,00	56,03
26	25,00	60,54
27	28,00	64,49
28	32,00	69,00
29	36,00	72,81
30	40,00	76,04
31	45,00	79,40
32	50,00	82,15
33	56,00	84,84
34	63,00	87,31
35	75,00	90,37
36	90,00	92,88
37	106,0	94,63
38	125,0	96,02
39	150,0	97,22
40	175,0	98,04
41	200,0	98,62
42	225,0	99,04

43	250,0	99,36
44	280,0	99,64
45	315,0	99,85
46	355,0	99,94
47	400,0	99,99
48	450,0	100,0

Delges **Cementa AB , Stefan Sandelin, ref 205875**
Cementa AB , Erik Viggh, ref 183100
Cementa AB , Mikael Westerholm

Ingen hänsyn tagen till renheten på kalkstenen.

Mätosäkerhet enligt "SWEDAC:s policy för mätosäkerhet vid kalibrering och provning", SWEDAC DOC 04:05. Den angivna mätosäkerheten är beräknad med täckningsfaktor 2, vilket ger konfidensnivå på ca 95%. Mätosäkerheten anges som (%) relativ eller absolut(abs%) eller i övrigt gällande enhet t.ex. Mpa, mg/kg.

* SLUT PÅ RAPPORTEN *

PROVRESULTAT

CEMENTA
HEIDELBERGCEMENT Group
Cementa Research

Sid: 1 (1)
Provnr: 171104

Cementa AB
Erik Viggh, ref 183100
Dockplatsen 1
211 19 MALMÖ

2016-04-29

Provnr	171104		
Märkning	F35		
Uppdrag / grupp	Analyser för LTH-doktorand - Refnr: 121034856142		
Variant		Ankomstdatum	2016-04-11
Handläggare	Stina Hammar	Klardatum	2016-04-29
Provtagningsdatum	2016-04-25		
Provtagning	Insänt av kund		
Provtagare		Namn (Stina Hammar)	

* ackrediterad analys

Analys	**Metod**	**Resultat**	**Mätosäkerhet**	**Kommentar**
ICP-Analys				
Na2O-ekvivalent H2O-löslig	Saknas	0,23 %		
K2O H2O-lösl	CR 0401	0,29 %		
Na2O H2O-lösl	CR 0401	0,04 %		

Delges **Cementa AB , Mikael Westerholm**
Cementa AB , Erik Viggh, ref 183100

Mätosäkerhet enligt "SWEDAC:s policy för mätosäkerhet vid kalibrering och provning", SWEDAC DOC 04:05. Den angivna mätosäkerheten är beräknad med täckningsfaktor 2, vilket ger konfidensnivå på ca 95%. Mätosäkerheten anges som (%) relativ eller absolut(abs%) eller i övrigt gällande enhet t.ex. Mpa, mg/kg.

* SLUT PÅ RAPPORTEN *

Cementa Research
Skeppargatan 1
P.O Box 104
SE-624 22 Slite
Sweden

Phone +46 (0)498-28 11 00
Fax +46 (0)498-28 13 91
www.cementaresearch.se
johan.larsson@cementa.se
VAT no. SE556102778901

PROVRESULTAT

utfärdat av ackrediterat provningslaboratorium

Cementa AB
Stefan Sandelin, ref 205875
Box 47210
10074 STOCKHOLM

2015-10-14

Provnr	168953		
Märkning	LTH S20; Degerhamn anläggningscement+ Slagg(Merit)		
Uppdrag / grupp	Analyser för LTH-doktorand		
Variant		Ankomstdatum	2015-06-18
Handläggare	Karin Lindhe	Klardatum	2015-10-14
Provtagningsdatum	2015-06-17		
Provtagning	Insänt av kund		
Provtagare		Namn (Karin Lindhe)	

* ej ackrediterad analys

	Analys	Metod	Resultat	Mätosäkerhet	Kommentar
Leco Apparatur					
	Gl.f 950°C	ER 9213 :2005	1,17 **%**	**0,18 %**	
Fysikaliska Bestämningar					
	Densitet	ER 9228	3167 **kg/m3**	**40 kg/m3**	
	Blaine, manuell	EN 196-6 :2010	371 **m2/kg**	**3 %**	
Bindetid					
	Vatten	EN 196-3 :2005	26,0 **%**	**3,7 %**	
	Vicat vatten	EN 196-3 :2005	215 **min**	**4 %**	
Normprov Tryckhållfasthet					
	2 d	EN 196-1 :2005	16,5 **MPa**	**5 %**	
	28 d	EN 196-1 :2005	52,1 **MPa**	**5 %**	
	56 d	EN 196-1 :2005	63,3 **MPa**	**5 %**	
	91 d	EN 196-1 :2005	65,3 **MPa**	**5 %**	
	Std.av. 2 dygn	EN 196-1 :2005	0,2 **MPa**	**5 %**	
	Std.av. 28 dygn	EN 196-1 :2005	0,8 **MPa**	**5 %**	
	Std.av. 56 dygn	EN 196-1 :2005	1,3 **MPa**	**5 %**	
	Std.av. 91 dygn	EN 196-1 :2005	1,3 **MPa**	**5 %**	
ICP-Analys					
*	K2O H2O-lösl	CR 0401	0,35 **%**		
*	Na2O H2O-lösl	CR 0401	0,03 **%**		
XRF - Cement - wroxi					
	Na2O-ekvivalent	ER 9214	0,63 **%**		
	CaO	ER 9214	57,8 **%**	**0,233 %abs**	
	SiO2	ER 9214	23,9 **%**	**0,100 %abs**	
	Al2O3	ER 9214	5,61 **%**	**0,052 %abs**	
	Fe2O3	ER 9214	3,78 **%**	**0,019 %abs**	
	MgO	ER 9214	3,68 **%**	**0,025 %abs**	
	K2O	ER 9214	0,699 **%**	**0,032 %abs**	
	Na2O	ER 9214	0,17 **%**		
Partikelstorleksdistribution (Laserdiffraktionsteknik)					
	D(0.5)	ER 9322	16,142 **µm**		

LECO instrument CS 230

SO3	ER 9212	2,60 **%**	**3 %**
CO2	ER 9212	0,84 **%**	**3 %**
* Kalksten beräknad Degerhamn	Saknas	2,12 **%**	

Partikelstorleksdistribution (Laserdiffraktionsteknik)

Analys	**Siktstorlek**	**Passerande på sikt**
Enhet	µm	%
Metod	ER 9322	ER 9322
Mätosäkerhet		
RAD		
1	1,00	0,63
2	1,20	1,05
3	1,40	1,52
4	1,60	2,05
5	1,80	2,63
6	2,00	3,26
7	2,20	3,93
8	2,60	5,38
9	3,00	6,93
10	3,50	8,95
11	4,00	11,02
12	4,50	13,09
13	5,00	15,15
14	5,50	17,18
15	6,30	20,33
16	7,00	22,98
17	8,00	26,60
18	9,00	30,02
19	10,00	33,25
20	12,00	39,25
21	15,00	47,23
22	16,00	49,66
23	18,00	54,22
24	20,00	58,39
25	22,00	62,21
26	25,00	67,33
27	28,00	71,80
28	32,00	76,85
29	36,00	81,01
30	40,00	84,42
31	45,00	87,81
32	50,00	90,45
33	56,00	92,82
34	63,00	94,80
35	75,00	96,86
36	90,00	98,10
37	106,0	98,66
38	125,0	98,91
39	150,0	99,04
40	175,0	99,14
41	200,0	99,27
42	225,0	99,41
43	250,0	99,55
44	280,0	99,71

45	315,0	99,86
46	355,0	99,96
47	400,0	100,0
48	450,0	100,0

Delges **Cementa AB , Stefan Sandelin, ref 205875**
Cementa AB , Erik Viggh, ref 183100
Cementa AB , Mikael Westerholm

Mätosäkerhet enligt "SWEDAC:s policy för mätosäkerhet vid kalibrering och provning", SWEDAC DOC 04:05. Den angivna mätosäkerheten är beräknad med täckningsfaktor 2, vilket ger konfidensnivå på ca 95%. Mätosäkerheten anges som (%) relativ eller absolut(abs%) eller i övrigt gällande enhet t.ex. Mpa, mg/kg.

* SLUT PÅ RAPPORTEN *

SWEDAC ACKREDITERING
2026
ISO/IEC 17025

PROVRESULTAT

utfärdat av ackrediterat provningslaboratorium

Cementa Research

Cementa AB
Stefan Sandelin, ref 205875
Box 47210
10074 STOCKHOLM

2015-10-14

Provnr	168954		
Märkning	LTH S35; Degerhamn anläggningscement + Slagg (Merit)		
Uppdrag / grupp	Analyser för LTH-doktorand		
Variant		Ankomstdatum	2015-06-18
Handläggare	Karin Lindhe	Klardatum	2015-10-14
Provtagningsdatum	2015-06-17		
Provtagning	Insänt av kund		
Provtagare			

Namn (Karin Lindhe)

* ej ackrediterad analys

Analys	Metod	Resultat	Mätosäkerhet	Kommentar
Leco Apparatur				
Gl.f 950°C	ER 9213 :2005	0,56 **%**	**0,18 %**	
Fysikaliska Bestämningar				
Densitet	ER 9228	3123 **kg/m3**	**40 kg/m3**	
Blaine, manuell	EN 196-6 :2010	395 **m2/kg**	**3 %**	
Bindetid				
Vatten	EN 196-3 :2005	26,0 **%**	**3,7 %**	
Vicat vatten	EN 196-3 :2005	230 **min**	**4 %**	
Normprov Tryckhållfasthet				
2 d	EN 196-1 :2005	12,9 **MPa**	**5 %**	
28 d	EN 196-1 :2005	53,9 **MPa**	**5 %**	
56 d	EN 196-1 :2005	63,5 **MPa**	**5 %**	
91 d	EN 196-1 :2005	67,4 **MPa**	**5 %**	
Std.av. 2 dygn	EN 196-1 :2005	0,1 **MPa**	**5 %**	
Std.av. 28 dygn	EN 196-1 :2005	0,6 **MPa**	**5 %**	
Std.av. 56 dygn	EN 196-1 :2005	0,7 **MPa**	**5 %**	
Std.av. 91 dygn	EN 196-1 :2005	0,5 **MPa**	**5 %**	
ICP-Analys				
* K2O H2O-lösl	CR 0401	0,27 **%**		
* Na2O H2O-lösl	CR 0401	0,03 **%**		
XRF - Cement - wroxi				
Na2O-ekvivalent	ER 9214	0,75 **%**		
CaO	ER 9214	52,7 **%**	**0,233 %abs**	
SiO2	ER 9214	25,9 **%**	**0,100 %abs**	
Al2O3	ER 9214	7,10 **%**	**0,052 %abs**	
Fe2O3	ER 9214	3,11 **%**	**0,019 %abs**	
MgO	ER 9214	5,92 **%**	**0,025 %abs**	
K2O	ER 9214	0,748 **%**	**0,032 %abs**	
Na2O	ER 9214	0,26 **%**		
Partikelstorleksdistribution (Laserdiffraktionsteknik)				
D(0.5)	ER 9322	15,339 **µm**		

LECO instrument CS 230

	SO3	ER 9212	2,76 **%**	**3 %**
	CO2	ER 9212	0,73 **%**	**3 %**
*	Kalksten beräknad Degerhamn	Saknas	1,84 **%**	

Partikelstorleksdistribution (Laserdiffraktionsteknik)

Analys	**Siktstorlek**	**Passerande på sikt**
Enhet	µm	%
Metod	ER 9322	ER 9322
Mätosäkerhet		
RAD		
1	1,00	0,71
2	1,20	1,17
3	1,40	1,70
4	1,60	2,28
5	1,80	2,91
6	2,00	3,59
7	2,20	4,32
8	2,60	5,88
9	3,00	7,54
10	3,50	9,70
11	4,00	11,90
12	4,50	14,11
13	5,00	16,29
14	5,50	18,44
15	6,30	21,75
16	7,00	24,53
17	8,00	28,29
18	9,00	31,83
19	10,00	35,14
20	12,00	41,22
21	15,00	49,18
22	16,00	51,57
23	18,00	56,02
24	20,00	60,06
25	22,00	63,73
26	25,00	68,63
27	28,00	72,87
28	32,00	77,64
29	36,00	81,57
30	40,00	84,78
31	45,00	87,98
32	50,00	90,47
33	56,00	92,72
34	63,00	94,60
35	75,00	96,57
36	90,00	97,79
37	106,0	98,38
38	125,0	98,69
39	150,0	98,92
40	175,0	99,13
41	200,0	99,36
42	225,0	99,57
43	250,0	99,76
44	280,0	99,92

45	315,0	99,99
46	355,0	100,0
47	400,0	100,0
48	450,0	100,0

Delges **Cementa AB , Erik Viggh, ref 183100**
Cementa AB , Stefan Sandelin, ref 205875
Cementa AB , Mikael Westerholm

Mätosäkerhet enligt "SWEDAC:s policy för mätosäkerhet vid kalibrering och provning", SWEDAC DOC 04:05. Den angivna mätosäkerheten är beräknad med täckningsfaktor 2, vilket ger konfidensnivå på ca 95%. Mätosäkerheten anges som (%) relativ eller absolut(abs%) eller i övrigt gällande enhet t.ex. Mpa, mg/kg.

* SLUT PÅ RAPPORTEN *

SWEDAC ACKREDITERING
2026
ISO/IEC 17025

PROVRESULTAT

utfärdat av ackrediterat provningslaboratorium

CEMENTA
HEIDELBERGCEMENT Group
Cementa Research

Cementa AB
Stefan Sandelin, ref 205875
Box 47210
10074 STOCKHOLM

2015-10-14

Provnr	168955		
Märkning	LTH S70; Degerhamn anläggningscement + Slagg		
Uppdrag / grupp	Analyser för LTH-doktorand		
Variant		Ankomstdatum	2015-06-18
Handläggare	Karin Lindhe	Klardatum	2015-10-14
Provtagningsdatum	2015-06-17		
Provtagning	Insänt av kund		
Provtagare		Namn (Karin Lindhe)	

* ej ackrediterad analys

Analys	Metod	Resultat	Mätosäkerhet	Kommentar
Leco Apparatur				
Gl.f 950°C	ER 9213 :2005	-0,59 **%**	**0,18 %**	
Fysikaliska Bestämningar				
Densitet	ER 9228	3025 **kg/m3**	**40 kg/m3**	
Blaine, manuell	EN 196-6 :2010	448 **m2/kg**	**3 %**	
Bindetid				
Vatten	EN 196-3 :2005	26,0 **%**	**3,7 %**	
Vicat vatten	EN 196-3 :2005	330 **min**	**4 %**	
Normprov Tryckhållfasthet				
2 d	EN 196-1 :2005	4,4 **MPa**	**5 %**	
28 d	EN 196-1 :2005	42,4 **MPa**	**5 %**	
56 d	EN 196-1 :2005	49,3 **MPa**	**5 %**	
91 d	EN 196-1 :2005	51,8 **MPa**	**5 %**	
Std.av. 2 dygn	EN 196-1 :2005	0,1 **MPa**	**5 %**	
Std.av. 28 dygn	EN 196-1 :2005	0,4 **MPa**	**5 %**	
Std.av. 56 dygn	EN 196-1 :2005	0,9 **MPa**	**5 %**	
Std.av. 91 dygn	EN 196-1 :2005	1,1 **MPa**	**5 %**	
ICP-Analys				
* K2O H2O-lösl	CR 0401	0,14 **%**		
* Na2O H2O-lösl	CR 0401	0,02 **%**		
XRF - Cement - wroxi				
Na2O-ekvivalent	ER 9214	1,00 **%**		
CaO	ER 9214	41,6 **%**	**0,233 %abs**	
SiO2	ER 9214	29,9 **%**	**0,100 %abs**	
Al2O3	ER 9214	10,2 **%**	**0,052 %abs**	
Fe2O3	ER 9214	1,67 **%**	**0,019 %abs**	
MgO	ER 9214	10,7 **%**	**0,025 %abs**	
K2O	ER 9214	0,842 **%**	**0,032 %abs**	
Na2O	ER 9214	0,44 **%**		
Partikelstorleksdistribution (Laserdiffraktionsteknik)				
D(0.5)	ER 9322	13,957 **µm**		

LECO instrument CS 230

	SO3	ER 9212	3,02 **%**	**3 %**
	CO2	ER 9212	0,54 **%**	**3 %**
*	Kalksten beräknad Degerhamn	Saknas	1,38 **%**	

Partikelstorleksdistribution (Laserdiffraktionsteknik)

Analys	**Siktstorlek**	**Passerande på sikt**
Enhet	µm	%
Metod	ER 9322	ER 9322
Mätosäkerhet		
RAD		
1	1,00	0,82
2	1,20	1,42
3	1,40	2,11
4	1,60	2,86
5	1,80	3,67
6	2,00	4,54
7	2,20	5,45
8	2,60	7,35
9	3,00	9,32
10	3,50	11,83
11	4,00	14,33
12	4,50	16,78
13	5,00	19,18
14	5,50	21,49
15	6,30	25,02
16	7,00	27,94
17	8,00	31,83
18	9,00	35,43
19	10,00	38,78
20	12,00	44,80
21	15,00	52,53
22	16,00	54,82
23	18,00	59,04
24	20,00	62,84
25	22,00	66,26
26	25,00	70,78
27	28,00	74,67
28	32,00	79,00
29	36,00	82,53
30	40,00	85,40
31	45,00	88,26
32	50,00	90,46
33	56,00	92,45
34	63,00	94,12
35	75,00	95,88
36	90,00	97,00
37	106,0	97,58
38	125,0	97,97
39	150,0	98,34
40	175,0	98,71
41	200,0	99,07
42	225,0	99,40
43	250,0	99,67
44	280,0	99,89

45	315,0	99,98
46	355,0	100,0
47	400,0	100,0
48	450,0	100,0
49	500,0	100,0
50	560,0	100,0

Delges **Cementa AB , Erik Viggh, ref 183100**
Cementa AB , Stefan Sandelin, ref 205875
Cementa AB , Mikael Westerholm

Mätosäkerhet enligt "SWEDAC:s policy för mätosäkerhet vid kalibrering och provning", SWEDAC DOC 04:05. Den angivna mätosäkerheten är beräknad med täckningsfaktor 2, vilket ger konfidensnivå på ca 95%. Mätosäkerheten anges som (%) relativ eller absolut(abs%) eller i övrigt gällande enhet t.ex. Mpa, mg/kg.

* SLUT PÅ RAPPORTEN *

SWEDAC ACKREDITERING
2026
ISO/IEC 17025

PROVRESULTAT

utfärdat av ackrediterat provningslaboratorium

CEMENTA
HEIDELBERGCEMENT Group
Cementa Research

Provnr: 168956

Cementa AB
Stefan Sandelin, ref 205875
Box 47210
10074 STOCKHOLM

2015-10-14

Provnr	168956		
Märkning	LTH K35; Degerhamn anläggningscement + Slagg och Kalksfiller		
Uppdrag / grupp	Analyser för LTH-doktorand		
Variant		Ankomstdatum	2015-06-18
Handläggare	Karin Lindhe	Klardatum	2015-10-14
Provtagningsdatum	2015-06-17		
Provtagning	Insänt av kund		
Provtagare			

Namn (Karin Lindhe)

* ej ackrediterad analys

Analys	**Metod**	**Resultat**	**Mätosäkerhet**	**Kommentar**
Leco Apparatur				
Gl.f 950°C	ER 9213 :2005	5,04 **%**	**0,18 %**	
Fysikaliska Bestämningar				
Densitet	ER 9228	3104 **kg/m3**	**40 kg/m3**	
Blaine, manuell	EN 196-6 :2010	397 **m2/kg**	**3 %**	
Bindetid				
Vatten	EN 196-3 :2005	26,0 **%**	**3,7 %**	
Vicat vatten	EN 196-3 :2005	210 **min**	**4 %**	
Normprov Tryckhållfasthet				
2 d	EN 196-1 :2005	12,8 **MPa**	**5 %**	
28 d	EN 196-1 :2005	47,9 **MPa**	**5 %**	
56 d	EN 196-1 :2005	55,2 **MPa**	**5 %**	
91 d	EN 196-1 :2005	58,3 **MPa**	**5 %**	
Std.av. 2 dygn	EN 196-1 :2005	0,3 **MPa**	**5 %**	
Std.av. 28 dygn	EN 196-1 :2005	1,2 **MPa**	**5 %**	
Std.av. 56 dygn	EN 196-1 :2005	0,6 **MPa**	**5 %**	
Std.av. 91 dygn	EN 196-1 :2005	0,6 **MPa**	**5 %**	
ICP-Analys				
* K2O H2O-lösl	CR 0401	0,20 **%**		
* Na2O H2O-lösl	CR 0401	0,02 **%**		
TGA				
* CaCO3	Saknas	10,60 **%**		
XRF - Cement - wroxi				
Na2O-ekvivalent	ER 9214	0,66 **%**		
CaO	ER 9214	54,1 **%**	**0,233 %abs**	
SiO2	ER 9214	22,9 **%**	**0,100 %abs**	
Al2O3	ER 9214	5,94 **%**	**0,052 %abs**	
Fe2O3	ER 9214	3,11 **%**	**0,019 %abs**	
MgO	ER 9214	4,77 **%**	**0,025 %abs**	
K2O	ER 9214	0,685 **%**	**0,032 %abs**	
Na2O	ER 9214	0,21 **%**		

Partikelstorleksdistribution (Laserdiffraktionsteknik)

D(0.5)	ER 9322	16,439 **µm**	

LECO instrument CS 230

SO3	ER 9212	2,40 **%**	**3 %**

Partikelstorleksdistribution (Laserdiffraktionsteknik)

Analys	**Siktstorlek**	**Passerande på sikt**
Enhet	µm	%
Metod	ER 9322	ER 9322
Mätosäkerhet		
RAD		
1	1,00	0,59
2	1,20	1,16
3	1,40	1,83
4	1,60	2,58
5	1,80	3,39
6	2,00	4,24
7	2,20	5,11
8	2,60	6,91
9	3,00	8,72
10	3,50	10,96
11	4,00	13,16
12	4,50	15,28
13	5,00	17,33
14	5,50	19,30
15	6,30	22,31
16	7,00	24,79
17	8,00	28,13
18	9,00	31,26
19	10,00	34,20
20	12,00	39,64
21	15,00	46,86
22	16,00	49,06
23	18,00	53,19
24	20,00	56,99
25	22,00	60,47
26	25,00	65,16
27	28,00	69,28
28	32,00	73,98
29	36,00	77,90
30	40,00	81,17
31	45,00	84,50
32	50,00	87,15
33	56,00	89,63
34	63,00	91,80
35	75,00	94,26
36	90,00	96,00
37	106,0	97,00
38	125,0	97,65
39	150,0	98,11
40	175,0	98,41
41	200,0	98,65
42	225,0	98,88
43	250,0	99,09
44	280,0	99,30

45	315,0	99,51
46	355,0	99,67
47	400,0	99,81
48	450,0	99,91
49	500,0	99,99
50	560,0	100,0

Delges **Cementa AB , Stefan Sandelin, ref 205875**
Cementa AB , Erik Viggh, ref 183100

Ingen hänsyn tagen till renheten på kalkstenen.

Mätosäkerhet enligt "SWEDAC:s policy för mätosäkerhet vid kalibrering och provning", SWEDAC DOC 04:05. Den angivna mätosäkerheten är beräknad med täckningsfaktor 2, vilket ger konfidensnivå på ca 95%. Mätosäkerheten anges som (%) relativ eller absolut(abs%) eller i övrigt gällande enhet t.ex. Mpa, mg/kg.

* SLUT PÅ RAPPORTEN *

Appendix 8

Luftporeanalyse (ASTM C 457)

Udført: April 2015 v/AB & PL

Sags nr. 15-044

Prøvemærke : 02 17 02-1

Målelinier : 40 stk.
Pastaindhold : 30 %
(skønnet)

ANALYSE RESULTATER:

Luftindhold	Beton	Kitmasse
Total :	2,6 %	7,9 %
< 0,350 mm :	0,9 %	2,8 %
0,350-1,5 mm :	1,3 %	
1,5 - 2,0 mm :	0,2 %	
>2,0 mm :	0,2 %	

Specifik overflade : 16 mm^{-1}
Afstandsfaktor : 0,43 mm

Bemærkninger
'Kitmasse" er defineret som pastaindhold + luftindhold.
Hvis indhold af indkapslet luft (korder > 2 mm) udelades, kan ovenstående værdier genberegnes til:
Luftporer i beton: 2,4 % (i kitmasse: 7,3 %). Specifik overflade: 17 mm-1. Afstandsfaktor: 0,41 mm.

Luftporeanalyse (ASTM C 457)

Udført: April 2015 v/AB & PL

Sags nr. 15-044

Prøvemærke : 02 27 02-2

Målelinier : 40 stk.

Pastaindhold : 30 %

(skønnet)

ANALYSERESULTATER:

Luftindhold	Beton	Kitmasse
Total :	2,7 %	8,0 %
< 0,350 mm :	0,9 %	2,8 %
0,350-1,5 mm :	1,2 %	
1,5 - 2,0 mm :	0,2 %	
>2,0 mm :	0,3 %	

Specifik overflade : 17 mm^{-1}

Afstandsfaktor : 0,40 mm

Bemærkninger

'Kitmasse" er defineret som pastaindhold + luftindhold.
Hvis indhold af indkapslet luft (korder > 2 mm) udelades, kan ovenstående værdier genberegnes til:
Luftporer i beton: 2,4 % (i kitmasse: 7,1 %). Specifik overflade: 19 mm-1. Afstandsfaktor: 0,38 mm.

Luftporeanalyse (ASTM C 457)

Udført: April 2015 v/AB & PL

Sags nr. 15-044

Prøvemærke : 02 37 02-3

Målelinier : 40 stk.
Pastaindhold : 30 %
(skønnet)

ANALYSE RESULTATER:

Luftindhold	Beton	Kitmasse
Total :	2,8 %	8,4 %
< 0,350 mm :	1,3 %	3,9 %
0,350-1,5 mm :	1,3 %	
1,5 - 2,0 mm :	0,1 %	
>2,0 mm :	0,1 %	

Specifik overflade : 20 mm^{-1}
Afstandsfaktor : 0,33 mm

Bemærkninger
'Kitmasse" er defineret som pastaindhold + luftindhold.
Hvis indhold af indkapslet luft (korder > 2 mm) udelades, kan ovenstående værdier genberegnes til:
Luftporer i beton: 2,7 % (i kitmasse: 7,9 %). Specifik overflade: 21 mm-1. Afstandsfaktor: 0,32 mm.

Luftporeanalyse (ASTM C 457)

Udført: April 2015 v/AB & PL

Sags nr. 15-044

Prøvemærke : 02 47 02-4

Målelinier :	40 stk.
Pastaindhold : (skønnet)	30 %

ANALYSE RESULTATER:

Luftindhold	Beton	Kitmasse
Total :	4,1 %	11,9 %
< 0,350 mm :	1,9 %	5,7 %
0,350-1,5 mm :	1,3 %	
1,5 - 2,0 mm :	0,1 %	
>2,0 mm :	0,7 %	

Specifik overflade :	20 mm^{-1}
Afstandsfaktor :	0,27 mm

Bemærkninger
'Kitmasse" er defineret som pastaindhold + luftindhold.
Hvis indhold af indkapslet luft (korder > 2 mm) udelades, kan ovenstående værdier genberegnes til:
Luftporer i beton: 3,4 % (i kitmasse: 9,8 %). Specifik overflade: 24 mm-1. Afstandsfaktor: 0,25 mm.

Luftporeanalyse (ASTM C 457)

Prøvemærke :	7	F20-1
Målelinier :	40 stk.	
Pastaindhold : (skønnet)	30 %	

ANALYSE RESULTATER:

Luftindhold	Beton	Kitmasse
Total :	3,5 %	10,3 %
< 0,350 mm :	0,3 %	0,9 %
0,350-1,5 mm :	1,2 %	
1,5 - 2,0 mm :	0,4 %	
>2,0 mm :	1,6 %	

Specifik overflade : 6 mm^{-1}

Afstandsfaktor : 1,00 mm

Bemærkninger

'Kitmasse" er defineret som pastaindhold + luftindhold.

Hvis indhold af indkapslet luft (korder > 2 mm) udelades, kan ovenstående værdier genberegnes til:

Luftporer i beton: 1,9 % (i kitmasse: 5,6 %). Specifik overflade: 10 mm-1. Afstandsfaktor: 0,78 mm.

Luftporeanalyse (ASTM C 457)

Udført: April 2015 v/AB & PL

Sags nr. 14-186

Prøvemærke : 2 F20-2

Målelinier : 40 stk.
Pastaindhold : 30 %
(skønnet)

ANALYSE RESULTATER:

Luftindhold	Beton	Kitmasse
Total :	2,0 %	6,1 %
< 0,350 mm :	0,9 %	2,6 %
0,350-1,5 mm :	0,8 %	
1,5 - 2,0 mm :	0,2 %	
>2,0 mm :	0,1 %	

Specifik overflade :	23 mm^{-1}
Afstandsfaktor :	0,33 mm

Bemærkninger
'Kitmasse" er defineret som pastaindhold + luftindhold.
Hvis indhold af indkapslet luft (korder > 2 mm) udelades, kan ovenstående værdier genberegnes til:
Luftporer i beton: 1,9 % (i kitmasse: 5,6 %). Specifik overflade: 25 mm-1. Afstandsfaktor: 0,32 mm.

Luftporeanalyse (ASTM C 457)

Udført: April 2015 v/AB & PL

Sags nr. 14-186

Prøvemærke :	5	F20-3
Målelinier :	40 stk.	
Pastaindhold : (skønnet)	30 %	

ANALYSE RESULTATER:

Luftindhold	Beton	Kitmasse
Total :	3,1 %	9,3 %
< 0,350 mm :	1,1 %	3,3 %
0,350-1,5 mm :	1,2 %	
1,5 - 2,0 mm :	0,2 %	
>2,0 mm :	0,6 %	

Specifik overflade : 15 mm^{-1}

Afstandsfaktor : 0,41 mm

Bemærkninger

'Kitmasse" er defineret som pastaindhold + luftindhold.
Hvis indhold af indkapslet luft (korder > 2 mm) udelades, kan ovenstående værdier genberegnes til:
Luftporer i beton: 2,5 % (i kitmasse: 7,6 %). Specifik overflade: 18 mm-1. Afstandsfaktor: 0,37 mm.

Luftporeanalyse (ASTM C 457)

Udført: April 2015 v/AB & PL

Sags nr. 14-186

Prøvemærke : 11 F20-4

Målelinier : 40 stk.
Pastaindhold : 30 %
(skønnet)

ANALYSE RESULTATER:

Luftindhold	Beton	Kitmasse
Total :	3,5 %	10,3 %
< 0,350 mm :	2,0 %	5,9 %
0,350-1,5 mm :	1,2 %	
1,5 - 2,0 mm :	0,1 %	
>2,0 mm :	0,1 %	

Specifik overflade :	21 mm^{-1}
Afstandsfaktor :	0,28 mm

Bemærkninger
'Kitmasse" er defineret som pastaindhold + luftindhold.
Hvis indhold af indkapslet luft (korder > 2 mm) udelades, kan ovenstående værdier genberegnes til:
Luftporer i beton: 3,4 % (i kitmasse: 9,9 %). Specifik overflade: 22 mm-1. Afstandsfaktor: 0,27 mm.

Luftporeanalyse (ASTM C 457)

Udført: April 2015 v/AB & PL

Sags nr. 15-044

Prøvemærke : F35 13 F35-1

Målelinier : 40 stk.
Pastaindhold : 30 %
(skønnet)

ANALYSERESULTATER:

Luftindhold	Beton	Kitmasse
Total :	1,8 %	5,4 %
< 0,350 mm :	0,3 %	1,0 %
0,350-1,5 mm :	0,8 %	
1,5 - 2,0 mm :	0,0 %	
>2,0 mm :	0,7 %	

Specifik overflade : 15 mm^{-1}
Afstandsfaktor : 0,53 mm

Bemærkninger
'Kitmasse" er defineret som pastaindhold + luftindhold.
Hvis indhold af indkapslet luft (korder > 2 mm) udelades, kan ovenstående værdier genberegnes til:
Luftporer i beton: 1,1 % (i kitmasse: 3,4 %). Specifik overflade: 24 mm-1. Afstandsfaktor: 0,41 mm.

Luftporeanalyse (ASTM C 457)

Udført: April 2015 v/AB & PL

Sags nr. 15-044

Prøvemærke :	F35 27	F35-2
Målelinier :	40 stk.	
Pastaindhold : (skønnet)	30 %	

ANALYSE RESULTATER:

Luftindhold	Beton	Kitmasse
Total :	3,8 %	11,2 %
< 0,350 mm :	0,8 %	2,2 %
0,350-1,5 mm :	1,3 %	
1,5 - 2,0 mm :	0,3 %	
>2,0 mm :	1,4 %	

Specifik overflade :	13 mm^{-1}
Afstandsfaktor :	0,44 mm

Bemærkninger

'Kitmasse" er defineret som pastaindhold + luftindhold.
Hvis indhold af indkapslet luft (korder > 2 mm) udelades, kan ovenstående værdier genberegnes til:
Luftporer i beton: 2,4 % (i kitmasse: 7 %). Specifik overflade: 20 mm-1. Afstandsfaktor: 0,35 mm.

Luftporeanalyse (ASTM C 457)

Udført: April 2015 v/AB & PL

Sags nr. 15-044

Prøvemærke : F35 37 F35-3

Målelinier : 40 stk.
Pastaindhold : 30 %
(skønnet)

ANALYSERESULTATER:

Luftindhold	Beton	Kitmasse
Total :	3,2 %	9,5 %
< 0,350 mm :	1,6 %	4,7 %
0,350-1,5 mm :	1,0 %	
1,5 - 2,0 mm :	0,3 %	
>2,0 mm :	0,4 %	

Specifik overflade : 30 mm^{-1}
Afstandsfaktor : 0,20 mm

Bemærkninger
'Kitmasse" er defineret som pastaindhold + luftindhold.
Hvis indhold af indkapslet luft (korder > 2 mm) udelades, kan ovenstående værdier genberegnes til:
Luftporer i beton: 2,9 % (i kitmasse: 8,4 %). Specifik overflade: 34 mm-1. Afstandsfaktor: 0,19 mm.

Luftporeanalyse (ASTM C 457)

Udført: April 2015 v/AB & PL

Sags nr. 15-044

Prøvemærke : F35 47 F35-4

Målelinier : 40 stk.
Pastaindhold : 30 %
(skønnet)

ANALYSERESULTATER:

Luftindhold	Beton	Kitmasse
Total :	4,8 %	13,8 %
< 0,350 mm :	2,0 %	5,8 %
0,350-1,5 mm :	1,2 %	
1,5 - 2,0 mm :	0,2 %	
>2,0 mm :	1,4 %	

Specifik overflade : 19 mm^{-1}
Afstandsfaktor : 0,27 mm

Bemærkninger
'Kitmasse" er defineret som pastaindhold + luftindhold.
Hvis indhold af indkapslet luft (korder > 2 mm) udelades, kan ovenstående værdier genberegnes til:
Luftporer i beton: 3,4 % (i kitmasse: 9,7 %). Specifik overflade: 27 mm-1. Afstandsfaktor: 0,22 mm.

Luftporeanalyse (ASTM C 457)

Udført: April 2015 v/AB & PL

Sags nr. 14-186

Prøvemærke : 6 S20-1

Målelinier : 40 stk.

Pastaindhold : 30 %
(skønnet)

ANALYSE RESULTATER:

Luftindhold	Beton	Kitmasse
Total :	3,6 %	10,6 %
< 0,350 mm :	0,7 %	2,2 %
0,350-1,5 mm :	1,3 %	
1,5 - 2,0 mm :	0,3 %	
>2,0 mm :	1,3 %	

Specifik overflade : 9 mm^{-1}

Afstandsfaktor : 0,66 mm

Bemærkninger

'Kitmasse" er defineret som pastaindhold + luftindhold.
Hvis indhold af indkapslet luft (korder > 2 mm) udelades, kan ovenstående værdier genberegnes til:
Luftporer i beton: 2,3 % (i kitmasse: 6,8 %). Specifik overflade: 13 mm-1. Afstandsfaktor: 0,55 mm.

Luftporeanalyse (ASTM C 457)

Udført: April 2015 v/AB & PL

Sags nr. 14-186

Prøvemærke :	3 S20-2
Målelinier :	40 stk.
Pastaindhold : (skønnet)	30 %

ANALYSERESULTATER:

Luftindhold	Beton	Kitmasse
Total :	5,1 %	14,5 %
< 0,350 mm :	1,1 %	3,0 %
0,350-1,5 mm :	1,3 %	
1,5 - 2,0 mm :	0,5 %	
>2,0 mm :	2,2 %	

Specifik overflade :	10 mm^{-1}
Afstandsfaktor :	0,49 mm

Bemærkninger

'Kitmasse" er defineret som pastaindhold + luftindhold.
Hvis indhold af indkapslet luft (korder > 2 mm) udelades, kan ovenstående værdier genberegnes til:
Luftporer i beton: 2,9 % (i kitmasse: 8,2 %). Specifik overflade: 17 mm-1. Afstandsfaktor: 0,38 mm.

Luftporeanalyse (ASTM C 457)

Udført: April 2015 v/AB & PL

Sags nr. 14-186

Prøvemærke : 8 S20-3

Målelinier : 40 stk.
Pastaindhold : 30 %
(skønnet)

ANALYSE RESULTATER:

Luftindhold	Beton	Kitmasse
Total :	2,3 %	6,9 %
< 0,350 mm :	1,2 %	3,7 %
0,350-1,5 mm :	0,5 %	
1,5 - 2,0 mm :	0,1 %	
>2,0 mm :	0,4 %	

Specifik overflade : 22 mm^{-1}
Afstandsfaktor : 0,32 mm

Bemærkninger
'Kitmasse" er defineret som pastaindhold + luftindhold.
Hvis indhold af indkapslet luft (korder > 2 mm) udelades, kan ovenstående værdier genberegnes til:
Luftporer i beton: 1,9 % (i kitmasse: 5,6 %). Specifik overflade: 27 mm-1. Afstandsfaktor: 0,29 mm.

Luftporeanalyse (ASTM C 457)

Udført: April 2015 v/AB & PL

Sags nr. 14-186

Prøvemærke : 1 S20-4

Målelinier : 40 stk.

Pastaindhold : 30 %
(skønnet)

ANALYSE RESULTATER:

Luftindhold	Beton	Kitmasse
Total :	3,7 %	10,9 %
< 0,350 mm :	2,1 %	6,1 %
0,350-1,5 mm :	1,2 %	
1,5 - 2,0 mm :	0,1 %	
>2,0 mm :	0,3 %	

Specifik overflade : 27 mm^{-1}

Afstandsfaktor : 0,21 mm

Bemærkninger

'Kitmasse" er defineret som pastaindhold + luftindhold.
Hvis indhold af indkapslet luft (korder > 2 mm) udelades, kan ovenstående værdier genberegnes til:
Luftporer i beton: 3,4 % (i kitmasse: 9,9 %). Specifik overflade: 30 mm-1. Afstandsfaktor: 0,2 mm.

Luftporeanalyse (ASTM C 457)

Udført: April 2015 v/AB & PL

Sags nr. 15-044

Prøvemærke : S35 14 S35-1

Målelinier : 40 stk.
Pastaindhold : 30 %
(skønnet)

ANALYSERESULTATER:

Luftindhold	Beton	Kitmasse
Total :	3,1 %	9,1 %
< 0,350 mm :	0,5 %	1,5 %
0,350-1,5 mm :	0,8 %	
1,5 - 2,0 mm :	0,2 %	
>2,0 mm :	1,5 %	

Specifik overflade :	8 mm^{-1}
Afstandsfaktor :	0,75 mm

Bemærkninger
'Kitmasse" er defineret som pastaindhold + luftindhold.
Hvis indhold af indkapslet luft (korder > 2 mm) udelades, kan ovenstående værdier genberegnes til:
Luftporer i beton: 1,5 % (i kitmasse: 4,6 %). Specifik overflade: 16 mm-1. Afstandsfaktor: 0,54 mm.

PELCON

Luftporeanalyse (ASTM C 457)

Udført: April 2015 v/AB & PL

Sags nr. 15-044

Prøvemærke : S35 26 S35-2

Målelinier : 40 stk.
Pastaindhold : 30 %
(skønnet)

ANALYSE RESULTATER:

Luftindhold	Beton	Kitmasse
Total :	3,6 %	10,4 %
< 0,350 mm :	1,3 %	3,9 %
0,350-1,5 mm :	1,2 %	
1,5 - 2,0 mm :	0,4 %	
>2,0 mm :	0,7 %	

Specifik overflade : 16 mm^{-1}
Afstandsfaktor : 0,37 mm

Bemærkninger
'Kitmasse" er defineret som pastaindhold + luftindhold.
Hvis indhold af indkapslet luft (korder > 2 mm) udelades, kan ovenstående værdier genberegnes til:
Luftporer i beton: 2,9 % (i kitmasse: 8,4 %). Specifik overflade: 19 mm-1. Afstandsfaktor: 0,33 mm.

Luftporeanalyse (ASTM C 457)

Udført: April 2015 v/AB & PL

Sags nr. 15-044

Prøvemærke : S35 37 S35-3

Målelinier : 40 stk.
Pastaindhold : 30 %
(skønnet)

ANALYSERESULTATER:

Luftindhold	Beton	Kitmasse
Total :	3,1 %	9,1 %
< 0,350 mm :	1,5 %	4,3 %
0,350-1,5 mm :	1,0 %	
1,5 - 2,0 mm :	0,2 %	
>2,0 mm :	0,4 %	

Specifik overflade : 22 mm^{-1}
Afstandsfaktor : 0,29 mm

Bemærkninger
'Kitmasse" er defineret som pastaindhold + luftindhold.
Hvis indhold af indkapslet luft (korder > 2 mm) udelades, kan ovenstående værdier genberegnes til:
Luftporer i beton: 2,7 % (i kitmasse: 8 %). Specifik overflade: 25 mm-1. Afstandsfaktor: 0,27 mm.

Luftporeanalyse (ASTM C 457)

Udført: April 2015 v/AB & PL

Sags nr. 15-044

Prøvemærke : S35 45 S35-4

Målelinier : 40 stk.
Pastaindhold : 30 %
(skønnet)

ANALYSE RESULTATER:

Luftindhold	Beton	Kitmasse
Total :	5,6 %	15,8 %
< 0,350 mm :	2,4 %	6,7 %
0,350-1,5 mm :	2,0 %	
1,5 - 2,0 mm :	0,2 %	
>2,0 mm :	1,1 %	

Specifik overflade : 18 mm^{-1}
Afstandsfaktor : 0,26 mm

Bemærkninger
'Kitmasse" er defineret som pastaindhold + luftindhold.
Hvis indhold af indkapslet luft (korder > 2 mm) udelades, kan ovenstående værdier genberegnes til:
Luftporer i beton: 4,5 % (i kitmasse: 12,8 %). Specifik overflade: 23 mm-1. Afstandsfaktor: 0,23 mm.

Luftporeanalyse (ASTM C 457)

Udført: April 2015 v/AB & PL

Sags nr. 15-044

Prøvemærke : S70 17 S70-1

Målelinier : 40 stk.

Pastaindhold : 30 %
(skønnet)

ANALYSERESULTATER:

Luftindhold	Beton	Kitmasse
Total :	2,9 %	8,6 %
< 0,350 mm :	0,9 %	2,6 %
0,350-1,5 mm :	1,2 %	
1,5 - 2,0 mm :	0,4 %	
>2,0 mm :	0,4 %	

Specifik overflade : 13 mm^{-1}

Afstandsfaktor : 0,52 mm

Bemærkninger

'Kitmasse" er defineret som pastaindhold + luftindhold.
Hvis indhold af indkapslet luft (korder > 2 mm) udelades, kan ovenstående værdier genberegnes til:
Luftporer i beton: 2,5 % (i kitmasse: 7,4 %). Specifik overflade: 14 mm-1. Afstandsfaktor: 0,48 mm.

Luftporeanalyse (ASTM C 457)

Udført: April 2015 v/AB & PL

Sags nr. 15-044

Prøvemærke : S70 27 S70-2

Målelinier : 40 stk.
Pastaindhold : 30 %
(skønnet)

ANALYSE RESULTATER:

Luftindhold	Beton	Kitmasse
Total :	2,7 %	8,1 %
< 0,350 mm :	1,1 %	3,2 %
0,350-1,5 mm :	1,0 %	
1,5 - 2,0 mm :	0,2 %	
>2,0 mm :	0,5 %	

Specifik overflade : 17 mm^{-1}
Afstandsfaktor : 0,38 mm

Bemærkninger
'Kitmasse" er defineret som pastaindhold + luftindhold.
Hvis indhold af indkapslet luft (korder > 2 mm) udelades, kan ovenstående værdier genberegnes til:
Luftporer i beton: 2,2 % (i kitmasse: 6,7 %). Specifik overflade: 21 mm-1. Afstandsfaktor: 0,35 mm.

Luftporeanalyse (ASTM C 457)

Udført: April 2015 v/AB & PL

Sags nr. 15-044

Prøvemærke : S70 37 S70-3

Målelinier : 40 stk.
Pastaindhold : 30 %
(skønnet)

ANALYSE RESULTATER:

Luftindhold	Beton	Kitmasse
Total :	4,3 %	12,4 %
< 0,350 mm :	1,4 %	4,1 %
0,350-1,5 mm :	1,6 %	
1,5 - 2,0 mm :	0,3 %	
>2,0 mm :	1,0 %	

Specifik overflade : 14 mm^{-1}
Afstandsfaktor : 0,39 mm

Bemærkninger
'Kitmasse" er defineret som pastaindhold + luftindhold.
Hvis indhold af indkapslet luft (korder > 2 mm) udelades, kan ovenstående værdier genberegnes til:
Luftporer i beton: 3,3 % (i kitmasse: 9,5 %). Specifik overflade: 18 mm-1. Afstandsfaktor: 0,35 mm.

Luftporeanalyse (ASTM C 457)

Udført: April 2015 v/AB & PL

Sags nr. 15-044

Prøvemærke : S70 47 S70-4

Målelinier : 40 stk.
Pastaindhold : 30 %
(skønnet)

ANALYSERESULTATER:

Luftindhold	Beton	Kitmasse
Total :	3,3 %	9,6 %
< 0,350 mm :	1,2 %	3,5 %
0,350-1,5 mm :	1,4 %	
1,5 - 2,0 mm :	0,2 %	
>2,0 mm :	0,5 %	

Specifik overflade : 15 mm^{-1}
Afstandsfaktor : 0,42 mm

Bemærkninger
'Kitmasse" er defineret som pastaindhold + luftindhold.
Hvis indhold af indkapslet luft (korder > 2 mm) udelades, kan ovenstående værdier genberegnes til:
Luftporer i beton: 2,7 % (i kitmasse: 8 %). Specifik overflade: 17 mm-1. Afstandsfaktor: 0,38 mm.

Luftporeanalyse (ASTM C 457)

Udført: April 2015 v/AB & PL

Sags nr. 15-044

Prøvemærke : K35 17 K35-1

Målelinier : 40 stk.
Pastaindhold : 30 %
(skønnet)

ANALYSERESULTATER:

Luftindhold	Beton	Kitmasse
Total :	3,3 %	9,8 %
< 0,350 mm :	1,0 %	3,0 %
0,350-1,5 mm :	1,5 %	
1,5 - 2,0 mm :	0,2 %	
>2,0 mm :	0,6 %	

Specifik overflade : 14 mm^{-1}
Afstandsfaktor : 0,45 mm

Bemærkninger
'Kitmasse" er defineret som pastaindhold + luftindhold.
Hvis indhold af indkapslet luft (korder > 2 mm) udelades, kan ovenstående værdier genberegnes til:
Luftporer i beton: 2,7 % (i kitmasse: 7,9 %). Specifik overflade: 17 mm-1. Afstandsfaktor: 0,4 mm.

Luftporeanalyse (ASTM C 457)

Udført: April 2015 v/AB & PL

Sags nr. 15-044

Prøvemærke : K35 27 K35-2

Målelinier : 40 stk.
Pastaindhold : 30 %
(skønnet)

ANALYSE RESULTATER:

Luftindhold	Beton	Kitmasse
Total :	3,7 %	10,7 %
< 0,350 mm :	1,2 %	3,5 %
0,350-1,5 mm :	1,4 %	
1,5 - 2,0 mm :	0,3 %	
>2,0 mm :	0,8 %	

Specifik overflade : 15 mm^{-1}
Afstandsfaktor : 0,40 mm

Bemærkninger
'Kitmasse" er defineret som pastaindhold + luftindhold.
Hvis indhold af indkapslet luft (korder > 2 mm) udelades, kan ovenstående værdier genberegnes til:
Luftporer i beton: 2,9 % (i kitmasse: 8,4 %). Specifik overflade: 18 mm-1. Afstandsfaktor: 0,35 mm.

Luftporeanalyse (ASTM C 457)

Udført: April 2015 v/AB & PL

Sags nr. 15-044

Prøvemærke : K35 37 K35-3

Målelinier : 40 stk.
Pastaindhold : 30 %
(skønnet)

ANALYSE RESULTATER:

Luftindhold	Beton	Kitmasse
Total :	3,5 %	10,2 %
< 0,350 mm :	1,5 %	4,5 %
0,350-1,5 mm :	1,2 %	
1,5 - 2,0 mm :	0,3 %	
>2,0 mm :	0,4 %	

Specifik overflade : 20 mm^{-1}
Afstandsfaktor : 0,29 mm

Bemærkninger
'Kitmasse" er defineret som pastaindhold + luftindhold.
Hvis indhold af indkapslet luft (korder > 2 mm) udelades, kan ovenstående værdier genberegnes til:
Luftporer i beton: 3,1 % (i kitmasse: 9,1 %). Specifik overflade: 23 mm-1. Afstandsfaktor: 0,27 mm.

Luftporeanalyse (ASTM C 457)

Udført: April 2015 v/AB & PL

Sags nr. 15-044

Prøvemærke : K35 47 K 35-4

Målelinier : 40 stk.
Pastaindhold : 30 %
(skønnet)

ANALYSERESULTATER:

Luftindhold	Beton	Kitmasse
Total :	3,2 %	9,5 %
< 0,350 mm :	1,6 %	4,9 %
0,350-1,5 mm :	1,3 %	
1,5 - 2,0 mm :	0,1 %	
>2,0 mm :	0,2 %	

Specifik overflade : 22 mm^{-1}
Afstandsfaktor : 0,28 mm

Bemærkninger
'Kitmasse" er defineret som pastaindhold + luftindhold.
Hvis indhold af indkapslet luft (korder > 2 mm) udelades, kan ovenstående værdier genberegnes til:
Luftporer i beton: 3,1 % (i kitmasse: 9,1 %). Specifik overflade: 23 mm-1. Afstandsfaktor: 0,27 mm.